Alma Mater Studiorum – Università di Bologna

DOTTORATO DI RICERCA IN SCIENZE CHIMICHE

Ciclo XXVIII

Settore Concorsuale di afferenza: 03/B1

Settore Scientifico disciplinare: CHIM/03

TITOLO TESI

Novel Ruthenium Complexes for Bifunctional Catalysis: the Dual Role of Cyclopentadienone and N-Heterocyclic Carbene.

Presentata da: Cristiana Cesari

Coordinatore Dottorato	**Relatore**
Prof. Aldo Roda	Prof. Valerio Zanotti
	Correlatore
	Dott. ssa Rita Mazzoni

Esame finale anno 2016

Abstract

The PhD thesis herein presented deal with the synthesis, characterization and catalytic application of new ruthenium transition metal complexes which exhibit unprecedented combination of ligands: cyclopentadienones and N-heterocyclic carbenes (NHC). In the first year of the PhD work it was developed a straightforward and efficient synthetic route to novel Ru N-heterocyclic carbenes (NHC) complexes by transmetallation of non-bulky imidazolylidene silver complexes to ruthenium dicarbonyl tetraarylcyclopentadienone. The same procedure with sterically demanding NHC resulted in the formation of unprecedented heterobimetallic Ru-Ag(NHC) complexes. During the second year six months (from March to September 2014) have been spent at the UCD School of Chemistry and Chemical Biology, University College of Dublin, under the supervision of Professor Martin Albrecht investigating the steric and electronic tunability of the catalyst precursors by replacing imidazolylidenes with triazolylidenes. Triazolylidenes are stronger donors than imidazolylidenes, and hence they further activate the ruthenium(0) oxidation state in dicarbonyl tetraarylcyclopentadienone Ru (NHC) complexes, which resulted to be beneficial in catalytic applications. During the second and third year the novel classes of ruthenium complexes were successfully employed as catalyst precursors in the transfer hydrogenation of ketones and aldehydes using iPrOH as hydrogen source. Fine tuning of several molecular parameters and reaction conditions allowed to improve catalytic performances. Furthermore, the catalysts were employed for the oxidation of alcohol with promising results. Heterogenization of the catalyst on polypropylene imine dendrimers has been also developed, moreover ionic ruthenium complexes have been also exploited as potential catalyst in ionic liquids. Greener synthetic conditions have been found both for the synthesis of ruthenium complexes under microwave irradiation and for the acid catalysed transformation of the bio-based bis-hydroxymethylfuran. Preliminary electrochemical measurements have been carried out on a triazolylidene Ru(0) complex. Its redox behaviour could be exploited in the development of electrocatalysis.

Table of contents

CHAPTER I

General Introduction

CHAPTER II

Sterically driven synthesis of ruthenium and ruthenium-silver N-heterocyclic carbene complexes

CHAPTER III

Ruthenium(0) complexes with triazolylidene spectator ligands: oxidative activation for (de)hydrogenation catalysis

CHAPTER IV

Ruthenium hydroxycyclopentadienyl *N*-heterocyclic carbene complexes as transfer hydrogenation catalysts

CHAPTER V

Synthesis and catalytic performance of poly(propylene imine) (PPIs) dendrimers modified with ruthenium cyclopentadienone N-heterocyclic carbene complexes

CHAPTER VI

Imidazolium salts of ruthenium anionic cyclopentadienone complexes: ion pair for bifunctional catalysts in ionic liquids

CHAPTER VII

Straightforward synthesis of iron cyclopentadienone *N*-heterocyclic carbene complexes

CHAPTER VIII

Microwave-assisted synthesis of functionalized Shvo's type complexes

CHAPTER IV

Oxidant free one-pot transformation of bio-based 2,5-bis-hydroxymethylfuran into α-6-hydroxy-6-methyl-4-enyl-2H-pyran-3-one in water

LIST OF PUBLICATIONS

CHAPTER I

General Introduction

The development of highly efficient and selective catalysts is one of the major research goals in chemistry and is expected to provide a significant contribution to the issue of sustainability. New catalysts need to be developed, and the demand for more selective and efficient synthetic methods has led to renewed interest toward homogeneous catalysis, particularly in the development of new ligands which can be tuned to specific needs. Indeed, the properties of a metal complex are the result of the interaction of the metal center and its surrounding ligands. In traditional approaches, the steric and electronic properties of the ligands are used to control the performance of the catalyst, but the ligands play a spectator role (the reactivity takes place at the metal center). Recent new approaches deviate from this concept, and make use of more reactive (actor) ligands, that can play a much more prominent role in the elementary bond activation steps in a catalytic cycle. The central idea is that the metal and the ligand can cooperate in a synergistic manner, and their interplay facilitates the chemical process.[1] Starting from this idea, the main goal of this thesis concerned the design of a new class of ruthenium carbonylic bifunctional catalyst that combine two versatile and popular class of ligands such as cyclopentadienone/hydroxycyclopentadienyl and N-Heterocyclic carbenes, in order to exploit this new metal-ligand combination for application in homogeneous catalysis. The unique features of the both ligands will be considered in details in the following paragraphs.

1. N-heterocyclic carbenes (NHCs) as spectator ligands

N-heterocyclic carbenes (NHCs) are probably the class of ligands that has attracted the most attention during the past decade, and has also witnessed the most impressive advances, which had produced a wider availability, applicability and a deeper understanding of their properties.

The first complex with a heteroatom-stabilized carbene ligand dates back to almost a century ago by Tschugajeff (Chugaev),[2] even though the molecular structure was only solved decades later providing evidence for the formation of the diaminocarbene complexes.

Discussions about N-heterocyclic carbenes were initialized by Wanzlick's report in the early 1960s; shortly thereafter, in 1968, Wanzlick and Öfele[3] independently published the first transition metal-carbene complexes (Hg and Cr respectively) predating the isolation of a free NHC by over 20 years (Figure 1.1).

Nevertheless, the field of N-heterocyclic carbenes as ligands in transition metal chemistry remained a lab curiosity until 1991 when a report on the extraordinary stability, isolation and storability of crystalline NHC IAd by Arduengo *et al.*[4] ignited a rapidly growing research field. The discovery that some carbenes could be isolated and easily handled triggered a true explosion of interest in their coordination ability. A few years later, this new class of ligands exploded in the literature, so that NHCs have become a ubiquitous class of ligands (Figure 1.1).
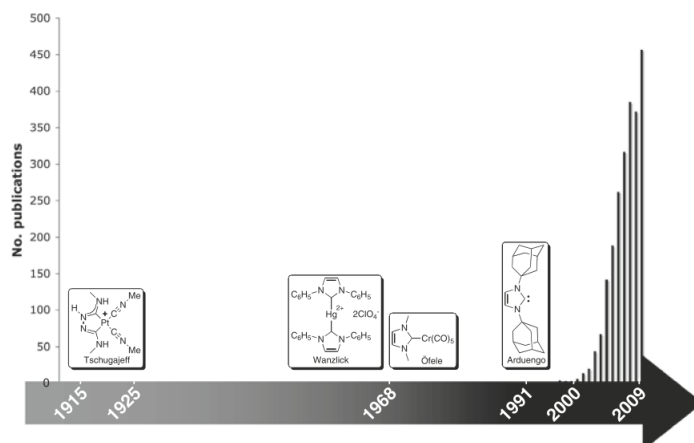
Figure 1.1. Number of publications (*N-heterocyclic carbene* as research topic).[5]

As excellent ligands for transition metals, NHCs have found multiple applications in some of the most important catalytic transformations in the chemical industry, while their reactivity upon coordination to main group elements and as organocatalysts has opened up new areas of research.

However, the largest application of NHC-transition metal complexes is in homogeneous catalysis directed to organic synthesis. The success encountered by NHC spectator ligands in this transformation is often attributed to their strong σ-electron donating properties, which allow a very strong NHC-metal bonds preventing decomposition of the catalyst and improving the catalytic activity.

1.1 Attractive Features of NHC

In many reviews the NHC are defined as heterocyclic species containing a carbene carbon and at least one nitrogen atom in the ring structure. Within these criteria fall many different classes of carbene compound with various substituent patterns, ring size and degrees of heteroatom stabilization (Figure 1.2). Nowadays the most common NHC used in catalysis are five-membered ring imidazolylidene, imidazolinylidenes and triazolylidenes that probably constitute the largest group of stable heterocyclic carbenes.[6]

imidazolidinylidene   **imidazol**ylidene   **triazol**ylidene   **tetrazol**ylidene

thiazolylidene   **oxazol**ylidene   **pyrrolidin**ylidene
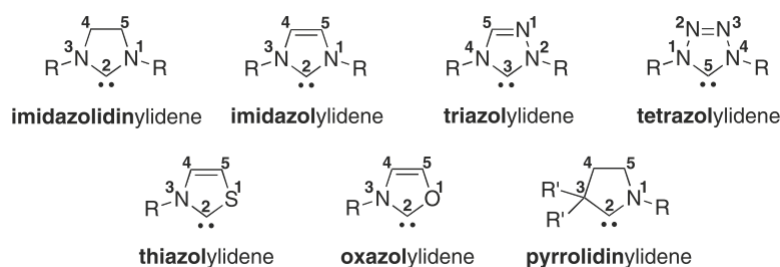
Figure 1.2. Common five-membered heterocyclic carbenes.

A representation of the general structures of NHCs is shown in Figure 1.3a for the first reported compound IAd by Arduengo. The remarkable stability of the carbene centre C^2 is explained by the combination of electronic and steric effects of these structural features. As demonstrated in IAd by the two adamantyl groups bound to the nitrogen atoms, NHCs generally include bulky substituents adjacent to the carbene carbon, which help to kinetically stabilize the species by sterically disfavouring dimerization to the corresponding olefin (the Wanzlick equilibrium).

1.1.1 Electronic and Steric Properties of NHC

The most important factor in the NHC ligands is the electronic stabilization provided by the nitrogen atoms. In contrast to classical carbenes, the NHCs such as IAd contain an sp^2-hybridized C^2 carbon in a singlet ground-state electronic configuration with the σ molecular orbital filled with two electrons in antiparallel spin orientation at highest energy and an unoccupied p-orbital at lowest energy (Figure 1.3b).[7]
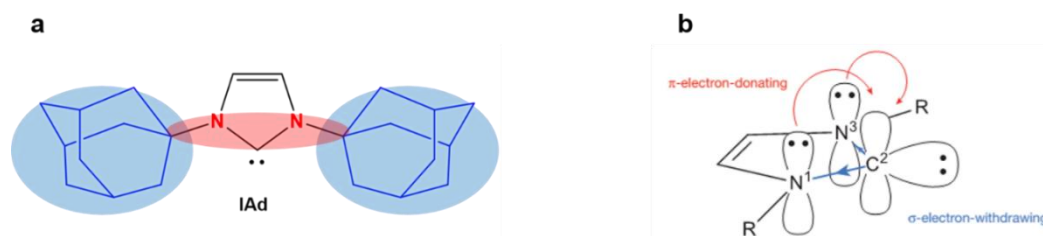
Figure 1.3. (**a**) General structural features of IAd. (**b**) Ground-state electronic structure of imidazol-2-ylidenes. The mesomeric (*red*) and inductive (*blue*) effects help to stabilize the singlet carbene structure.[7]

The adjacent σ -electron-withdrawing and π-electron-donating nitrogen atoms stabilize this structure both inductively by lowering the energy of the occupied σ-orbital (HOMO) and mesomerically by donating electron density into the empty p-orbital (LUMO). Furthermore, the cyclic nature of NHCs also helps to favour the singlet state by forcing the carbene carbon into a bent, more sp^2-like arrangement.

This ground state electronic structure, and in particular the presence of a lone pair on the plane of the heterocyclic ring of NHC, makes these compound nucleophilic with the tendency to act as σ-donors and bind to a wide range of metallic and non-metallic compound. This peculiarity influences the stability, structure and reactivity of the resulting complexes.

Although σ-donation is the most important component of metal–ligand binding, the contribution of both π-back-bonding into the carbene p-orbital and π-donation from the carbene p-orbital can be relevant (Figure 1.4). The degree of π-acceptor power of N-heterocyclic carbenes is still disputed and unclear. From experimental and theoretical results, Frenking and co-workers calculated that π-contributions account for about 20% of the complexes' overall orbital interaction.[4]
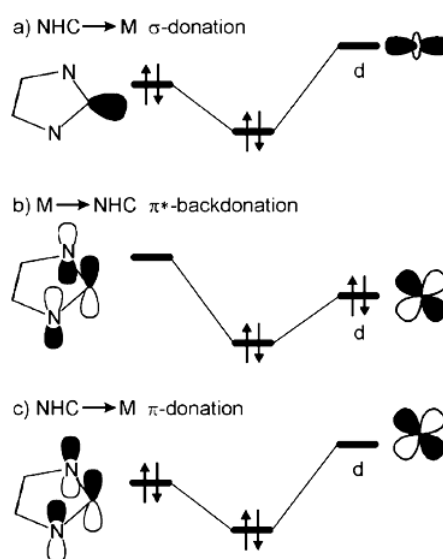
Figure 1.4. Diagram illustrates the σ→ d (**a**), the d →π* (**b**), and the π→ d (**c**) bonding modes occurring between NHCs and transition metals.[6]

The strong σ-donor and comparatively weak π-acceptor properties of NHCs bear similarities to the coordination characteristics of phosphines, so that NHCs were initially considered as mimics for this ubiquitous class of ancillary ligand in transition-metal coordination chemistry. There are, however, a number of differences between the two classes of ligands.[8]

As indicated by their lower TEP (Tolman Electronic Parameter) values (evaluation of the electron-donating ability of ligand by measuring the infrared-stretching frequencies of carbonyl ligands in model transition metal carbonyl complexes), NHCs are in general more electron-donating than phosphines. This leads to thermodynamically stronger metal–ligand bonds and is reflected in the typically greater bond dissociation energies and shorter metal–ligand bond lengths observed for NHC complexes over their phosphine counterparts. As a rule, the stronger metal–ligand interaction renders NHC–metal coordination less labile than metal–phosphine binding and the complexes are more thermally and oxidatively stable. Therefore, the equilibrium between the free carbene and the carbene metal complex lies far more on the side of the complex than in the case for phosphines (Figure 1.5b)[9]
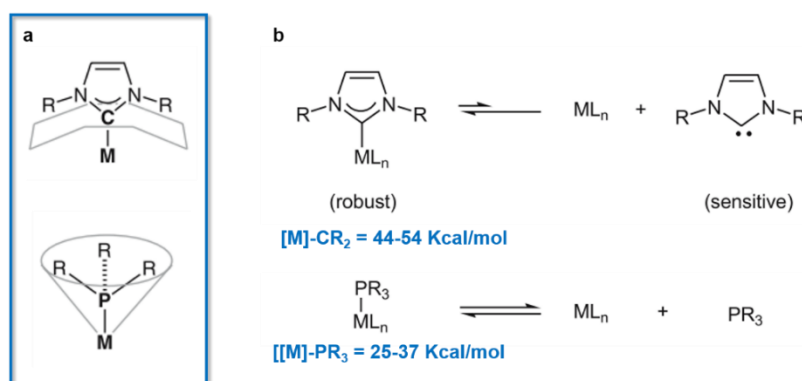
Figure 1.5. Comparison between the steric (**a**) and electronic (**b**) properties of phosphine and NHC metal complexes.

A comparison of the steric properties of NHCs and phosphines also reveals significant differences. Whereas the sp^3-hybridization of phosphines results in a cone-shaped spatial arrangement of the steric bulk, most classes of NHCs, including the most commonly employed imidazole-derived types, can be better described as fan- or umbrella-shaped with the nitrogen-substituents adjacent to the carbene carbon oriented more towards the metal (Figure 1.5a). In an attempt to quantify the steric demand of NHC ligands Nolan *et al.*[10] have introduced the %V$_{bur}$, (volume buried parameter) by overlap between a sphere with a radius of 3Å centered around the metal with the atoms of the ligand within this sphere. As a result, NHCs are generally considered to be sterically demanding ligands with variations in the nitrogen substituents and class of heterocycle having a large effect on the steric environment at the metal centre. In contrast to phosphines, where changing the phosphorus substituents invariably affects both the steric and electronic properties in that the substituents are directly attached to the donor atom itself, the NHC provide the possibility to separately modify the nitrogen substituents, the backbone functionality and the class of heterocycle, allowing independent variation of each parameter. With these attractive features, NHCs nowadays rival phosphines and cyclopentadienyls as ligands across organometallic chemistry and the extensive range of accessible complexes continues to grow at amazing rate.[9b]

1.1.2 Synthesis of NHC precursors and NHC-Transition Metal Complexes

An additional advantges associated to NHCs is the relative ease with which libraries of structurally diverse analogues can be prepared and studied.

Various methods of synthesizing complexes may be employed, and the main synthetic routes leading to the formation of NHC complexes are depicted in Scheme 1.1. The methodologies given are shown with imidazolydene ligands, however, they are applicable to other NHCs.
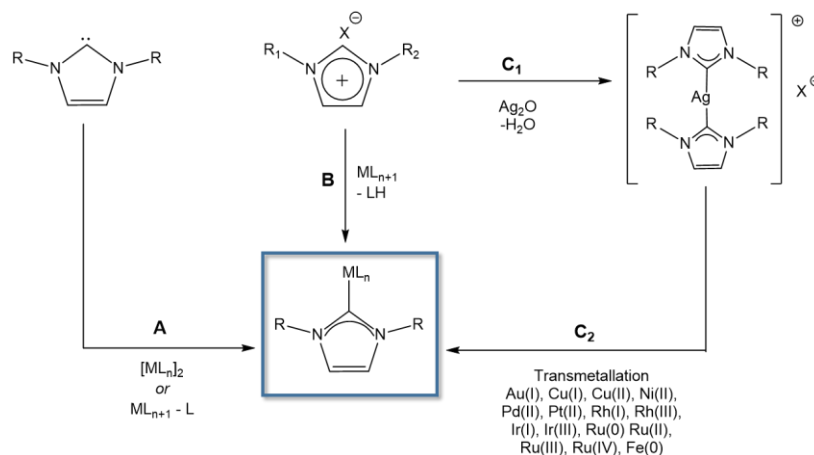
Scheme 1.1. Main synthetic strategies for the formation of NHC-complexes.

Route **A** consists of generating the free carbene (by deprotonation of the corresponding salt) followed by coordination to a metal centre (often with concomitant ligand displacement). Method **B** consists of using a metal precursor containing a base as ligand. The base deprotonates the imidazolium salt, leading to the coordination of the NHC and of the counter anion of the salt (if X is a coordinating anion). Method **C** employs a carbene transfer reagent (often a Ag-complex) that, by transmetallation reaction, delivers the NHC to a second metal centre.[5]

Arguably, imidazolium-based carbenes synthesis have proven to be especially versatile and useful, in fact the synthesis of imidazolium salts has been developed over many decades and numerous powerful methods exist. Two main different routes can be distinguished:[6]

1) imidazoles obtained by deprotonation of the corresponding cationic heterocyclic azolium salt with the help of suitable bases (pKa = 21-24), can be alkylated using appropiate electrophiles (*eg.* alkyl halide) resulting in the formation of N-alkyl-substituted imidazolium salts (Scheme 1.2).
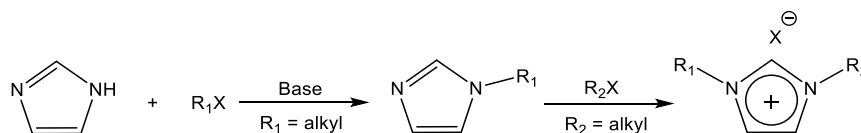
Scheme 1.2. Synthesis of imidazolium salts by alkylation reactions.

2) the imidazolium ring can be built up by condensation reaction. For example, glyoxal is reacted with formaldehyde and a primary amine in the presence of a strong acid, resulting in the formation of imidazolium salts (Scheme 1.3). Symmetric imidazolium salts can be easily obtained by similar synthetic procedures when two equivalents of primary amine are employed ($R_1 = R_2$). This latter route has become the method of choice for many sterically demanding imidazolium salts.
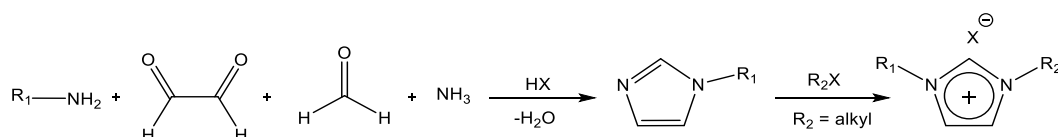
Scheme 1.3. Synthesis of imidaziolium salts by cyclization reaction followed by alkylation.

The general applicability of these synthetic routes allow to modulate the steric and electronic properties of the NHC ligand by changing the R substituents. The insertion of appropriate functional groups on the R substituents can:

- increase the complex stability through the formation of chelating system;
- promote hemilability;
- adjust the steric and electronic factor around the metal centre;
- induce chirality;
- increase the solubility in polar solvent.

Furthermore, the insertion of a donor substituent in the side chain of the NHC can:

- be used for the immobilization of organic imidazolium salts or organometallic complexes by means of NHC linker;
- act as a further coordination site.

1.2 Catalytic applications of NHC-Transition Metal Complexes

The attractive features of NHC-metal coordination previously described have led to a wide range of different applications in many field of chemistry. As mentioned above, the largest application is in homogeneous catalysis; in particular the most important transformations mediated by NHC-transition metal complexes includes Ir- and Ru- catalysed hydrogenation and hydrogen transfer, gold-catalysed activation of π -bonds and Rh- and Pt-catalysed hydrosilylation[11]. The two most extensively studied classes of catalytic reactions, however, are cross-coupling (catalysed by Pd or other metals) and Ru-catalysed olefin metathesis. Much of the success of NHC spectator ligands in these transformations can be attributed to the increased catalyst stability, and consequent lower rates of catalyst decomposition resulting from strong metal–ligand binding.

1st Generation
Grubbs

2nd Generation
Grubbs

2nd Generation
Hoveyda-Grubbs
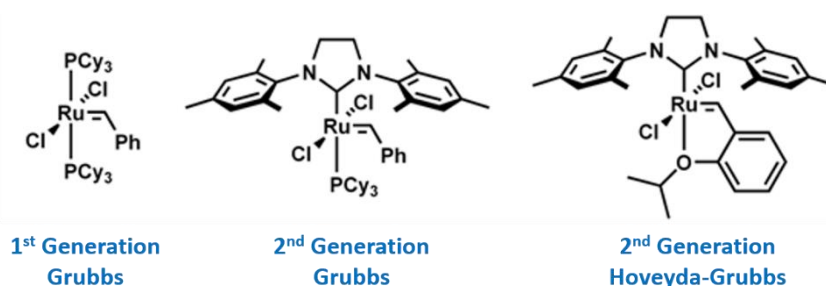
Figure 1.6. Comparison of Grubbs' first- and second- generation catalyst in olefin metathesis.

Arguably, the best example is provided by the excellent efficiency of the Grubbs' second-generation olefin metathesis catalyst in comparison to the first-generation (Figure 1.6), which displays two PCy$_3$ ligands bound to ruthenium(II).[12] The substitution of one of the two phosphines with the SIMes carbene ligand in the second Grubbs generation displays significantly higher reactivity than its predecessor and has dramatically expanded the range of suitable substrates for metathesis reactions. Numerous related NHC–ruthenium complexes, including the widely used Hoveyda–Grubbs second-generation catalyst (Figure 1.6), have been developed for

applications in metathesis and the importance of these reactions was recognized with the award of the Nobel Prize for chemistry in 2005.[7]

The major role of Ruthenium on the NHC chemistry of group 8 is the direct consequence of the immense interest raised by the Grubbs [(NHC)Ru] complexes in olefin metathesis. A downside of this success is that the other catalytic applications of [(NHC)Ru] compounds have long been overshadowed.[13]

1.2.1 Ru(NHC) complexes as homogeneous catalysts

In the last decade the ruthenium-based NHC complexes have found applications in a wide homogeneous catalytic reaction, some examples are listed below:

- Transfer Hydrogenation:[14]

The reduction of carbonyl compounds using a hydrogen donor, typically isopropanol that is oxidized into acetone, has emerged as an attractive alternative to protocols based on dihydrogen and metal hydrides protocols. In this context, Ru(NHC) complexes have proven to be excellent catalysts, and have become the benchmark for newly developed catalytic transformation.

The presence of a NHC ligands in the design of new catalysts enhanced the stability of the complex resulting in good catalytic performances, furthermore the ligand choice is a key issue toward both selectivity and activity of the metal center.

Beller and co-workers evaluated the potential of a wide range of common N-heterocyclic carbenes in the transfer hydrogenation of acetophenone. Among differently substituent aryl and alkyl NHCs, IPr (isopropyl group) proved to be the most active, resulting in very high TON.[15] Another example, (Figure 1.7) shows two type of transfer hydrogenation catalysts that contain an abnormal N-Heterocycle Carbene (aNHC) as ligand.
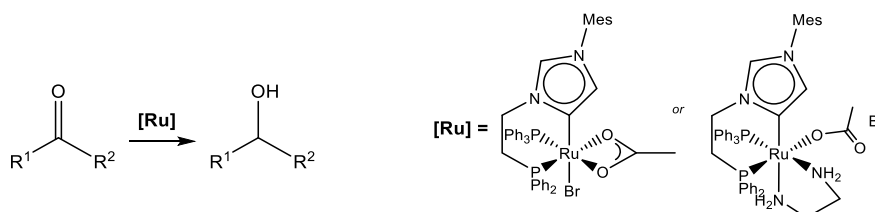
Figura 1.7 Transfer hydrogenation of ketones by [Ru(aNHC)] catalysts.

In this kind of carbene the imidazolylidenes bind the metal centers *via* the C4 or C5 position of the heterocycle. This peculiar coordination is considerably more electron-donating due to the reduced σ-withdrawal from the carbene center leading to a different electron properties and enhances reactivity.

- Synthesis of amide from alcohol and nitrile:[16]
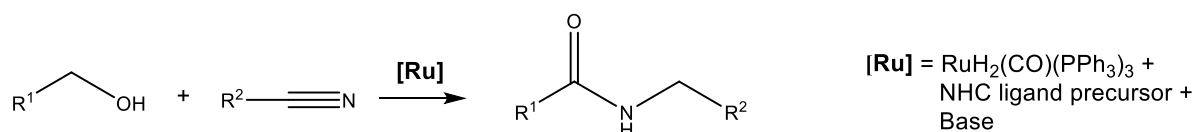
Figure 1.8. Catalytic amide synthesis from an alcohol and a nitrile by an NHC-based Ru hydride catalyst.

The synthesis of amide according to the principles of "atom-economic" is one of the top challenges in green organic synthesis and industrial processes in particular for pharmaceutical industries. The first catalytic, single-

step, and redox-neutral transformation of alcohols and nitriles into amide with 100% atom economy was performed by a Ru hydride complexes (*eg.* RuH$_2$(CO)(PPh$_3$)$_3$) as pre-catalyst in the presence of an N-heterocyclic carbene precursor such as 1,3-diisopropylimidazolium bromide and a base (Figure 1.8). The amide C−N bond is efficiently formed between the nitrogen atom of nitrile and the α-carbon of alcohol, with the help of an N-heterocyclic carbene-based ruthenium catalyst, without a single by-product.

- H$_2$-Mediated Hydrogenation:

Whittlesey and co-workers combined the potential of NHCs with that of metal borohydrides in molecular hydrogen-based reduction leading to the synthesis of a series of η^2-BH$_4$ ruthenium catalysts (Scheme 1.4) that displayed good activities in the reduction of acetophenone derivatives under 10 atm of H$_2$.[17] Similarly to Beller's findings, the IPr-containing complex was found to be the most active.

NHC = L = IMes
NHC = L = IPr
NHC = L = SIPr
NHC = IMes, L = PPh$_3$
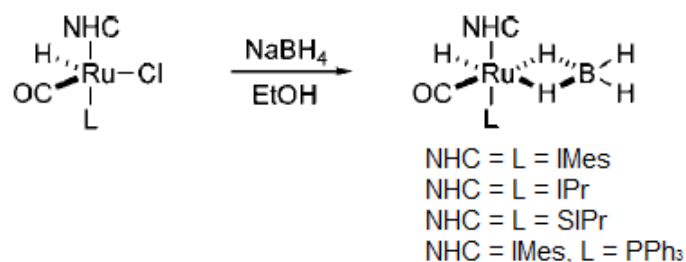
Scheme 1.4. Synthesis of η^2-BH$_4$ ruthenium carbene complexes.

Recently, Albrecht *et al.*[18] have proven that Ru(arene) complexes (Figure 1.9) containing a bidentate chelating NHC ligand, are effective catalyst precursors for the direct hydrogenation of olefin using H$_2$. The chelating groups have a pronounced effect on the catalytic activity and the stability of the complexes. Whereas the olefin donor group in **Ru1** was rapidly hydrogenated, thus inducing complex decomposition and predominantly heterogeneous hydrogenation, the carboxylate group in **Ru2** markedly increased the stability of the complex.
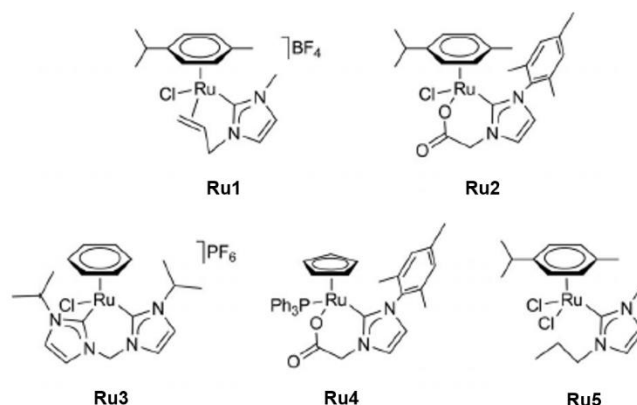
Figure 1.9. Chelate (**Ru1-4**) and monodentate (**Ru5**) ruthenium carbene complexes.

- Water Oxidation:[19]

The discovery of efficient catalysts for water splitting is currently a major challenge due to need of technologies for fuel production in order to address the growing global energy demand.

Mononuclear and dinuclear ruthenium complexes containing a pyridine-functionalized NHC (Figure 1.10) result active in this reaction. Tailoring the catalytic activity, still rare in water oxidation catalysis, is readily achieved by appropriate modification of the substituents at the imidazolylidene nitrogens.
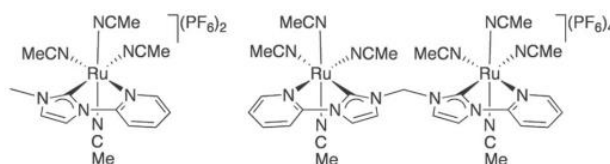
Figure 1.10. Ru(NHC) water oxidation catalyst synthetized by Albrecht group.

- Antitumor metallodrugs:[20]

Recently, NHCs came into the focus as carrier ligands for cytotoxic metal complexes because they perfectly fit prerequisites for an efficient drug design and fast optimization. NHCs are readily accessible in few steps and their substituents can be widely varied allowing an easy fine-tuning of both the physicochemical properties and the reactivity in biological medium of the final metal–NHC complexes. Additionally, their high stability and ease of derivatization make them suitable candidates for drug development. Figure 1.11 shows two examples Ru(NHC) complexes synthetized as potential chemotherapeutic agents.
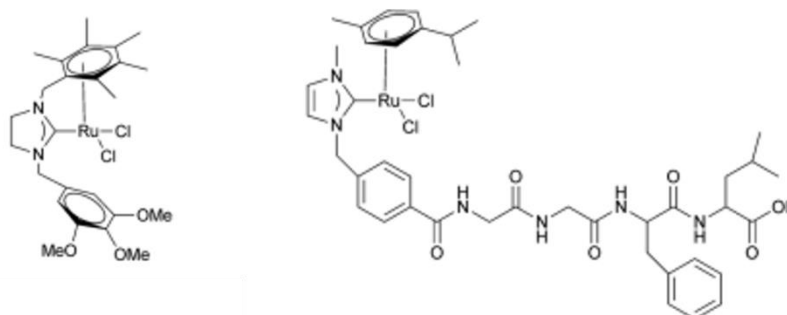
Figura 1.11. Ru(NHC) as potential chemotherapeutic agents.

Until recently, only two classes of ligands, both sterically and electronically tuneable, can be considered of very broad use in organometallic catalysis: phosphines (PR_3) and cyclopentadienyls (C_5R_5). Comparison between NHCs and phosphines properties, being both monodentate 2 electron ligands, has discussed previously in the paragraph 1.1.1 Cyclopentadienyls, as 5 electron ligands (6e$^-$ on the ionic model), are less closely related to NHCs than phosphines, nevertheless both type of ligand can adopt the role of spectator or actor ligands in the activation steps of a catalytic cycle.[21] Indeed, beside modulation of the electronic and steric properties of the ligand to affect the catalytic activity, bifunctional catalyst are emerging as powerful tools, provided that the ligands contain non-innocent functional groups, which are directly involved in the catalytic cycle.[22]

2. Cyclopentadienone as non-innocent ligand in bifunctional catalysts

The development of new metal-ligand bifunctional hydrogenation catalysts has dramatically changed the face of catalytic reduction. These catalysts provide attractive "green" alternatives to stoichiometric $LiAlH_4$ and $NaBH_4$ reductions and utilize environmentally friendly terminal reductants, such as hydrogen and 2-propanol. The first metal-ligand bifunctional catalyst, the hydroxycyclopentadienyl diruthenium bridging hydride (Figure 1.12, **A**), was reported by Shvo in the mid-1980s; it showed an efficient catalytic activity in a large variety of reactions and notably in hydrogenation and oxidation transformations. Fundamental contributions in this area have delivered by Noyori with a number of ruthenium catalysts, including the ruthenium(diamine)(BINAP) (Figure 1.12, **B**), which has displayed an extraordinary activity in the asymmetric reduction of ketones.[23]
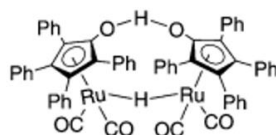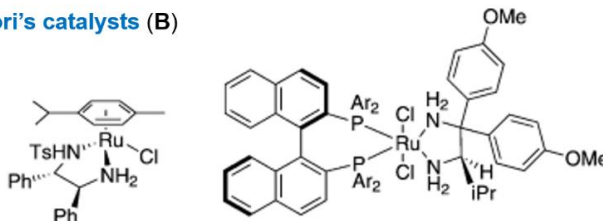
Figure 1.12. Shvo,s and Noyori's metal-ligand bifunctional catalysts.

2.1 Outer Sphere mechanism in hydrogenation catalysis

Shvo and of Noyori bifunctional catalysts, which contain a proton donor site (AH) on the ligand and a hydride donor sites (BH) on the metal center, suggest an outer sphere (OS) transfer mechanism, in contrast to the traditional inner sphere (IS) mechanism operated by the majority of homogeneous hydrogenation catalysts. In the OS mechanism the substrate does not bind to the metal but H^+ and H^- are instead transferred, either together or stepwise, from the catalyst to the unbound substrate. The proton donor site is typically an ancillary ligand such as cyclopentadienyl containing an OH or NH unit adjacent to the metal, and the hydride donor is a metal hydride, typically Ru–H. The two sites being adjacent and coupled electronically facilitates concerted $(H^+ + H^-)$ transfer (Figure 1.13.).[24]
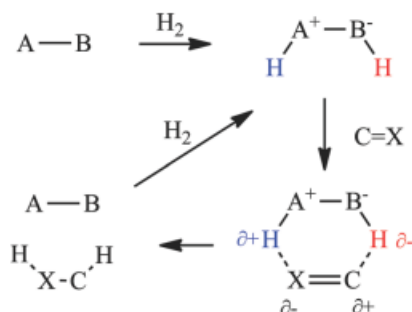
Figure 1.13. A general scheme for the catalytic H_2 hydrogenation of polar bonds where the hydride addition to the substrate in the outer coordination sphere is assisted by an ancillary ligand.

An example of non-classical outer sphere mechanism for the hydrogenation of polar multiple bonds is shown in Scheme 1.5. In step I substrate **1** coordinates in step I by forming an outer sphere interaction between the atoms of its polar double bond and the proton and hydride of the complex **B**. This interaction allows for the simultaneous transfer of the hydride and the proton (step II) producing the hydrogenated substrate **2** and a ruthenium complex with a vacant coordination site, **C**. This 16-electron ruthenium center is usually stabilized by π-donation from the deprotonated ligand into the empty d-orbital. Hydrogen gas can then coordinate at this open site (III) producing a dihydrogen complex intermediate or transition state **D**. The dihydrogen ligand heterolytically cleaves in step IV to re- form the original hydride complex **A**.[25]
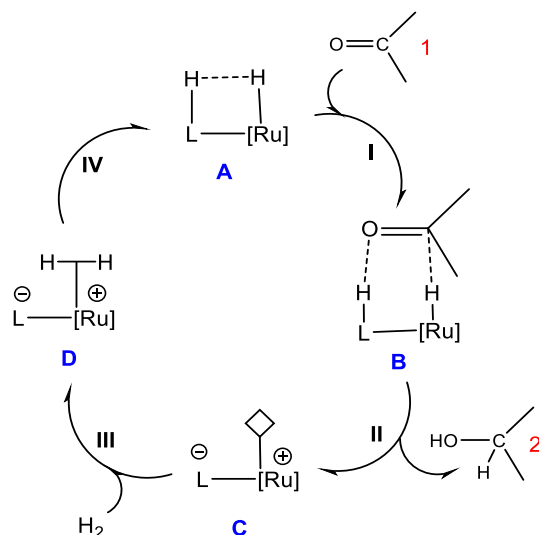
Scheme 1.5. A general scheme for the H$_2$ hydrogenation of polar bonds catalyzed by ruthenium catalysts where the hydride addition to the substrate in the outer coordination sphere is assisted by an ancillary ligand.

2.2 Nature of Shvo's catalyst and the role of the cyclopentadienone ligand

Catalytic cycles of the type described in the Scheme 1.5 involves a NH or OH group on the ancillary ligand. As far as it concerns the OH group as proton donor, the most famous example is the Shvo catalyst. Shvo's catalyst (Scheme 1.6, structure **I**)[26] is an air- and water-stable crystalline solid that is commercially available from several sources. Its discoverer, Youval Shvo, and co-workers discovered and introduced this versatile ruthenium catalyst that utilizes non innocent cyclopentadienone ligands to stabilize the metal in low oxidation states. This complex and its analogues have been extensively applied as catalyst for reactions such as hydrogenation of aldehydes, ketones, alkynes, and alkenes, transfer hydrogenation, disproportionation of aldehydes to esters, isomerization of allylic alcohols, dynamic kinetic resolution (DKR), amine–amine coupling, and hydroboration reactions.

2.2.1 Reactivity

Complex **I** is a dimeric pre-catalyst that forms monomeric oxidizing (**II**) and reducing (**III**) forms upon dissociation in solution. The concentrations of these active forms are governed by equilibrium effects; mutual conversion of **II** and **III** take place through the gain or loss of "H$_2$" from donors (AH$_2$) and acceptors (A) as shown in Scheme 1.6.
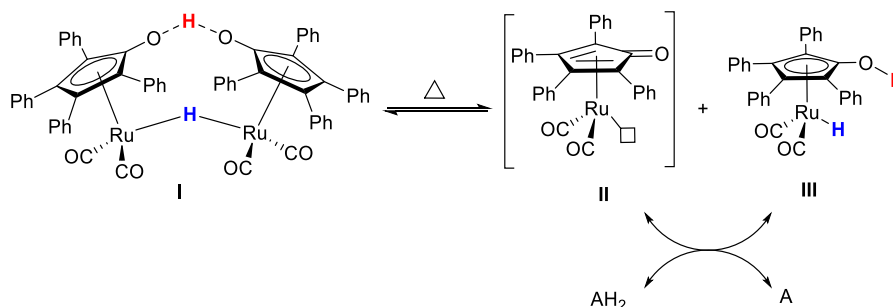
Scheme 1.6. Shvo's Catalyst (**I**): Heterodimer of oxidizing (**II**) and reducing (**III**) species.[27]

2.2.2 Catalytic mechanism in hydrogenation reaction

The dissociated monomeric forms of **I** are: a ruthenium hydride (**III**) and a coordinatively unsaturated dicarbonyl species (**II**). Upon dissociation both bridging hydrogen atoms are associated with the same monomer (**III**), this ruthenium is in the 2+ oxidation state while the other (**II**) is formally in the zero oxidation state. Curiosly, the species with higher formal oxidation state (Ru^{2+}) is the reducing agent, and the formal ruthenium(0) species is the oxidizing complement. This interesting situation can be explained by the conversion of a formally neutral cyclopentadienone ligand (coordination η^4) to a formally anionic hydroxycyclopentadienyl ligand (coordination η^5).[28]

Mechanistic studies by Casey, Backvall, and others have established that the catalyst transfers dihydrogen through a hydride on the transition metal (Ru-H) and a proton on the hydroxyl cyclopentadienyl ligand (O-H), as depicted in Scheme 1.7, thus it acts as a metal-ligand bifunctional catalyst.
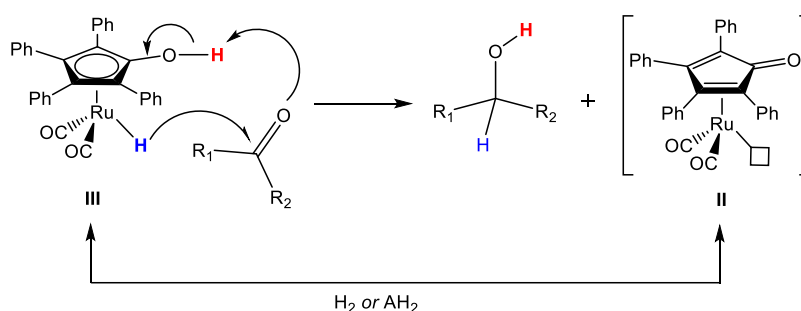
Scheme 1.7. Concerted delivery of H^+/H^-, and regeneration of the catalyst.

As mentioned above, the catalyst precursor **I** has the two metals joined by a bridging hydride, and an O-H-O hydrogen bond connects the two cyclopentadienone ligands. The cleavage of the bimetallic starting material occurs by heating producing a formally 16-electron Ru fragment (**II**) and the 18-electron Ru-hydride containing the substituted hydroxycyclopentadienyl ligand (**III**). In fact, the catalytic hydrogenation of ketones requires a temperature over 90°C to generate the mononuclear species that are catalytically active in hydrogenation, according to the sequence shown in Scheme 1.7. The catalytic cycle is an example of metal ligand cooperation in a non-classical outer sphere mechanism thereby allowing to operate in mild conditions leading to high selectivity and conversions of the substrate with a low hydrogen consumption.[29]

3. Catalytic Redox Processes

Redox transformations of coordination compounds have since long drawn considerable attention in consideration of the fact that catalytic reduction and oxidation reactions can be effectively mediated by transition metal complexes. The most common ("classical") behaviour of a transition complex in a redox process involves oxidation or reduction of the metal, leaving the ligand unaffected. In other cases, as the example of the Shvo catalyst reported above, ligands can also participate in the redox process. In such cases, the ligand is referred to as being "redox non-innocent" or "redox active". Such species have attracted substantial attention over the past decade, since they offer a unique opportunity to modify the reactivity of transition metal complexes.[1] Among the variety of transition-metal mediated redox reactions, hydrogenation and dehydrogenation have gained a special role due to the wide application of these reactions in many laboratory and industrial processes, and in consideration of the increasing demand for "green" and suitable

transformations. In particular, this latter point has strongly motivated the development of a large number of new catalyst for hydrogenation – dehydrogenation reactions.[30]

3.1 Transfer Hydrogenation

Hydrogenation is one of the most fundamental transformations in organic synthesis, and its industrial applications span from fine chemicals to pharmaceuticals synthesis. Direct hydrogenation, under H_2 gas pressure, and transfer hydrogenation (TH) are the two most common strategies for hydrogenation.[31]

TH reaction, referring to the addition of hydrogen to a molecule from a non-H_2 hydrogen source, is a convenient and powerful method to access various hydrogenated compounds. It is an attractive alternative to direct hydrogenation, and it has recently become the subject of an interest research activity. The advantages of transfer hydrogenation are:

(i)   it does not require hazardous pressurized H_2 gas nor elaborate experimental setup,

(ii)   the hydrogen donors are readily available, inexpensive, and easy to handle,

(iii)   the major side product deriving from the oxidation of the hydrogen donors can be recycled,

(iv)   the catalysts involved are usually readily accessible and not sensitive.

3.1.1 Main historical milestones of Transfer Hydrogenation reaction

The hydrogen transfer reaction dates back more than a century. TH, is by far the most important and widely used subfield. TH reactions are divided according to the catalyst type in Meerwein−Ponndorf−Verley (MPV) reductions, late transition metal-catalyzed reactions, organocatalytic, enzyme-catalyzed, thermal, base-catalyzed, and uncatalytic processes.

The illustrious MPV reduction[32] was first published independently by Meerwein and Verley in 1925, and it was the first TH reaction of carbonyl compounds. In the MPV process, an aluminum alkoxide acts as a promoter for the reduction of a ketone to the corresponding alcohol in the presence of a secondary alcohol as a hydrogen donor. The transition state is a six-membered cycle in which both the reducing alcohol and the carbonyl are coordinated to the same metal center (Scheme 1.8).
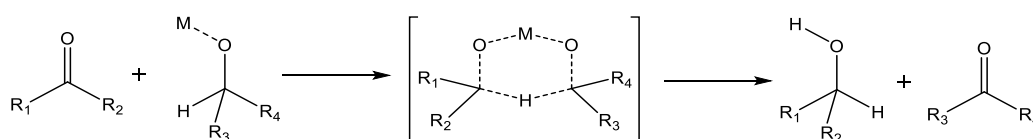
Scheme 1.8. Hydrogen Transfer in the MPV Reduction via a cyclic transition state.

The MPV reduction has been extensively applied in both academic and industrial syntheses, particularly in the chemical manufacture of flavor agents, due to its chemoselectivity toward the keto functionality and the mild reaction conditions. However, the well-known drawbacks of this method are the requirements of a large amount of reagents, side reactions that led to the formation of undesired products and moisture sensitivity (especially for Al catalysts).

The next milestone of TH was the discovery of late transition-metal catalysts involving the metals of groups 8, 9, 10, and 11. In the 1960s Mitchell and co-workers[33] reported that an iridium hydride complex catalyzed the hydrogenation of cyclohexanones and α,β-unsaturated ketones to alcohols with isopropanol.

Subsequently, Sasson and Blum[34] demonstrated that the complex [RuCl$_2$(PPh$_3$)$_3$] is active in the biphasic TH of acetophenone in the presence of isopropanol at high temperature. Two decades later, Chowdhury and Backvall[35] found that the catalytic activity of [RuCl$_2$(PPh$_3$)$_3$] is strongly enhanced by adding NaOH as co-catalyst.

In the early 1980s, the first reports of the Ru- catalyzed asymmetric TH emerged. Since then, asymmetric TH (ATH) has received significant and increasing attention, culminating with the Nobel Prize award to Noyori and Knowles in 2001.[36] ATH based on late transition-metal catalysts has proven to be among the most powerful methods for asymmetric reduction of various unsaturated substrates to produce chiral compounds. This is due to the excellent stereo-selectivity, the availability of various hydrogen sources, operational simplicity, and the use of readily accessible and little sensitive catalysts.
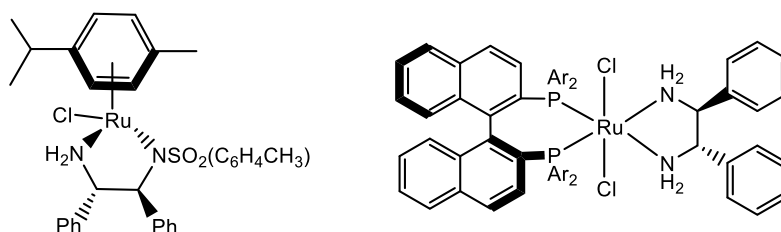
Figure 1.14. Noyori catalysts.

The chiral ruthenium complexes shown in Figure 1.14 are two examples of catalyst precursors synthetized by Noyori and used in the stereoselective hydrogenation of various ketone, aldehydes, and imines.

Ir, Ru, and Rh complexes bearing N, P, O, S, C element-based ligands are perhaps the most classic and popular catalysts for TH. In the last decades, the family of N-heterocyclic carbene (NHC) ligands has arrived at the forefront of coordination chemistry and organometallic catalysis as ubiquitous ancillary ligands due to their attractive features such as strong coordination ability and the tuneable character of their steric and electronic properties which have been thoroughly described in the paragraph 1.1. The use of NHC as ligands in transition-metal complexes for catalytic TH was pioneered by Nolan *et al.*[37] who designed and synthesized the complexes [Ir(cod)(py)(NHC)]PF$_6$ (**Ir1**) (Figure 1.15).

R = 2,4,6-trimethylphenyl
2,6-di-iso-propylphenyl
cyclohexyl
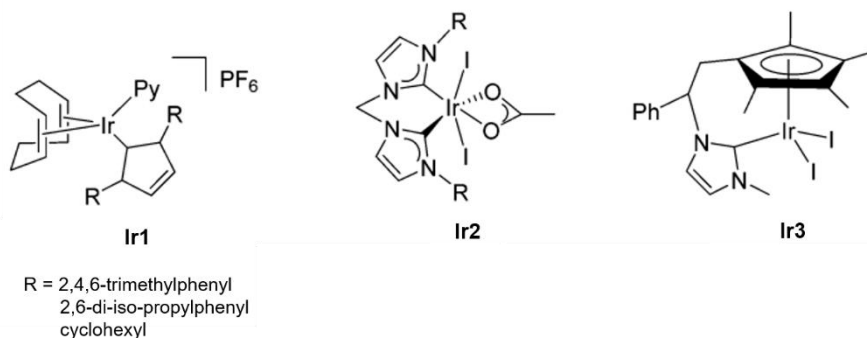
Figure 1.15. [Ir(NHC)] catalysts synthetized by Nolan (**Ir1**), Crabtree (**Ir2**) and Royo (**Ir3**).[30]

These complexes were used as TH catalysts for the reduction of several unsaturated substrates including ketones, olefins, and nitroarenes using isopropanol as hydrogen source. In the light of these results, many other Ir(NHC) complexes have been investigated. Crabtree and his group[38] reported the new air-stable and moisture-insensitive Ir catalyst (**Ir2**, Figure 1.15) bearing a chelating bis(N-heterocyclic carbene) ligand for

efficient TH of ketones. Royo and co-workers[39] prepared the first Cp*-functionalized NHC (Cp* = η^5-C$_5$Me$_5$) (Figure 1.15, **Ir3**).

3.1.2 Ru(NHC) complexes as transfer hydrogenation catalysts

Recent years have witnessed great improvements in the field of ruthenium-catalyzed Tranfer Hydrogenation, in particular due to the development of the diversity of ligands. Ligand choice is a key issue toward both selectivity and activity of the metal center. In consideration of the peculiar properties of NHCs mentioned above (paragraph 1.2), it is not surprising that a variety of ruthenium NHC complexes with different oxidation states, coordination geometries of ruthenium, and structural motifs have recently disclosed good activity and selectivity in catalytic TH.[30] In particular, NHC ligands functionalized with an additional donor group have been extensively investigated, due to the potential hemilability of the additional donor group involving reversible dissociation from the ruthenium center. These donor groups include pyridine, pyrimidine, phosphine, carboxylate, indenyl, oxazoline, thioether, and ether.

Early pioneering work on TH using Ru(NHC) catalysts was reported by Peris and Danopoulos;[40] these authors used 2,6-bis(1-alkylimidazo-lium-3-yl)pyridine salts as a new source of tridentate CNC bis(carbenes) to coordinate Ru and readily assemble the Ru "pincer" NHCs complexes **Ru6** and **Ru7** (Figure 1.16). Both the complexes exhibited high catalytic activity in the TH reduction of carbonyl compounds.

Ru6   **Ru7**
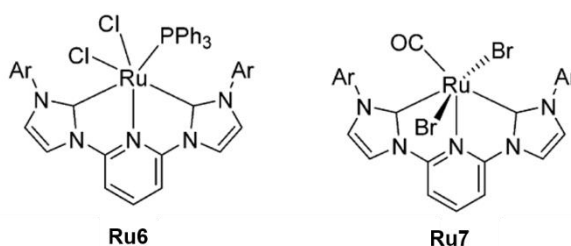
Figure 1.16. [Ru(NHC)] catalysts reported by Peris and Danopoulos.[30]

Ruthenium complexes with NHCs containing a pyridine moiety (*e.g.* complexes **Ru8** and **Ru9** Figure 1.17) have been established as effective catalysts in TH. Remarkably, only 0.1 mol% catalyst loading of **Ru9** appeared to be sufficient for the TH of a wide range of ketones and imines (Figure 1.17).[41]

Ru8   **Ru9**
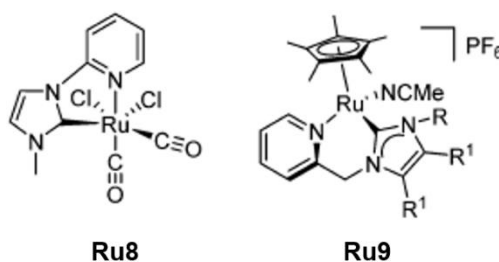
Figure 1.17. [Ru(NHC)] complexes bearing a pyridine group.

Albrecht' s group readily prepared a series of ruthenium complexes containing different donor substituent-functionalized NHCs (Figure 1.18).[42] Among them, the olefin-tethered NHC ruthenium complex **Ru10** was a very efficient and versatile catalyst toward reduction of olefins, alkynes, ketones, nitrobenzene and benzonitrile under various conditions. Furthermore, the study on the double TH of α,β-unsaturated ketones catalyzed by a revealed fast isomerization of the enol intermediate to its saturated ketone tautomer prior to the second hydrogenation.
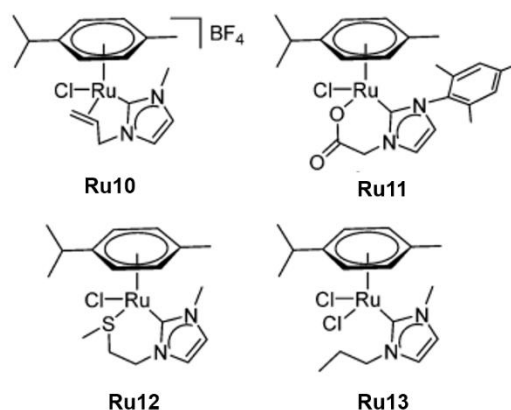
Figure 1.18. [Ru(NHC)] complexes synthetized by Albrecht.

Most NHC ligands that are used in TH catalysis coordinate to the ruthenium center in a monodentate fashion. Chelating bis- or tetra-NHCs in general are of great interest, because they extend the range of possible NHC ligands, and their properties have been tuned. The complex **Ru14** shown in Figure 1.19 displays an excellent activity in the reduction of ketones under TH conditions with 0.1 mol % of catalyst loading.[43]
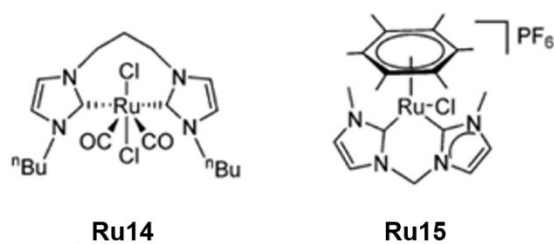
Figure 1.19. Ru catalysts with chelating NHC ligand.[30]

Peris and co-workers reported that the complexes [Ru(η^6-arene)(bis-NHC)] (Figure 1.19, **Ru15**),[44] gave good results in TH of carbon dioxide to formate using 2-PrOH as hydrogen source. The reaction was conducted at 110°C under 50atm of carbon dioxide. These severe reaction conditions require a high stable catalyst; the presence of a bis-NHC ligand enhanced the stability of catalyst resulting in good catalytic performances.

3.2 Dehydrogenation reaction

Reverse process of hydrogenation is called dehydrogenation (Scheme 1.9). Dehydrogenation involves loss of hydrogen from a molecule and converts a saturated substrate to an unsaturated one.
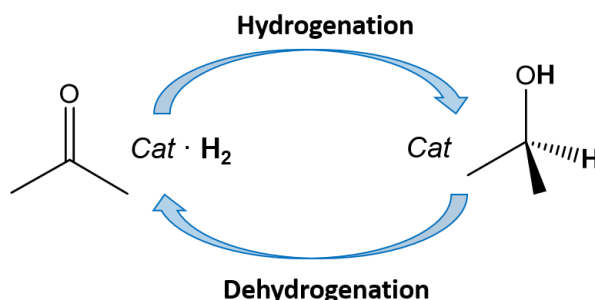
Scheme 1.9. Hydrogenation is the same reaction of dehydrogenation but on the other way around.

Carbonyls such as ketones and aldehydes are synthetically prevalent functional groups because of their outstanding versatility for derivatization. Amongst the various procedures to prepare carbonyl compounds, selective oxidation from alcohol is a mostly valuable approach in that precursors are abundant and readily available.[45]

Hydrogen transfer in the context of alcohol oxidation in organic chemistry has been studied and developed since the 1930s. An early milestone in the chemistry of catalyzed hydrogen transfer from an alcohol is Oppenauer's report of aluminum *tert*-butoxide oxidation of secondary alcohols in the presence of acetone.[46] Though aluminum alkoxides had been previously utilized in the reduction of aldehydes and ketones by Meerwein, Ponndorf, and Verley, Oppenauer was the first to use the method for oxidizing an alcohol to ketone. Generally, the 'catalysts' used in classical Oppenauer oxidations are simple bases added in stoichiometric quantities.

Subsequently, several groups have developed transition-metal catalyzed systems showing Oppenauer-type alcohol oxidation reactivity. Many of the first catalysts discovered for hydrogen transfer from alcohols to carbonyls incorporated iridium, rhodium, or ruthenium. These catalysts tend to require harsh conditions for good conversion. Among the first Oppenauer oxidation catalysts were [RhCl(PPh$_3$)$_3$] (Wilkinson's catalyst) and [IrCl$_3$(dmso)$_3$].[47]

The base often serves as an activator of hydrogen transfer catalysts and as a promoter for hydrogen transfer reactions. Therefore, the majority of alcohol activation reactions require at least catalytic amounts of base. The high use of oxidant in these systems is the main drawback due to the fact that provides significant quantities of (sometimes toxic) side-products and a low atom-economy of the overall reaction. In the recent years, the attention has been focused on more benign oxidants such as H_2O_2 and O_2 as terminal oxidants, leading to substantial progresses, in particular in ruthenium- palladium-, and copper-catalyzed alcohol oxidation.[48] Furthermore, the recent quest for hydrogen as an alternative that does not impact the global carbon cycle has strongly stimulated research into acceptorless alcohol (and amine) dehydrogenation processes. Ruthenium-catalyzed protocols for the dehydrogenation of primary and secondary alcohols have been developed for example by the groups of Beller, Milstein, and Williams.[49]

Homogeneous dehydrogenative catalytic activation of alcohols can be considered as a development of hydrogen transfer catalysis. This reaction leads to transfer of 2H from a sacrificial secondary alcohol to a

ketone facilitated by a transition-metal catalyst. One H is removed from a CH bond, hence is relevance to CH activation, and the other comes from the hydroxyl group. The classic early examples employed secondary alcohols such as isopropanol, in part because they are greater reducing alcohols.[46]

As for hydrogenation, also dehydrogenation mechanism can be divided into two:

- Inner-sphere or "classical" mechanism;
- Outer-sphere or bifunctional mechanism.

In inner-sphere mechanism, catalysts usually need a base for activation and heating for displacement of a labile ligand. The substrate is coordinated to the metal and a labile ligand is displaced in order to have a vacant site at metal center. By this way, a β-hydride elimination occurs and the product can be released from the metal complex. An example of this mechanism is reported in Scheme 1.10. After dehydrogenation, the catalyst is regenerated via H_2 acceptorless release, or by hydrogen transfer to another molecule, which can be a sacrificial acceptor or substrate itself.
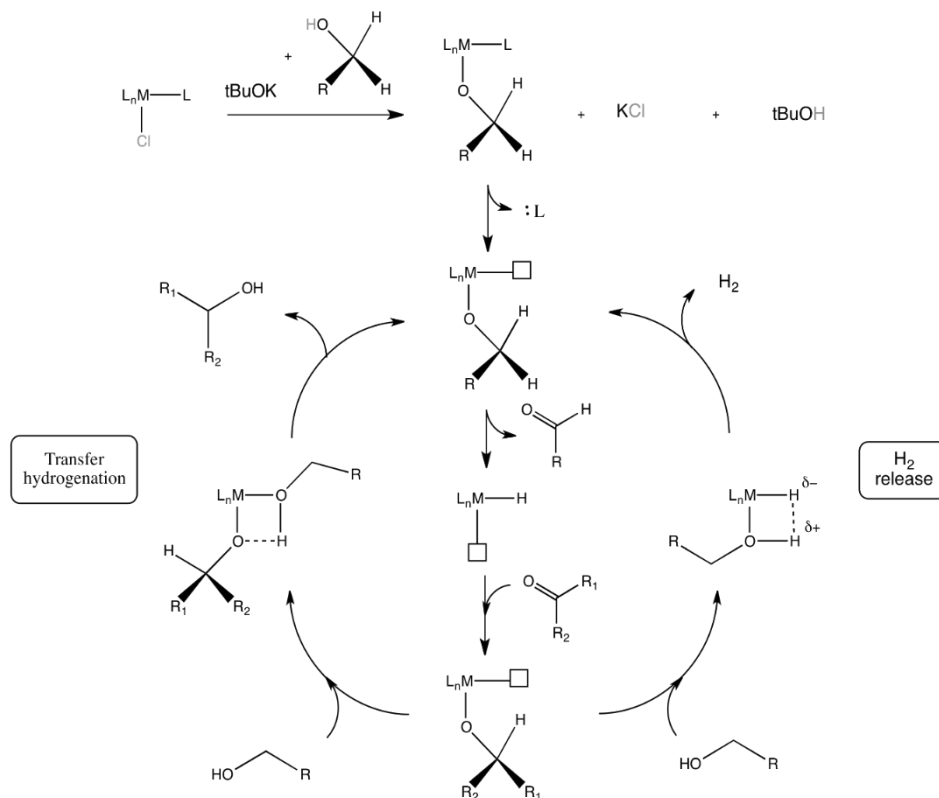
Scheme 1.10. A schematic example of a traditional dehydrogenation mechanism.

Outer-sphere catalysts are characterized by a basic site, usually a nitrogen in one ligand, and acidic site, on metal center. Also in this case dehydrogenation is typically performed using a base to obtain the active catalyst, but it is also possible to work without any base. This reaction is usually described as a concerted transfer, where the transition state with H_2 transfer is shown as one single step. An example is described in Scheme 1.11, where the active catalyst is a 16 electron complex. After dehydrogenation the catalyst becomes an 18 electron complex. Catalyst needs to be recycled in the same way of inner-sphere catalyst, so by H_2 release or by hydrogen transfer to another molecule.
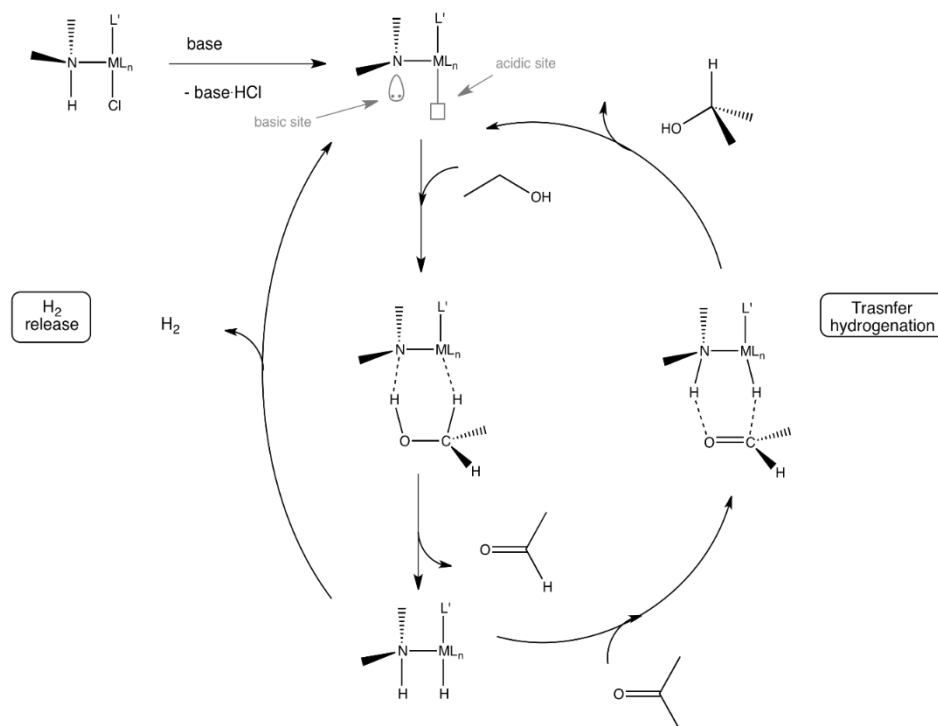
Scheme 1.11. Example of outer-sphere mechanism.

Many catalysts, which are believed to operate via outer-sphere or metal–ligand bifunctional mechanisms, have been utilized in hydrogen transfer, including Noyori and Shvo's diruthenium complexes previously described in the paragraph 2.2.2.

3.2.1 Ru(NHC) complexes as catalysts for dehydrogenation reaction

In the last decade several ruthenium catalysts for the dehydrogenation of primary and secondary alcohols have been developed. Among them the Shvo's catalyst is one of the most representative examples in terms of both efficiency and versatility.

As mentioned above (see paragraph 3.1.2), N-heterocyclic carbene (NHC) ruthenium based catalysts have recently played an important role in the hydrogen transfer catalysis and thus include the catalytic dehydrogenation of alcohol. Notably, simple well-defined (η^6-arene)Ru-(NHC) complexes are among the best catalysts for this transformation, which can be performed using a wide variety of substrates.[50]

The use of NHC-based ligands seems to bring a series of advantages, in that the NHCs combine a number of attractive features (see paragraph 1.1 for more details). First, the azolium ligand precursor is stable toward oxidation. Second, the number of possible coordination modes of the carbene to the metal, paired with the large library of NHC-type ligands, may allow the electronic properties of the metal to be fine-tuned, with obvious implications for catalytic outcomes. Third, the carbene ligand displays a pronounced mesoionic character, thus accommodating positive and negative partial charges in the same heterocycle that allow to coordinate the metal centers in different oxidation states.[51]

Albrecht's group recently reported a series of Ru(II)(η^6-arene) complexes containing 1,2,3-triazolylidene ligands with different aryl and alkyl wingtip groups (Figure 1.20) that are active catalyst precursors for the base- and oxidant-free dehydrogenation of alcohols to the corresponding carbonyl compounds with concomitant release of H_2. The absence of base and oxidant is appealing in terms of atom economy and experimental setup and should allow for wide functional group tolerance.[47]
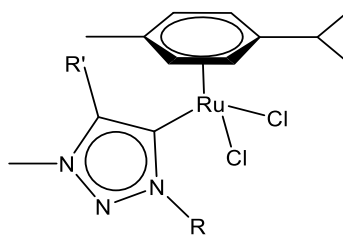
Figure 1.20. Example of a triazolylidene Ruthenium(II) complex synthetized by Albrecht's group.

4. Scope of the thesis

Starting from the above reported state-of-the-art the main scope of this thesis concerned the synthesis, characterization and catalytic application of new ruthenium-based transition metal complexes that combine cyclopentadienones and *N*-heterocyclic carbenes ligands with ruthenium carbonyl fragments.

The main goal was to design a new class of carbonylic ruthenium complexes bearing tetraarylcyclopentadienone ligands and N-heterocyclic carbenes in order to develop a novel bifunctional catalyst with the aim to exploit this new metal-ligand combination for applications in homogeneous catalysis. As already mentioned the tetraarylcyclopentadienones ligands behave as non-innocent ligands in reactions promoted by the well-known ruthenium based Shvo catalyst and the NHC are ancillary ligands due to their strong coordination ability and the possibility to modulate their steric and electronic properties by changing the R substituents.
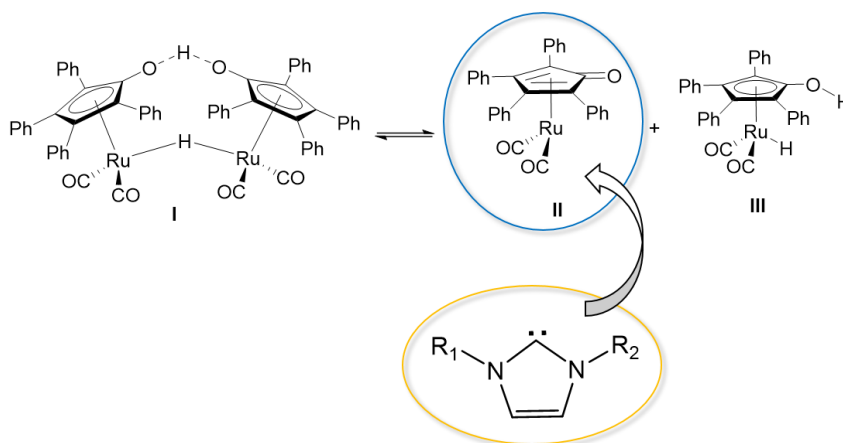
Figure 1.21. A schematic illustration of the two classes of ligands concerned: in *blue* the cyclopentadienone ligand on the Shvo catalyst (**I**); in *yellow* a general representation of a free N-heterocyclic carbene.

On this bases the **first** scope of the thesis has been to synthetized a series of cyclopentadienone Ru carbene complexes by transmetallation reaction thought a dimeric ruthenium precursor and silver carbene complexes intermediates. The same synthetic route has been employed with imidazolylidene and triazolylidene leading to the formation of, respectively, normal and abnormal Ru(0) carbene complexes.

The **second** object has been the evaluation of the catalytic activity of this new kind of mononuclear ruthenium complexes in redox reactions such as transfer hydrogenation of ketones and alcohol oxidation. A particular attention was focused on the activation of this catalyst precursors testing different routes (*e.g.* oxidizing additives, protonation reactions, photolysis) and on the investigation of the catalytic mechanism.

In order to expand the scope of these kind of complexes to a more "green" chemistry with the aim of high atom-efficiency and more environment friendly, the **third** goal of the research has been focused on the

developing and characterization of a new iron-based complex, inspired by the ruthenium one. The iron would be a good choice due to his low toxicity, low price and high availability.

Finally, the **fourth** aim has been addressed around the immobilization of these complexes on a dendritic support in order to allow the separation of the supported complexes from the reaction mixture combining advantages from both homogeneous and heterogeneous catalysis.

References

[1] V. Lyaskovskyy, B. de Bruin, *ACS Catal.* **2012**, *2*, 270.

[2] L. Tschugajeff, M. Skanawy-Grigorjewa, A. Posnjak, *Z Anorg Chem*, **1925**, 148:37–421991.

[3] (a) K.Öfele, *J. Organomet. Chem.*, **1968**, *12*, 42; (b) H. W. Wanzlick, H. J. Shönherr, Angew. *Chem. Int. Ed. Engl.*, **1968**, *7*, 141.

[4] (a) A. J. Arduengo, M. Kline, J. C. Galabrese, F. Davidson, *J. Am. Chem. Soc.*, **1991**, *113*, 9704; (b) A. J. Arduengo, R. L. Harlow, M. Kline, *J. Am. Chem. Soc.*, **1991**, *113*, 361.

[5] L. Cavallo, C. S. J. Cazin (ed.), *N-Heterocyclic Carbenes in Transition Metal Catalysis and Organocatalysis, Catalysis by Metal Complexes*, DOI 10.1007/978-90-481-2866-2_1, © Springer Science+Business Media B.V. **2011**.

[6] (a) H. D. Velazquez, F. Verpoort, *Chem. Soc. Rev.*, **2012**, *41*, 7032; (b) S. Diez-González, N. Marion, S. P. Nolan, *Chem. Rev.*, **2009**, *109*, 3612; (d) W. A. Herrmann, *Angew. Chem. Int. Ed.*, **2002**, *41*, 1290.

[7] M. N. Hopkinson, C. Richter, M. Schedler, F. Glorius, *Nature*, **2014**, *510*, 485.

[8] R. H. Crabtree, *J. Organomet. Chem.*, **2005**, *690*, 5451-5457.

[9] (a) L. Cavallo, A. Correa, C. Costabile, H. Jacobsen, *J Organomet Chem,* **2005**, *690*, 5407; (b)C. M. Crudden, D. P. Allen, *Coord. Chem. Rev.*, **2004**, *248*, 2247–2273.

[10] S.P. Nolan (ed), *N-Heterocyclic Carbenes: Effective Tools for Organometallic Synthesis*, © Wiley-VCH Verlag, **2014**

[11] (a) A. T. Normand, K. J. Cavell, *Eur. J. Inorg. Chem.*, **2009**, 2781–2800; (b) N. Marion, S.P. Nolan, *Chem. Soc. Rev.*, **2008**, *37*, 1776–1782; (c) B. Marciniec, *Advances in Silicon Science*, **2009**, *1*, 3–51.

[12] R. H. Grubbs, S. Chang, *Tetrahedron*, **1998**, *54*, 4413.

[13] S. Díez-González, N. Marion, S.P. Nolan, *Chem. Rev.*, **2009**, *109*, 3612-3676.

[14] J. Witt, A. Pöthig, F. E. Kühn, W. Baratta, *Organometallics*, **2013**, *32*, 4042.

[15] S. Enthaler, R. Jackstell, B. Hagemann, K. Junge, G. Erre, M. Beller, *J. Organomet. Chem.*, **2006**, *691*, 4652–4659.

[16] B. Kang, Z. Fu, S. H. Hong, *J. Am. Chem. Soc.*, **2013**, *135*, 11704.

[17] V.L. Chantler, S.L. Chatwin, R.F.R. Jazzar, M.F. Mahon, O. Saker, M.K. Whittlesey, *Dalton Trans.,* **2008**, 2603–2614.

[18] S. Horn, C. Gandolfi, M. Albrecht, *Eur. J. Inorg. Chem.,* **2011**, 2863–2868.

[19] L. Bernet, R. Larlempuia, W. Ghattas, H. Mueller-Bunz, L. Vigara, A. Llobet, M. Albrecht, *Chem. Commun.*, **2011**, *47*, 8058.

[20] W. Liu, R. Gust, *Chem. Soc. Rev.*, **2013**, *42*, 755.

[21] R.H. Crabtree, J. *Organomet. Chem.,* **2005**, *690*, 5451–5457.

[22] A. Quintard, J. Rodriguez, *Angew. Chem., Int. Ed.,***2014**, *53*, 4044.

[23] P. Casey, J. B. Johnson, S. W. Singer, Q. Cui, *J. Am. Chem. Soc.,* **2005**, *127*, 3100 – 3109.

[24] O. Eisenstein, R. H. Crabtree, *New J. Chem.*, **2013**, *37*, 21—27.

[25] S. E. Clapham, A. Hadzovic, R.H. Morris, *Coord. Chem. Rev.,* **2004**, 2201-2237.

[26] Y. Shvo, D. Czarkie, Y. Rahamim, *J. Am. Chem. Soc.,* **1986**, *108*, 7400.

[27] B. L. Conley, M. K. Pennington-Boggio, E. Boz, T. J. Williams, *Chem. Rev.,* **2010**, *110*, 2294-2312.

[28] (a) R. M. Bullock, *Chem. Eur. J.,* **2004**, *10*, 2366; (b) S. E. Clapham, A. Hadzovic, R.H. Morris, *Coord. Chem. Rev.*, **2004**, *248*, 2201.

[29] (a) G. Csjernvik, A.H. Eu, L. Ladini, B. Pugin, J. E. Backvall, *J. Org. Chem.*, **2002**, *67,* 1657; (b) C. P. Casey, S. W. Singer, D. R. Powell, R. K. Hayashi, M. Kavana, *J. Am. Chem. Soc.*, **2001**,*123*, 1090.

[30] (a) D. J. Ager, A. H. M. de Vries, J. G. de Vries, *Chem. Soc. Rev.* **2012**, *41*, 3340; (b) H. Shimizu, I. Nagasaki, K. Matsumara, N. Sayo, T. Saito, *Acc. Chem. Res.* **2007**, *40*, 1385; (c) N. B. Johnson, I. C. Lennon, P. H. Moran, J. A. Ramsden, *Acc. Chem. Res.* **2007**, *40*, 1291.

[31] D. Wang, D. Astruc, *Chem. Rev.*, **2015**, *115*, 6621–6686.

[32] (a) A. Verley, *Bull. Soc. Chim. Fr.*, **1925**, *37*, 537–542; (b) H. Meerwein, R. Schmidt, Liebigs *Ann. Chem.*, **1925**, *444*, 221–238.

[33] (a) Y. M. Haddad, H. B. Henbest, J. Husbands, T. R. Mitchell, *Proc. Chem. Soc. London*, **1964**, 361-365; (b) J. Trochagr, H. B. Henbest, *Chem. Commun.*, **1967**, 544–544; (c) M. McPartli, R. Mason, *Chem. Commun.*, **1967**, 545–546.

[34] (a) Y. Sasson, J. Blum, *Tetrahedron Lett.*, **1971**, *12*, 2167–2170; (b) J. Blum, Y. Sasson, S. Iflah, *Tetrahedron Lett.,* **1972**, *13*, 1015–1018; (c) Y. Sasson, J. Blum, *J. Org. Chem.*, **1975**, *40*, 1887–1896.

[35] R. L. Chowdhury, J. Backvall, *Chem. Commun.*, **1991**, 1063–106.

[36] R. Noyori, *Angew. Chem., Int. Ed.*, **2002**, *41*, 2008–2022.

[37] A. C. Hillier, H. M. Lee, E. D. Stevens, S. P. Nolan, *Organometallics*, **2001**, *20*, 4246–4252.

[38] M. Albrecht, J. R. Miecznikowski, A. Samuel, J. W. Faller, R. H. Crabtree, *Organometallics*, **2002**, *21*, 3596–3604.

[39] A. P. da Costa, M. Viciano, M. Sanaú, S. Merino, J. Tejeda, E. Peris, B. Royo, *Organometallics,* **2008**, *27*, 1305–1309.

[40] (a) A. A. Danopoulos, S. Winston, W. B. Motherwell, *Chem. Commun.,* **2002**,1376–1377. (b) M. Poyatos, J. A. Mata, E. Falomir, R. H. Crabtree, E. Peris, *Organometallics,* **2003**, *22*, 1110–1114.

[41] (a) X.-W. Li, G.-F. Wang, F. Chen, Y.-Z. Li, X.-T. Chen, Z.-L. Xue, *Inorg. Chim. Acta,* **2011**, *378*, 280–287 (b) F. E. Fernandez, M. C. Puerta, P. Valerga, *Organometallics,* **2011**, *30*, 5793–5802 (c) F. E. Fernandez, M. C. Puerta, P. Valerga, *Organometallics,* **2012**, *31*, 6868–6879.

[42] (a) S. Horn, M. Albrecht, *Chem. Commun.,* **2011**, *47*, 8802–8804 (b) S. Horn, C. Gandolfi, M. Albrecht, *Eur. J. Inorg. Chem.,* **2011**, 2863–2868.

[43] Y. Cheng, X.-Y. Lu, H.-J. Xu, Y.-Z Li, X.-T Chen, Z.- L Xue, *Inorg. Chim. Acta,* **2010**, *363,* 430−437.

[44] S. Sanz, A. Azua, E. Peris, *Dalton Trans.,* **2010**, *39*, 6339–6343.

[45] (a) *Modern Oxidation Methods,* ed. J.-E. Bäckvall, Wiley-VCH, Weinheim, Germany, **2008**; (b) I. E. Marko, P. R. Giles, M. Tsukazaki, A. Gautier, R. Dumeunier, K. Doda, F. Philippart, I. Chelle-Gegnault, J.-L. Mutonkole, S. M. Brown and C. J. Urch, in *Transition Metals for Organic Synthesis*, ed. M. Beller and C. Bolm, Wiley-VCH, Weinheim, Germany, **2008**, 437–478; (c) R. Noyori and S. Hashigushi*, Acc. Chem. Res.*, **1997**, *30*, 97–102.

[46] R. V. Oppenauer, *Recl. Tra V. Chim. Pay-Bas*. **1937**, *56*, 137.

[47] E. D. Graham, R. H. Crabtree, *Chem. Rev.*, **2010**, *110*, 2.

[48] D. Canseco-Gonzalez, M. Albrecht, *Dalton Trans.*, **2013**, *42*, 7424.

[49] (a) J. Zhang, M. Gandelman, L. J. W. Shimon, H. Rozenberg and D. Milstein, *Organometallics*, **2004**, *23*, 4026–4033; (b) H. Junge and M. Beller, *Tetrahedron Lett.*, **2005**, *46*, 1031–1034; (c) G. R. A. Adair and J. M. J. Williams, *Tetrahedron Lett.*, **2005**, *46*, 8233–8235; (d) J. van Buijtenen, J. Meuldijk, J. A. J. M. Vekemans, L. A. Hulshof, H. Kooijman and A. L. Spek, *Organometallics*, **2006**, *25*, 873–881.

[50] Y. Zhang, C. Chen, S.C. Ghosh, Y. X. Li, S. H. Hong, *Organometallics,* **2010**, *29*, 1374.

[51] A. Prades, E. Peris, M. Albrecht, *Organometallics,* **2011**, *30*, 1162–1167.

<div align="center">

CHAPTER II

Sterically driven synthesis of ruthenium and ruthenium-silver N-heterocyclic carbene complexes

</div>

Abstract

A straightforward and efficient synthetic route to novel Ru *N*-heterocyclic carbenes (NHC) complexes by transmetallation of non-bulky silver NHC to ruthenium dicarbonyl tetraarylcyclopentadienone is described. The same procedure with sterically demanding NHC leads to unprecedent heterobimetallic Ru-Ag(NHC) complexes.

Introduction

As reported in the introduction, ruthenium based *N*-heterocyclic carbene complexes are among the most versatile homogeneous catalysts. In addition to the well-known second generation Grubb's metathesis catalysts,[1] Ru(NHC) catalysts have found application in a broad variety of reactions,[2] including: transfer hydrogenation,[3] hydrogenation of olefins[4] and esters,[5] asymmetric hydrogenation,[6] amide synthesis from alcohols and nitriles,[7] dehydrogenation of esters and imines from alcohols,[8] racemization of chiral alcohols,[9] alcohol[10] and water oxidation.[11] Moreover, Ru(NHC) are also employed in medical and material science as potential antitumoral drugs,[12] and in the development of sensitizers.[13] From a more general perspective *N*-heterocyclic carbenes (NHCs) are widely documented as ubiquitous ancillary ligands due to their strong coordination ability and the tuneable character of their steric and electronic properties.[14]

Another class of versatile ligands is represented by tetraarylcyclopentadienones, which behave as non-innocent ligands in reactions promoted by the well-known ruthenium based Shvo catalyst.[15]

Since our research interests recently focused on both *N*-heterocyclic carbenes[16] and cyclopentadienone ligands,[17] we wondered about the possibility to exploit both ligands in the preparation of novel Ru(0) complexes. Indeed, most of the literature on Ru(NHC) complexes, is based on Ru(II), whereas the chemistry of Ru(0)(NHC) is essentially limited to the combination of NHCs (or their precursors) with $Ru_3(CO)_{12}$ and $Ru(CO)_2(PPh_3)_3$.[18]

In this chapter we report the sterically driven synthesis of ruthenium(0) and ruthenium-silver dicarbonyl tetraarylcyclopentadienone *N*-heterocyclic carbene complexes.

Results and discussion

2.1 Synthesis of imidazolium salts

As a first step, we prepared a small library of variously encumbered imidazolium salts, NHC precursors, by following procedures reported in the literature (Figure 2.1). As described in the introduction (paragraph 1.1.2) the two main synthetic routes leading to the formation of NHC precursors are by bis-alkylation or cyclization reactions. All the imidazolium salts **1a-l** depicted in Figure 2.1 have been prepared following these two methodologies.
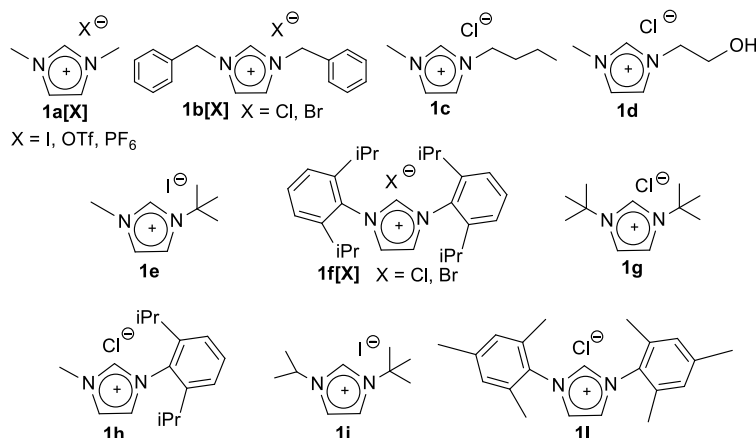
Figure 2.1. Imidazolium salts precursors of NHC ligands.

2.2 Synthesis of tetraarylcyclopentadienone Ru(0)-NHC complexes

At a later stage, imidazolium salts **1a-e** have been reacted with Ag_2O, and the corresponding silver complexes (**2**, Experimental section) directly treated *in situ* with the dimeric precursor dicarbonyl(η^4-3,4-bis(4-methoxyphenyl)-2,5-diphenylcyclopenta-2,4-dienone) (**3**). A quantitative and instant transmetallation reaction leads to the formation of the neutral Ru(0) complexes **4a-e** (Scheme 2.1). The reaction is general with non-bulky *N*-heterocyclic carbenes and tolerant to functional groups, in fact it occurs in the presence of a primary alcohol in the lateral chain (**1d** to **4d**) without the need of protection.
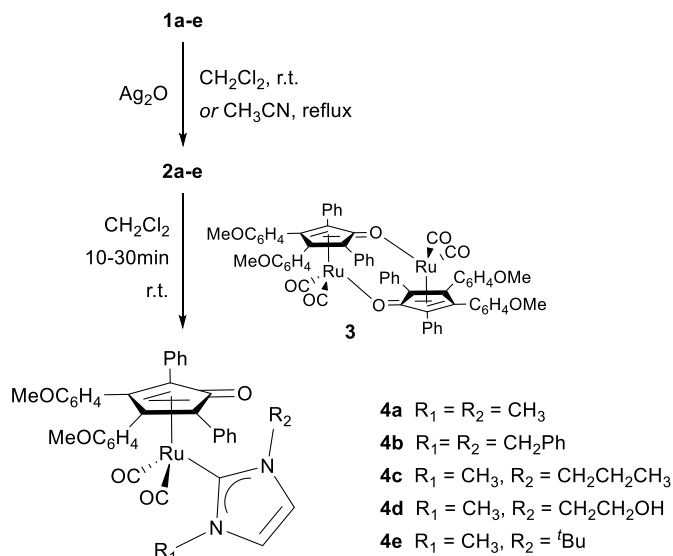
Scheme 2.1. Synthesis of dicarbonyl-cyclopentadienone-*N*-heterocyclic carbene ruthenium complexes (**4a-e**).

The synthesis of **4a-e** has been followed by IR spectroscopy observing in all the cases a lowering in the CO stretching frequencies (*e.g.* **4a**: v(CO) = 2004, 1945 cm^{-1} *vs.* **3**: 2018, 1967 cm^{-1}) due to the strong σ donor properties of N-heterocyclic carbenes. IR spectra are very similar for complexes **4a-c**, whereas, in the case of the hydroxyl-functionalized complex **4d**, increased frequency for terminal CO and lowering of cyclopentadienone v C=O are observed [v(CO) = 2011, 1952 cm^{-1}; v(C=O) = 1558 cm^{-1} *vs.* 1586 cm^{-1} for **4a**] which is ascribable to the formation of hydrogen bond between –OH and the carbonyl group, as demonstrated by X-Ray diffraction. ^{13}C-NMRs show a diagnostic signal for the Ru-C$_{carbene}$ within the range 172-173 ppm (Figure 2.2) and molecular ions of complexes **4a-e** are detectable by ESI-MS (see Experimental section).
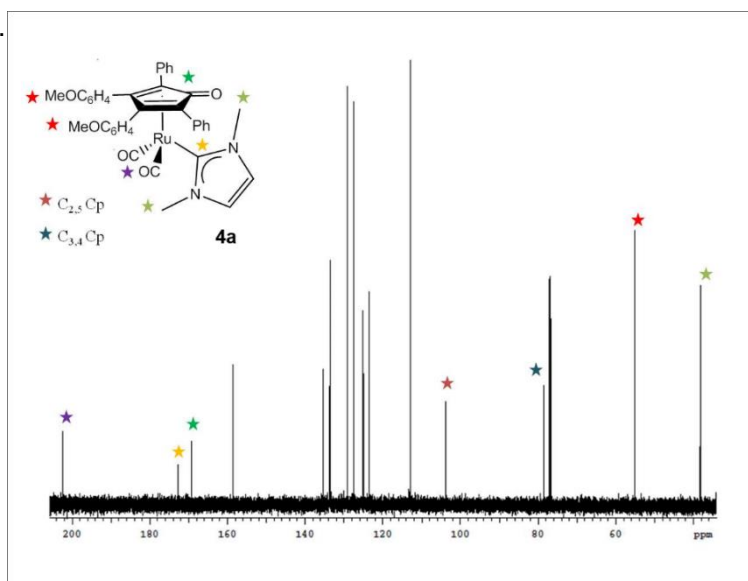
Figure 2.2. ^{13}C-NMR spectrum of **4a** in CDCl$_3$.

Complexes **4a**, **4b** and **4d** have been also characterized by X-Ray diffraction studies. The molecular structure of **4a** is reported in Figure 2.3, whereas those of **4b** and **4d** as well a list of their main bonding parameters are given in the Experimental section (Figs. 2.15 and 2.16, Table 2.1). The three complexes display almost identical structures, apart from the different substituents on the *N*-heterocyclic carbene ligand. The Ru(1)-C(3) distance [2.470(4) Å in **4a**] is significantly longer than Ru(1)-C(4-7) [2.206(4)-2.270(3) Å, average 2.237(7) Å in **4a**] and C(3)-O(3) [1.245(4) Å] is essentially a double bond.[19] The Ru(1)-C(34) contact [2.117(3) Å] is in the typical range for the interaction between Ru(0) and a *N*-heterocyclic carbene.[18a]
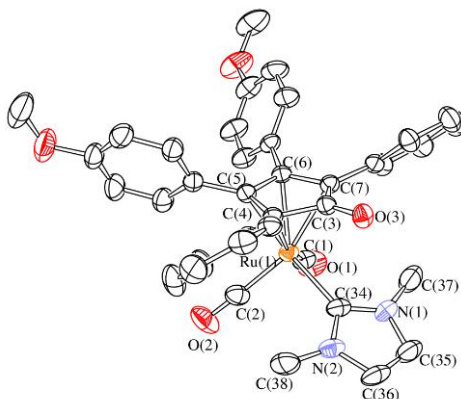
Figure 2.3. ORTEP drawing of **4a**. Displacement ellipsoids are at the 30% probability level. H-atoms have been omitted for clarity. Selected bond lengths (Å): Ru(1)-C(1) 1.893(5), Ru(1)-C(2) 1.874(5), Ru(1)-C(3) 2.470(4), Ru(1)-C(4) 2.263(4), Ru(1)-C(5) 2.206(4), Ru(1)-C(6) 2.208(3), Ru(1)-C(7) 2.270(3), Ru(1)-C(34) 2.117(4), C(3)-O(3) 1.245(4).

2.3 Synthesis of dimetallic Ru-Ag-NHC complexes

The use of the more sterically hindered imidazolium salts **1f-l** led to the unexpected hitherto unreported heterodimetallic ruthenium-silver complexes of type **5** (Scheme 2.2). As reviewed by Kuhl,[20] implications of the wingtip groups in *N*-heterocyclic carbene complexes are normally ascribable to steric factors, and this is also our case, in that encumbrance arise by both the tetraarylcyclopentadienone and the *N*-heterocyclic carbene moiety. On the other hand, a possible role of the donor properties of NHCs, in addition to their steric effects should not be excluded. Indeed, NHCs with bulky substituents generally display better donor properties, as evaluated by TEP values (Tolman Electronic Parameters).[21] For example, **1g** containing t-butyl groups is a better donor compared to **1a**, containing methyls.[21a] A combination of these steric and electronic effects might increase both stability and inertness of the silver complexes intermediates (in case of **2f-l**) and consequently disfavor carbene transmetallation compared with halide coordination. If this hypothesis is realistic the observed formation of bimetallic products, in the case of bulky NHCs, should be the consequence of both steric congestion at the ruthenium products and lower tendency to transmetallation of the silver intermediates.

This remarkable reactivity is likely to be favoured by the formation of a Ru-Cl-Ag bridge and by the concomitant interaction between the silver metal and the carbonyl of the cyclopentadienone.
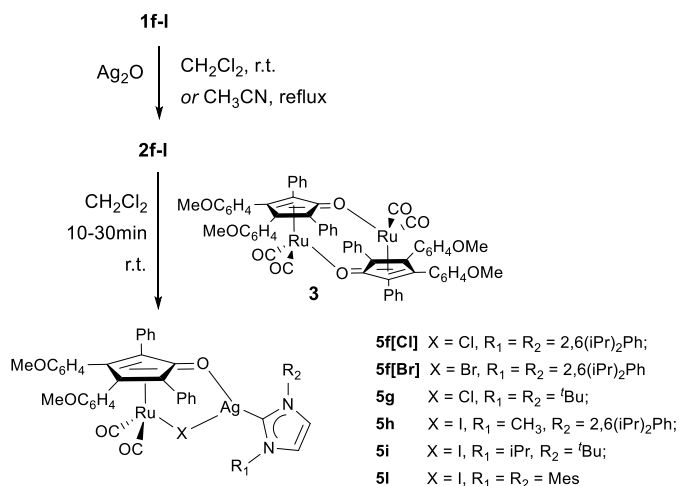
Scheme 2.2 Synthesis of heterodimetallic Ru-Ag(NHC) complexes (**5f-l**).

The dinuclear complexes **5f-l** have been characterized by IR, ^{1}H and ^{13}C-NMR and ESI-MS (see Experimental section). Suitable crystals for X-Ray diffraction have been obtained for **5f[Cl]**. FT-IR CO stretching frequencies are in the range 2013-2014 cm^{-1} and 1953-1955 cm^{-1} (Figure 2.4), while at the ^{13}C-NMR spectra the Ag-C$_{carbene}$ resonates as a doublet of doublet (*e.g.* **5f[Cl]**: 188.6 ppm; dd, J ([109]Ag-^{13}C) = 271 Hz; J ([108]Ag-^{13}C) = 235 Hz).
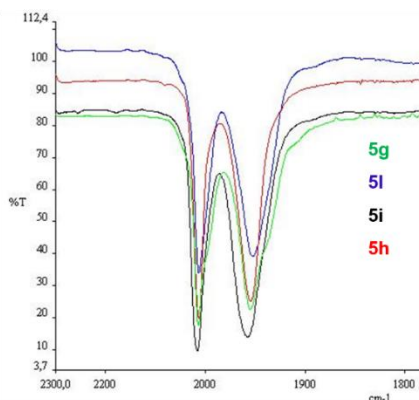
Figure 2.4. IR spectra of **5g**, **5h**, **5i**, **5l**: range of terminal CO stretching frequencies.

The structure of **5f[Cl]** has been crystallographically determined (Figure 2.5 and Table 2.2). This is composed by a RuCl(CO)$_2$(tetraarylcyclopentadienone) moiety chelating on the Ag(*N*-heterocyclic carbene) *via* O(3) and Cl(1). The C(3)-O(3) distance [1.246(7) Å] is almost identical to the one found in **4a** [1.245(4) Å] retaining its double bond character and suggesting a dative bond between O(3) and Ag(1).
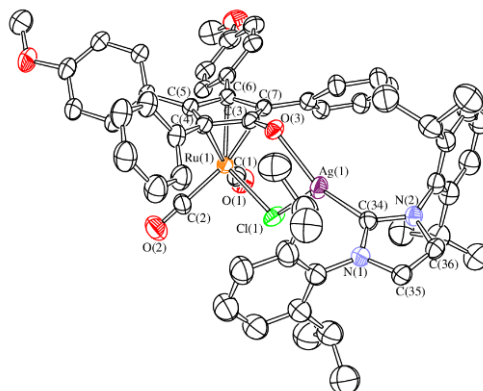
Figure 2.5. ORTEP drawing of **5f[Cl]**. Displacement ellipsoids are at the 30% probability level. H-atoms have been omitted for clarity. Selected bond lengths (Å): Ru(1)-C(1) 1.873(8), Ru(1)-C(2) 1.865(8), Ru(1)-C(3) 2.424(6), Ru(1)-C(4) 2.248(6), Ru(1)-C(5) 2.194(6), Ru(1)-C(6) 2.190(6), Ru(1)-C(7) 2.245(6), Ru(1)-Cl(1) 2.4370(17), C(3)-O(3) 1.246(7), Ag(1)-O(3) 2.223(4), Ag(1)-Cl(1) 2.6282(18), Ag(1)-C(34) 2.086(6).

2.4 Synthesis of dimetallic Ru-Cu(NHC) complex

Once investigated the substrate scope, we have extended our studies to copper. The reaction between 1,3-di-(2,6-diisopropylphenyl)imidazole-2-ylidene copper chloride and **3** confirmed the same reactivity as demonstrated by X-Ray crystal structure of the Ru-Cl-Cu-O complex **6** (Figure 2.17 and Table 2.2).
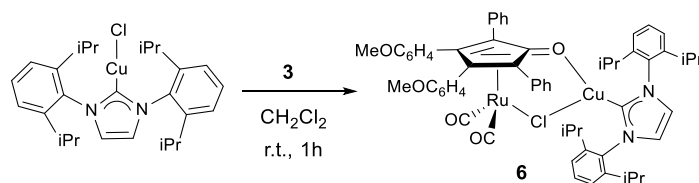
Scheme 2.3. Synthesis of heterodimetallic Ru-Cu(NHC) complex (**6**).

The heterodimetallic complexes **5** and **6** are stable in the solid state, while in solution they decompose in more than 24h.

2.5 Synthesis of bis-trimethylsilyl-cyclopentadienone Ru(NHC) complexes

In order to further extend the ligand scope, with the principal aim to change the solubility of the complex in polar solvents such as water the ruthenium triscarbonyl bis(TMS)-substituted cyclopentadienone complex **7**, has been prepared with a novel method that exploit microwave irradiation (see Experimental section); our way of synthesis is indeed by far faster than that reported in the literature.[22] By treating **7** with Me$_3$NO in CH$_3$CN, intermediate **8** has been obtained and employed as a precursor for the synthesis of NHC complexes **9** by transmetallation with silver carbene complexes prepared *in situ* (Scheme 2.4).
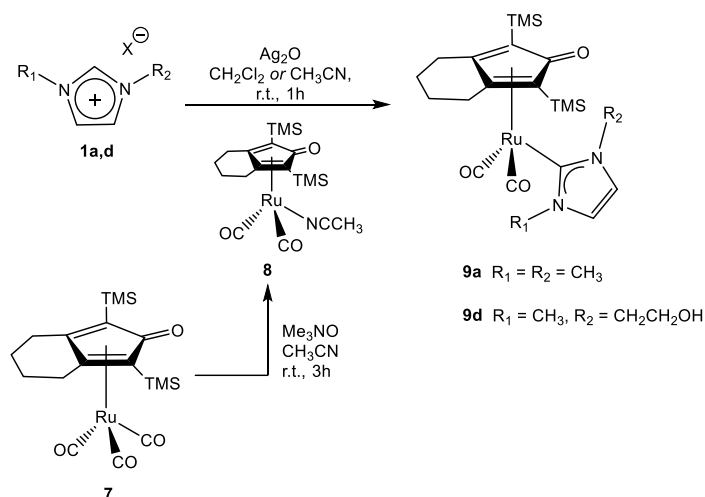
Scheme 2.4. Synthesis of dicarbonyl-bis(TMS)-substituted cyclopentadienone Ru(NHC) complexes (**9a,d**).

Complexes **9a,d** have been completely characterized by IR, ^{1}H and ^{13}C-NMR and ESI-MS (see Experimental section). It is important to underline that complex **9d** can be protonated leading to a complex partially soluble in water. The latter complex for the sake of clarity will be discussed in Chapter V.

Conclusions

In summary, a very efficient and rapid synthetic route for obtaining novel Ru(0) complexes, which combine *N*-heterocyclic carbenes and tetraarylcyclopentadienone ligands, has been found. The reaction scope is general and transmetallation proved to be tolerant to primary alcohol. A role of the steric hindrance of the ligands has been observed leading to the remarkable formation of heterobimetallic complexes containing both Ru and Ag or Cu. The novel synthetic methods for the preparation of complexes of type **4**, **5** and **6** pave the way for future developments in both homogeneous catalysis and medical applications. Finally, preliminary results showed that the solubility of the ruthenium complexes in polar solvents such as water can be increased by employing a bis-(TMS)-substituted cyclopentadienone ligand instead of the very lipophilic tetraarylcyclopentadienone.

Experimental Section

Materials and procedures. Solvents: dichloromethane (CH_2Cl_2), tetrahydrofuran (THF), diethyl ether (Et2O), petroleum ether referring to a fraction of bp 60-80 °C, acetonitrile (CH_3CN) were dried and distilled prior to use. Acetone has been degassed and stored under inert atmosphere on molecular sieves. Other solvents such as ethylacetate (EtOAc), chloroform, ethanol (EtOH), methanol (MeOH), heptane, toluene, $CDCl_3$, D_2O, CD_3CN (Sigma Aldrich) have been employed without further purification. Reagents: triruthenium-dodecacarbonil ($Ru_3(CO)1_2$) (Strem), methyl iodide, methyl bromide, bromidric and chloridric acid, silver oxide, 1-methylimidazole, 1,3 diphenylacetone, benzyl bromide, benzyl chloride, paraformaldehyde, tert-butylamine, 2,6-dimethylaniline, 2,6-diisopropylaniline, glyoxal, acetic acid, 2,4,6-trimethylaniline (Sigma Aldrich), 4,4'dimethoxybenzil (Alfa Aesar), 1,7-octadiyne have been employed as purchased.

1,3-dimethylimidazolium iodide (**1a[I]**),[23] 1,3-dimethylimidazolium trifluoromethanesulfonate (**1a[OTf]**), 1,3-dimethylimidazolium hexafluorophosphate (**1a[PF₆]**), 1,3-dibenzylimidazolium bromide (**1b[Br]**), 1,3-dibenzylimidazolium chloride (**1b[Cl]**),[24] 1-methyl-3-butyl-imidazolium chloride (**1c**), 1-methyl-3-(2-hydroxyethyl)imidazolium chloride (**1d**),[25] 1-methyl-3-tert-butylimidazolium iodide (**1e**), N,N′-bis(2,6-diisopropylphenyl)-1,4-diaza-1,3-butadiene, 1,3-bis(2,6-diisopropylphenyl)imidazolium chloride (**1f[Cl]**), 1,3-bis(2,6-diisopropylphenyl)imidazolium bromide (**1f[Br]**),[26] 1,3-di-tert-butylimidazolium chloride (**1g**),[27] 1-methyl-3-(2,6-diisopropylphenyl)imidazolium iodide (**1h**),[28] 1-isopropyl-3-tert-butylimidazolium iodide (**1i**),[23] 2 1,4-bis(2,4,6-trimethylphenyl)-1,4-diaza-1,3-butadiene, 1,3-bis(2,4,6-trimethylphenyl)imidazolium chloride (**1l**), 1,3-dimethylimidazol-2-ylidene silver iodide (**2a[I]**),[29] 1,3-dimethylimidazol-2-ylidene silver trifluoromethanesulfonate (**2a[OTf]**), 1,3-dimethylimidazol-2-ylidene silver hexafluorophosphate (**2a[PF₆]**), 1,3-dibenzylimidazol-2-ylidene silver chloride (**2b[Cl]**),[30] 1,3-dibenzylimidazol-2-ylidene silver bromide (**2b[Br]**),[31] 1-methyl-3-butylimidazol-2-ylidene silver chloride (**2c**), 1-methyl-3-(2-hydroxyethyl)imidazol-2-ylidene silver chloride (**2d**),[32] 1-methyl-3-tert-butylimidazol-2-ylidene silver iodide (**2e**), 1,3-bis(2,6-diisopropylphenyl)imidazol-2-ylidene silver chloride (**2f[Cl]**),[33] 1,3-bis(2,6-diisopropylphenyl)imidazol-2-ylidene silver bromide (**2f[Br]**),[34] 1,3-di-tert-butylimidazol-2-ylidene silver chloride (**2g**), 1-methyl-3-(2,6-diisopropylphenyl)imidazol-2-ylidene silver chloride (**2h**), 1-isopropyl-3-tert-butylimidazol-2-ylidene silver iodide (**2i**), 1,3-bis(2,4,6-trimethylphenyl)imidazole-2-ylidene silver chloride (**2l**), 1,3-di-(2,6-diisopropylphenyl)imidazol-2-ylidene copper chloride,[35] 3,4-Bis(4-methoxyphenyl)-2,5-diphenylcyclopenta-2,4-dienone,[36] have been prepared following procedures reported in the literature.

The prepared derivatives were characterized by spectroscopic methods. The NMR spectra were recorded using Varian Inova 300 (^{1}H, 300.1; ^{13}C, 75.5 MHz), Varian Mercury Plus VX 400 (^{1}H, 399.9; ^{13}C, 100.6 MHz), Varian Inova 600 (^{1}H, 599.7; ^{13}C, 150.8 MHz) spectrometers at 298 K; chemical shifts were referenced internally to residual solvent peaks. Full ^{1}H- and ^{13}C-NMR assignments were done, when necessary, by gHSQC and gHMBC NMR experiments using standard Varian pulse sequences. Infrared spectra were recorded at 298 K on a Perkin-Elmer Spectrum 2000 FT-IR spectrophotometer. ESI-MS spectra were recorded on Waters Micromass ZQ 4000 with samples dissolved in MeOH or CH_3CN. Elemental analyses were performed on a Thermo-Quest Flash 1112 Series EA instrument.

Synthesis of Ag-NHC complexes (2)

Imidazolium salts (**1**), were reacted with Ag$_2$O (1.2 eq.) in the appropriate solvent under inert atmosphere and with protection from light. After stirring the reaction for the time and at the temperature required in order to reach complete conversion to silver complexes (**2**), the solvent was then removed under vacuum and the silver complexes characterized by NMR spectroscopy observing the disappearance of the NC(H)N signal of imidazolium salts **1a-l** (around 8-9 ppm: ^{1}H-NMR)[1-6] and the concomitant arising of the NMR signals of the silver complexes **2a-l** which are consistent with literature data.[7-12]

2a[X]: X = I, OTf, PF$_6$; R$_1$ = R$_2$ = CH$_3$;
2b[X]: X = Cl, Br; R$_1$ = R$_2$ = CH$_2$Ph;
2c: X = Cl, R$_1$ = CH$_3$, R$_2$ = CH$_2$CH$_2$CH$_3$;
2d: X = Cl, R$_1$ = CH$_3$, R$_2$ = CH$_2$CH$_2$OH;
2e: X = I, X = Cl, R$_1$ = CH$_3$, R$_2$ = ^{t}Bu;

2f[X]: X = Cl, Br; R$_1$ = R$_2$ = 2,6(iPr)$_2$Ph;
2g: X = Cl, R$_1$ = R$_2$ = ^{t}Bu;
2h: X = I, R$_1$ = CH$_3$, R$_2$ = 2,6(iPr)$_2$Ph;
2i: X = I, R$_1$ = iPr, R$_2$ = ^{t}Bu;
2e: X = I, R$_1$ = R$_2$ = Mes
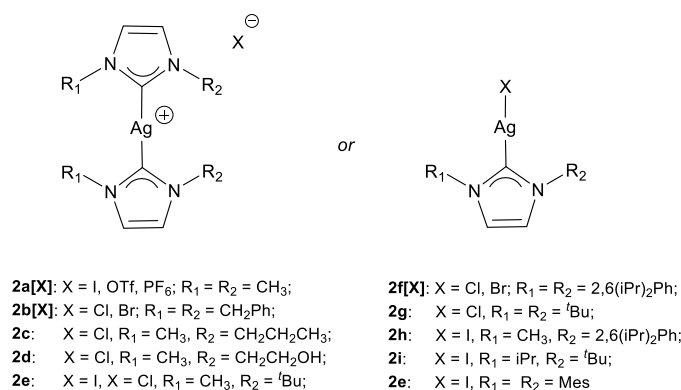
Figure 2.6. Mono and bis-carbene silver complexes (**2**)

1,3-dimethylimidazol-2-ylidene silver iodide (2a[I]): 1,3-dimethylimidazolium iodide 0.149 g (0.665 mmol), Ag$_2$O 0.185 g (0.798 mmol), room temperature, CH$_2$Cl$_2$, 3h. ^{1}H-NMR (399.9 MHz, CDCl$_3$): δ 6.97 (s, 2H, CH$_{NHC}$), 3.84 (s, 6H, NCH$_3$).

1,3-dimethylimidazol-2-ylidene silver trifluoromethanesulfonate (2a[OTf]): 1,3-dimethylimidazolium trifluoromethanesulfonate 0.075 g (0.35 mmol), Ag$_2$O 0.093 g (0.40 mmol) room temperature, CH$_2$Cl$_2$, 3h. ^{1}H-NMR (399.9 MHz, CDCl$_3$): δ 6.96 (s, 2H, CH$_{NHC}$), 3.90 (s, 6H, NC*H$_3$*). ^{19}F-NMR (282.4 MHz, CDCl$_3$): δ -78.38 (s, 3F).

1,3-dimethylimidazol-2-ylidene silver hexafluorophosphate (2a[PF$_6$]): 1,3-dimethylimidazolium hexafluorophosphate 0.075 g (0.35 mmol), Ag$_2$O 0.093 g (0.40 mmol), 40 °C, CH$_2$Cl$_2$, 16h. ^{1}H-NMR (399.9 MHz, CDCl$_3$): δ 7.00 (s, 2H, CH$_{NHC}$), 3.84 (s, 6H, NCH$_3$). ^{19}F-NMR (282.4 MHz, CDCl$_3$): δ -72.91 (d, 6F, J_{P-F} = 757 Hz).

1,3-dibenzylimidazol-2-ylidene silver chloride (2b[Cl]): 1,3-dibenzylimidazolium chloride 0.024 g (0.083 mmol), Ag$_2$O 0.023 g (0.099 mmol), 80 °C reflux, CH$_3$CN, 3h. ^{1}H-NMR (399.9 MHz, CDCl$_3$): δ 7.34-7.24 (m, 10H, CH$_{Ph}$), 7.05 (s, 2H, CH$_{NHC}$), 5.23 (s, 4H, CH$_2$). Suitable crystals of **2b[Cl]** has been obtained by CH$_2$Cl$_2$/petroleum ether double layer.

1,3-dibenzylimidazol-2-ylidene silver bromide (2b[Br]): 1,3-dibenzylimidazolium bromide 0.027 g (0.083 mmol), Ag$_2$O 0.023 g (0.099 mmol), 80 °C reflux, CH$_3$CN, 3h. ^{1}H-NMR (399.9 MHz, CDCl$_3$): δ 7.29-7.18 (m, 10H, CH$_{Ph}$), 6.99 (s, 2H, CH$_{NHC}$), 5.21 (s, 4H, CH$_2$).

1-methyl-3-butylimidazol-2-ylidene silver chloride (2c): 1-methyl-3-butyl-imidazolium bromide 0.018 g (0.083 mmol), Ag$_2$O 0.023 g (0.099 mmol), 80 °C reflux, CH$_3$CN, 3h. ^{1}H-NMR (399.9 MHz, CDCl$_3$): δ 6.96 (m, 1H, CH$_{NHC}$), 6.93 (m, 1H, CH$_{NHC}$), 4.46 (t, 2H, J = 7.5 Hz, NCH$_2$), 4.06 (s, 3H, NCH$_3$), 1.92 (m, 2H, CH$_2$), 1.37 (m, 2H, CH$_2$), 1.07 (t, 3H, J = 7.2 Hz, CH$_3$).

1-methyl-3-(2-hydroxyethyl)imidazol-2-ylidene silver chloride (2d): 1-methyl-3-(2-hydroxyethyl)imidazolium chloride 0.014 g (0.083 mmol), Ag$_2$O 0.023 g (0.099 mmol), room temperature,

CH$_3$CN, 3h. ^{1}H-NMR (399.9 MHz, CDCl$_3$): δ 7.17 (s, 1H, CH$_{NHC}$), 6.99 (s, 1H, CH$_{NHC}$), 4.24 (t, *J* = 5,2 Hz, 2H, CH$_2$), 3.86 (t, *J* = 5,2 Hz, 2H, CH$_2$), 3.68 (s, 3H, CH$_3$).

1-methyl-3-*tert*-butylimidazol-2-ylidene silver iodide (2e): 1-methyl-3-*tert*-butylimidazolium iodide 0.026 g (0.098 mmol), Ag$_2$O 0.027 g (0.117 mmol), room temperature, CH$_2$Cl$_2$, 4h. ^{1}H-NMR (399.9 MHz, CDCl$_3$): δ 7.14 (s, 1H, CH$_{NHC}$), 6.93 (s, 1H, CH$_{NHC}$), 3.77 (s, 3H, NCH$_3$), 1.72 (s, 9H, CH$_{3tBu}$).

1,3-bis(2,6-diisopropylphenyl)imidazol-2-ylidene silver chloride (2f[Cl]): 1,3-bis(2,6-diisopropylphenyl)imidazolium chloride 0.070 g (0.17 mmol), Ag$_2$O 0.047 g (0.20 mmol), 40 °C, CH$_2$Cl$_2$, 3h. ^{1}H-NMR (399.9 MHz, CDCl$_3$): δ 7.49 (d, *J* = 7.8 Hz, 2H, CH$_{Ph}$), 7.29 (d, *J* = 7.8 Hz, 4H, CH$_{Ph}$), 7.21 (s, 2H, CH$_{NHC}$), 2.54 (sept, *J* = 6.8 Hz, 4H, CH$_{iPr}$), 1.23 (d, *J* = 6.8 Hz, 12 H, CH$_{3iPr}$), 1.18 (d, *J* = 6.8 Hz, 12 H, CH$_{3iPr}$).

1,3-bis(2,6-diisopropylphenyl)imidazol-2-ylidene silver bromide (2f[Br]): 1,3-bis(2,6-diisopropylphenyl)imidazolium bromide 0.038 g (0.083 mmol), Ag$_2$O 0.023 g (0.099 mmol), 40 °C, CH$_2$Cl$_2$, 3h. ^{1}H-NMR (399.9 MHz, CDCl$_3$): δ 7.49 (m, 2H, CH$_{Ph}$), 7.30 (m, 4H, CH$_{Ph}$), 7.21 (s, 2H, CH$_{NHC}$), 2.54 (sept, *J* = 6.8 Hz, 2H, CH$_{iPr}$), 1.28 (d, *J* = 6.8 Hz, 12 H, CH$_{3iPr}$), 1.20 (d, *J* = 6.8 Hz, 12 H, CH$_{3iPr}$).

1,3-di-*tert*-butylimidazol-2-ylidene silver chloride (2g): 1,3-di-*tert*-butylimidazolium chloride 0.018 g (0.083 mmol), Ag$_2$O 0.023 g (0.099 mmol), room temperature, CH$_2$Cl$_2$, 3h. ^{1}H-NMR (399.9 MHz, CDCl$_3$): δ 7.11 (s, 2H, CH$_{NHC}$), 1.76 (s, 18H, CH$_{3tBu}$).

1-methyl-3-(2,6-diisopropylphenyl)imidazol-2-ylidene silver chloride (2h): 1-methyl-3-(2,6-diisopropylphenyl)imidazolium iodide 0.038 g (0.10 mmol), Ag$_2$O 0.028 g (0.12 mmol) room temperature, CH$_2$Cl$_2$, 3h. ^{1}H-NMR (399.9 MHz, CDCl$_3$): δ 7.46 (t, *J* = 7.8 Hz, 1H, CH$_{Ph}$), 7.23 (m, 2H, CH$_{Ph}$), 7.17 (m, 1H, CH$_{NHC}$), 6.98 (m, 1H, CH$_{NHC}$), 3.98 (s, 3H, NCH$_3$), 2.35 (sept, *J* = 6.8 Hz, 2H, CH$_{iPr}$), 1.22 (d, *J* = 6.8 Hz, 6 H, CH$_{3iPr}$), 1.10 (d, *J* = 6.8 Hz, 6 H, CH$_{3iPr}$).

1-isopropyl-3-*tert*-butylimidazol-2-ylidene silver iodide (2i): 1-isopropyl-3-*tert*-butylimidazolium iodide 0.031 g (0.11 mmol), Ag$_2$O 0.029 g (0.13 mmol), room temperature, CH$_2$Cl$_2$, 24h. ^{1}H-NMR (399.9 MHz, CDCl$_3$): δ 7.16 (s, 1H, CH$_{NHC}$), 6.97 (s, 1H, CH$_{NHC}$), 4.83 (sept, *J* = 6.8 Hz, 1H, CH$_{iPr}$), 1.72 (s, 9H, CH$_{3tBu}$), 1.46 (d, *J* = 6.8 Hz, 6H, CH$_{3iPr}$).

1,3-bis(2,4,6-trimethylphenyl)imidazole-2-ylidene silver chloride (2l): 1,3-bis(2,4,6-trimethylphenyl)imidazolium chloride 0.028 g (0,083 mmol), Ag$_2$O 0.023 g (0,099 mmol), 40 °C, CH$_2$Cl$_2$, 4h. ^{1}H-NMR (399.9 MHz, CDCl$_3$): 7.13 (s, 2H, CH$_{NHC}$), 6.99 (s, 4H, CH$_{Ph}$), 2.35 (s, 6H, *p*-CH$_{3Ph}$), 2.07 (s, 12H, *o*-CH$_{3Ph}$).

Synthesis of dicarbonyl(η4-3,4-bis(4-methoxyphenyl)-2,5-diphenylcyclopenta-2,4-dienone) ruthenium dimer (3).
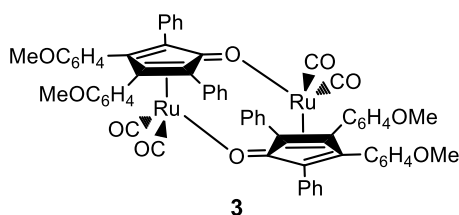
Figure 2.7. Structure of the dimeric ruthenium precursor (**3**).

Dicarbonyl(η4-3,4-bis(4-methoxyphenyl)-2,5-diphenylcyclopenta-2,4-dienone) ruthenium dimer (**3**) has been prepared following a procedure reported in the literature for a similar complex,[37] by reacting 3,4-bis(4-methoxyphenyl)-2,5-diphenylcyclopenta-2,4-dienone 1.04 g (2.35 mmol) and Ru$_3$(CO)$_{12}$ 0.50 g (0.78 mmol) in

heptane (130°C for 5 days, inert atmosphere). **3** was purified by filtration as a yellow solid and obtained with a yield of 80%. ^{1}H-NMR (399.9 MHz, CDCl$_3$): δ 7.10-6.40 (m, 36H, CH$_{aryl}$), 3.60 (s, 12H, -OCH$_3$); ^{13}C-NMR (100.6 MHz, CDCl$_3$): δ 206.91 (CO), 169.65 (C=O), 158.53 (-COCH3), 132.70 (CH$_{aryl}$), 130.96 (Cq$_{aryl}$), 130.58 (CH$_{aryl}$), 126.27 (CH$_{aryl}$), 122.67 (Cq$_{aryl}$), 113.32 (-CH$_{aryl}$), 112.54 (CH$_{aryl}$), 97.78 (C2,5 Cp), 87.76 (C$_{3,4}$ Cp), 54.90 (-OCH$_3$). IR (CH$_2$Cl$_2$, cm^{-1}): 2018, 1967 (v_{CO}); 1610, 1519 ($v_{C=C}$).

Synthesis of Ru(NHC) complexes (4)

I step: imidazolium salts (**1**), were reacted with Ag$_2$O (1.2 eq.) in the appropriate solvent under inert atmosphere and with protection from light. After stirring the reaction for the time and at the temperature required in order to reach complete conversion to silver complexes (**2**), the solvent, if different from CH$_2$Cl$_2$, was removed under vacuo and the solid obtained dissolved in CH$_2$Cl$_2$. II step: then dicarbonyl(η^4-3,4-bis(4-methoxyphenyl)-2,5-diphenylcyclopenta-2,4-dienone) ruthenium dimer (**3**) (0.5 eq. vs. imidazolium salts) was straightforwardly added to the *in situ* prepared silver complexes solution. The reaction mixture was stirred until the end of the reaction at room temperature. Upon filtration on a celite pad and removal of the solvent the quantitative formation of the dicarbonyl-η^4-3,4-bis(4-methoxyphenyl)-2,5-diphenylcyclopenta-2,4-dienone)(NHC)ruthenium complexes (**4**) was verified by ^{1}H-NMR, ^{13}C-NMR, ESI-MS and X-Ray crystal structure when suitable crystals were available.

4a	R$_1$ = R$_2$ = CH$_3$
4b	R$_1$= R$_2$ = CH$_2$Ph
4c	R$_1$ = CH$_3$, R$_2$ = CH$_2$CH$_2$CH$_3$
4d	R$_1$ = CH$_3$, R$_2$ = CH$_2$CH$_2$OH
4e	R$_1$ = CH$_3$, R$_2$ = ^{t}Bu
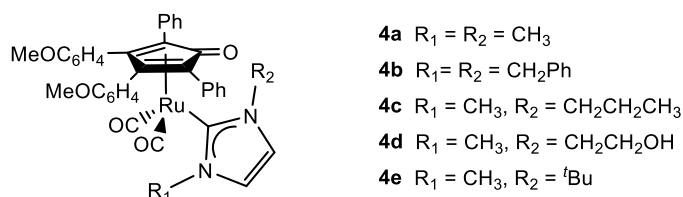
Figure 2.8. Structure of the mononuclear Ru carbene complexes (**4**).

Dicarbonyl(η^4-3,4-bis(4-methoxyphenyl)-2,5-diphenylcyclopenta-2,4-dienone)(1,3-dimethylimidazol-2-ylidene)ruthenium (4a): I step: 1,3-dimethylimidazolium iodide 0.149 g (0.665 mmol), Ag$_2$O 0.185 g (0.798 mmol), room temperature, CH$_2$Cl$_2$, 3h. II step: **3** 0.400 g (0.332 mmol), 10 min. The beige solid obtained was identified as **4a** (0.208 g, 90% yield). Suitable crystals of **4a** for X-Ray diffraction were obtained by slow diffusion (CH$_2$Cl$_2$/Et$_2$O).

The same reaction performed in a J-Young valve equipped NMR tube in CDCl$_3$ (0.7 mL) led to the *in situ* formation of the silver complex **2a** by sonication of the sample containing 1,3-dimethylimidazolium iodide 0.011 g (0.050 mmol) and Ag$_2$O 0.014 g (0.060 mmol) for 2h. Afterwards **3** 0.030 g (0.025 mmol) was added and ^{1}H-NMR analysis showed the quantitative and immediate formation of the complex **4a**. Complex **4a** is stable to air, moisture, in solution of organic solvents and in the presence of water. **4a** has been analyzed by IR, ^{1}H-NMR, ^{13}C-NMR, ESI-MS and X-Ray diffraction. ^{1}H-NMR (599.7 MHz, CDCl$_3$): δ 7.79 (m, 4H, CH$_{aryl}$), 7.17-7.04 (m, 10H, CH$_{aryl}$), 6.76 (s, 2H, CH$_{NHC}$), 6.65 (m, 4H, CH$_{aryl}$), 3.71 (s, 6H, -OCH$_3$), 3.09 (s, 6H, -NCH$_3$). ^{13}C-NMR (150.8 MHz, CDCl$_3$, g-HSQC, g-HMBC): δ 202.47 (CO), 172.72 (C$_{carbene}$), 169.33 (C=O, Cp), 158.54 (-COCH$_3$), 135.43 (Cq$_{aryl}$), 133.62 (CH$_{aryl}$), 129.16 (CH$_{aryl}$), 127.43 (CH$_{aryl}$), 125.27 (Cq$_{aryl}$), 124.90 (CH$_{aryl}$), 123.62 (CH$_{NHC}$), 112.93 (CH$_{aryl}$), 103.85 (C$_{2,5}$, Cp), 78.46 (C$_{3,4}$, Cp), 55.00 (-OCH$_3$), 38.23 (-NCH$_3$). IR (CH$_2$Cl$_2$, cm^{-1}): 2004, 1945 (v_{CO}); 1586 cm^{-1} ($v_{C=O}$); 1601, 1518 ($v_{C=C}$). ESI-MS (m/z) (+): 699 [M+H]$^+$; 721 [M + Na]$^+$. Anal. Calcd (%) for C$_{38}$H$_{32}$N$_2$O$_5$Ru: C, 65.41; H, 4.62. Found: C, 65.33; H, 4.58.

By using imidazolium salts with non-coordinating anions such as 1,3-dimethylimidazolium trifluoromethanesulfonate or 1,3-dimethylimidazolium hexafluorophosphate the formation of the corresponding silver complexes **2a[OTf]** and **2a[PF₆]** occurs. The latter undergo a transmetallation reaction with **3** leading to the formation of complex **4a**.

Dicarbonyl(η^4-3,4-bis(4-methoxyphenyl)-2,5-diphenylcyclopenta-2,4-dienone)(1,3-dibenzylimidazol-ylidene)ruthenium (4b): I step: 1,3-dibenzylimidazolium bromide 0.027 g (0,083 mmol), Ag₂O 0.023 g (0.099 mmol), 80 °C reflux, CH₃CN, 3h. II step: **3** 0.050 g (0.042 mmol), 2h. The beige solid obtained was identified as **4b** (0.081 g, 97% yield). Suitable crystals of **4b** for X-Ray diffraction were obtained by slow diffusion (toluene/hexane). The same result is obtained employing 1,3-dibenzylimidazolium chloride as imidazolium salt. **4b** has been analyzed by IR, ^{1}H-NMR, ^{13}C-NMR, ESI-MS and X-Ray diffraction. ^{1}H-NMR (300.1 MHz, CDCl₃): δ 7.85-6.60 (m, 28H, CH$_{aryl}$), 6.57 (s, 2H, CH$_{NHC}$), 4.67 (s, 4H, -CH₂Ph), 3.69 (s, 6H, -OCH₃). ^{13}C-NMR (150.8 MHz, CDCl₃): δ 201.69 (CO), 174.73 (C$_{carbene}$), 169.90 (C=O, Cp), 158.54 (-COCH₃), 136.13-112.90 (C$_{aryl}$), 122.71 (CH$_{NHC}$), 104.03 (C$_{2,5}$, Cp), 78.87 (C$_{3,4}$, Cp), 54.99, 54.27 (CH₂Ph, -OCH₃). IR (CH₂Cl₂, cm^{-1}): 2006, 1947 (v$_{CO}$); 1586 (v$_{C=O}$); 1603, 1518 (v$_{C=C}$). ESI-MS (m/z) (+): 851 [M+H]$^+$. Anal. Calcd (%) for C₅₀H₄₀N₂O₅Ru: C, 70.66; H, 4.74. Found: C, 70.58; H, 4.71.

Dicarbonyl(η^4-3,4-bis(4-methoxyphenyl)-2,5-diphenylcyclopenta-2,4-dienone)(1-methyl-3-butyl-imidazol-ylidene)ruthenium (4c): I step: 1-methyl-3-butyl-imidazolium bromide 0.018 g (0.083 mmol), Ag₂O 0.023 g (0.099 mmol), 80 °C reflux, CH₃CN, 3h. II step: **3** 0.050 g (0.042 mmol), 1h. The beige solid obtained was identified as **4c** (0.059 g, 96% yield). **4c** has been analyzed by IR, ^{1}H-NMR, ^{13}C-NMR, ESI-MS. ^{1}H-NMR (300.1 MHz, CDCl₃): δ 7.67-6.63 (m, 18H, CH$_{aryl}$), 7.82 (s, 1H, CH$_{NHC}$), 6.77 (s, 1H, CH$_{NHC}$), 3.69 (s, 6H, -OCH₃), 3.31 (m, 2H, -NCH₂), 3.05 (s, 3H, -NCH₃), 1.39, 0.89 (m, 2H, -CH₂CH₂), 0.72 (-CH₃). ^{13}C-NMR (150.8 MHz, CDCl₃): δ 202.44 (CO), 172.23 (C$_{carbene}$), 169.50 (C=O, Cp), 158.50 (-COCH₃), 135.41-112.90 (C$_{aryl}$), 124.04 (CH$_{NHC}$), 121.41 (CH$_{NHC}$), 103.88 (C$_{2,5}$, Cp), 78.35 (C$_{3,4}$, Cp), 54.97 (-OCH₃), 50.22 (-NCH₂), 38.12 (-NCH₃), 33.24, 19.38 (-CH₂CH₂-), 13.72 (-CH₃). IR (CH₂Cl₂, cm^{-1}): 2003, 1943 (v$_{CO}$); 1586 (v$_{C=O}$); 1600, 1517 (v$_{C=C}$). ESI-MS (m/z) (+): 741 [M+H]$^+$. Anal. Calcd (%) for C₄₁H₃₈N₂O₅Ru: C, 66.56; H, 5.18. Found: C, 66.51; H, 5.17.

Dicarbonyl(η^4-3,4-bis(4-methoxyphenyl)-2,5-diphenylcyclopenta-2,4-dienone)(1-methyl-3-(2-hydroxyethyl)imidazol-ylidene)ruthenium (4d): I step: 1-methyl-3-(2-hydroxyethyl)imidazolium chloride 0.014 g (0.083 mmol), Ag₂O 0.023 g (0.099 mmol), room temperature, CH₃CN, 3h. II step: **3** 0.050g (0.042 mmol), 1h. The beige solid obtained, was identified as **4d**, (0.060 g, 98% yield). Suitable crystals of **4d** for X-Ray diffraction were obtained by slow diffusion (CH₂Cl₂/petroleum ether). **4d** has been analyzed by IR, ^{1}H-NMR, ^{13}C-NMR, ESI-MS and X-Ray diffraction. ^{1}H-NMR (300.1 MHz, CDCl₃): δ 7.67-6.65 (m, 18H, CH$_{aryl}$), 7.01 (s, 1H, CH$_{NHC}$), 6.86 (s, 1H, CH$_{NHC}$), 3.86 (m, 2H, -NCH₂), 3.72 (s, 6H, -OCH₃), 3.22 (s, 3H, -NCH₃), 3.15 (m, 2H, -CH₂OH). ^{13}C-NMR (150.8 MHz, CDCl₃): δ 201.82 (CO), 172.88 (C$_{carbene}$), 166.15 (C=O, Cp), 158.67 (-COCH₃), 134.07-112.95 (C$_{aryl}$), 124.23 (CH$_{NHC}$), 121.03 (CH$_{NHC}$), 104.98 (C$_{2,5}$, Cp), 80.68 (C$_{3,4}$, Cp), 58.94 (-NCH₂), 55.04 (-OCH₃), 52.47 (-CH₂OH), 38.29 (-NCH₃). IR (CH₂Cl₂, cm^{-1}): 2011, 1952 (v$_{CO}$); 1558 (v$_{C=O}$); 1609, 1518 (v$_{C=C}$). ESI-MS (m/z) (+): 729 [M+H]$^+$, 751 [M+Na]$^+$. Anal. Calcd (%) for C₃₉H₃₄N₂O₆Ru: C, 64.36; H, 4.71. Found: C, 64.29; H, 4.69.

Dicarbonyl(η^4-3,4-bis(4-methoxyphenyl)-2,5-diphenylcyclopenta-2,4-dienone)(1-methyl-3-*tert*-butyl-imidazol-ylidene)ruthenium (4e): I step: 1-methyl-3-(*tert*-butyl)imidazolium iodide 0.026 g (0.097 mmol),

Ag$_2$O 0.027 g (0.17 mmol), room temperature, CH$_2$Cl$_2$, 4h. II step: **3** 0.059 g (0.049 mmol), 2h. The beige solid obtained, was identified as **4e**, (0.070 g, 98% yield). **4e** has been analyzed by IR, ^{1}H-NMR, ^{13}C-NMR, ESI-MS. ^{1}H-NMR (300.1 MHz, CDCl$_3$): δ 7.73 (s, 1H, CH$_{NHC}$), 7.71-6.62 (m, 18H, CH$_{aryl}$), 6.08 (s, 1H, CH$_{NHC}$), 3.71 (s, 6H, -OCH$_3$), 3.24 (s, 3H, -NCH$_3$), 1.31 (s, 9H, CH$_{3tBu}$). ^{13}C-NMR (150.8 MHz, CDCl$_3$): 203.75 (CO), 182.15 (C$_{carbene}$), 168.31 (C=O, Cp), 158.29 (-COCH$_3$), 149.03 (CH$_{NHC}$), 135.86-112.73 (C$_{aryl}$, CH$_{NHC}$), 103.18 (C$_{2,5}$, Cp), 79.42 (C$_{3,4}$, Cp), 56.62 (Cq$_{tBu}$), 55.00 (-OCH$_3$), 37.63 (-NCH$_3$), 29.69 (CH$_{3tBu}$). IR (CH$_2$Cl$_2$, cm^{-1}): 1996, 1933 (ν$_{CO}$); 1590 (ν$_{C=O}$); 1604, 1518 (ν$_{C=C}$). ESI-MS (m/z) (+): 741 [M+H]$^+$. Anal. Calcd (%) for C$_{41}$H$_{38}$N$_2$O$_5$Ru: C, 66.56; H, 5.18. Found: C, 66.53; H, 5.19.

Synthesis of Ru-Ag(NHC) complexes (5)

I step: imidazolium salts (**1**), were reacted with Ag$_2$O in the appropriate solvent under inert atmosphere and with protection from light. After stirring the reaction for the time and at the temperature requested in order to reach complete conversion, the solvent, if different from CH$_2$Cl$_2$, was removed and the solid obtained dissolved in CH$_2$Cl$_2$. II step: successively dicarbonyl(η^4-3,4-bis(4-methoxyphenyl)-2,5-diphenylcyclopenta-2,4-dienone) ruthenium dimer (**3**) (0.5 eq. vs. imidazolium salts) was straightforwardly added to the *in situ* prepared silver complexes solution. The reaction mixture was stirred until the end of the reaction at room temperature. Upon filtration on a celite pad and removal of the solvent the quantitative formation of the dicarbonyl-η^4-3,4-bis(4-methoxyphenyl)-2,5-diphenylcyclopenta-2,4-dienone)(NHC)silver halidee)ruthenium complexes (**5**) was verified by ^{1}H-NMR, ^{13}C-NMR, ESI-MS and X-Ray crystal structure when suitable crystals were available.

5f[Cl] X = Cl, R$_1$ = R$_2$ = 2,6(iPr)$_2$Ph;
5f[Br] X = Br, R$_1$ = R$_2$ = 2,6(iPr)$_2$Ph
5g X = Cl, R$_1$ = R$_2$ = ^{t}Bu;
5h X = I, R$_1$ = CH$_3$, R$_2$ = 2,6(iPr)$_2$Ph;
5i X = I, R$_1$ = iPr, R$_2$ = ^{t}Bu;
5l X = I, R$_1$ = R$_2$ = Mes
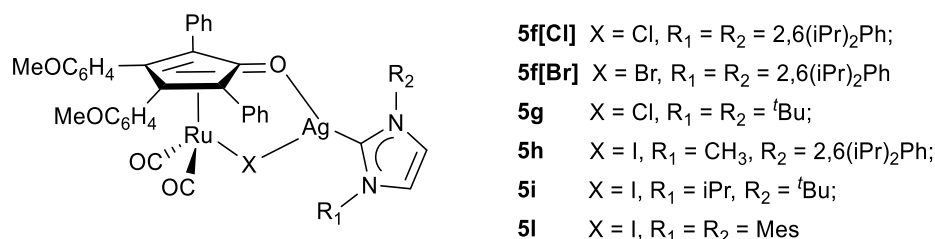
Figure 2.9. Structure of the dimetallic Ru-Ag carbene complexes (**5**).

Dicarbonyl(η^4-3,4-bis(4-methoxyphenyl)-2,5-diphenylcyclopenta-2,4-dienone)(1,3-di-(2,6-diisopropylphenyl)imidazol-2-ylidene silver chloride)ruthenium (5f[Cl]): I step: 1,3-bis(2,6-diisopropylphenyl)imidazolium chloride 0.070 g (0.17 mmol), Ag$_2$O 0.047 g (0.20 mmol), 40 °C, CH$_2$Cl$_2$, 3h. II step: **3** 0.100 g (0.083 mmol), 1h. The beige solid obtained, was identified as **5f[Cl]**, (0.187 g, 96% yield). Suitable crystals of **5f[Cl]** for X-Ray diffraction were obtained by slow diffusion (CH$_2$Cl$_2$/petroleum ether). **5f[Cl]** has been analyzed by IR, ^{1}H-NMR, ^{13}C-NMR, ESI-MS and X-Ray diffraction. **5f[Cl]** is stable in the solid state; it decomposes in solution of CH$_2$Cl$_2$, CDCl$_3$, Tol-d$_8$ in more than 24h. ^{1}H-NMR (399.9 MHz, CDCl$_3$): δ 7.57-6.51 (m, 24H, CH$_{aryl}$), 7.24 (s, 2H, CH$_{NHC}$), 3.68 (s, 6H, -OCH$_3$), 2.53 (sept, *J* = 6.8 Hz, 4H, CH$_{iPr}$), 1.16 (d, *J* = 6.8 Hz, 12H, CH$_{3iPr}$), 1.13 (d, *J* = 6.8 Hz, 12H, CH$_{3iPr}$). ^{13}C-NMR (150.8 MHz, CDCl$_3$): δ 200.54 (CO), 188.6 (dd, *J* (^{109}Ag-^{13}C) = 271 Hz; *J* (^{108}Ag-^{13}C) = 235 Hz), 165.38 (C=O, Cp), 158.47 (-COCH$_3$), 145.53-112.55 (C$_{aryl}$), 123.04, 122.96 (CH$_{NHC}$), 99.61 (C$_{2,5}$, Cp), 83.12 (C$_{3,4}$, Cp), 55.03 (-OCH$_3$), 28.60 (CH$_{iPr}$), 24.34, 24.05 (CH$_{3iPr}$). IR (CH$_2$Cl$_2$, cm^{-1}): 2013, 1953 (ν$_{CO}$); 1608, 1518 (ν$_{C=C}$). ESI-MS (m/z) (-): 1169 [M+Cl]$^-$. Anal. Calcd (%) for C$_{60}$H$_{60}$AgClN$_2$O$_5$Ru: C, 63.58; H, 5.34. Found: C, 63.49; H, 5.29.

The same reaction was performed on 1,3-bis(2,6-diisopropylphenyl)imidazolium bromide as starting material leading to the formation of the equivalent dicarbonyl-η^4-3,4-bis(4-methoxyphenyl)-2,5-diphenylcyclopenta-2,4-dienone)(1,3-di-(2,6-diisopropylphenyl)imidazol-2-ylidene silver bromide)]ruthenium (**5f[Br]**) which show a ^{1}H-NMR and IR characterization superimposable to the one of **5f[Cl]**. ^{1}H-NMR (399.9 MHz, CDCl$_3$): δ 7.57-6.51 (m, 24H, CH$_{aryl}$), 7.24 (s,2H, CH$_{NHC}$), 3.68 (s, 6H, -OCH$_3$), 2.53 (sept, J = 6.8 Hz, 4H, CH$_{iPr}$), 1.16 (d, J = 6.8 Hz, 12H,CH$_{3iPr}$), 1.14 (d, J = 6.8 Hz, 12H, CH$_{3iPr}$). IR (CH$_2$Cl$_2$, cm^{-1}): 2013, 1953 (v$_{CO}$); 1608, 1518 (v$_{C=C}$).

Dicarbonyl(η^4-3,4-bis(4-methoxyphenyl)-2,5-diphenylcyclopenta-2,4-dienone)(1,3-di-*tert*-butylimidazol-2-ylidene silver chloride)ruthenium (5g): I step: 1,3-di-*tert*-butylimidazolium chloride 0.018 g (0.083 mmol), Ag$_2$O 0.023 g (0.10 mmol), room temperature, CH$_2$Cl$_2$, 3h. II step: **3** 0.050 g (0.042 mmol), 2h. The beige solid obtained was identified as **5g** (0.088 g, 95% yield). **5g** has been analyzed by IR, ^{1}H-NMR, ^{13}C-NMR, ESI-MS. **5g** is stable in the solid state; it decomposes in solution in more than 24h. ^{1}H-NMR (300.1 MHz, CDCl$_3$): δ 7.50-6.55 (m, 18H, CH$_{aryl}$), 7.01 (s, 2H, CH$_{NHC}$), 3.70 (s, 6H, -OCH$_3$), 1.60 (s, 18H, CH$_{3tBu}$). ^{13}C-NMR (150.8 MHz, CDCl$_3$): δ 200.46 (CO), 177.51(s, C$_{carbene}$), 165.20 (C=O, Cp), 158.60 (-*C*OCH$_3$), 133.14-112.75 (CH$_{aryl}$), 116.16 (CH$_{NHC}$), 99.71 (C$_{2,5}$, Cp), 84.00 (C$_{3,4}$, Cp), 55.00 (-OCH$_3$), 57.45 (Cq$_{tBu}$), 31.60 (CH$_{3tBu}$). IR (CH$_2$Cl$_2$, cm^{-1}): 2014, 1955 (v$_{CO}$); 1608, 1518 (v$_{C=C}$). ESI-MS (m/z) (-): 961 [M+Cl]$^-$. Anal. Calcd (%) for C$_{44}$H$_{44}$AgClN$_2$O$_5$Ru: C, 57.12; H, 4.79. Found: C, 57.02; H, 4.75.

Dicarbonyl(η^4-3,4-bis(4-methoxyphenyl)-2,5-diphenylcyclopenta-2,4-dienone)(1-methyl-3-(2,6-diisopropylphenyl)imidazol-2-ylidene silver chloride)ruthenium (5h): I step: 1-methyl-3-(2,6-diisopropylphenyl)imidazolium iodide 0.038 g (0.10 mmol), Ag$_2$O 0.028 g (0.12 mmol), room temperature, CH$_2$Cl$_2$, 3h. II step: **3** 0.061 g (0.051 mmol), 2h. The beige solid obtained was identified as **5h** (0.096 g, 97% yield). **5h** has been analyzed by IR, ^{1}H-NMR, ^{13}C-NMR, ESI-MS. **5h** is stable in the solid state; it decomposes in solution in more than 24h. ^{1}H-NMR (300.1 MHz, CDCl$_3$): δ 7.53-6.54 (m, 21H, CH$_{aryl}$), 7.07, 7.09 (m, 2H, CH$_{NHC}$) 3.73 (3H, -NCH$_3$), 3.72 (s, 6H, -OCH$_3$), 2.33 (sept, J = 6.8 Hz, 2H, CH$_{iPr}$), 1.20 (d, J = 6.8 Hz, 6H, CH$_{3iPr}$), 1.09 (d, J = 6.8 Hz, 6H, CH$_{3iPr}$). ^{13}C-NMR (150.8 MHz, CDCl$_3$): δ 200.27 (CO), 176.85 (C$_{carbene}$), 168.36 (C=O, Cp), 158.59 (-*C*OCH$_3$), 145.68-112.71 (C$_{aryl}$), 123.33, 121.23 (CH$_{NHC}$),100.39 (C$_{2,5}$, Cp), 83.60 (C$_{3,4}$, Cp), 55.00 (-OCH$_3$), 38.55 (-NCH$_3$), 28.06 (CH$_{iPr}$), 24.40, 24.35 (CH$_{3iPr}$). IR (CH$_2$Cl$_2$, cm^{-1}): 2014, 1955 (v$_{CO}$); 1609, 1518 (v$_{C=C}$). ESI-MS (m/z) (-): 1023 [M+Cl]$^-$. Anal. Calcd (%) for C$_{49}$H$_{46}$AgClN$_2$O$_5$Ru: C, 59.61; H, 4.70. Found: C, 59.54; H, 4.67.

Dicarbonyl(η^4-3,4-bis(4-methoxyphenyl)-2,5-diphenylcyclopenta-2,4-dienone)(1-isopropyl-3-*tert*-butyl)imidazol-2-ylidene silver iodide)ruthenium (5i): I step: 1-isopropyl-3-*tert*-butylimidazolium iodide 0.062 g (0.22 mmol), Ag$_2$O 0.058 g (0.26 mmol), room temperature, CH$_2$Cl$_2$, 24h. II step: **3** 0.128 g (0.106 mmol), 2h. The beige solid obtained, was identified as **5i** by IR and ^{1}H-NMR. **5i** decomposed in solution preventing ^{13}C-NMR analysis. ^{1}H-NMR (399.9 MHz, CDCl$_3$): δ 7.54-6.56 (m, 20H, CH$_{aryl}$, CH$_{NHC}$), 3.71 (s, 6H, -OCH$_3$), 4.52 (m, 1H, CH$_{iPr}$), 1.56 (s, 9H, CH$_{3tBu}$), 1.31 (d, 6H, J = 6.8 Hz, CH$_{3iPr}$). IR (CH$_2$Cl$_2$, cm^{-1}): 2016, 1958 (v$_{CO}$); 1609, 1518 (v$_{C=C}$).

Dicarbonyl(η^4-3,4-bis(4-methoxyphenyl)-2,5-diphenylcyclopenta-2,4-dienone)(1,3-bis-(2,4,6-trimethylphenyl)imidazol-2-ylidene silver chloride)ruthenium (5l): I step: 1,3-bis-(2,4,6-trimethylphenyl)imidazolium chloride 0.056 g (0.17 mmol), Ag$_2$O 0.046 g (0.20 mmol), room temperature, CH$_2$Cl$_2$, 2h. II step: **3** 0.100 g (0.083 mmol), 1h. The beige solid obtained, was identified as **5l** by IR and ^{1}H-NMR. **5l** decomposed in solution preventing ^{13}C-NMR analysis. ^{1}H-NMR (399.9 MHz, CDCl$_3$): δ 7.25-6.41 (m,

22H, CH$_{aryl}$, CH$_{NHC}$), 3.59 (s, 6H, -OCH$_3$), 2.35 (s, 6H, *p*-CH$_{3Ph}$), 1.91 (s, 12H, *o*-CH$_{3Ph}$). IR (CH$_2$Cl$_2$, cm^{-1}): 2013, 1954 (v$_{CO}$); 1608, 1517 (v$_{C=C}$).

Synthesis of Ru-Cu(NHC) complex (6)

Dicarbonyl(η^4-3,4-bis(4-methoxyphenyl)-2,5-diphenylcyclopenta-2,4-dienone)(1,3-di-(2,6-diisopropylphenyl)imidazol-2-ylidene copper chloride)ruthenium (6)
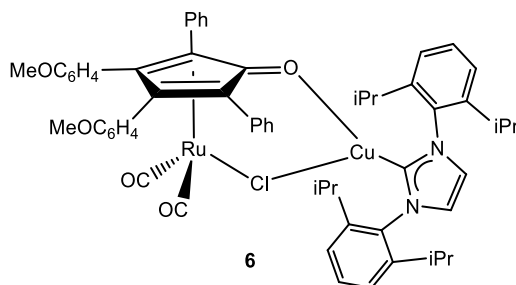
Figure 2.10. Structure of the dimetallic Ru-Cu carbene complex (**6**).

To a CH$_2$Cl$_2$ solution of 1,3-di-(2,6-diisopropylphenyl)imidazol-2-ylidene copper chloride 0.081 g (0.16 mmol), **3** 0.100 g (0.083 mmol) was added. The reaction mixture was stirred for 1h at room temperature. Upon filtration on a celite pad and removal of the solvent the quantitative formation of **6** as a beige solid (0.164 g, 94% yield) was verified by ^{1}H-NMR, ^{13}C-NMR, ESI-MS. Suitable crystals of **6** for X-Ray diffraction were obtained by slow diffusion (toluene/hexane). **6** is stable in the solid state. It decomposes in solution in more than 24h. ^{1}H-NMR (399.9 MHz, CDCl$_3$): δ 7.57-6.52 (m, 24H, CH$_{aryl}$), 7.05 (s, 2H, CH$_{NHC}$), 3.69 (s, 6H, -OCH$_3$), 2.68 (sept, *J* = 6.6 Hz, 4H, CH$_{iPr}$), 1.17 (d, *J* = 6.6 Hz, 12H, CH$_{3iPr}$). ^{13}C-NMR (150.8 MHz, CDCl$_3$): δ 200.43 (CO), 183.45 (C$_{carbene}$), 165.56 (C=O, Cp), 158.47 (-COCH$_3$), 145.66-112.70 (C$_{aryl}$), 130.76 (CH$_{NHC}$), 99.17 (C$_{2,5}$, Cp), 84.94 (C$_{3,4}$, Cp), 54.91 (-OCH$_3$), 28.44 (CH$_{iPr}$), 24.23, 23.84 (CH$_{3iPr}$). IR (CH$_2$Cl$_2$, cm^{-1}): 2014, 1956 (v$_{CO}$); 1609, 1520 (v$_{C=C}$). ESI-MS (m/z) (-): 1125 [M+Cl]$^-$. Anal. Calcd (%) for C$_{60}$H$_{60}$CuClN$_2$O$_5$Ru: C, 66.16; H, 5.55. Found: C, 66.10; H, 5.51.

Synthesis of bis-trimethylsilyl-cyclopentadienone Ru complexes

Triscarbonyl-(2,4-bis(trimethylsilyl)bicyclo[3.3.0]nona-1,4-dien-3-one)ruthenium (7)
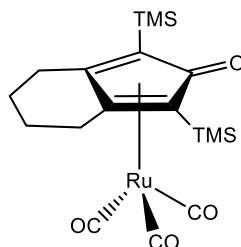
Figure 2.11. Structure of ruthenium triscarbonyl bis(TMS)-substituted cyclopentadienone complex (**7**).

In a 75 mL Teflon tube equipped with magnetic stirrer, 1,7-octadiyne 0.150 g (0.6 mmol) and $Ru_3(CO)_{12}$ 0.191 g (0.3 mmol) were dissolved in 40 mL of toluene. The container is closed with a cap, equipped with a temperature sensor, and placed into microwave. The reaction is heated to 140 °C for 4h. Upon removal of the solvent, the crude was purified by neutral alumina column chromatography eluting, at first, with hexane, then with dichloromethane and finally with ethyl acetate to afford the yellow triscarbonyl-(2,4-bis(trimethylsilyl)bicyclo[3.3.0]nona-1,4-dien-3-one)iron complex (**7**) with a yield of 52%. ^{1}H-NMR (399.9 MHz, CDCl$_3$): δ (ppm) 2.65 (m, 4H, CH$_2$), 1.80 (m, 4H, CH$_2$), 0.26 (s, 18H, CH$_3$, TMS). ^{13}C-NMR (150.8 MHz, CDCl$_3$, g-HSQC, g-HMBC): δ (ppm) 195.06 (CO), 184.54 (C=O), 112.62 (C$_{2,5}$, Cp), 68.69 (C$_{3,4}$, Cp), 24.96 (CH$_2$, 2C), 22.59 (CH$_2$, 2C), 0.14 (CH$_3$, TMS, 6C).vIR (CH$_2$Cl$_2$, cm^{-1}): 2076, 2017, 2000 (v$_{CO}$), 1614 (v$_{C=O}$).ESI-MS (m/z) (+): 465 [M+H]$^+$; 487 [M + Na]$^+$; 503 [M+K]$^+$.

Dicarbonyl-(2,4-bis(trimethylsilyl)bicyclo[3.3.0]nona-1,4-dien-3-one)[acetonitrile]ruthenium (8)

9
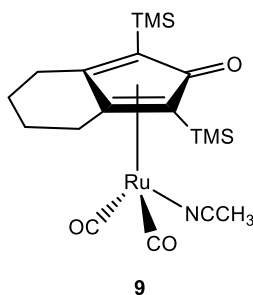
Figure 2.12. Structure of dicarbonyl-(2,4-bis(TMS)bicyclo[3.3.0]nona-1,4-dien-3-one)[acetonitrile]Ru precursor (**8**).

In a dried 10 mL Schlenk flask, triscarbonyl-(2,4-bis(trimethylsilyl)bicyclo[3.3.0]nona-1,4-dien-3-one)ruthenium (**7**) 0.065 g (0.140 mmol) and trimethylamine-N-oxide 0.016 g (0.210 mmol) were dissolved in 3 mL of anhydrous acetonitrile. Reaction mixture was stirred at room temperature and protected from light for 3 hours. A pale-yellow precipitate appeared. The solid was filtered and washed with cold hexane to afford the complex dicarbonyl-(2,4-bis(trimethylsilyl)bicyclo[3.3.0]nona-1,4-dien-3-one)[acetonitrile]ruthenium (**8**) with a yield of 75%.^{1}H-NMR (399.9 MHz, CDCl$_3$): δ (ppm) 2.42 (m, 4H, CH$_2$), 2.25 (s, 3H, CH$_3$), 1.60 (m, 4H, CH$_2$), 0.26 (s, 18H, CH$_3$, TMS). ^{13}C-NMR (150.8 MHz, CDCl$_3$, g-HSQC, g-HMBC): δ (ppm) 199.10 (CO), 182.47 (C=O), 124.51 (Cq, -CH$_3$*C*N), 107.27 (C$_{2,5}$, Cp), 67.99 (C$_{3,4}$, Cp), 25.17 (CH$_2$, 2C), 22.44 (CH$_2$, 2C), 4.09 (-*C*H$_3$CN), 0.14 (CH$_3$, TMS, 6C). IR (CH$_2$Cl$_2$, cm^{-1}): 2010, 1948 (v$_{CO}$), 1591 (v$_{C=O}$). ESI-MS (m/z) (+): 478 [M+H]$^+$; 500 [M + Na]$^+$.

Dicarbonyl-(2,4-bis(trimethylsilyl)bicyclo[3.3.0]nona-1,4-dien-3-one)[1,3-dimethyl-ilidene]ruthenium (9a)
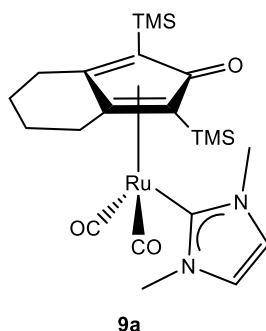
Figure 2.13. Structure of bis(TMS)-substituted cyclopentadienone Ru carbene complex (**9a**)

A mixture of 1,3-dimethylimidazolium iodide (**1a**) (0.013g, 0.056mmol), Ag_2O (1.2eq, 0.016g, 0.067mmol) and dicarbonyl-(2,4-bis(trimethylsilyl)bicyclo[3.3.0]nona-1,4-dien-3-one)[acetonitrile]ruthenium precursor (**8**) (0.027g, 0.056mmol) were reacted in dry CH_2Cl_2 under inert atmosphere and with protection from light stirring for 1h at room temperature. Upon filtration on a celite pad and removal of the solvent the quantitative formation of the dicarbonyl-(2,4-bis(trimethylsilyl)bicyclo[3.3.0]nona-1,4-dien-3-one)[1,3-dimethyl-ilidene]ruthenium (**9a**) was verified by ^{1}H-NMR, ^{13}C-NMR and ESI-MS. ^{1}H-NMR (399.9 MHz, $CDCl_3$): δ (ppm) 6.98 (s, 2H, CH_{NHC}), 3.88 (s, 6H, CH_3), 2.54 (m, 4H, CH_2), 1.77 (m, 4H, CH_2), 0.19 (s, 18H, CH_3, TMS). ^{13}C-NMR (150.8 MHz, $CDCl_3$, g-HSQC, g-HMBC): δ (ppm) 202.60 (CO), 181.75 ($C_{carbene}$), 177.12 (C=O), 122.98 (CH_{NHC}), 105.88 ($C_{2,5}$, Cp), 68.03 ($C_{3,4}$, Cp), 40.38 (-NCH$_3$), 24.82 (CH_2, 2C), 22.87 (CH_2, 2C), 0.98 (CH_3, TMS, 6C). IR (CH_2Cl_2, cm^{-1}): 1997, 1935 (v_{CO}), 1563 ($v_{C=O}$). ESI-MS (m/z) (+): 533 [M+H]$^+$; 555 [M + Na]$^+$.

Dicarbonyl-(2,4-bis(trimethylsilyl)bicyclo[3.3.0]nona-1,4-dien-3-one)[1-(2-hydroxyethyl))-3-methylilidene]ruthenium (9d)
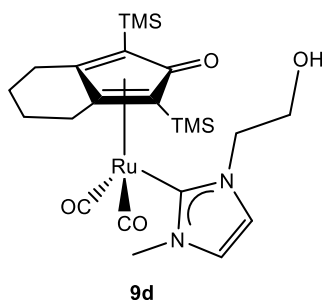
Figure 2.14. Structure of bis(TMS)-substituted cyclopentadienone Ru carbene complex (**9d**).

1-methyl-3-(2-hydroxyethyl) imidazolium chloride (**1d**) (0.014g, 0.096mmol), was reacted with Ag_2O (1.2eq., 0.027g, 0.115mmol) in dry CH_3CN under inert atmosphere and with protection from light. The reaction mixture was stirred for 3h at room temperature in order to reach complete conversion to the corresponding silver carbene complex. Then, the solvent was removed under vacuum, the solid obtained dissolved in CH_2Cl_2 and 0.046g (0.096mmol) of dicarbonyl-(2,4-bis(trimethylsilyl)bicyclo[3.3.0]nona-1,4-dien-3-one)[acetonitrile]ruthenium precursor (**2**) was straightforwardly added to the *in situ* prepared silver complex solution. After stirring for 1h at room temperature, the reaction mixture was filtered on a celite pad and the solvent removed under vacuum leading to the quantitative formation of the dicarbonyl-(2,4-bis(trimethylsilyl)bicyclo[3.3.0]nona-1,4-dien-3-one)[1-(butyl-3-(2-pyridinyl)-imidazol-2-ylidene]ruthenium

complex (**9d**). ^{1}H-NMR (399.9 MHz, CDCl$_3$): δ (ppm) 7.24 (s, 1H, CH$_{NHC}$), 7.06 (s, 1H, CH$_{NHC}$), 4.23 (t, 2H, -NCH$_2$), 3.92 (t, 2H, CH$_2$OH), 3.87 (s, 3H, -NCH$_3$), 2.59 (m, 4H, CH$_2$), 1.77 (m, 4H, CH$_2$), 0.19 (s, 18H, CH$_3$, TMS). ^{13}C-NMR (150.8 MHz, CDCl$_3$, g-HSQC, g-HMBC): δ (ppm) 202.94 (CO), 176.47 (C$_{carbene}$), 175.68 (C=O), 124.22 (CH$_{NHC}$), 120.17 (CH$_{NHC}$), 105.64 (C$_{2,5}$, Cp), 70.04 (C$_{3,4}$, Cp), 59.16 (-NCH$_2$), 53.91 (-CH$_2$OH), 40.65 (-NCH$_3$), 25.12 (CH$_2$, 2C), 22.87 (CH$_2$, 2C), 1.00 (CH$_3$, TMS, 6C). IR (CH$_2$Cl$_2$, cm^{-1}): 2003, 1939 (v$_{CO}$), 1525 (v$_{C=O}$). ESI-MS (m/z) (+): 563 [M+H]$^+$; 585 [M + Na]$^+$.

X-Ray diffraction studies
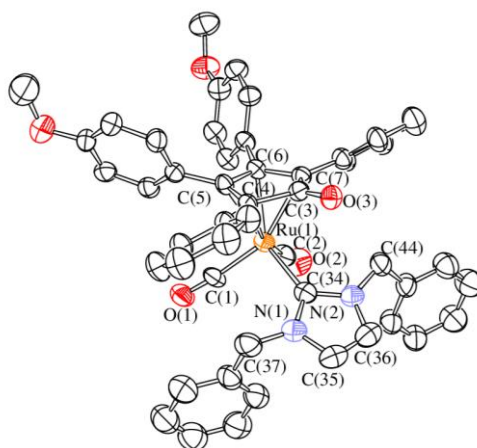
Figure 2.15. ORTEP drawing of **4b**. Displacement ellipsoids are at the 30% probability level. H-atoms have been omitted for clarity.
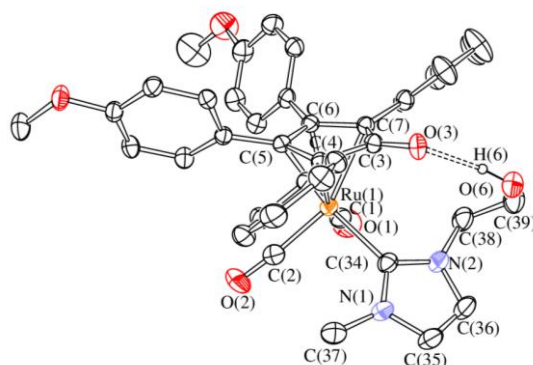
Figure 2.16. ORTEP drawing of **4d**. Displacement ellipsoids are at the 30% probability level. H-atoms, except H(6), have been omitted for clarity. The H-bond between O(6)H(6) and O(3) is represented as a dashed line.
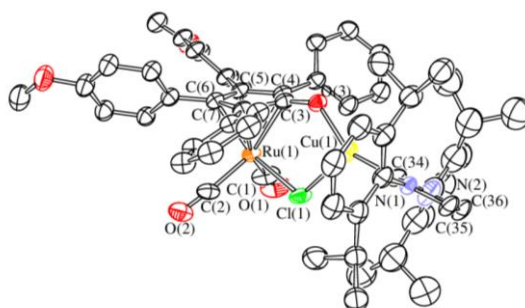
Figure 2.17. ORTEP drawing of **6**. Displacement ellipsoids are at the 30% probability level. H-atoms have been omitted for clarity.
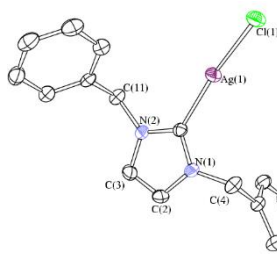
Figure 2.18. ORTEP drawing of **2b[Cl]**. Displacement ellipsoids are at the 30% probability level. H-atoms have been omitted for clarity.

Table 2.1. Main bond lengths (Å) and angles (deg) of **4a**, **4b** and **4d**.

	4a	4b	4d
Ru(1)-C(1)	1.893(5)	1.868(10)	1.884(3)
Ru(1)-C(2)	1.874(5)	1.840(11)	1.879(4)
Ru(1)-C(3)	2.470(4)	2.503(10)	2.474(3)
Ru(1)-C(4)	2.263(4)	2.242(8)	2.269(3)
Ru(1)-C(5)	2.206(4)	2.203(8)	2.217(3)
Ru(1)-C(6)	2.208(3)	2.181(8)	2.197(3)
Ru(1)-C(7)	2.270(3)	2.269(8)	2.291(3)
Ru(1)-C(34)	2.117(4)	2.103(10)	2.128(3)
C(1)-O(1)	1.128(5)	1.144(9)	1.139(4)
C(2)-O(2)	1.151(5)	1.170(10)	1.145(4)
C(3)-O(3)	1.245(4)	1.235(9)	1.259(3)
C(3)-C(4)	1.464(5)	1.510(11)	1.472(4)
C(4)-C(5)	1.454(5)	1.418(11)	1.445(4)
C(5)-C(6)	1.426(5)	1.412(11)	1.426(4)
C(6)-C(7)	1.445(5)	1.439(11)	1.453(4)
C(7)-C(3)	1.475(5)	1.481(11)	1.463(4)
C(34)-N(1)	1.352(6)	1.361(11)	1.357(4)
C(34)-N(2)	1.355(5)	1.369(11)	1.357(4)
N(1)-C(35)	1.370(6)	1.392(12)	1.384(4)
N(1)-C(37)	1.456(7)	1.409(11)	1.454(5)
N(2)-C(36)	1.379(6)	1.378(12)	1.387(4)
N(2)-C(38)	1.427(7)	1.439(12)	1.460(5)
C(35)-C(36)	1.310(7)	1.284(13)	1.322(6)
C(3)-C(4)-C(5)	108.5(3)	108.0(7)	107.9(2)
C(4)-C(5)-C(6)	108.2(3)	109.3(7)	108.7(2)
C(5)-C(6)-C(7)	108.1(3)	108.7(8)	108.0(2)
C(6)-C(7)-C(3)	108.7(3)	108.5(8)	108.4(2)
C(7)-C(3)-C(4)	105.0(3)	103.2(8)	105.7(2)
C(7)-C(3)-O(3)	127.1(3)	128.7(8)	126.5(2)
C(4)-C(3)-O(3)	127.6(3)	127.7(8)	127.6(3)
Ru(1)-C(34)-N(1)	127.6(3)	130.2(8)	128.2(2)
Ru(1)-C(34)-N(2)	128.4(3)	127.6(8)	127.2(2)
N(1)-C(34)-N(2)	103.9(3)	102.2(9)	104.5(3)
C(34)-N(1)-C(35)	111.2(4)	111.7(9)	110.6(3)
N(1)-C(35)-C(36)	107.0(5)	106.5(11)	107.1(3)
C(35)-C(36)-N(2)	107.8(4)	108.8(11)	107.5(3)
C(36)-N(2)-C(34)	110.2(4)	110.7(9)	110.3(3)
Ru(1)-C(1)-O(1)	178.7(4)	174.1(9)	178.3(3)
Ru(1)-C(2)-O(2)	177.9(4)	177.0(9)	174.8(3)

Table 2.2. Main bond lengths (Å) and angles (deg) of **5f[Cl]** and **6**.

	5f[Cl]	6
Ru(1)-C(1)	1.873(8)	1.885(12)
Ru(1)-C(2)	1.865(8)	1.895(13)
Ru(1)-C(3)	2.424(6)	2.386(10)
Ru(1)-C(4)	2.248(6)	2.263(10)
Ru(1)-C(5)	2.194(6)	2.205(9)
Ru(1)-C(6)	2.190(6)	2.205(9)
Ru(1)-C(7)	2.245(6)	2.247(9)
Ru(1)-Cl(1)	2.4370(17)	2.411(3)
C(1)-O(1)	1.149(8)	1.123(13)
C(2)-O(2)	1.142(9)	1.130(14)
C(3)-O(3)	1.246(7)	1.263(11)
C(3)-C(4)	1.452(9)	1.448(13)
C(4)-C(5)	1.451(9)	1.465(14)
C(5)-C(6)	1.450(9)	1.462(13)
C(6)-C(7)	1.437(8)	1.429(13)
C(7)-C(3)	1.471(9)	1.460(14)
O(3)-M(1)	2.223(4)	1.922(6)
Cl(1)-M(1)	2.6282(18)	2.449(3)
M(1)-C(34)	2.086(6)	1.869(10)
N(1)-C(34)	1.351(8)	1.360(12)
N(2)-C(34)	1.351(7)	1.343(13)
N(1)-C(35)	1.389(8)	1.373(12)
N(2)-C(36)	1.389(8)	1.389(15)
C(35)-C(36)	1.329(9)	1.309(15)
C(3)-C(4)-C(5)	108.6(5)	107.2(9)
C(4)-C(5)-C(6)	107.4(5)	107.8(8)
C(5)-C(6)-C(7)	108.4(5)	107.9(8)
C(6)-C(7)-C(3)	108.1(5)	108.5(8)
C(7)-C(3)-C(4)	106.2(5)	107.8(8)
C(7)-C(3)-O(3)	125.8(6)	127.8(8)
C(4)-C(3)-O(3)	127.7(6)	124.3(9)
Ru(1)-Cl(1)-M(1)	112.36(6)	110.08(10)
C(3)-O(3)-M(1)	127.9(4)	129.0(6)
M(1)-C(34)-N(1)	124.2(4)	131.3(7)
M(1)-C(34)-N(2)	132.0(4)	125.5(8)
N(1)-C(34)-N(2)	103.8(5)	103.2(9)
C(34)-N(1)-C(35)	111.8(5)	111.3(8)
N(1)-C(35)-C(36)	106.0(6)	107.3(9)
C(35)-C(36)-N(2)	107.4(6)	106.7(10)
C(36)-N(2)-C(34)	111.0(5)	111.4(10)
Ru(1)-C(1)-O(1)	175.5(7)	177.4(16)
Ru(1)-C(2)-O(2)	179.7(9)	174.4(10)

X-ray Crystallography

Crystal data and collection details for **4a·0.5CH₂Cl₂·0.5H₂O**, **4b**, **4d·0.5CH₂Cl₂**, **5f[Cl]·0.5CH₂Cl₂·0.5C₅H₁₂·0.25H₂O**, **6·0.5CHCl₃·0.5C₅H₁₂·0.5H₂O** and **2b[Cl]** (CCDC 1016378-1016383) are reported in Table 3. The diffraction experiments were carried out on a Bruker APEX II diffractometer equipped with a CCD detector using Mo–Kα radiation. Data were corrected for Lorentz polarization and absorption effects (empirical absorption correction SADABS).[38] Structures were solved by direct methods and refined by full-matrix least-squares based on all data using F^2.[39] All non-hydrogen atoms were refined with anisotropic displacement parameters unless otherwise stated. All hydrogen atoms were fixed at calculated positions and refined by a riding model.

4a·0.5CH₂Cl₂·0.5H₂O: The asymmetric unit of the unit cell contains one Ru-complex (located on a general position), one CH₂Cl₂ molecule disordered over two symmetry related (by 2) positions (occupancy factor 0.5) and half of a H₂O molecule (located on 2). The CH₂Cl₂ and H₂O molecules have been refined isotropically. Similar U restraints [SIMU line in SHELXL, *s.u.* 0.01] were applied to the CH₂Cl₂ molecule and its C-Cl distances restrained to 1.75 Å [*s.u.* 0.01]. The independent H-atom bonded to O(50) in the H₂O molecule has been located in the Fourier Map and refined isotropically using the 1.5 fold U_{iso} value of the parent O(50); the O(50)-H(50) distance was restrained to 0.87 Å [*s.u.* 0.01].

4b: The asymmetric unit of the unit cell contains one Ru-complex located on a general position. 4b crystallizes in very small and low-quality plate-like crystals. Therefore, the data have been cut at 2θ = 47.06° and several restraints have been applied during the refinement. Similar U restraints [SIMU line in SHELXL, *s.u.* 0.01] have applied to all the C-atoms. Some of the C and O atoms have been restrained to as isotropic like behavior [ISOR line in SHELXL, *s.u.* 0.01]. The aromatic rings have been constrained to fit regular hexagons [AFIX 66 line in SHELXL].

4d·0.5CH₂Cl₂: The asymmetric unit of the unit cell contains one Ru-complex (located on a general position) and half of a CH₂Cl₂ molecule located on a 2-fold axis. Similar *U* restraints [SIMU line in SHELXL, *s.u.* 0.01] have applied to all the C-atoms. H(6) bonded to O(6) has been located in the Fourier Map and refined isotropically using the 1.5 fold U_{iso} value of the parent O(6); the O(6)-H(6) distance was restrained to 0.89 Å [*s.u.* 0.02].

5e[Cl]·0.5CH₂Cl₂·0.5C₅H₁₂·0.25H₂O: The asymmetric unit of the unit cell contains two Ru-complexes (located on general positions), one CH₂Cl₂ molecule (on a general position), one C₅H₁₂ molecule (on a general position) and half of a H₂O molecule disordered over two symmetry related (by an inversion center) positions. It has not been possible to locate the H-atoms of the H₂O molecule. Similar *U* restraints [SIMU line in SHELXL, *s.u.* 0.005] have applied to all the C, O and N-atoms. Some of the C and O atoms have been restrained to as isotropic like behavior [ISOR line in SHELXL, *s.u.* 0.005]. The aromatic rings have been constrained to fit regular hexagons [AFIX 66 line in SHELXL]. Restraints to bond distances have been applied as follows [*s.u.* 0.01]: 1.75 Å to C-Cl in CH₂Cl₂; 1.53 Å to C-C in C₅H₁₂.

6·0.5CHCl₃·0.5C₅H₁₂·0.5H₂O: The asymmetric unit of the unit cell contains two Ru-complexes, one CHCl₃ molecule, one C₅H₁₂ molecule and one H₂O molecule (all located on general positions). The H₂O molecule is disordered over two independent positions and has been refined isotropically with one occupancy parameter. It has not been possible to located the H-atoms of the H2O molecule. The crystals appear to be pseudo-merohedrally twinned with twin matrix 1 0 0 0 -1 0 0 0 -1 and refined batch factor 0.2580(13). Similar *U*

restraints [SIMU line in SHELXL, *s.u.* 0.005] have applied to all the C-atoms. Some of the C and O atoms have been restrained to as isotropic like behavior [ISOR line in SHELXL, *s.u.* 0.01]. The aromatic rings have been constrained to fit regular hexagons [AFIX 66 line in SHELXL]. Restraints to bond distances have been applied as follows *[s.u.* 0.01]: 1.75 Å to C-Cl in CH_2Cl_2; 1.53 Å to C-C in C_5H_{12}.

2b[Cl]: The asymmetric unit of the unit cell contains one Ag complex located on a general position.

Table 2.3. Crystal data and experimental details for **4a·0.5CH₂Cl₂·0.5H₂O**, **4b**, **4d·0.5CH₂Cl₂**, **5f[Cl]·0.5CH₂Cl₂·0.5C₅H₁₂·0.25H₂O**, **6·0.5CHCl₃·0.5C₅H₁₂·0.5H₂O** and **2b[Cl]**.

	4a·0.5CH₂Cl₂·0.5H₂O	**4b**	**4d·0.5CH₂Cl₂**
Formula	$C_{38.5}H_{34}ClN_2O_{5.5}Ru$	$C_{50}H_{40}N_2O_5Ru$	$C_{39.5}H_{35}ClN_2O_6Ru$
Fw	749.2	849.91	770.22
T, K	295(2)	293(2)	294(2)
λ, Å	0.71073	0.71073	0.71073
Crystal system	Monoclinic	Monoclinic	Monoclinic
Space group	*P2/c*	*P2₁/n*	*C2/c*
a, Å	16.2736(16)	14.602(4)	24.188(4)
b, Å	13.5024(13)	15.790(4)	14.213(3)
c, Å	17.6132(17)	17.850(5)	24.171(4)
β, °	113.2960(10)	101.118(3)	117.822(2)
Cell Volume, Å³	3554.7(6)	4038.4(19)	7349(2)
Z	4	4	8
D_c, g cm⁻³	1.400	1.398	1.392
μ, mm⁻¹	0.563	0.440	0.547
F(000)	1536	1752	3160
Crystal size, mm	0.18×0.16×0.12	0.15×0.13×0.10	0.24×0.21×0.18
θlimits, °	1.66–25.66	1.65–23.53	1.72–25.02
Reflections collected	34990	31532	30056
Independent reflections	6728 [R_{int}= 0.0387]	6003 [R_{int}= 0.1717]	6287 [R_{int}= 0.0324]
Data / restraints /parameters	6728 / 8 / 732	6003 / 378 / 451	6287 / 211 / 450
Goodness on fit on F^2	1.048	0.966	1.051
R_1 (*I*> 2σ(*I*))	0.0427	0.0675	0.0327
wR_2 (all data)	0.1348	0.1946	0.1060
Largest diff. peak and hole, e Å⁻³	0.732 / –0.658	0.638 / –0.600	0.496 / –0.490

	5f[Cl]·0.5CH₂Cl₂·0.5C₅H₁₂·0.25H₂O	6·0.5CHCl₃·0.5C₅H₁₂·0.5H₂O	2b[Cl]
Formula	$C_{63}H_{67}AgCl_2N_2O_{5.25}Ru$	$C_{63}H_{66.5}Cl_{2.5}CuN_2O_{5.5}Ru$	$C_{17}H_{16}AgClN_2$
Fw	1216.03	1192.92	391.64
T, K	295(2)	291(2)	293(2)
λ, Å	0.71073	0.71073	0.71073
Crystal system	Monoclinic	Monoclinic	Triclinic
Space group	$P2_1/c$	$P2_1/c$	$P\bar{1}$
a, Å	15.6360(14)	15.469(3)	8.1352(9)
b, Å	20.8474(19)	20.983(5)	10.0028(11)
c, Å	38.030(4)	37.639(8)	10.5175(11)
α, °	90	90	88.1710(10)
β, °	90.6730(10)	90.260(3)	68.1080(10)
γ, °	90	90	85.0180(10)
Cell Volume, Å³	12396(2)	12217(5)	791.14(15)
Z	8	8	2
D_c, g cm⁻³	1.303	1.297	1.644
μ, mm⁻¹	0.693	0.753	1.437
F(000)	5008	4944	392
Crystal size, mm	0.19×0.16×0.13	0.19×0.16×0.14	0.21×0.19×0.12
θlimits, °	1.07–25.03	0.97–25.03	2.04–26.00
Reflections collected	116087	114878	8194
Independent reflections	21858 [R_{int}= 0.0524]	21522 [R_{int}= 0.0838]	3092 [R_{int}= 0.0176]
Data / restraints /parameters	21858 / 1014 / 1153	21522 / 909 / 1163	3092 / 0 / 190
Goodness on fit on F²	1.022	1.014	1.064
R_1 (*I*> 2σ(*I*))	0.0613	0.0812	0.0270
wR_2 (all data)	0.1956	0.2550	0.0667
Largest diff. peak and hole, e Å⁻³	1.313 / –0.759	0.939 / –1.064	0.643 / –0.268

References

[1] (a) G. C. Vougioukalakis and R. H. Grubbs, *Chem. Rev.,* **2010**, *110,* 1746; A. H. Hoveyda, S. J. Malcolmson, S. J. Meek and A. R. Zhugralin, *Angew. Chem. Int. Ed.,* **2010**, *49*, 34; (b) S. P. Nolan and H. Clavier, *Chem. Soc. Rev.,* **2010**, *39*, 3305.

[2] (a) S. Diez-Gonzalez, N. Marion and S. P. Nolan, *Chem. Rev.,* **2009**, *109*, 3612; (b) H. D. Velazquez and F. Verpoort, *Chem. Soc. Rev.,* **2012,** *41***,** 7032.

[3] (a) J. Witt, A. Pothig, F. E. Kuhn, W. Baratta, *Organometallics,* **2013**, *32*, 4042; (b) N. Gurbuz, E. O. Ozcan, I. Ozdemir, B. Cetinkaya, O. Sahin and O. Buyukgungor, *Dalton Trans.,* **2012**, *41*, 2330; (c) S. Horn, C. Gandolfi and M. Albrecht, *Eur. J. Inorg. Chem.,* **2011**, 2863; (d) S. Kuwata and T. Ikariya, *Chem. Eur. J.,* **2011**, *17*, 3542; (e) H. Ohara, W. W. N. O, A. J. Lough and R. H. Morris, *Dalton Trans.,* **2012**, *41*, 8797; (f) W. W. N. O, A. J. Lough and R. H. Morris, *Organometallics,* **2012**, *31*, 2137.

[4] T. Wang, C. Pranckevicius, C. L. Lund, M. J. Sgro and D. W. Stephan, *Organometallics*, **2013**, *32*, 2168 and references cited therein.

[5] E. Fogler, E. Balaraman, Y. Ben-David, G. Leitus, L. J. W. Shimon and D. Milstein, *Organometallics*, **2011**, *30*, 3826.

[6] (a) S. Urban, B. Beiring, N. Ortega, D. Paul and F. Glorius, *J. Am. Chem. Soc.,* **2012**, *134*, 1541; (b) J. Wysocki, N. Ortega and F. Glorius, *Angew. Chem. Int. Ed.,* **2014**, *53*, 8751.

[7] B. Kang, Z. Fu and S. H. Hong, *J. Am. Chem. Soc.,* **2013**, *135*, 11704.

[8] I. S. Makarov and R. Madsen*, J. Org. Chem.,* **2013**, *78*, 6593 and references cited therein.

[9] J. Balogh, A. M. Z. Slawin and S. P. Nolan, *Organometallics,* **2012**, *31*, 3259.

[10] (a) A. Prades, E. Peris and M. Albrecht, *Organometallics*, **2011**, *30*, 1162; (b) D. Canseco-Gonzalez and M. Albrecht, *Dalton Trans.,* **2013**, *42*, 7424.

[11] L. Bernet, R. Larlempuia, W. Ghattas, H. Mueller-Bunz, L. Vigara, A. Llobet and M. Albrecht, *Chem. Commun.,* **2011**, *47*, 8058.

[12] (a) O. Schuster, L. Yang, H. G. Raubenheimer and M. Albrecth, *Chem. Rev.,* **2009**, *109*, 3445; (b) K. M. Hindi, M. J. Panzer, C. A. Tessier, C. L. Cannon, W. J. Youngs, *Chem. Rev.,* **2009**, *109,* 3859; (c) A. Monney, M. Albrecht, *Coord. Chem. Rev.,* **2013**, *257*, 2420; (d) W. Liu, R. Gust, *Chem. Soc. Rev.,* **2013**, *42*, 755.

[13] (a) V. Leigh, W. Ghattas, R. Lalrempuia, H. Muller-Bunz, M. T. Pryce and M. Albrecht, *Inorg. Chem.,* **2013**, *52*, 5395; (b) S. Sinn, B.Schultze, C. Friebe, D. G. Brown, M. Jager, E. Altuntas, J. Kubel, O. Gunter, C. P. Berlinguette, B. Dietzek and U. S. Schubert, *Inorg. Chem.,* **2014**, *53*, 2083; (c) W.-C. Chang, H.-S. Chen, T.-Y. Li, N.-M. Hsu, Y. S. Tingare, C.-Y. Li, Y.-C. Liu, C. Su and W.-R. Li, *Angew. Chem., Int. Ed.,* **2010**, *49*, 8161.

[14] Selected reviews on *N*-heterocyclic carbenes: (a) L. A. Schaper, S. J. Hock, W. A. Herrmann and F. E. Kühn, *Angew. Chem., Int. Ed.,* **2013**, *52*, 270; (b) K. F. Donnelly, A. Petronilho and M. Albrecth, *Chem. Commun.,* **2013**, *49*, 1145; (c) L. Benhamou, E. Chardon, G. Lavigne, S. Bellemin-Laponnaz and V. César, *Chem. Rev.,* **2011**, *111*, 2705; (d) L. Mercs and M. Albrecht, *Chem. Soc. Rev.,* **2010**, *39*, 1903; (e) H. Jacobsen, A. Correa, A. Poater, C. Costabile and L. Cavallo, *Coord. Chem. Rev.,* **2009**, *253*, 687; (f) C. M. Crudden and D. P. Allen, *Coord. Chem. Rev.,* **2004**, *248*, 2247; (g) W. A. Herrmann, *Angew. Chem., Int. Ed.,* **2002**, *41*, 1290; (h) D. Bourissou, O. Guerret, F. P. Gabbai and G. Bertrand, *Chem. Rev.,* **2000**, *100*, 39.

[15] (a) M. C. Warner, C. P. Casey and J.-E. Backvall, *Top. Organomet. Chem.,* **2011**, *37*, 85; (b) B. L. Conley, M. K. Pennington-Boggio, E. Boz and T. J. Williams, *Chem. Rev.,* **2010**, *110*, 2294; (c) T. Pasini, G. Solinas, V. Zanotti, S. Albonetti, F. Cavani, A. Vaccari, A. Mazzanti, S. Ranieri and R. Mazzoni, *Dalton Trans.,* **2014**, *43*, 10224.

[16] (a) L. Busetto, M. C. Cassani, C. Femoni, M. Mancinelli, A. Mazzanti, R. Mazzoni and G. Solinas, *Organometallics,* **2011**, *30*, 5258; (b) M. C. Cassani, M. A. Brucka, C. Femoni, M. Mancinelli, A. Mazzanti, R. Mazzoni and G. Solinas, *New J. Chem.,* **2014**, *38*, 1768.

[17] (a) C. Cesari, L. Sambri, S. Zacchini, V. Zanotti and R. Mazzoni, *Organometallics,* **2014**, *33*, 2814; (b) M. Boiani, A. Baschieri, C. Cesari, R. Mazzoni, S. Stagni, S. Zacchini and L. Sambri, *New. J. Chem.,* **2012**, *36*, 1469.

[18] See for examples: (a) J. A. Cabeza and P. Garcia-Alvarez, *Chem. Soc. Rev.,* **2011**, *40*, 5389; (b) J. A. Cabeza, M. Damonte and E. Perez-Carreno, *Organometallics,* **2012**, *31*, 8355; (c) J. A. Cabeza, M. Damonte, P. Garcia-Alvarez and E. Perez-Carreno, *Chem. Commun.,* **2013**, *49*, 2813; (d) C. E. Ellul, M. F. Mahon, O. Saker and M. K. Whittlesey, *Angew. Chem. Int. Ed.,* **2007**, *46*, 6343; (e) L. Benhamou, J. Wolf, V. Cesar, A. Labande, R. Poli, N. Lugan and G. Lavigne, *Organometallics,* **2009**, *28*, 6981.

[19] F. H. Allen, O. Kennard, D. G. Watson, L. Brammer, A. G. Orpen and R. Taylor, *J. Chem. Soc., Perkin Trans.,* **1987**, *2*, S1-S19.

[20] O. Kuhl, *Coord. Chem. Rev.,* 2009, *253*, 2481.

[21] (a) D. G. Gusev, *Organometallics,* **2009**, *28*, 6458; (b) R. Tonner and G. Frenking, *Organometallics,* **2009**, *28*, 3901; (c) A. Furstner, M. Alcarazo, H. Krause and C. W. Lehmann, *J. Am. Chem. Soc.,* **2007**, *129*, 12676.

[22] Y. Yamamoto, Y. Miyabe, K. Itoh, *Eur. J. Inorg. Chem.* **2004**, 3651-3661.

[23] a) A. M. Oertel, V. Ritleng, L. Burr, C. Harwig and M. J. Chetcuti, *Organometallics,* **2011**, *30*, 6685; b) L. B. Benac, E. M. Burgess, L. Burr and A. J. Arduengo, *Organic Syntheses, Coll.,* **1990**, *7*, 195; **1986**, *64*, 92*.*

[24] S. Patil, J. Claffey, A. Deally, M. Hogan, B. Gleeson, L. M. Menéndez Méndez, H. Müller-Bunz, F. Paradisi and M. Tacke, *Eur. J. Inorg. Chem.,* **2010***, 7*, 1020.

[25] L. C. Branco, J. N. Rosa, J. J. Moura Ramos and C. A. M. Afonso, *Chem. Eur. J.,* **2002**, *8*, 3671.

[26] a) L. Jafarpour, E. D. Stevens and S. P. Nolan, *J. Organomet. Chem.,* **2000**, *606*, 49; b) A. J. Arduengo, R. Krafczyk, H. A. Schmutzler, J. Craig, R. Goerlich, W. J. Marshall and M. Unverzagt, *Tetrahedron*, **1999**, *55*, 14523.

[27] a) W. A. Herrmann, V. P. W. Böhm, C. W. K. Gstöttmayr, M. Grosche, C. P. Reisinger and T. Weskamp, *J. Organomet. Chem.*, **2001**, *616–617*, 616; b) E. C. Hurst, K. Wilson, I. J. S. Fairlamb and V. Chechick, *New J. Chem.*, **2009**, *33*, 1837.

[28] J. Liu, J. Chen, J. Zhao, Y. Zhao, L. Li and H. Zhang, *Synthesis*, **2003**, *17*, 2661.

[29] W. Chen and F. Liu, *J. Organomet. Chem.*, **2003**, *673*, 5.

[30] M. Bouhrara, E. Jeanneau, L. Veyre, C. Copéret and C. Thieuleux, *Dalton Trans.*, **2011**, *40*, 2995.

[31] S. Patil, A. Deally, F. Hackenberg, L. Kaps, H. Muller-Bunz, R. Schobert and M. Tacke *Helv. Chim. Acta*, **2011**, *94*, 1551.

[32] S. Hameury, P. de Frémont, P. -A. R. Breuil, H. Olivier-Bourbigou and P. Braunstein, *Dalton Trans.*, **2014**, *43*, 4700.

[33] X. Yu, B. O. Patrick and B. R. James, *Organometallics,* **2006**, *25*, 2359.

[34] D. V. Partyka and N. L. Deligonul, *Inorg. Chem.*, **2009**, *48*, 9463.

[35] J. Chun, H. S. Lee, I. G. Jung, S. W. Lee, H. J. Kim, and S. U. Son, *Organometallics,* **2010**, *29*, 1518.

[36] K. R. J. Thomas, M. Velusamy, J. T. Lin, C. H. Chuen and Y. T. Tao, *J. Mater. Chem.*, **2005**, *15*, 4453.

[37] Y. Mum, D. Czarkle, Y. Rahamlm and Y. Shvo, *Organometallics*, **1985**, *4*, 1461.

[38] G. M. Sheldrick, *SADABS*, Program for empirical absorption correction, University of Göttingen, Germany, **1996**.

[39] G. M. Sheldrick, *SHELX97*, Program for crystal structure determination, University of Göttingen, Germany, **1997**.

CHAPTER III

Ruthenium(0) complexes with triazolylidene spectator ligands: oxidative activation for (de)hydrogenation catalysis

Abstract

Transmetallation of silver triazolylidene intermediates with the ruthenium(0) precursor [Ru(Cp=O)(CO)$_2$]$_2$ afforded low-valent ruthenium(0) complexes containing a triazole-derived NHC ligand (Cp=O = 3,4-di(4-methoxyphenyl)-2,5-diphenyl-cyclopentadienone). Protonation of the carbonyl group of the Cp=O ligand significantly reduces the π character of the Ru–CO bond as deduced from v$_{CO}$ analysis. The new triazolylidene ruthenium(0) complexes were evaluated as catalyst precursors in transfer hydrogenation of 4-fluoro-acetophenone and in the acceptorless dehydrogenation of benzyl alcohol. Low activities were noted, though in both reactions, catalytic performance is markedly increased when cerium(IV) was added. Electrochemical analysis indicates that activation of the catalyst precursor proceeds via cerium-mediated oxidation of the ruthenium center, which facilitates dissociation of a CO ligand to enter the catalytic cycle. Such oxidative activation of catalyst precursors may be of more general scope.

Introduction

N-Heterocyclic carbenes (NHCs), as pointed out in the Chapter I, have become some of the most popular ligands in transition metal chemistry due to their efficiency as ancillary ligands to improve catalytic activity.[1] Their success is due to a combination of unique properties, such as their easily tuneable electronic and steric properties that influence the metal center and which allow catalytic activity to be rationally optimized. The exploitation of such concepts is particularly appealing because the synthesis of NHC ligand precursors as well as NHC metal complexes is fairly simple and highly versatile.[2]

Accordingly, a variety of catalytic reactions have strongly benefited from introduction of NHC ligands, such as ruthenium-catalyzed olefin metathesis,[3] palladium-catalyzed cross-coupling reaction,[4] iridium-catalyzed reductions and oxidations,[5] and gold-catalyzed activation of π-bonds, to name but a few.[6] Apart from olefin metathesis, NHC ruthenium complexes have shown catalytic activity in various redox transformations,[7] including: transfer hydrogenation,[8] hydrogenation of olefins[9] and esters,[10] asymmetric hydrogenation,[11] amide synthesis from alcohols and nitriles,[12] dehydrogenation of esters and imines from alcohols,[13] racemization of chiral alcohols,[14] oxidation of alcohols[15] and water oxidation[16] (for more details see chapter I, paragraph 1.2.1). Most of the literature on NHC ruthenium chemistry features ruthenium(II) complexes, while low-valent NHC ruthenium(0) systems are restricted to a few examples based on either [Ru$_3$(CO)$_{12}$] or [Ru(CO)$_2$(PPh$_3$)$_3$] as precursors.[17] In the chapter II a straightforward approach towards NHC ruthenium(0) complexes has been presented,[18] which is based on a dimeric ruthenium(0) cyclopentadienone dicarbonyl dimer (**3**).[19] Cleavage of the dimer in the presence of a free carbene or a silver carbene precursor provided access to a new class of ruthenium complexes (**4**).

Here we have expanded this synthetic methodology to 1,2,3-triazolylidenes as strong donor NHC-type ligands.[20] The present work has been carried out in collaboration with Prof. Martin Albrecht, a pioneer of this research area, in the UCD School of Chemistry and Chemical Biology, University College of Dublin.

The triazolylidenes are so-called abnormal carbenes (aNHC) because the binding to the metal center occurs *via* the C4 or C5 position, often the substitution pattern is chosen to block the C2 position. The triazolylidenes

are thus stabilized by only one nitrogen moiety, as the π-donating and σ-accepting properties of the second nitrogen atom are greatly reduced, in fact the donor properties can be significantly influenced by the number and position of heteroatoms within the heterocycle (Figure 3.1).
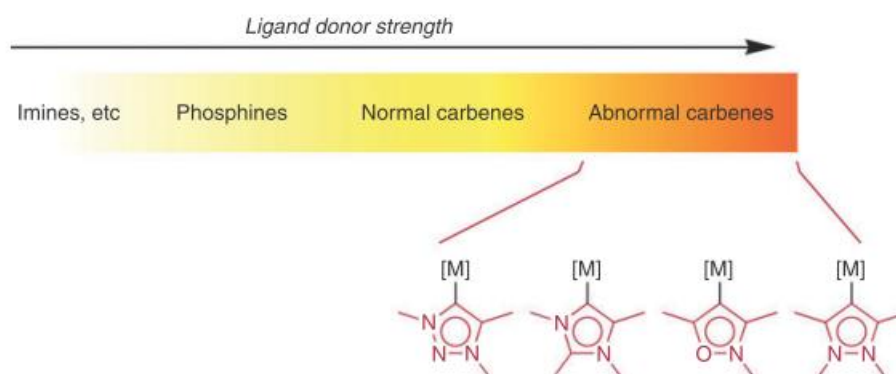
Figure 3.1 Schematic and simplified donor ability scale illustrating the donor ability of different abnormal NHC ligands.[20]

Such aNHC provide great scope for achieving different properties from so-called normal carbenes. They are considerably more electron-donating due to the reduced σ-withdrawal from the carbene center, in addition, they have been shown to be more π -accepting (due to reduced $p_\pi - p_\pi$ delocalization). The different properties of these ligands will naturally confer different properties and reactivity to the metal centers to which they are coordinated directly affecting the catalytic activity of the complexes.

Triazolylidenes offer a vast synthetic flexibility due to their convenient accessibility through [2+3] dipolar cycloaddition of alkynes and azides.[21] In addition, their enhanced donor properties as compared to more commonly utilized imidazolylidenes may further destabilize the ruthenium(0) oxidation state and hence facilitate substrate activation by metal/ligand cooperation in analogy to the reduced portion of Shvo's catalyst.[22] Thus, it will be of particular interest to evaluate the propensity of the new triazolylidene ruthenium(0) complexes to dehydrogenate substrates via formal H_2 transfer, as this process may lead to efficient catalysts for acceptorless oxidation (alcohol dehydrogenation) or transfer hydrogenation.

Results and Discussion

3.1 Synthesis of triazolylidene Ru complexes

The triazolium salts **10a-d**, readily accessible by "click" cycloaddition of the corresponding alkynes and azides and subsequent alkylation,[21] were successfully transformed into the silver triazolylidene intermediates as reported previously.[23] Transmetallation with the low-valent ruthenium precursor afforded complexes **11a–d** in very high yields (Scheme 3.1). Complexes **11** constitute a class of ruthenium(0) complexes which contain exclusively carbon-donor ligands.
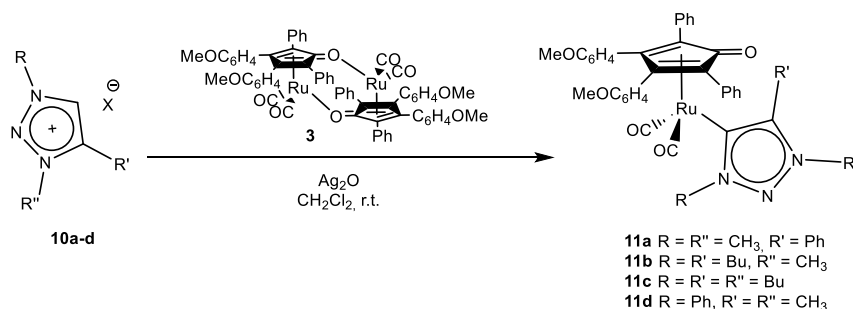
Scheme 3.1. Synthesis of cyclopentadienone triazolylidene ruthenium(0) complexes **11a-d**.

Formation of complexes **11a–d** was established by ^{1}H NMR, ^{13}C{^{1}H} NMR, and IR spectroscopy as well as ESI-MS and for representative examples, by single crystal X-ray diffraction analysis (see Experimental section). IR spectroscopy provided a particularly convenient methodology for monitoring the progress of the transmetallation reaction, as the Ru–CO stretch vibrations of the precursor complex shifted distinctly by 20 cm^{-1} to lower energy upon triazolylidene coordination (ν_{CO} = 2018, 1967 cm^{-1} in **3**, and 1999, 1938 cm^{-1} in **11b**, Table 3.1). The bathochromic shift is slightly but consistently more pronounced when the triazolylidene ligand contained only alkyl substituents, and less strong when a phenyl substituent is present, irrespective of the connectivity pattern. The carbene ligand in **11a** with the phenyl group attached to the carbon induced the same shift as the analogous carbene with the phenyl group attached to nitrogen (**11d**). These data suggest that the CO stretch vibration may be used as a probe for the qualitative assessment of the carbene donor properties.[23,24] In line with this notion, coordination of 2-imidazolylidenes induces a slightly smaller bathochromic shift ($\Delta\nu$= 4 cm^{-1}), which reflects their weaker donor properties when compared to triazolylidenes.[20a,b] Potentially, backbonding from the electron-rich ruthenium(0) center to the carbene ligand may affect the CO stretch vibration and may thus complicate a simple linear correlation between IR frequencies and donor properties.

Table 3.1. Relevant carbonyl stretch vibrations (cm^{-1}) of the complexes.

complex	Ru–CO	Cp=O
3	2018, 1967	---
11a	2004, 1945	1577
11b	1999, 1938	1583
11c	1998, 1937	1584
11d	2003, 1944	1578
11a + HBF$_4$	2036, 1979	---

Further evidence of the formation of complexes **11a–d** was obtained from NMR data, in particular the disappearance of the low field signal of the triazolium precursor in the ^{1}H NMR spectrum and the downfield shift of the carbenic resonance in the ^{13}C NMR spectra. This nucleus resonates in the 154–158 ppm range

and hence some 20 ppm higher field than in ruthenium(II) complexes, indicative for a low valent and electron-rich metal center (Figure 3.2).
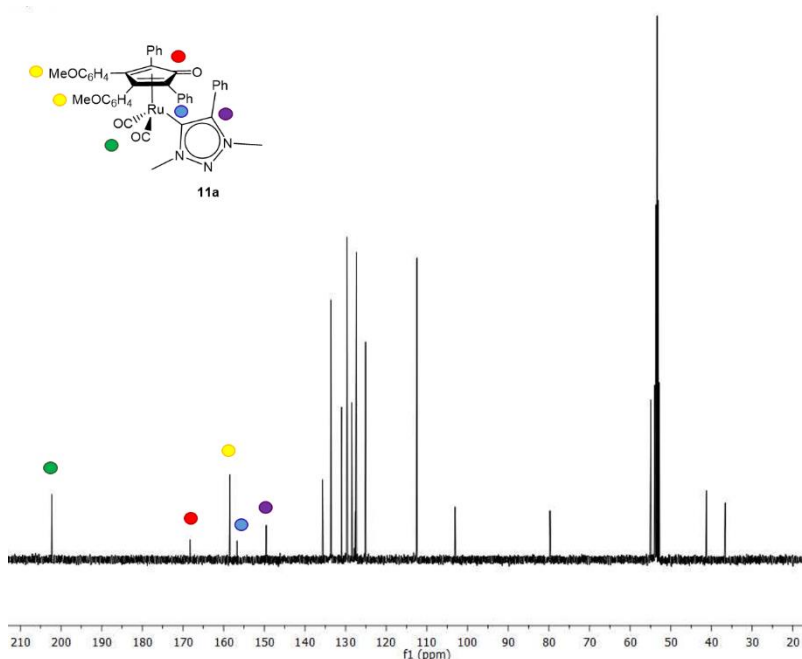
Figure 3.2 ^{13}C NMR spectrum of triazolylidene Ru complex **11a** in CD_2Cl_2.

Unambiguous structural evidence was obtained by X-ray diffraction analysis of single crystals of complexes **11a** and **11d**. The molecular structure reveals the expected piano-stool geometry with the cyclopentadienone ligand occupying one face and the two CO ligands and the triazolylidene forming the three legs (Figure 3.3). Bond lengths and angles (Table 3.2) are very similar in both complexes, suggesting only marginal steric consequences upon swapping the methyl and phenyl wingtip groups in the triazolylidene ligand. As expected, the Ru–C_{trz} bond is longer in complexes **11** than in analogues featuring a higher-valent ruthenium(II) metal center (Δd = 0.06 Å).[15]

Table 3.2. Selected bond lengths (Å) and angles (deg) for complexes **11a** and **11d**.

	11a	**11d**
Ru–C1	2.1196(12)	2.120(2)
Ru–C42	1.8965(13)	1.878(2)
Ru–C43	1.8825(13)	1.898(2)
Ru–Cg [a)]	1.930(<1)	1.932(<1)
C1–Ru–C42	95.18(5)	91.08(8)
C1–Ru–C43	91.66(6)	95.90(8)
C1–Ru–Cg [a)]	116.44(3)	115.02(5)
C42–Ru–Cg [a)]	125.76(4)	125.60(7)
C43–Ru–Cg [a)]	127.83(4)	127.44(6)
C42–Ru–C43	90.99(6)	92.96(9)
C11–O1	1.2464(14)	1.239(2)

a) Cg = centroid of cyclopentadienone ligand
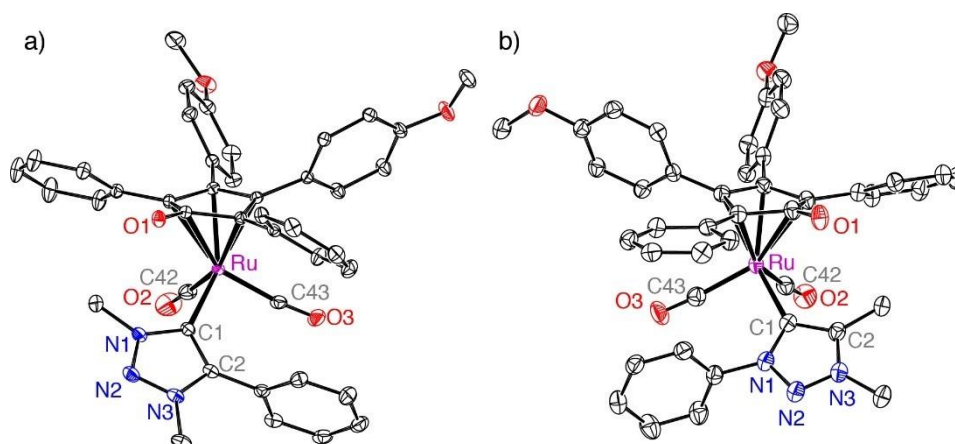
Figure 3.3. ORTEP representations (50% probability level, hydrogen atoms omitted for clarity) of complexes **11a** (a) and **11d** (b).

3.2 Catalytic alcohol oxidation

The triazolylidene Ru(0) complex **11a** was evaluated as catalyst precursor for the oxidation of alcohols using benzyl alcohol (BnOH) as model substrate. While ruthenium(II) systems with a cymene spectator ligand gave attractive conversions even in the absence of oxidants or base,[15] runs performed with **11a** in the absence of such additives were essentially non-productive with <5% conversion (Table 3.3, entry 1). Better results were obtained upon adding $[Ce(NO_3)_6](NH_4)_2$ (CAN) as oxidizing agent to activate the catalyst precursor **11a**.

Table 3.3. Ruthenium/cerium-catalyzed BnOH oxidation [a]
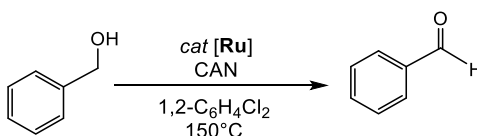
Entry	Ru^0 complex	mol% Ce^{IV}	Yield 2h (%)	Yield 24h (%)
1	**11a**	---	<5	<5
2	---	10	25	80
3	---	5	12	42
4	---	2.5	12	31
5	**11a**	10	57	97[b]
6	**11a**	5	24	85
7	**11a**	2.5	20	84
8	**3**	10	19	81

a) General conditions: 0.19 mmol BnOH, 5 mol% Ru^0 complex, 3 mL 1,2-$C_6H_4Cl_2$, mol% Ce^{IV} and Ru relative to BnOH; 150 °C, yield of PhCHO determined by ^{1}H NMR spectroscopy by using anisole as internal standard; b) reaction complete after 8 h.

Initial background measurements indicated that in the absence of a ruthenium complex, CAN catalyzes the oxidation of BnOH to benzaldehyde on its own under the applied reaction conditions. Background conversions reached 80% when 10 mol% CAN were used, and dropped to 40% and 30% approximately, if the CAN loading was reduced to 5 and 2.5 mol%, respectively (entries 2–4, Figures 3.9-3.11). Addition of complex **3**, *i.e.* the carbene-free ruthenium(0) precursor, had no notable effect and conversions mirrored those of CAN only (entry 8). Possibly, the lack of a stabilizing ligand for ruthenium(II) induces rapid decomposition, supported also by the brown color that rapidly developed upon heating the mixture. In contrast, complex **11a** induced a considerable acceleration (entries 5–7). For example, with 5 mol% **11a** and 2.5 mol% CAN, 84% conversion

were accomplished within 24 h (*cf.* 31% conversion in the background reaction). At higher CAN loading (10 mol%), the catalytic competence of **11a** is evident in particular at early stages of the oxidation. After 2 h, 57% conversion were observed with the Ru[0]/Ce[IV] couple (25% with Ce[IV] only, 0% with Ru[0] only), and oxidation was essentially complete after less than 8 h. Further improvement of the catalytic performance of **11a** may need to focus on an oxidant for ruthenium that is less catalytically active than CAN.

3.3 Catalytic transfer hydrogenation

In addition to alcohol dehydrogenation, we were also interested to see whether complexes **11** are active in transfer hydrogenation. A model reaction employed complex **11a** as catalyst precursor and 4-fluoroacetophenone as substrate under standard transfer hydrogenation conditions,[25] *i.e.* refluxing *i*PrOH as hydrogen source (Table 3.4).

Table 3.4. Catalytic transfer hydrogenation of 4-fluoroacetophenone.[a]
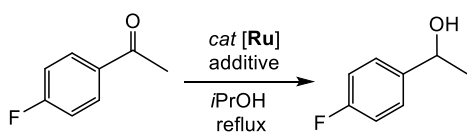
entry	**Ru⁰** complex	additive [b]	Yield 8h (%)	Yield 24h (%)
1	**11a**	---	0	<6
2	**3**	---	96	n.d.[c]
3	**11a**	KOH	0	<6
4	**3**	KOH	94	n.d.[c]
5	**11a**	HBF₄	<6	31
6	**3**	HBF₄	55	58
7	**11a**	CAN	58	88
8	**3**	CAN	0	6.5
9	**11a**	CAN + HBF₄	41	43
10	**11a**	CAN + KOH	<6	17

a) General conditions: Ruthenium complex (5 mol% Ru), *i*PrOH (5 mL), reflux; yield of alcohol determined by ¹H NMR spectroscopy, n.d. = not determined; b) quantities of additives as follows: HBF₄ 1 molequiv., KOH 2 molequiv., CAN 1 molequiv. per ruthenium center. c) n.d. = not determined due to complete conversion after 8h.

Catalytic runs were performed in particular for comparing the catalytic activity of the triazolylidene ruthenium(0) complex **11a** and the triazolylidene-free dimeric precursor **3** under various conditions. In the absence of any additives (entries 1,2), complex **11a** is inactive and essentially no conversion was observed, while precursor **3** reaches almost complete conversion within 8 h in pure *i*PrOH. Addition of KOH did not change the relative performance and conversions were indifferent to those in *i*PrOH only (entries 3,4). These results suggest that KOH is not a suitable additive for the activation of the ruthenium center in complex **11a**, probably because the electron-rich ruthenium(0) center has no affinity for binding a hard alkoxide ligand, nor for dissociation of a CO ligand due to the high donor properties of the triazolylidene ligand, which are assumed to enhance Ru-CO backbonding. Conversely, the activity observed for complex **3** probably arises from splitting of the dimeric precursor into two monomeric forms which, in the presence of a hydrogen source lead to a derivative of Shvo's catalyst (**A**, Figure 3.4).[22] Such complexes are well-known to catalyze the transfer hydrogenation of a broad range of ketones.
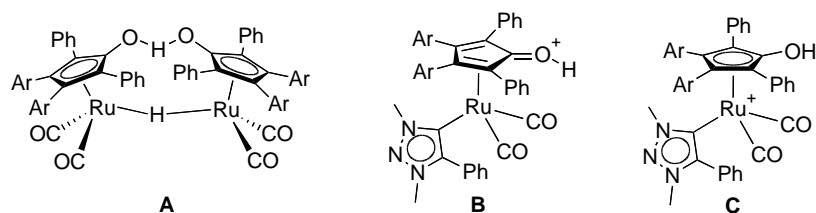
Figure 3.4. Shvo-type catalyst **A** resulting from cleavage of dimer **3** in *i*PrOH, and cationic complexes **B** and **C** from protonation of complex **11a**, featuring a ruthenium(0) and a ruthenium(II) center, respectively.

In an attempt to labilize the CO ligands, a proton source was introduced. Protonation at the dienone system has been reported and may provide a cationic structure with a positive charge either at the oxygen (complex **B**, Figure 3.4) or at the ruthenium center (**C**), thus inducing formal oxidation of the metal center to ruthenium(II) and depletion of electron density, which in turn is expected to substantially reduce the π character of the Ru–CO bond. Stoichiometric experiments using HCl (10 molequiv.) or HBF$_4$ (5 molequiv.) in CH$_2$Cl$_2$ with complex **11a** indeed gave cationic complexes in which the carbonyl stretch vibration was significantly shifted to higher frequency (v_{CO} = 2036 and 1979 cm^{-1}, *cf.* 2004 cm^{-1}, 1945 cm^{-1} in **11a**), and the ketone C=O vibration observed in **11a** for the Cp=O ligand disappeared in the cationic complexes. These data strongly suggesting formation of a cyclopentadienyl-type ligand as in complex **C**. Transfer hydrogenation in the presence of HBF$_4$ (1 equiv) did indeed increase the catalytic activity of complex **11** (entry 5), however the 30% conversion after 24 h are unremarkable when compared with other ruthenium carbene systems.[26] The dimeric complex **3** performs significantly less in the presence of acid (entry 6), in agreement with the formation of a Shvo-type active system from formal dihydrogen transfer rather than protonation. Best result for complex **11a** were obtained when using CAN as an oxidizing agent. Under these conditions, oxidation of the metal center from ruthenium(0) to ruthenium(II) takes place (see Electrochemical measurement), which weakens the bonding of CO and hence produces a methodology to activate the complex. In the presence of CAN, conversion of 4-fluoroacetophenone reaches 58% after 8 h and 89% after 24 h (entry 7). In contrast, CAN efficiently quenches the activity of complex **3** (entry 8). Hence, conditions have been developed that favor catalytic transfer hydrogenation using the dimer **3** but not **11a** (entries 1,2), and inversely, conditions that favor activity of complex **11a** but not **3** (entries 7,8). These results demonstrate the orthogonality induced upon bonding of a triazolylidene ligand. Addition of either base or acid to the CAN-activated complex **11a** are not advantageous and conversions were consistently lower (entries 9,10). Variation of the amount of CAN did not result in further enhancement of activity. Both lowering the amount to 0.25 or 0.5 equivalents relative to **11a** as well as increasing the amount to 2, 4 or 6 equivalents resulted in slower and generally incomplete conversion (Figure 3.12). In particular using excess CAN lead to substantial catalyst deactivation after around 5 h.

3.4 Electrochemical measurement

Electrochemical analysis of the triazolylidene ruthenium(0) complex **11a** by cyclic voltammetry measurements reveal a quasi-reversible oxidation of **11a** in CH$_2$Cl$_2$ solution with $E_{1/2}$ = +0.952(±3) *vs* SCE (Figure 3.5, Figure 3.14-Experimental). The redox process likely involves a Ru^0/Ru^I oxidation which is according to the peak-current ratio reversible at higher scan rates (i_{pc}/i_{pa} = 0.96 at 200 mV s^{-1}) and less reversible at slower scan rates (i_{pc}/i_{pa} = 0.56 at 20 mV s^{-1}), suggesting a slow chemical transformation of the oxidized species (EC mechanism).[27] The i_{pc}/i_{pa} ratio at different scan rates fits excellently with an irreversible first-order reaction after the oxidation process, with a rate constant k = 0.58 s^{-1} for the

homogeneous follow-up reaction (correlation > 0.99, Table 3.6, Figure 3.16-Experimental).

These data are in agreement with a metal-centered oxidation process and subsequent slow dissociation of CO from the coordination sphere due to the lower electron-density upon ruthenium oxidation (*cf.* CAN-mediated activity of **11a** in transfer hydrogenation). Consistent with this model, electrochemical analysis of **11a** measured in MeCN shows a largely irreversible oxidation process (E_{pa} = +0.96 V, (i_{pc}/i_{pa} = 0.64) even at high scan rates (500 mV s^{-1}; Figure 3.16). The coordinating properties of MeCN may thus accelerate the substitution of CO and thus the EC mechanism.
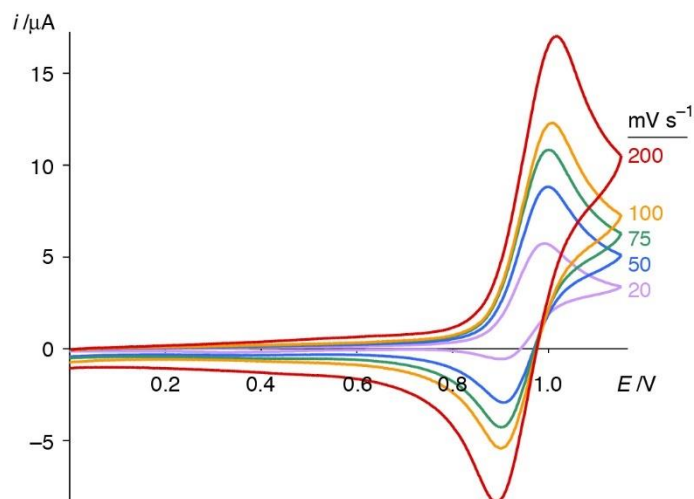
Figure 3.5. Cyclic voltammograms for **11a** in CH$_2$Cl$_2$ at different scan rates (potential *vs* SCE, Fc as internal standard).

Since the catalytic activity of the ruthenium complex **11a** was considerably enhanced when pre-activated with CAN, both for transfer hydrogenation and alcohol dehydrogenation, a series of electrochemical measurements was performed on **11a** in the presence of CAN. When 0.5 molequiv CAN were added to a solution of **11a** in MeCN, differential pulse voltammetry revealed three oxidation processes (Figure 3.6). The first process at E = +0.90 V pertains to the Ru^0/Ru^I oxidation of complex **11a** and was also observed in measurements without CAN,[28] and the second process with E = +1.06 V corresponds to a cerium-centered oxidation.[29] A third oxidation process at E = +1.22 V with equal ratio to the first process is assumed to belong to a new species resulting from oxidation of complex **11a** and has thus tentatively been attributed to a Ru^I/Ru^{II} oxidation. The equal relative intensity of the first and last oxidation process remains constant over several hours, suggesting an equilibrium. The 1:1 ratio indicates equal quantities of two ruthenium species, which agrees well with the provision of 0.5 molequiv CAN at the onset of the experiment and suggests a complete one-electron transfer from ruthenium(0) to cerium(IV), thus resulting in 50% **[11a]$^+$** and 50% of the parent complex **11a**. In support of such a model, no oxidation process at +0.9 V was detected after addition of 1 molequiv CAN, thus indicating absence of significant amounts of the original complex **11a**. Instead, only an oxidation process at E = +1.22 V was detected, together with the cerium-centered oxidation. These measurements are thus consistent with a CAN-mediated oxidation of the ruthenium-center in **11a** to ruthenium(II) by consumption of two equivalents of cerium(IV), and concomitant release of CO (EC mechanism) as a process for entering the catalytic cycle. Such processes require the presence of a stabilizing donor ligand such as the triazolylidene used in this study.
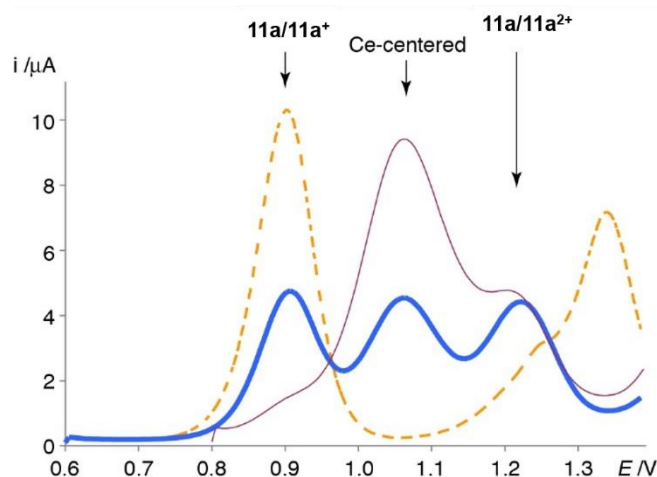
Figure 3.6. Relevant section of differential pulse voltammetry analysis of complex **11a** in presence of different equivalent of CAN: 0 equiv (orange dashed line), 0.5 equiv (blue bold line) and 1.0 equiv (red thin line; all measurements in MeCN at 50 mV s^{-1}, potential *vs* SCE, Fc as internal standard).

Conclusions

A set of ruthenium(0) complexes **11** has been prepared which contain differently substituted triazolylidene ligands, thus demonstrating the suitability of such strongly donating NHC ligands to stabilize low-valent metal centers. Catalytic activity in hydrogen transfer reactions has been evidenced, though oxidative activation with CAN as a potent auxiliary is required. For alcohol dehydrogenation, both CAN and the ruthenium complex are pre-catalysts and the relative quantities of the two components can be used to increase the relevance of either the Ce- or the Ru-catalyzed transformation. Detailed electrochemical analyses lend support to a fast two-step oxidation of the ruthenium center of **11** in order to enter the catalytic cycle, an activation process that is complementary to that of the dimeric ruthenium carbonyl complex **3**. Upon insertion of a triazolylidene ligand, loss of CO appears to be essential for the generation of an open coordination site for substrate coordination and catalytic turnover. Triazolylidene ligands with their strongly mesoionic character may be particularly useful for facilitating the metal oxidation and for entailing such catalyst activation. This concept may become particularly useful when employing other low-valent complexes as catalyst precursors and may provide an interesting opportunity for exploiting base metals in catalysis.

Experimental Section

Materials and procedures. The syntheses of the ruthenium complexes were carried out under an inert atmosphere of N_2 using Schlenk techniques and dry solvents. Purifications were performed in air using commercial solvents. ^1H and $^{13}C\{^1H\}$ NMR spectra were recorded at room temperature on Varian spectrometers operating at 400 or 500 MHz unless stated otherwise. Chemical shifts (δ in ppm, *J* in Hz) were referenced to SiMe$_4$. Signal assignments are based on homo- and heteronuclear (multiple-bond) correlation spectroscopy. Elemental analyses were performed by the Microanalytical Laboratory at the University College Dublin, Ireland. Infra-red spectra were recorded on a Perkin Elmer FTIR at 1 cm^{-1} resolution. Electrochemical studies were carried out on a Metrohm Autolab PGSTAT101 potentiostat using a gas-tight three electrode cell under an argon atmosphere. A platinum disk with 3.8 mm^2 surface area was used as the working electrode and was polished before each measurement. The reference electrode was Ag/AgCl, the counter electrode was a Pt wire. In all experiments, [Bu$_4$N]PF$_6$ (100 mM in dry CH$_2$Cl$_2$ or MeCN) was used as supporting electrolyte with analyte concentrations of approximately 1 mM. The redox potentials were referenced to ferrocenium/ferrocene (Fc$^+$/Fc; $E_{1/2}$ = 0.46 V *vs.* SCE in CH$_2$Cl$_2$; $E_{1/2}$ = 0.40 V *vs.* SCE in MeCN).[30] The ruthenium precursors **3**[28] and the triazolium salts **10a–d** were prepared according to literature procedures.[11] All other reagents were purchased from commercial sources and were used as received, unless otherwise stated.

Synthesis of the triazolylidene ruthenium complexes (11)

The triazolium salts **10a-d** were reacted at room temperature with Ag$_2$O (0.5 eq.) in CH$_2$Cl$_2$ solution under inert atmosphere and protected from light. After 2 h, the dimeric ruthenium precursor **3** (0.5 eq.) was added to the mixture and stirring continued for 2 h. The mixture was then filtered through a short pad of celite and filtrate was evaporated to yield the triazolylidene Ru(0) complexes **11a-d** in typically quantitative yield. Suitable crystals for X-Ray diffraction were obtained by slow diffusion of pentane into a CH$_2$Cl$_2$ solution of the complex.

11a R = R'' = CH$_3$, R' = Ph
11b R = R' = Bu, R'' = CH$_3$
11c R = R' = R'' = Bu
11d R = Ph, R' = R'' = CH$_3$
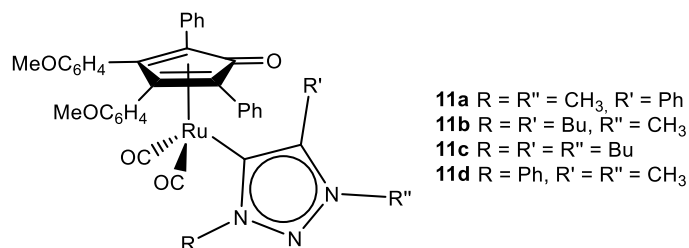
Figure 3.7 Structure of triazolylidene ruthenium complexes (**11**).

Dicarbonyl-(η^4-3,4-bis(4-methoxyphenyl)-2,5-diphenylcyclopenta-2,4-dienone)(1,3-dimethyl-4-phenyl-1,2,3-triazol-ylidene)ruthenium (11a): ^1H NMR (300 MHz, CD$_2$Cl$_2$): δ = 7.59–7.51 (m, 4H, CH$_{aryl}$), 7.32-7.01 (m, 15H, CH$_{aryl}$ + CH$_{Ph}$), 6.58–6.50 (m, 4H, CH$_{aryl}$), 3.63 (s, 6H, OCH$_3$), 3.61, 3.56 (2 × s, 3H, NCH$_3$); $^{13}C\{^1H\}$ NMR (400 MHz, CD$_2$Cl$_2$): δ = 203.11 (Ru–CO), 169.08 (C$_{Cp}$=O), 159.31 (COMe), 157.57 (Ru–C$_{trz}$), 150.38 (C$_{trz}$–Ph), 136.51 (C$_{aryl}$–Cp), 134.45 (CH$_{aryl}$), 131.83, 130.48, 129.33 (3 × C$_{Ph}$), 128.46 (CH$_{aryl}$), 128.19 (CH$_{aryl}$), 125.93 (C$_{aryl}$), 124.90 (CH$_{aryl}$), 113.34 (CH$_{aryl}$), 103.91 (C$_{2,5\ Cp}$), 80.59 (C$_{3,4\ Cp}$), 55.77 (OCH$_3$), 42.11, 37.48 (2 × NCH$_3$). IR (CH$_2$Cl$_2$) v$_{CO}$: 2004 cm^{-1}, 1945 cm^{-1}, 1577 cm^{-1}. ESI-MS (m/z) = 776 [M+H]$^+$; 798 [M+Na]$^+$. Anal. Calcd (%) for C$_{43}$H$_{35}$N$_3$O$_5$Ru (774.82): C, 66.66; H, 4.55; N 5.42. Found: C, 65.95; H, 4.64; N 5.34.

Dicarbonyl-(η^4-3,4-bis(4-methoxyphenyl)-2,5-diphenylcyclopenta-2,4-dienone)(1,4-dibutyl-3-methyl-1,2,3-triazolylidene)ruthenium (11b): ^{1}H NMR (300 MHz, CDCl$_3$): δ = 7.79–7.20 (m, 4H, CH$_{aryl}$), 7.37–6.63 (m, 10H, CH$_{aryl}$), 6.62–6.50 (m, 4H, CH$_{aryl}$), 3.81 (s, 3H, NCH$_3$), 3.63 (s, 6H, OCH$_3$), 3.61 (m, 2H, NCH$_2$), 1.87-1.03 (m, 10H, -–CH$_2$–), 0.73 (m, 6H, CH$_2$CH_3). ^{13}C{^{1}H} NMR (400 MHz, CDCl$_3$): δ = 202.90 (CO), 158.44 (COMe), 154.01 (Ru–C$_{trz}$), 148.55 (C$_{trz}$–Bu), 135.59 (C$_{aryl}$), 133.71 (CH$_{aryl}$), 129.11 (CH$_{aryl}$), 127.37 (CH), 125.25 (C$_{aryl}$), 125.06 (CH$_{aryl}$), 112.87 (CH$_{aryl}$), 103.85 (C$_{2,5\ Cp}$), 78.43 (C$_{3,4\ Cp}$), 55.02 (OCH$_3$), 53.31 (NCH$_2$), 36.05 (NCH$_3$), 32.08 (NCH$_2$CH_2), 31.24 (C$_{trz}$-CH_2), 23.55 (C$_{trz}$-CH$_2$CH_2), 22.38, 19.39 (2 × CH_2CH$_3$), 14.05, 13.60 (2 × CH$_2$CH_3). IR (CH$_2$Cl$_2$) v$_{CO}$: 1999 cm^{-1}, 1938 cm^{-1}, 1583 cm^{-1}.

Dicarbonyl-(η^4-3,4-bis(4-methoxyphenyl)-2,5-diphenylcyclopenta-2,4-dienone)(1,3,4-tributyl-1,2,3-triazolylidene)ruthenium (11c): ^{1}H NMR (300 MHz, CD$_2$Cl$_2$): δ = 7.70 (m, 4H, CH$_{aryl}$), 7.21-7.03 (m, 10H, CH$_{aryl}$), 6.66 (m, 4H, CH$_{aryl}$), 4.03 (m, 2H, NCH$_2$), 3.70 (s, 6H, -OCH$_3$), 3.64 (m, 2H, NCH$_2$), 1.79-1.04 (m, 14H, -CH$_2$, ^{n}Bu), 0.95-0.67 (m, 9H, -CH$_2$CH_3, ^{n}Bu); ^{13}C{^{1}H} NMR (400 MHz, CD$_2$Cl$_2$): δ = 204.09 (CO), 169.47 (C$_{Cp}$=O), 159.45 (COMe), 157.58 (Ru–C$_{trz}$), 148.96 (C$_{trz}$–Bu), 136.81 (C$_{aryl}$), 134.60 (CH$_{aryl}$), 129.90 (CH$_{aryl}$), 128.10 (CH), 126.36 (C$_{aryl}$), 125.80 (CH$_{aryl}$), 113.56 (CH$_{aryl}$), 104.48 (C$_{2,5\ Cp}$), 79.07 (C$_{3,4\ Cp}$), 55.82 (OCH$_3$), 50.13 (NCH$_2$), 34.96 (NCH$_3$), 32.77, 32.67 (2 x NCH$_2$CH_2), 32.19 (C$_{trz}$-CH_2), 24.28 (C$_{trz}$-CH$_2$CH_2), 23.18, 20.36, 20.17 (3 × CH_2CH$_3$), 14.63, 14.14, 14.09 (3 × CH$_2$CH_3). IR (CH$_2$Cl$_2$) v$_{CO}$: 1998 cm^{-1}, 1937 cm^{-1}, 1584 cm^{-1}.

Dicarbonyl-(η^4-3,4-bis(4-methoxyphenyl)-2,5-diphenylcyclopenta-2,4-dienone)(1-phenyl-3,4-dimethyl-1,2,3-triazol-ylidene)ruthenium (11d): ^{1}H NMR (300 MHz, CDCl$_3$) δ (ppm): 7.59–7.49 (m, 4H, CH$_{aryl}$), 7.28–6.92 (m, 15H, CH$_{aryl}$ + CH$_{Ph}$), 6.64–6.55 (m, 4H, CH$_{aryl}$), 3.87 (s, 3H, NCH$_3$), 3.66 (s, 6H, OCH$_3$), 1.79 (s, 3H, C$_{trz}$–CH$_3$); ^{13}C{^{1}H} NMR (400 MHz, CDCl$_3$): δ = 202.41 (CO), 167.75 (C$_{Cp}$=O), 159.84 (Ru–C$_{trz}$), 158.27 (COMe), 145.38 (C$_{trz}$–Me), 139.18 (C$_{aryl}$), 135.45–112.64 (C$_{aryl}$), 133.57, 129.54, 127.31 (3 × C$_{Ph}$), 103.34 (C$_{2,5\ Cp}$), 79.72 (C$_{3,4\ Cp}$), 54.95 (OCH$_3$), 35.99 (NCH$_3$), 10.53 (C$_{trz}$–CH$_3$). ESI-MS (m/z): 798 [M+Na]$^+$. IR (CH$_2$Cl$_2$) v$_{CO}$: 2003 cm^{-1}, 1944 cm^{-1}, 1578 cm^{-1}.

General condition for alcohol oxidation
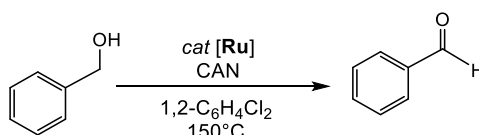
Figure 3.8 Oxidation of BnOH catalyzed by Ruthenium/CAN.

Complex **11a** (7.4 mg, 9.5 μmol, 5 mol%), 1,2-dichlorobenzene (3 mL), and the appropriate amount of [Ce(NH$_3$)$_6$](NO$_3$)$_2$ dissolved in MeCN (0.5 mL) were stirred at reflux for 15 min. Benzyl alcohol (20 μL, 190 μmol) was then added. Aliquotes (0.05 mL) were taken from the mixture at selected intervals, diluted with CDCl$_3$ (0.5 mL) and conversions were determined by ^{1}H NMR spectroscopy.

General conditions for transfer hydrogenation
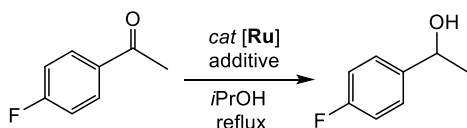
Figure 3.9 Catalytic transfer hydrogenation of 4-fluoroacetophenone.

Complex **11a** (12 mg, 15 µmol, 5 mol%), CAN (8 mg, 15 µmol, 5 mol%) and *i*PrOH (5 mL) were stirred at reflux for 15 min. Then 4-fluoroacetophenone (36 µL, 300 µmol) was added and samples were taken at regular intervals. Aliquots (ca. 0.05mL) were diluted with $CDCl_3$ (0.5 mL) and conversions were determined by ^1H NMR spectroscopy.

Crystallographic details

Crystal data for complexes **11a** and **11d** were collected by using an Agilent Technologies SuperNova A diffractometer fitted with an Atlas detector using Mo-K_α radiation (0.71073 Å; **11a**) or Cu-K_α radiation (1.54184 Å; **11d**). A complete dataset was collected, assuming that the Friedel pairs are not equivalent. An analytical numeric absorption correction was performed.[31] The structure was solved by direct methods using SHELXS-97[32] and refined by full-matrix least-squares fitting on F^2 for all data using SHELXL-97.[32] Hydrogen atoms were added at calculated positions and refined by using a riding model. Their isotropic temperature factors were fixed to 1.2 times (1.5 times for methyl groups) the equivalent isotropic displacement parameters of the carbon atom the H-atom is attached to. Anisotropic thermal displacement parameters were used for all nonhydrogen atoms.

Table 3.5 Crystallographic details for complexes **11a** and **11d**

CCDC No.	1043258		1043259	
Empirical formula	$C_{43}H_{35}N_3O_5Ru$		$C_{43}H_{35}N_3O_5Ru$	
Formula weight	774.81		774.81	
Temperature	100(2) K		100(2) K	
Wavelength	0.71073 Å		1.54184 Å	
Crystal system	Monoclinic		Triclinic	
Space group	P2$_1$/n (#14)		P–1 (#2)	
Unit cell dimensions	a = 14.2501(1) Å		a = 11.59996(7) Å	α = 96.3043(6)°
	b = 12.8432(1) Å	β = 91.0445(6)°	b = 12.4497(1) Å	β = 107.6103(6)°
	c = 19.6923(2) Å		c = 13.3559(1) Å	γ = 105.4593(6)°
Volume	3603.42(5) Å^3		1733.40(2) Å^3	
Z	4		2	
Density (calculated)	1.428 Mg m^{-3}		1.484 Mg m^{-3}	
Absorption coefficient	0.486 mm^{-1}		4.088 mm^{-1}	
F(000)	1592		796	
Crystal size	0.3520 x 0.2699 x 0.1758 mm^3		0.2053 x 0.1485 x 0.0444 mm^3	
θ range for data collection	2.86 to 32.88°		3.55 to 76.91°	
Reflections collected	112232		69936	
Independent reflections	12821 [R(int) = 0.0412]		7272 [R(int) = 0.0366]	
Completeness to θ = 32.00°	98.9 %		99.4 %	
Absorption correction	Analytical		Analytical	
Max. and min. transmission	0.932 and 0.882		0.867 and 0.588	
Refinement method	Full–matrix least–squares on F^2		Full–matrix least–squares on F^2	
Data / restraints / parameters	12821 / 0 / 609		7272 / 0 / 473	
Goodness–of–fit on F^2	1.062		1.063	
Final R indices [I>2$\square$(I)]	R1 = 0.0276, wR2 = 0.0633		R1 = 0.0262, wR2 = 0.0657	
R indices (all data)	R1 = 0.0361, wR2 = 0.0680		R1 = 0.0280, wR2 = 0.0667	
Largest diff. peak and hole	0.651 and –0.562 e Å^{-3}		0.842 and –0.659 eÅ^{-3}	

Time-conversion profiles

Selected profiles of the conversion in the function of time are summarized in the following.
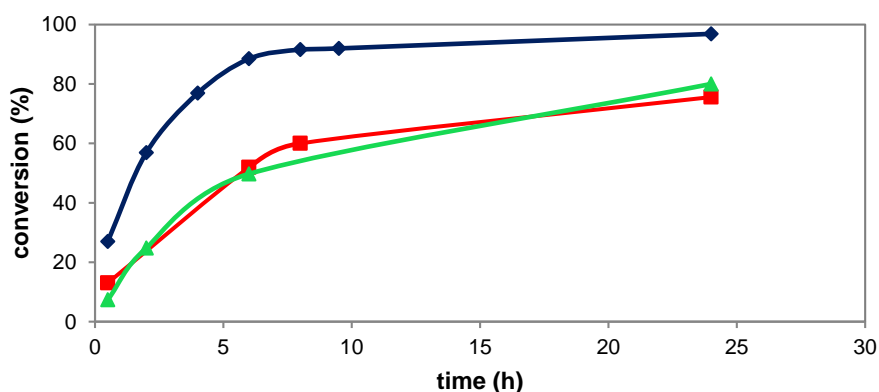
Figure 3.10 Comparison of conversion for the alcohol oxidation of BnOH with 2 equivalents of CAN using as pre-catalyst the ruthenium dimer (▲), the carbene complex **11a** (♦), and the blank without any precursor (■)
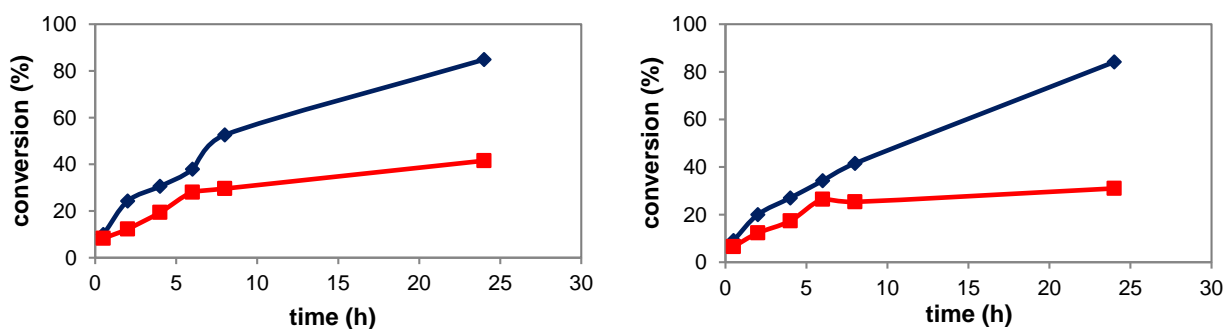
Figure 3.11 Comparison of conversions for the alcohol oxidation of BnOH with complex **11a** as pre-catalyst (♦), and the blank without any precursor (■) with 0.5 molequiv CAN (*left*) and 1 molequiv CAN (*right*) relative to **11a**.
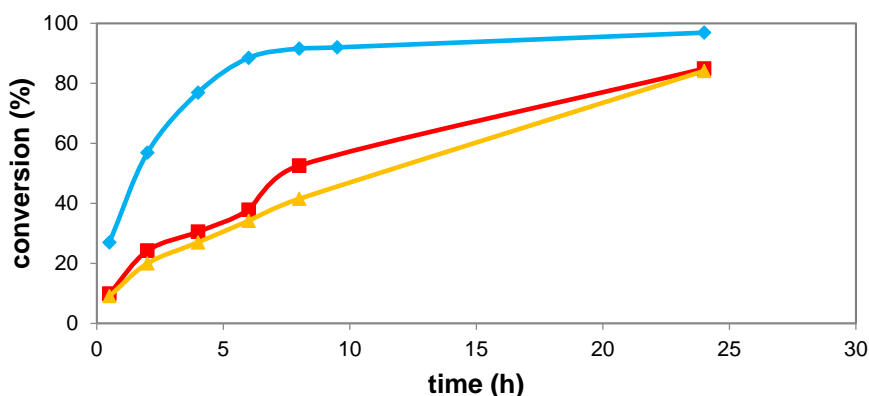
Figure 3.12 Comparison of conversions for the alcohol oxidation of BnOH with 5 mol% complex **11a** as pre-catalyst with 2 equivalents (♦),1 equivalent (■) and 0.5 equivalent (▲) of CAN as activator.
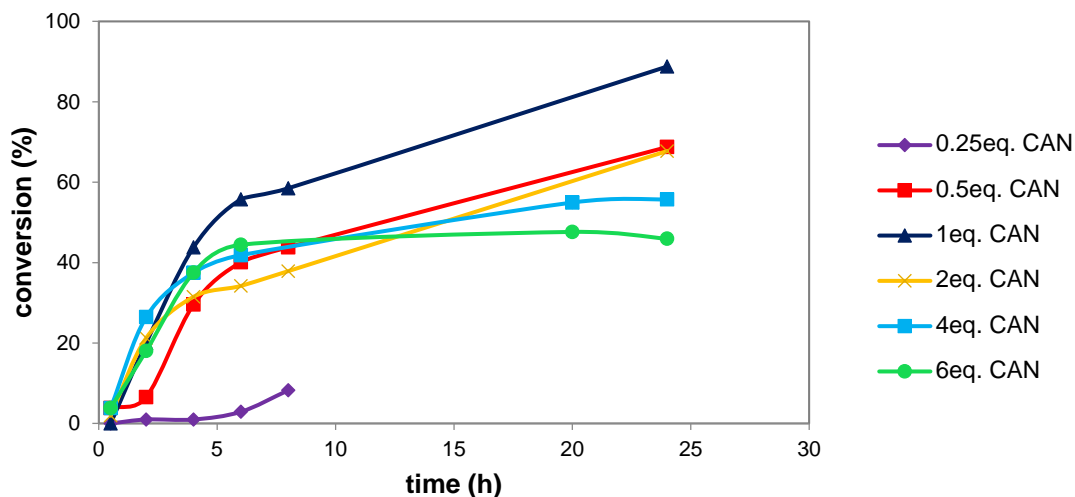
Figure 3.13 Comparison of the catalytic results for the transfer hydrogenation of 4-fluoroacetophenone with **11a** in the presence of different amounts of CAN. Best results were obtained with stoichiometric quantities of the oxidazing agent; lower amounts of CAN give a lower conversion, probably due to a higher induction time. Higher CAN concentrations induced catalyst deactivation after 4–8 h and gave incomplete conversions. A blank experiment using 10 mol% CAN showed no conversion.

Electrochemical analysis

Further details on the electrochemical analysis performed on **11a** are depicted in Figure 3.13 and 3.16 and in Table 3.6.
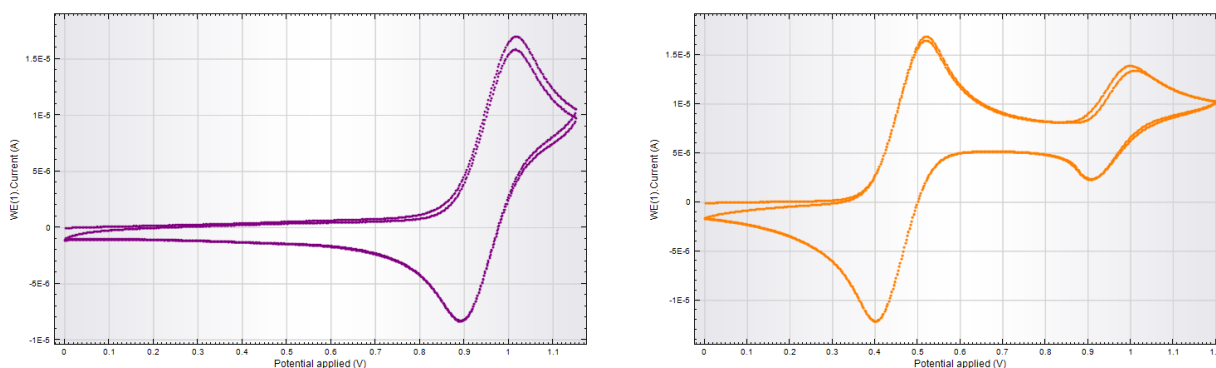
Figure 3.14 Cyclic Voltammetry of **11a** in CH_2Cl_2 at 200 mV s^{-1} (*left*) and in the presence of ferrocene (*right*): E_{pc} = 1.013 V and E_{pa} = 0.894 V, hence $E_{1/2}$ = 0.953 V (ΔE = 120 mV); i_{pa} = 17.0 □A and i_{pc} = 16.3 □A, thus i_{pc}/i_{pa} = 0.96.

Table 3.6 Scan rate dependence of the +0.95 V oxidation of complex **11a**.

Scan rate	$E_{1/2}$ (V)	ΔE (mV)	i_{pc}/i_{pa}
20 mV s^{-1}	0.946	90.3	0.56
50 mV s^{-1}	0.953	95.2	0.80
75 mV s^{-1}	0.954	111	0.84
100 mV s^{-1}	0.956	110	0.91
200 mV s^{-1}	0.953	120	0.96
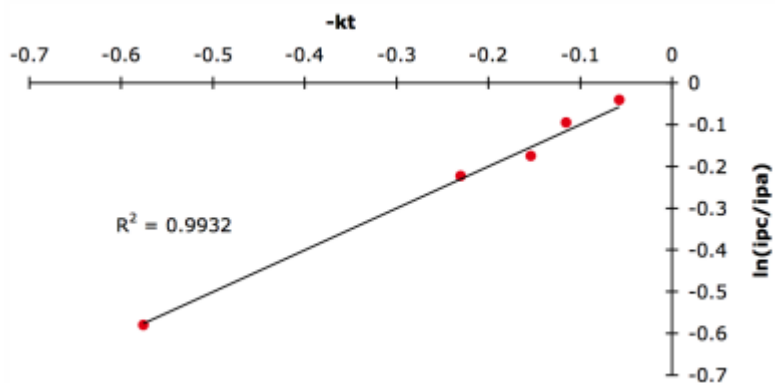
Figure 3.15 Analysis of i_{pc}/i_{pa} ratios at different scan rates provides a linear fit for a coupled first-order irreversible follow-up reaction to the oxidation (EC mechanism) with a first-order rate constant k = 0.58 s^{-1} (t = time between passing the $E_{1/2}$ potential and reaching the switching potential E_{max}, here 0.95 V and 1.15 V, respectively).
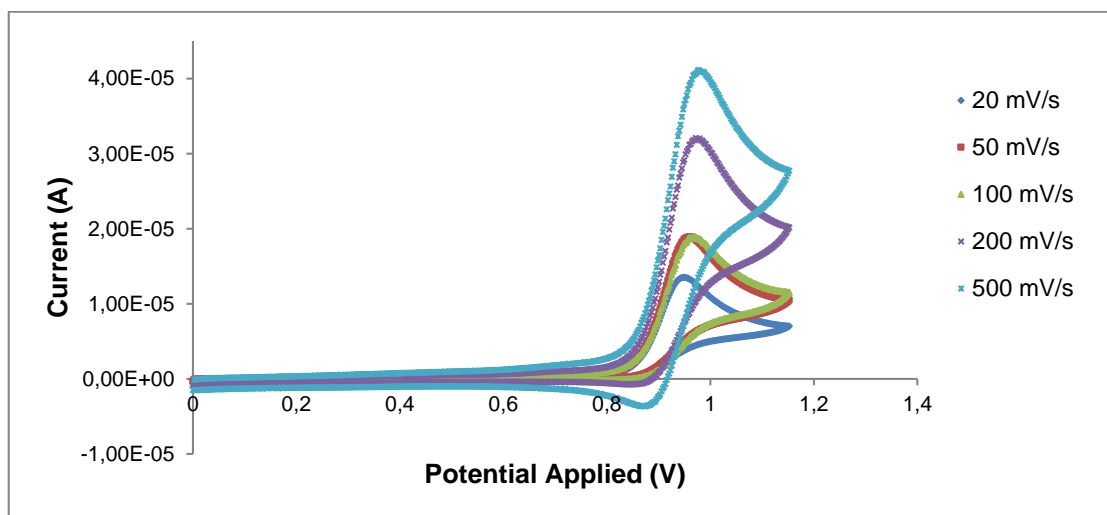
Figure 3.16 Cyclic Voltammetry diagrams of **11a** in MeCN with different scan rates.
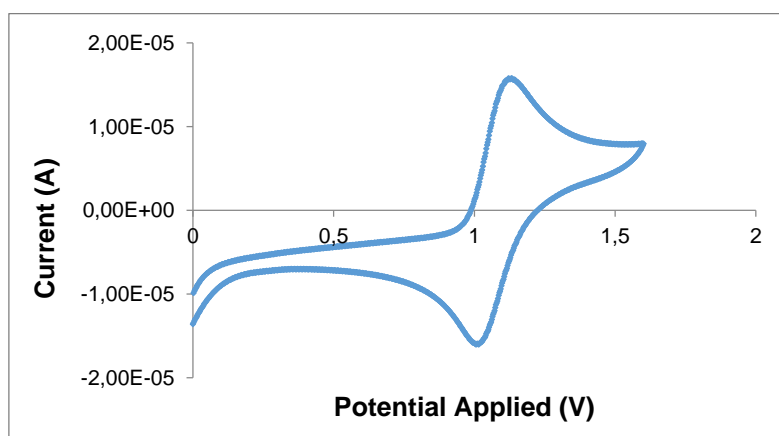
Figure 3.17 Cyclic voltammogram of CAN measured in MeCN at 100 mV s^{-1}.

References

[1] For selected reviews, see: a) D. Bourissou, O. Guerret, F. P. Gabbai, G. Bertrand, *Chem. Rev.* **2000**, *100*, 39; b) W. A. Herrmann, *Angew. Chem. Int. Ed.* **2002**, *41*, 1290; c) C. M. Crudden, D. P. Allen, *Coord. Chem. Rev.* **2004**, *248*, 2247; d) M. Poyatos, J. A. Mata, E. Peris, *Chem. Rev.* **2009**, *109*, 3677; e) O. Schuster, L. Yang, H. G. Raubenheimer, M. Albrecht, *Chem. Rev.* **2009**, *109*, 3445; f) L. Mercs, M. Albrecht, *Chem. Soc. Rev.* **2010**, *39*, 1903; g) S. P. Nolan, *N-heterocyclic carbenes*, Wiley-VCH

[2] For reviews, see: a) F. E. Hahn, M. C. Jahnke, *Angew. Chem. Int. Ed.* **2008**, *47*, 3122; b) M. Melaimi, M. Soleilhavoup, G. Bertrand, *Angew. Chem. Int. Ed.* **2010**, *49*, 8810. c) L. Benhamou, E. Chardon, G. Lavigne, S. Bellemin-Laponnaz, V. Cesar, *Chem. Rev.* **2011**, *111*, 2705. d) L. A. Schaper, S. J. Hock, W. A. Herrmann, F. E. Kühn, *Angew. Chem. Int. Ed.* **2013**, *52*, 270.

[3] a) C. Samojlowicz, M. Bieniek, K. Grela, *Chem. Rev.* **2009**, *109*, 3708; b) S. Monfette, D. E. Fogg, *Chem. Rev.* **2009**, *109*, 3783; c) G. C. Vougioukalakis, R. H. Grubbs, *Chem. Rev.* **2010**, *110*, 1746.

[4] a) E. A. B. Kantchev, C. J. O'Brien, M. G. Organ, *Angew. Chem. Int. Ed.* **2007**, *46*, 2768; b) G. C. Fortman, S. P. Nolan, *Chem. Soc. Rev.* **2011**, *40*, 5151.

[5] For examples, see: a) R. Corberan, E. Peris, *Organometallics* **2008**, *27*, 1954; b) A. Savini, G. Bellachioma, G. Ciancaleoni, C. Zuccaccia, D. Zuccaccia, A. Macchioni, *Chem. Commun.* **2010**, *46*, 9218; c) A. Petronilho, J. A. Woods, H. Mueller-Bunz, S. Bernhard, M. Albrecht, *Chem. Eur. J.* **2014**, *20*, 15775

[6] a) A. Fürstner, P. W. Davies, *Angew. Chem. Int. Ed.* **2007**, *46*, 3410; b) N. Marion, S. P. Nolan, *Chem. Soc. Rev.* **2008**, *37*, 1776; c) A. S. K. Hashmi, *Angew. Chem. Int. Ed.* **2008**, *47*, 6754.

[7] a) S. Diez-Gonzalez, N. Marion and S. P. Nolan, Chem. Rev. 109 (2009) 3612; b) H. D. Velazquez, F. Verpoort, *Chem. Soc. Rev.* **2012**, *41*, 7032.

[8] (a) J. Witt, A. Pothig, F. E. Kuhn, W. Baratta, *Organometallics* **2013**, *32*, 4042; b) N. Gurbuz, E. O. Ozcan, I. Ozdemir, B. Cetinkaya, O. Sahin, O. Buyukgungor, *Dalton Trans.* **2012**, *41*, 2330; c) S. Horn, C. Gandolfi, M. Albrecht, *Eur. J. Inorg. Chem.* **2011**, 2863; d) S. Kuwata, T. Ikariya, *Chem. Eur. J.* **2011**, *17*, 3542; e) H. Ohara, W. W. N. O, A. J. Lough, R. H. Morris, *Dalton Trans.* **2012**, *41*, 8797; f) W. W. N. O, A. J. Lough, R. H. Morris, *Organometallics* **2012**, *31*, 2137.

[9] a) C. Gandolfi, M. Heckenroth, A. Neels, G. Laurenczy, M. Albrecht, *Organometallics* **2009**, *28*, 5112; b) T. Wang, C. Pranckevicius, C. L. Lund, M. J. Sgro, D. W. Stephan, *Organometallics* **2013**, *32*, 2168; c) B. Bagh, D. W. Stephan *Dalton Trans.* **2014**, *43*, 15638; via transfer hydrogenation: d) S. Horn, M. Albrecht, *Chem. Commun.* **2011**, *47*, 8802.

[10] E. Fogler, E. Balaraman, Y. Ben-David, G. Leitus, L. J. W. Shimon, D. Milstein, *Organometallics* **2011**, *30*, 3826.

[11] (a) S. Urban, B. Beiring, N. Ortega, D. Paul, F. Glorius, J. *Am. Chem. Soc.* **2012**, *134*, 1541; b) J. Wysocki, N. Ortega, F. Glorius, *Angew. Chem. Int. Ed.* **2014**, *53*, 8751.

[12] B. Kang, Z. Fu, S. H. Hong, *J. Am. Chem. Soc.* **2013**, *135*, 11704.

[13] I. S. Makarov, R. Madsen*, J. Org. Chem.* **2013**, *78*, 6593.

[14] J. Balogh, A. M. Z. Slawin, S. P. Nolan, *Organometallics* **2012**, *31*, 3259.

[15] a) A. Prades, E. Peris, M. Albrecht, *Organometallics* **2011**, *30*, 1162; b) A. Solvhoj, R. Madsen, *Organometallics* **2011**, *30*, 6044; c) D. Canseco-Gonzalez, M. Albrecht, *Dalton Trans.* **2013**, *42*, 7424; d) M. Delgado-Rebollo, D. Canseco-Gonzalez, M. Hollering, H. Müller-Bunz, M. Albrecht, *Dalton Trans.* **2014**, *43*, 4462; e) B. Bagh, A. M. McKinty, A. J. Lough, D. W. Stephan, *Dalton Trans.* **2014**, *43*, 12842.

[16] L. Bernet, R. Larlempuia, W. Ghattas, H. Mueller-Bunz, L. Vigara, A. Llobet, M. Albrecht, *Chem. Commun.* **2011**, *47*, 8058.

[17] a) J. A. Cabeza, P. Garcia-Alvarez, *Chem. Soc. Rev.* **2011**, *40*, 5389; b) J. A. Cabeza, M. Damonte, E. Perez-Carreno, *Organometallics* **2012**, *31*, 8355; c) J. A. Cabeza, M. Damonte, P. Garcia-Alvarez, E. Perez-Carreno, *Chem. Commun.* **2013**, *49*, 2813; d) C. E. Ellul, M. F. Mahon, O. Saker, M. K. Whittlesey*, Angew. Chem. Int. Ed.* **2007**, *46*, 6343; e) L. Benhamou, J. Wolf, V. Cesar, A. Labande, R. Poli, N. Lugan, G. Lavigne, *Organometallics* **2009**, *28*, 6981.

[18] C. Cesari, S. Conti, S. Zacchini, V. Zanotti, M. C. Cassani, R. Mazzoni, *Dalton Trans.* **2014**, *43*, 17240.

[19] a) C. Cesari, L. Sambri, S. Zacchini, V. Zanotti, R. Mazzoni, *Organometallics* **2014**, *33*, 2814; (b) M. Boiani, A. Baschieri, C. Cesari, R. Mazzoni, S. Stagni, S. Zacchini, L. Sambri, *New. J. Chem.* **2012**, *36*, 1469.

[20] a) P. Mathew, A. Neels, M. Albrecht, *J. Am. Chem. Soc.* **2008**, *130*, 13534; b) K. F. Donnelly, A. Petronilho, M. Albrecht, *Chem. Commun.* **2013**, *49*, 1145; c) G. Guisado-Barrios, J. Bouffard, B. Donnadieu, G. Bertrand, *Angew. Chem. Int. Ed.* **2010**, *49*, 4759. For recent applications of triazolylidenes as ligands, see *e.g.*: d) J. A. Woods, R. Lalrempuia, A. Petronilho, N. D. McDaniel, H. Müller-Bunz, M. Albrecht, S. Bernhard, *Energy Env. Sci.* **2014**, *7*, 2316; e) D. Canseco-Gonzalez, A. Petronilho, H. Müller-Bunz, K. Ohmatsu, T. Ooi, M. Albrecht, *J. Am. Chem. Soc.* **2013**, *135*, 13193.

[21] a) V. V. Rostovtsev, L. G. Green, V. V. Fokin, K. B. Sharpless, *Angew. Chem. Int. Ed.* **2002**, *41*, 2596; b) F. Himo, T. Lovell, R. Hilgraf, V. V. Rostovtsev, L. Noodleman, K. B. Sharpless, V. V. Fokin, *J. Am. Chem. Soc.* **2005**, *127*, 210; c) V. D. Bock, H. Hiemstra, J. H. van Maarseveen, *Eur. J. Org. Chem.* **2006**, 51; d) J. E. Moses, A. D. Moorhouse, *Chem. Soc. Rev.* **2007**, *36*, 1249; e) J. E. Hein, V. V. Fokin, *Chem. Soc. Rev.* **2010**, *39*, 1302.

[22] Y. Shvo, D. Czarkie, Y. Rahamim, D. F. Chodosh, *J. Am. Chem. Soc.* **1986**, *108*, 7400; b) M. C. Warner, O. Verho, J.-E. Bäckvall, *J. Am. Chem. Soc.* **2011**, *133*, 2820; c) Conley, B. L.; Pennington-Boggio M. K.; Boz, E.; Williams, T. J.; *Chem. Rev.* **2010**, *110*, 2294-2312.

[23] A. Poulain, D. Canseco-González, R. Hynes-Roche, H. Müller-Bunz, O. Schuster, H. Stoeckli-Evans, A. Neels, M. Albrecht, *Organometallics* **2011**, *30*, 1021.

[24] a) A. R. Chianese, X. Li, M. C. Janzen, J. W. Faller, R. H. Crabtree, *Organometallics* **2003**, *22*, 1663; b) R. A. Kelly, H. Clavier, S. Guidice, N. M. Scott, E. D. Stevens, J. Bordner, I. Samardjiev, C. D. Hoff, L. Cavallo, S. P. Nolan, *Organometallics* **2008**, *27*, 202.

[25] a) G. Zassinovich, G. Mestroni, S. Gladiali, *Chem. Rev.* **1992**, *92*, 1051; b) R. Noyori, S. Hashiguchi, *Acc. Chem. Res.* **1997**, *30*, 97; c) S. Gladiali, E. Alberico, *Chem. Soc. Rev.* **2006**, *35*, 226; (d) J. S. M. Samec, J.-E. Bäckvall, P. G.Andersson, P. Brandt, *Chem. Soc. Rev.* **2006**, *35*, 237.

[26] A. Prades, M. Viciano, M. Sanau, E. Peris, *Organometallics*, **2008**, *27*, 4254.

[27] J. Heinze, *Angew. Chem. Int. Ed. Engl.* **1984**, *23*, 831.

[28] A second oxidation process with E_{pa} = +1.34 V is probably a consequence of the EC process mentioned above.

[29] CAN in dry MeCN displays a reversible oxidation at $E_{1/2}$ = 1.069 V (ΔE = 126 mV, i_{pc}/i_{pa} = 0.95 at 100 mV s^{-1}), see also Fig. 3.17.

[30] N.G. Connelly, W.E. Geiger, *Chem. Rev.* **1996**, *96*, 877.

[31] R. C. Clark J. S. Reid, *Acta Crystallogr.* **1995**, *A51*, 887.

[32] G. M. Sheldrick, *Acta Crystallogr.* **2008**, *A64*, 112.

CHAPTER IV

Ruthenium hydroxycyclopentadienyl *N*-heterocyclic carbene complexes as transfer hydrogenation catalysts

Abstract

A series of novel cationic hydroxycyclopentadienyl and methoxycyclopentadienyl *N*-heterocyclic carbene ruthenium(II) complexes have been synthesized from the corresponding neutral ruthenium(0) complexes containing both the non-innocent cyclopentadienone ligand and variously functionalized *N*-heterocyclic carbenes (NHCs). In particular, an NHC derivative containing a pyridine group in the side chain has been designed and developed in order to evaluate the influence of a basic, potentially cooperative substituent in the catalytic activity of these complexes. All the prepared complexes were employed as selective catalysts for transfer hydrogenation reactions employing refluxing ^{i}PrOH as hydrogen source and several ketones and aldehydes as substrates. We found that while the presence of oxidizing additives such as CAN and benzoquinone is mandatory to activate the neutral ruthenium(0) complexes, no activation is needed for the cationic Ru(II) catalysts. The catalytic activity of the latter is also influenced by the coordinating ability of the counterion, and indeed the cationic complexes having a pyridine-functionalized NHC ligand and $CF_3SO_3^-$ as counterion, present the best conversion (> 99%) thus demonstrating the fundamental role played by the basic pyridine in the catalytic activity. With regard to the hydrogenation reaction mechanism, the release of the CO ligand was demonstrated to be the key step and the presence of hydride species has been detected at the end of the reaction.

Introduction

As emphasised many times in the previous chapters the attention of the research group was particularly focus on two popular classes of ligands: *N*-Heterocyclic carbenes, that are among the most popular ancillary ligands due to a combination of unique electronic and steric features[1] allowing to the rational design of transition metal catalysts and the improvement of catalytic activity,[2] and the cyclopentadienones which behave as non-innocent ligands exploiting the cyclopentadienone/hydroxycyclopentadienyl reversible transformation. The most famous example of its cooperativity with ruthenium in bifunctional catalysis is the Shvo catalyst, a well-known system employed in a plethora of catalytic applications.[3] In principle by combining NHC and cyclopentadienone ligands on ruthenium complexes the properties of both ligands should be exploited allowing the design of novel catalysts finely tuning steric and electronic properties, solubility and the insertion of substituents suitable for heterogenization. Furthermore, by choosing a proper substituent, NHC ligand itself could cooperate with the metal as a non-innocent species.[4]

With this aim in mind, a straightforward approach towards Ru(0)-NHC complexes has been developed as described in Chapter II,[5] based on a dimeric Ru(0) cyclopentadienone dicarbonyl dimer (**3**). Cleavage of **3** in the presence of a silver carbene precursor provided access to a new class of ruthenium complexes in quantitative yields (for the sake of clarity some examples are recalled in Scheme 4.1).
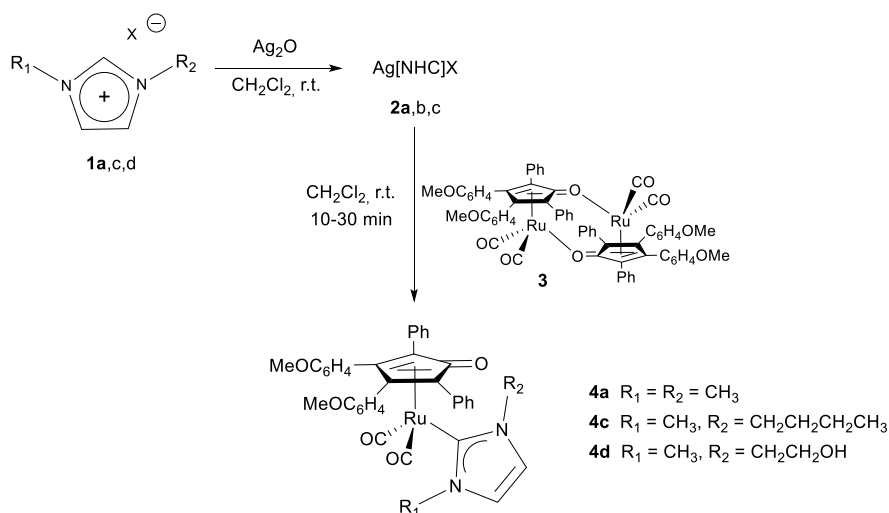
Scheme 4.1. Synthesis of cyclopentadienone imidazolylidene ruthenium(0) complexes **4a,c,d**.

In this chapter we first describe an extension of this synthetic methodology to a complex containing a basic nitrogen on the side chain of the NHC ligand (**4m**: R_1 = butyl; R_2 = 2-pyridine; **4n**: R_1 = methyl; R_2 = 2-BocNH-ethyl; **4o**: R_1 = methyl; R_2 = aminoethyl) then the main body of this work concerns the transformation of the cyclopentadienone imidazolylidene ruthenium(0) complexes (**4a,c,d,m,o**) into their corresponding cationic hydroxyl- and methoxy-cyclopentadienyl ruthenium(II) derivatives [**12a,c,d,m,o[X]** (X = Cl, BF_4, NO_3, CF_3SO_3) and **13a,m[CF$_3$SO$_3$]]**, and the use of both Ru(0) and Ru(II) complexes as catalysts for transfer hydrogenation of ketones and aldehydes in refluxing isopropanol. Comparison between monodentate and pyridine-functionalized NHC ligands, has provided some insights into the reaction mechanism.

Results and discussion

4.1 Synthesis of imidazolylidene Ru complexes

The novel complexes **4m** (R_1 = butyl; R_2 = 2-pyridine) and **4n** (R_1 = methyl; R_2 = 2-BocNH-ethyl) were prepared in one pot following the same procedure described in Scheme 4.1 and fully characterized by spectroscopic methods and elemental analysis. In particular, the ^{13}C NMR spectra show the downfield shifted resonance of the carbene (δ = 173.20 ppm (**4m**), 173.16 ppm (**4n**)), whereas in the IR spectrum the CO stretching bands are consistent with those of similar complexes (vCO = 2008 cm^{-1}, 1949 cm^{-1} (**4m**); 2008 cm^{-1}, 1948 cm^{-1} (**4n**) vs vCO = 2004 cm^{-1}, 1945 cm^{-1} (**4a**)). Further evidences were produced by ESI-MS and X-Ray diffraction analyses.

The molecular structure of **4m** has been determined by single crystal X-ray crystallography as its **4m·0.5CH₂Cl₂** solvate (Figure 4.1).

Figure 4.1. ORTEP drawing of **4m**. Displacement ellipsoids are at the 30% probability level. H-atoms have been omitted for clarity. Selected bond lengths (Å): Ru(1)-C(1) 1.845(16), Ru(1)-C(2) 1.883(12), Ru(1)-C(3) 2.511(11), Ru(1)-C(4) 2.279(11), Ru(1)-C(5) 2.199(11), Ru(1)-C(6) 2.212(10), Ru(1)-C(7) 2.280(11), Ru(1)-C(34) 2.139(12), C(3)-O(3) 1.246(13).

Its structure is similar to those previously reported for the analogous complexes **4a,c,d**.[5] In particular, the Ru(1)-C(3) distance [2.511(11) Å] is significantly longer than Ru(1)-C(4-7) [2.199(11)-2.280(11) Å, average 2.242(2) Å] and C(3)-O(3) [1.246(13) Å] is essentially a double bond.[6] The Ru(1)-C(34) contact [2.117(3) Å] is in the typical range for the interaction between Ru(0) and a N-heterocyclic carbene.[7]

The reaction of **4a,c,d,m** with strong acids or a methylating agent such as MeCF₃SO₃, leads to the quantitative formation of the hydroxycyclopentadienyl and methoxycyclopentadienyl cationic complexes **12a,c,d,m[X]** (X = Cl, BF₄, NO₃, CF₃SO₃) and **13a,m [CF₃SO₃]** (Scheme 4.2), in which Ru(0) is formally oxidized to Ru(II).

12a[X] $R_1 = R_2 = CH_3$; X = CF₃SO₃, Cl, BF₄.
12c[X] $R_1 = CH_3$, $R_2 = Bu$; X = CF₃SO₃
12d[X] $R_1 = CH_3$, $R_2 = CH_2CH_2OH$; X = CF₃SO₃
12m[X] $R_1 = Bu$, $R_2 = 2$-py; X = CF₃SO₃, Cl, BF₄.

13a[CF₃SO₃] $R_1 = R_2 = CH_3$;
13m[CF₃SO₃] $R_1 = Bu$, $R_2 = 2$-py

Scheme 4.2. Synthesis of hydroxycyclopentadienyl imidazolylidene ruthenium complexes **12a,c,d,m[X]** and methoxycyclopentadienyl imidazolylidene ruthenium complexes **13a,m[CF₃SO₃]**.

Infrared spectroscopy provides a convenient technique for monitoring the progress of the protonation as, in agreement with the reduced back-donation from the metal center to the carbonyl ligands, v-C≡O stretch vibrations undergo a significant high-energy shift upon formation of the cationic complex (Figure 4.2) [*e.g.* v_{CO} = 2008 cm^{-1}, 1949 cm^{-1} (**4m**), and 2041 cm^{-1}, 1991 cm^{-1} (**12m[CF₃SO₃]**)].
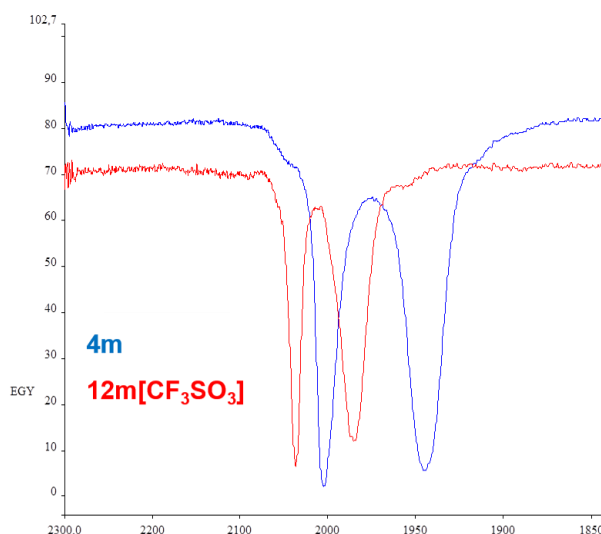
Figure 4.2 Comparison of CO stretching frequencies of the neutral (**4m**) and the cationic (**12m[CF₃SO₃]**) pyridine-functionalized NHC complexes.

The change in the coordination from η^4 (cyclopentadienone ligand) to η^5 (hydroxycyclopentadienyl ligand) is further evidenced by ^{13}C-NMR shift of the resonance due to the endocyclic carbon involved in the ketone-alcohol transformation [δ 169.33 ppm (C=O, Cp, in **4a**) vs δ 142.77 ppm (C-OH, Cp, in **12a[CF₃SO₃]**)]. Ru-carbene signals are also shifted to higher fields; from δ 172.72 ppm (**4a**) to δ 161.35 ppm (**12a[CF₃SO₃]**) (Figure 4.3).
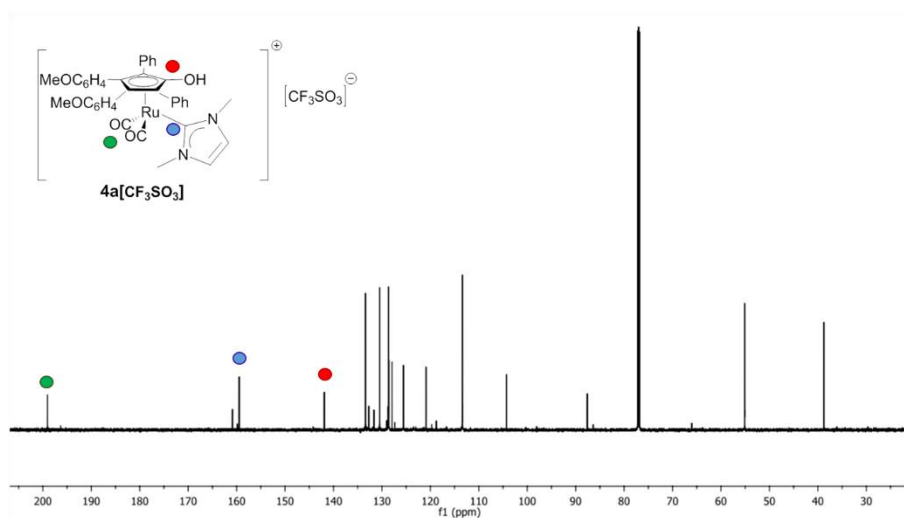
Figure 4.3. ^{13}C-NMR spectrum of **12a[CF₃SO₃]** in CDCl₃.

With regard to the methylated complexes **13a[CF₃SO₃]** and **13m[CF₃SO₃]** IR spectra show a shift of 40 cm^{-1} from the neutral to the cationic species (*e.g.* v_{CO} = 2004 cm^{-1}, 1945 cm^{-1} (**4a**), and 2045 cm^{-1}, 1995 cm^{-1} (**13a[CF₃SO₃]**) and both IR and NMR data are similar to those obtained for the hydroxycyclopentadienyl complexes **12a[CF₃SO₃]** and **12m[CF₃SO₃]** with the methyl group arising at δ 3.19 (^{1}H NMR) and δ 61.93 (^{13}C NMR) ppm.

Moreover, structural evidences were obtained by X-ray diffraction analysis of single crystals of the cationic complexes **[12a]⁺** and **[12d]⁺** as their **[12a][CF₃SO₃]·0.5toluene** and **[12d][CF₃SO₃]·CHCl₃** solvate salts (Figure 4.4). X-ray crystallography confirms that protonation has occurred on the O-atom of the cyclopentadienone ligand. As a consequence, the C(3)-O(3) interaction [1.335(6) and 1.339(9) Å for **[12a]⁺** and **[12d]⁺**, respectively] is considerably elongated compared to the parent neutral complexes [e.g., 1.246(13) Å for **4m**] and displays the character of a $C(sp_2)$-O single bond. In addition the Ru(1)-C(3) distance [2.323(5) and 2.319(7) Å for **[12a]⁺** and **[12d]⁺**, respectively] is shortened in respect to the parent complexes [e.g., 2.511(11) Å for **4m**] and comparable to the other Ru(1)-C(4-7) distances [2.227(5)- 2.290(5) Å, average 2.253(10) Å for **[12a]⁺**; 2.271(8)- 2.221(7) Å, average 2.248(12) Å for **[12d]⁺**]. Thus, the protonated ligand of **[12a]⁺** and **[12d]⁺** is better described as a η^5-cyclopentadienyl ligand, as previously reported for analogous complexes.[18d, 23] The O(3)-H(3) group of **[12a]⁺** is involved in an inter-molecular H-bond with the [CF₃SO₃]⁻ anion [O(3)-H(3) 0.885(10) Å, H(3)···O(301) 1.80(3) Å, O(3)···O(301) 2.626(5) Å, <O(3)H(3)O(301) 155(5)°]. Conversely, the O(3)-H(3) group of **[12d]⁺** forms an intra-molecular H-bond with the O(6) atom of the side chain of the NHC ligand [O(3)-H(3) 0.84 Å, H(3)···O(6) 1.83 Å, O(3)···O(6) 2.646(7) Å, <O(3)H(3)O(6) 163.7°]. In addition, there is in **[12d]⁺** also an inter-molecular H-bond between the O(6)-H(6) group of the complex and the [CF₃SO₃]⁻ [O(6)-H(6) 0.84 Å, H(6)···O(301)#1 1.91 Å, O(6)···O(301)#1 2.739(9) Å, <O(6)H(6)O(301)#1 167.7°; symmetry transformations used to generate equivalent atoms: #1 x+1,y,z   #2 -x+1,-y+1,-z+1]. The carbene interaction Ru(1)-C(34) [2.101(5) and 2.109(7) Å for **[12a]⁺** and **[12d]⁺**, respectively] is almost unchanged compared to the parent neutral complexes [e.g., 2.117(3) Å for **4m**].
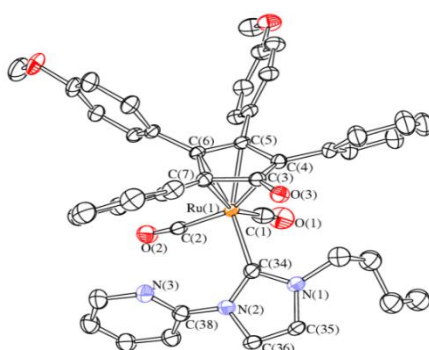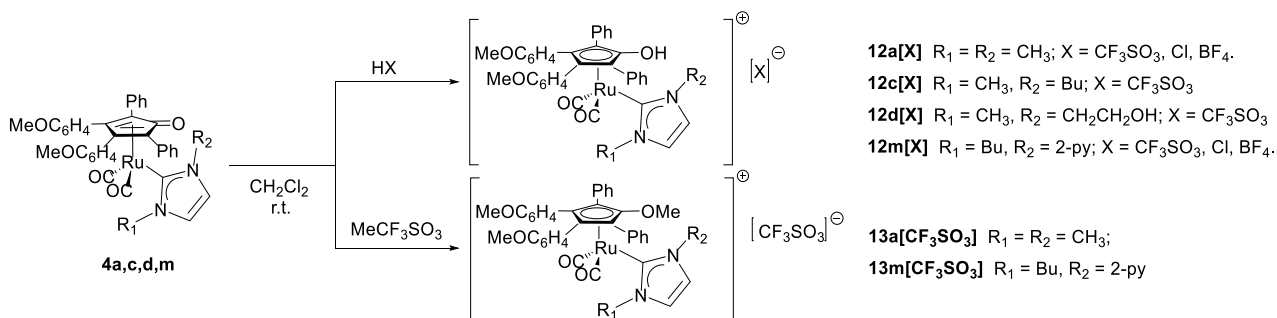

Figure 4.4. <u>Left</u>: ORTEP drawing of **[12a]⁺** Displacement ellipsoids are at the 30% probability level. H-atoms have been omitted for clarity, except H(3). Selected bond lengths (Å): Ru(1)-C(1) 1.882(7), Ru(1)-C(2) 1.881(7), Ru(1)-C(3) 2.323(5), Ru(1)-C(4) 2.290(5), Ru(1)-C(5) 2.238(5), Ru(1)-C(6) 2.227(5), Ru(1)-C(7) 2.256(5), Ru(1)-C(34) 2.101(5), C(3)-O(3) 1.335(6). <u>Right</u>: ORTEP drawing of **[12d]⁺**. Displacement ellipsoids are at the 30% probability level. H-atoms have been omitted for clarity, except H(3) and H(6). Selected bond lengths (Å): Ru(1)-C(1) 1.876(8), Ru(1)-C(2) 1.901(9), Ru(1)-C(3) 2.319(7), Ru(1)-C(4) 2.262(7), Ru(1)-C(5) 2.240(7), Ru(1)-C(6) 2.221(7), Ru(1)-C(7) 2.271(8), Ru(1)-C(34) 2.109(7), C(3)-O(3) 1.339(9).

In order to obtain a basic nitrogen on the side chain of the carbene, the complex **4n**, containing an amide-functionalized NHC ligand, has been treated with tetrafluoroboric acid diethyl ether complex allowing the cleaving of the NHBoc group and leading to the formation of the cationic complex **12o[BF₄]** with an amine group on the side chain of the carbene (Scheme 4.3). Infrared characterization evidences the presence of two species in equilibrium demonstrated by two set of CO stretching frequencies [v(CO): 2042 cm⁻¹, 1992 cm⁻¹ (**12o'[BF₄]**) and 2021 cm⁻¹, 1966 cm⁻¹(**12o''[BF₄]**)]. Conversely, the ¹H-NMR spectrum shows only one set of averaged signal resulting from a fast exchange between the two species (**12o'[BF₄]** and **12o''[BF₄]**). Indeed,

a VT-NMR experiment performed at T = -50°C in (in CDCl₃) reveals the presence of two set of signals belonging to the two cationic forms. Conversely, the ¹H-NMR spectrum shows only one set of averaged signal resulting from a fast exchange between the two species (**12o'[BF₄]** and **12o''[BF₄]**) at room temperature.

The protonation, in fact, can occurs on the cyclopentadienone ligand leading to the formation of the hydroxycyclopentadienyl cationic complex **12o'[BF₄]** or on the -NH₂ obtaining the complex **12o''[BF₄]** that contain a terminal ammonium cation on the side chain of the carbene (Scheme 4.3). Quite surprisingly the bis-cationic complex, which would arise from the bis-protonation, has never been observed even though an excess of HBF₄ is employed.
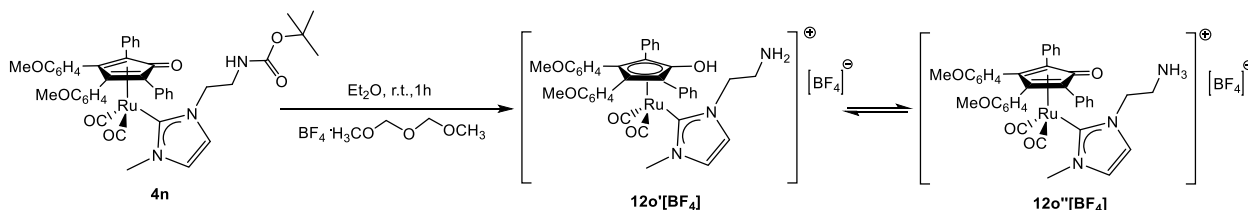
Scheme 4.3 Deprotection reaction of NHBoc group.

Furthermore, the treatment of **12o[BF₄]**, formally containing a protected amine, with bases such as K₂CO₃ and KOH led to the formation of the corresponding neutral complex **4o** that has been subsequently protonate with trifluoromethanesulfonic acid in order to achieve the cationic complex **12o[CF₃SO₃]** with the triflate as conterion (Scheme 4.4) thus demonstrating the reversibility of the protonation. It is important to underline that while employing triflic acid as protonating agent only one isomer is observed by IR spectroscopy [ν(CO): 2042 cm⁻¹, 1993 cm⁻¹].
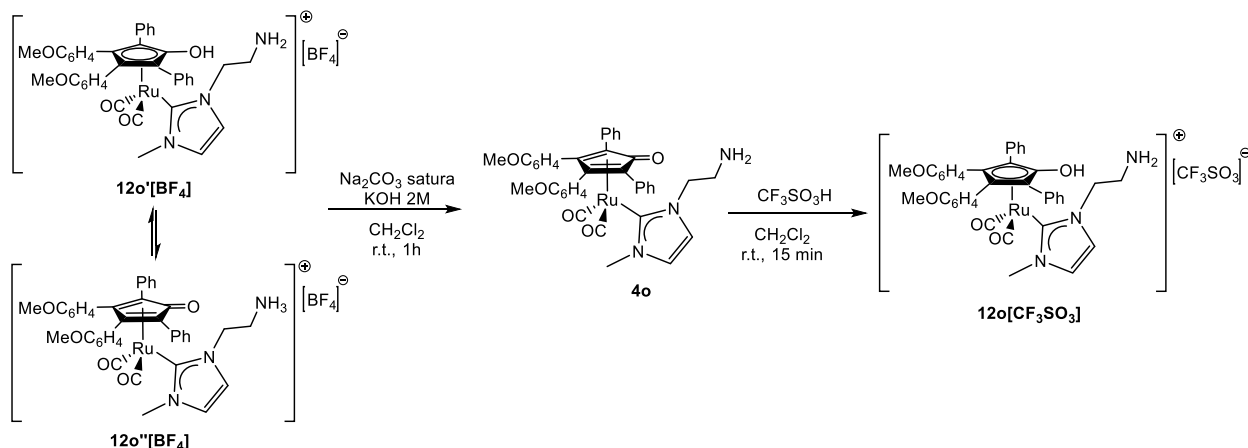
Scheme 4.4 Synthesis of dicarbonyl-η⁴-3,4-bis(4-methoxyphenyl)-2,5-diphenylcyclopenta-2,4-dienone)(1-(2-aminoethyl)-3-methylimidazol-2-ylidene)ruthenium (**4o**).

Due to the peculiar acid/base chemistry of amino-functionalized complexes, with the aim of allowing the coordination of a basic nitrogen to the metal centre, the pyridine containing complex **12m[CF₃SO₃]** has been irradiated with a UV lamp. The photolytic removal of one terminal CO led to the formation of the chelated complex **14m[CF₃SO₃]** in good yield (Scheme 4.5).
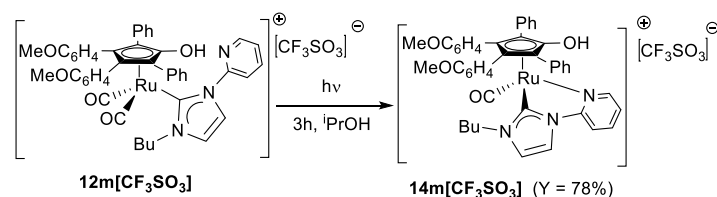
Scheme 4.5. Photolytic removal of terminal CO.

The IR spectrum shows the disappearance of the two absorptions due to the CO stretching of **12m[CF₃SO₃]**, and the appearance of a unique band at 1967 cm⁻¹ (**14m[CF₃SO₃]**). Carbene resonance, in ¹³C NMR spectrum, is shifted to lower fields (δ 185.63 ppm (**14m[CF₃SO₃]**) vs δ 166.07 ppm (**12m[CF₃SO₃]**).

The X-Ray molecular structure of **14m[CF₃SO₃]** further supports the characterization performed in solution (Figure 4.5) and consists of a Ru center coordinated to a η⁵-cyclopentadienyl ligand, a terminal CO and a chelating NHC ligand bonded to Ru *via* the carbene and the N-atom of the pyridine side group. The Ru(1)-Cp distances [2.216(7)- 2.302(8) Å, average 2.248(16) Å] are comparable to those reported above for **[12a]⁺** and **[12d]⁺** and analogous Ru-complexes containing protonated cyclopentadienone ligands.[3d, 8] As in the case of **[12a]⁺** and **[12d]⁺**, the C(3)-O(3) interaction [1.338(9) Å] is a single bond, in view of the presence of a H atom on the oxygen, which is involved in H-bond with the triflate anion.
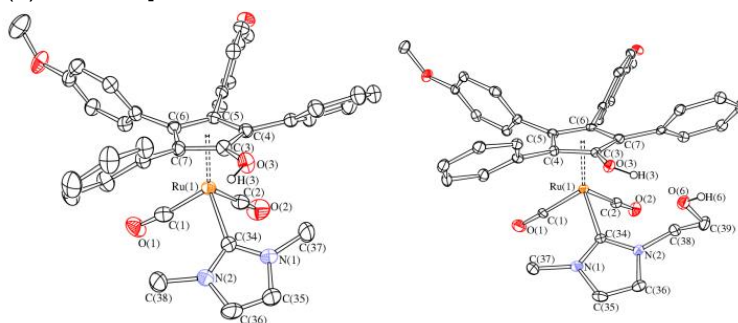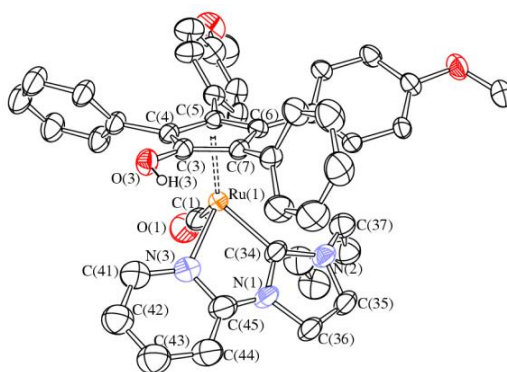

Figure 4.5. ORTEP drawing of **14m[CF₃SO₃]**. Displacement ellipsoids are at the 30% probability level. H-atoms have been omitted for clarity, except H(3). Selected bond lengths (Å): Ru(1)-C(1) 1.860(9), Ru(1)-C(3) 2.302(8), Ru(1)-C(4) 2.237(7), Ru(1)-C(5) 2.216(7), Ru(1)-C(6) 2.236(7), Ru(1)-C(7) 2.251(7), Ru(1)-C(34) 2.030(7), Ru(1)-N(3) 2.127(10), C(3)-O(3) 1.338(9).

It is worth mentioning that UV irradiation (3 h) of the neutral complexes **4a** and **4m** leaves the reactant unaltered indicating that the formal oxidation of Ru complex, upon protonation, favor the CO removal. The same result was surprisingly obtained with the cationic complexes **12a[CF₃SO₃]** and **13a[CF₃SO₃]**, for which CO release was expected (16 h of irradiation in ᶦPrOH). Nonetheless irradiating **12a[CF₃SO₃]** and **13a[CF₃SO₃]**, in the presence of a trapping agent such as pyridine, the formation of the complexes **15[CF₃SO₃]** and **16[CF₃SO₃]** was finally observed (Figure 4.6) actually demonstrating that the CO release occurs in the cationic complexes. Indeed, neutral complex **4a** did not lose CO under UV irradiation even in the presence of pyridine. It is thus likely that, in the case of cationic complexes, without the help of pyridine the removal of CO is an equilibrium in which ruthenium-CO bond is reformed at the end of the reaction leading to the recovery of the precursors **12a[CF₃SO₃]** and **13a[CF₃SO₃]**.
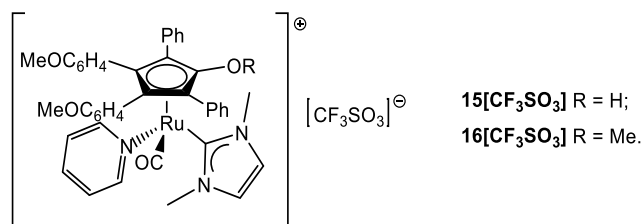
Figure 4.6. Molecular structure of **15CF₃SO₃]** and **16[CF₃SO₃]**.

Formation of **15[CF₃SO₃]** and **16[CF₃SO₃]** is evidenced by the disappearance of the two carbonyl stretching bands associated to **12a[CF₃SO₃]** (2037, 1985 cm^{-1}) and **13a[CF₃SO₃]** (2045, 1995 cm^{-1}), with the concomitant appearance of a single band associated with the new complex **15[CF₃SO₃]** (1943 cm^{-1}) and **16[CF₃SO₃]** (1948 cm^{-1}) (Figure 4.6). Complexes **15[CF₃SO₃]** and **16[CF₃SO₃]** have been found in mixture with other species and their characterization was not complete. However, the bathochromic shift observed in IR spectra is in agreement with the replacement of a strong π ligand with a σ N-donor ligand such as pyridine. Furthermore, ESI-MS analyses performed on complexes **15[CF₃SO₃]** and **16[CF₃SO₃]** showed the presence of the molecular ions.

4.2 Catalytic transfer hydrogenation

The Ru complexes **4a,c,d,m,o**, **12a,c,d,m,o[X]** [(X = Cl, BF₄, NO₃, CF₃SO₃)] and **13a,m[CF₃SO₃]** were evaluated as catalyst precursors under transfer hydrogenation conditions *i.e.* refluxing ^{i}PrOH as hydrogen source employing 4-fluoroacetophenone as model substrate. Catalytic runs were performed to investigate the role of different additives in the activation of **4a,c,d,m,o** to compare the catalytic activity of the ruthenium(0) complexes **4a,c,d,m,o** with the corresponding ruthenium(II) cationic complexes **12a,c,d,m,o[X]** and **13a,m[CF₃SO₃]** and finally to evaluate the influence of a pyridine substituent on the NHC side chain. Results are reported in Table 4.1: in all cases selectivity is complete and conversion corresponds to yield unless otherwise stated.

Table 4.1. Catalytic transfer hydrogenation of 4-fluoroacetophenone.[a]
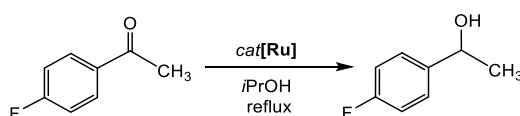
entry	[Ru]	additive	conversion 8h (%)	conversion 24h (%)
1	4a	---	0	0
2	4c	---	0	0
3	4d	---	0	0
4	4m	---	0	0
5	4o	---	0	0
6	4a	CAN[b]	25	61
7	4a[c]	CAN[b]	0	27
8	4c	CAN[b]	10	87
9	4d	CAN[b]	10	25
10	4m	CAN[b]	0	9
11	4o	CAN	<5	40
12	4a	$NaIO_4$[d]	0	0
13	4a	BQ[d]	25	55
14	12a[CF_3SO_3]	---	58	93
15	12a[CF_3SO_3][c]	---	5	29
16	12a[CF_3SO_3][e]	---	64	87
17	12a[CF_3SO_3]	KO^{t}Bu[d]	14	35
18	12a[BF_4]	---	41	71
19	12a[Cl]	---	16	24
20	4a	CF_3SO_3H[d]	32	>99[f]
21	4a	H_2SO_4[d]	45	92
22	4a	HNO_3[d]	60	65
23	12c[CF_3SO_3]	---	9	60
24	12d[CF_3SO_3]	---	35	46[g]
25	12m[CF_3SO_3]	---	84	>99
26	12m[Cl]	---	0	5
27	12m[BF_4]	---	37	40
28	12o[BF_4]	---	6	38
29	12o[CF_3SO_3]	---	81	88
30	4m	CF_3SO_3H[d]	84	>99[f]
31	4m	H_2SO_4[d]	76	86
32	4m	HNO_3[d]	0	36
33	13a[CF_3SO_3]	---	28	64
34	13m[CF_3SO_3]	---	10	13
35	14d[CF_3SO_3]	---	0	5
36	HCF_3SO_3	---	0	0

[a]General conditions: Ruthenium complex (5 mol% Ru), *i*PrOH (3 mL), reflux; conversions determined by ^{19}F NMR spectroscopy; [b]CAN 1 mol equiv. per ruthenium center; [c]catalyst loading reduced to 1 mol% Ru; [d]$NaIO_4$, BQ (benzoquinone), KO^{t}Bu and acids: 1 mol equiv. per ruthenium center; [e]recycling test; [f]yield ~70% the co-product arising from the acid catalyzed etherification of 4-fluoroacetophenol with the solvent 2-propanol; [g] yield ~ 35% the coproduct was not identified.

The neutral complexes **4a,c,d,m,o** did not present any catalytic activity in the absence of additives (entry 1-5), as well as by adding $NaIO_4$ (entry 12). However, we found that the addition of one equivalent of CAN (entry 6-11) results in the formation of active intermediates, likely deriving from the release of one CO ligand, favoured by oxidation as discussed in the previous section. In fact, the use of benzoquinone as oxidant additive under the same conditions (entry 13), activates the catalyst even though leading to a slightly lower conversion if compared with CAN.

Reduction of the catalyst loading to 1 mol% (**4a**) increases the induction time halving the conversion in 24 h (entry 6 vs 7). In general pre-catalysts **4a,c,d,m,o** resemble the behaviour of the triazolylidene ruthenium(0) congener, namely the dicarbonyl-(η^4-3,4-bis(4-methoxyphenyl)-2,5-diphenylcyclopenta-2,4-dienone)(1,3-dimethyl-4-phenyl-1,2,3-triazol-ylidene)ruthenium (**11**), previously tested as hydrogen transfer catalyst (see Chapter III).[9]

The oxidation state of the metal center appears to be the key point in order to activate the catalyst and indeed, better conversions are reached with the pre-catalysts **12a,c,d,m,o[X]** [(X = Cl, BF_4, NO_3, CF_3SO_3) (entries 14, 18, 19, 23-29)]. A recycling test has been performed with **12a[CF₃SO₃]**, the catalyst can be reused although a slight decrease in conversion from 93 to 87% was observed after 24 h (entry 16). Noteworthy also the counterion shows to influence the catalytic activity, and $CF_3SO_3^-$ provides the best results: for example, we observed almost complete conversion within 24 h in the case of **12a[CF₃SO₃]**, **12m[CF₃SO₃]** and **12o[CF₃SO₃]** (entries 14, 25, 29). Furthermore, the latter pyridine- and amine-functionalized catalyst **12m[CF₃SO₃]** and **12o[CF₃SO₃]** shows a faster activation if compared with **12a[CF₃SO₃]** (conversion of 84%, 81% and 58% respectively in 8 h). On the other hand, catalytic activity is suppressed in the case of **12a[Cl]** and **12m[Cl]** (entry 19, 26), possibly due to the coordinating ability of Cl^- counterion; on the contrary **12a[BF₄]**, **12m[BF₄]** and **12o[BF₄]** give intermediate results (entry 18, 27, 28). In particular in the case of **12o[BF₄]** the quite low conversion could be attributed also to the presence of two species in solution, it is assumed that the specie **12o''[BF₄]** (see Scheme 4.4) is less active compared to the other cationic complexes **12a,c,d,m,o'[X]**. The latter hypothesis is supported by IR spectrum of **12o''[BF₄]** for which a lowering in the CO stretching frequencies is observed reasonably due to the η^4 coordination of cyclopentadienonic ligand [v(CO): 2042 cm^{-1}, 1992 cm^{-1} (**12o'[BF₄]**) and 2021 cm^{-1}, 1966 cm^{-1}(**12o''[BF₄]**)]. Further investigations on the catalytic activity of this complex are being carried out.
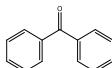
The *in situ* addition of various acids such as HCF_3SO_3, H_2SO_4 and HNO_3 to **4a** and **4m** (entries 20-22, 30-32) produces, in the case of triflic acid, similar conversions as for the corresponding preformed catalysts (*e.g.* entry 25, **12m[CF₃SO₃]** vs entry 30, **4m** + CF_3SO_3H *in situ*). However, a lower selectivity is observed due to the acid catalyzed etherification of 4-fluorobenzylalcohol and isopropanol. Best *in situ* performances are accomplished by sulfuric acid (entries 21, 31), which gives much better results than HNO_3 (entry 22, 32), confirming the detrimental effect of the coordination ability of counterions. A base, such as KO^tBu, has a negative effect on the reaction (entry 17), likely due to deactivation of the pre-catalyst by deprotonation. Finally, a blank experiment performed with HCF_3SO_3 in refluxing isopropanol rule out an exclusive role of the acid itself in the catalytic activity (entry 36).

With the aim of evaluating the role of the hydroxyl group in the catalytic reaction methylated complexes **13a[CF₃SO₃]** and **13m[CF₃SO₃]** have been also tested as catalysts (entry 33 and 34). Quite surprisingly, the

methylated complex **13a[CF₃SO₃]** shows a remarkable catalytic activity although in the absence of the acidic OH. Worst performances came from the pyridine-functionalized methylated complex **13m[CF₃SO₃]**, probably due to a deactivation pathway associated with the formation of stable species in the chelated form. Indeed, no conversion is observed when the chelated cationic complex **14m[CF₃SO₃]** is employed as pre-catalyst (entry 35).

The substrate scope has been also evaluated extending the reactivity of **4a**, **12a[CF₃SO₃]** and **12m[CF₃SO₃]** as hydrogen transfer catalysts to acetophenone, benzophenone and benzaldehyde. Data are reported in Table 4.2. All the substrates are converted to the corresponding alcohol by activated **4a** and by the cationic complex **12a[CF₃SO₃]**. As expected the catalysts are much more active in the case of benzaldehyde (entry 7 and 9), since aldehydes are substrates more prone to reduction than ketones. Additionally, the scale of activity is consistent with the electron withdrawing properties of the ketones examined. Again, **12m[CF₃SO₃]** (entry 3, 6, 9) shows a faster activation. As an example, benzaldehyde reaches complete conversion within 4 h, that becomes 8 h in the case of **12a[CF₃SO₃]** (entry 9[c] vs 8).

Table 4.2. Catalytic transfer hydrogenation.[a]

entry	substrate	[Ru]	Additive[b]	Conversion 8h (%)	Conversion 24h (%)
1		**4a**	CAN	10	77
2		**12a[CF₃SO₃]**	---	15	68
3		**12m[CF₃SO₃]**	---	45	48
4		**4a**	CAN	0	42
5		**12a[CF₃SO₃]**	---	0	36
6		**12m[CF₃SO₃]**	---	42	43
7		**4a**	CAN	31	39
8		**12a[CF₃SO₃]**	---	>99	
9		**12m[CF₃SO₃]**	---	>99%[c]	

[a]Reaction conditions: [Ru] = 5 mol%, iPrOH (3mL), reflux. Conversions determined by GC; [b]CAN 1 mol equiv. per ruthenium center; c) Complete conversion is reached within 4 h.

4.3 Mechanistic insight

On the basis of the results described above, we can draw some considerations regarding the active catalytic species. First of all, the trapping experiments with pyridine (see cyclization of **12m[CF₃SO₃]** to **14m[CF₃SO₃]**, Scheme 4.3 and complexes **15[CF₃SO₃]** and **16[CF₃SO₃]**, Figure 4.6) demonstrates that CO release is involved in the activation, leaving unaltered the Ru-carbene bond. Indeed, all the crude products of catalytic reactions have been analyzed by IR and NMR spectroscopy and only in a couple of cases traces of Shvo catalyst, which would results from NHC ligand release, were visible in NMR spectra, accompanied by a very bright yellow color of the solution typical of Shvo complex.[3] Furthermore, an outer sphere mechanism is likely to be followed, in that the complex [CpRu(CO)₂][CF₃SO₃], obtained by reaction between [Cp₂Ru₂(CO)₄] with AgOTf, did not present any catalytic activity, supporting the role of hydroxycyclopentadienyl complex as a bifunctional catalyst. Noteworthy, in the case of **12m[CF₃SO₃]** the pyridine itself can be involved in the catalytic cycle as a cooperative ligand through the formation of the active catalyst **A** in which a hydride and two different acid hydrogens should be available for the hydrogen transfer. (Figure 4.7).
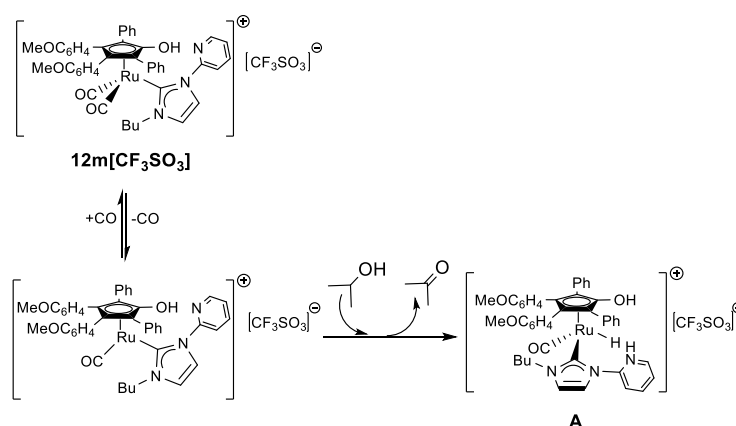
Figure 4.7. Proposed activation of the pre-catalyst **12m[CF₃SO₃]**.

Indeed, **12m[CF₃SO₃]** results to be the best pre-catalyst. Furthermore, from the crude reaction mixture at the end of the reaction some resonances in the ¹H-NMR spectrum are detected in the hydride region: a singlet at δ -10.18 ppm is presumably associated with monomeric Ru-H species, while the signal at δ -14.95 ppm falls in the region of bridging hydrides (Ru-H-Ru). Even though we were not able to isolate these hydride species, in analogy with what observed in the synthesis of Shvo catalyst (δ RuHRu -18.80 ppm for the dimeric specie and δ -9.37 ppm for the monomeric one),[3d, 8] the formation of active hydride complexes containing the NHC ligand in place of a terminal CO reasonably occurs.

Labeling experiments on the reduction of 4-fluoroacetophenone with **12a[CF₃SO₃]** and **12m[CF₃SO₃]** in isopropanol-d₈ (see Experimental section for reaction conditions and spectra) lead to the formation of the corresponding deuterated alcohol further confirming the role of isopropanol as hydrogen source as well as the action of the catalysts in its activation.

With regard to **12d[CF₃SO₃]**, which in our experiments leads to the worst conversion after 24h and lower selectivity (Table 4.1, entry 22), its molecular structure (Figure 4.4, right side) evidences a hydrogen bond between the hydroxycyclopentadienyl ligand and the –OH group in the NHC side chain. Furthermore, **12d[CF₃SO₃]**, upon CO release, would be prone to an intramolecular dehydrogenation, probably leading to

the formation of an inactive catalyst. By comparing the behavior of **12d[CF₃SO₃]** with that of an iridium complex containing the NHC hydroxymethyl ligand which

lead to the formation of an [Ir(Cp*)(I)(NHC-CH₂C=O)] complex upon oxidation and cyclometallation[10] we can propose a similar reactivity for our ruthenium complex in agreement with the ν(CO) and ν(C=O) bands found at 1950 cm⁻¹ and 1723 cm⁻¹.

Concerning monodentate NHC complexes **12a,c,d[X]** (X = Cl, BF₄, NO₃, CF₃SO₃) due to the absence of a *N*-containing side group able to be protonated, the active catalytic species has to be different from the proposed intermediate **A**. Once a vacant coordination site is formed by CO removal, proton abstraction from ᶦPrOH should be performed by the counteranion CF₃SO₃⁻ as external base, or by the oxygen of the -OH group (or -OMe group) on the catalyst itself, but at present we do not have any evidence to support such hypothesis.

Conclusions

A series of cationic hydroxy- or methoxy-cyclopentadienyl ruthenium(II) *N*-heterocyclic carbene complexes have been prepared in quantitative yield upon protonation with strong acids or methylation with MeCF₃SO₃ of neutral ruthenium(0) complexes containing both the non-innocent cyclopentadienone ligand and variously functionalized NHCs. These novel complexes have been successfully employed as selective catalysts in transfer hydrogenation. The reaction is general and several substrates such as various ketones and aldehydes can be selectively reduced to the corresponding alcohol. The catalytic activity can thus be tuned by the proper choice of both substituents on NHC ligand and counterions. Neutral Ru(0) complexes **4a,c,d,m,n,o** need an oxidizing agent such as CAN or benzoquinone in order to be activated, while the corresponding cationic complexes **12a,c,d,m,n,o[X]** (X = Cl, BF₄, NO₃, CF₃SO₃) and **13a,m[CF₃SO₃]**, formally containing a Ru(II) center are more prone to release a CO ligand and do not need any additives to be activated. In the cationic complexes the counterion plays a non-innocent role and CF₃SO₃⁻ showed the best outcome due to its coordinating ability.

Noteworthy the insertion of a pyridine substituent on the NHC side chain further improves the catalytic activity due to the presence of a second cooperative ligand containing a basic nitrogen.

With regard to the reaction mechanism CO release and its key role in the catalyst activation was demonstrated by trapping experiment with pyridine as well as by the UV-mediated formation of the chelated complex **14m[CF₃SO₃]**. Hydride species has been identified in the reaction mixture of the pyridine functionalized complex **12m[CF₃SO₃]** and the cooperative function of nitrogen- (pyridine in **12m[X]** and **13m[CF₃SO₃]**) and oxygen-containing (CF₃SO₃⁻ or -OH and -OMe in **12a,c,d[X]** and **13a[CF₃SO₃]**) moieties with the vacancy on ruthenium prone to accept an hydride species has been drawn as consideration in order to explain ᶦPrOH activation and subsequent active catalyst formation.

The versatility of NHC ligands which can be variously functionalized, together with the presence of the non-innocent cyclopentadienone open the way to the rational design of novel metal-ligand bifunctional catalysts liable to heterogenization and tunable solubility.

Experimental section

Material and procedures. Solvents: dichloromethane (CH_2Cl_2), tetrahydrofuran (THF), diethyl ether (Et_2O), petroleum ether referring to a fraction of bp 60-80 °C, acetonitrile (CH_3CN) were dried and distilled prior to use. Acetone has been degassed and stored under inert atmosphere on molecular sieves. Other solvents such as ethylacetate (EtOAc), chloroform, ethanol (EtOH), methanol (MeOH), heptane, hexane, 2-propanol, $CDCl_3$, D_2O, CD_3CN (Sigma Aldrich) have been employed without further purification. Reagents: triruthenium-dodecacarbonil ($Ru_3(CO)_{12}$) (Strem), methyl iodide, silver oxide, 1-methylimidazole, 1-chlorobutane, 1-butylimidazole, 1-chloroethanol, 1,3 diphenylacetone, 4,4'dimethoxybenzil (Alfa Aesar), 2-bromopyridine, 4-fluoroacetophenone, acetophenone, benzophenone, benzaldehyde, dodecane, trifluoromethanesulfonic acid, tetrafluoroboric acid diethyl ether complex (Sigma Aldrich), chloridric, nitric and sulfuric acid, methyl trifluoromethanesulfonate, pyridine, cerium ammonium nitrate (CAN), benzoquinone, sodium periodate have been employed as purchased. 1,3-dimethylimidazolium iodide (**1a**),[11] 1-methyl-3-butyl-imidazolium chloride (**1c**), 1-methyl-3-(2-hydroxyethyl)imidazolium chloride (**1d**),[12] 1-butyl-3-(2-pyridinyl)-imidazolium bromide (**1m**)[13], 3,4-Bis(4-methoxyphenyl)-2,5-diphenylcyclopenta-2,4-dienone,[14] dicarbonyl(η^4-3,4-bis(4-methoxyphenyl)-2,5-diphenylcyclopenta-2,4-dienone) ruthenium dimer (**3**),[15] dicarbonyl-η^4-3,4-bis(4-methoxyphenyl)-2,5-diphenylcyclopenta-2,4-dienone)-1,3(dimethyl)-imidazol-2-ylidene)ruthenium (**4a**), dicarbonyl-η^4-3,4-bis(4-methoxyphenyl)-2,5-diphenylcyclopenta-2,4-dienone)-1-methyl-3-butyl-imidazol-2-ylidene)ruthenium (**4c**), dicarbonyl-η^4-3,4-bis(4-methoxyphenyl)-2,5-diphenylcyclopenta-2,4- dienone)-1-methyl-3-butyl-imidazol-2-ylidene)ruthenium (**4d**),[5] have been prepared as previously reported. The prepared derivatives were characterized by spectroscopic methods. The NMR spectra were recorded using Varian Inova 300 (^{1}H, 300.1; ^{13}C, 75.5 MHz), Varian Mercury Plus VX 400 (^{1}H, 399.9; ^{13}C, 100.6 MHz), Varian Inova 600 (^{1}H, 599.7; ^{13}C, 150.8 MHz) spectrometers at 298 K; chemical shifts were referenced internally to residual solvent peaks. Full ^{1}H- and ^{13}C-NMR assignments were done, when necessary, by gHSQC and gHMBC NMR experiments using standard Varian pulse sequences. Infrared spectra were recorded at 298 K on a Perkin-Elmer Spectrum 2000 FT-IR spectrophotometer. ESI-MS spectra were recorded on Waters Micromass ZQ 4000 with samples dissolved in MeOH or CH_3CN. Elemental analyses were performed on a Thermo-Quest Flash 1112 Series EA instrument. The conversions were monitored by GC analysis (Agilent Technologies 7890A GC system) and ^{19}F-NMR. UV irradiation was performed by using a commercial Hg lamp (365 nm, 125 W).

Synthesis of neutral imidazolylidene Ru(0) complex (4)

4m R_1 = Bu R_2 = 2-py

4n R_1= CH_3 R_2 = CH_2CH_2NHBoc

4o R_1 = CH_3, R_2 = $CH_2CH_2NH_2$
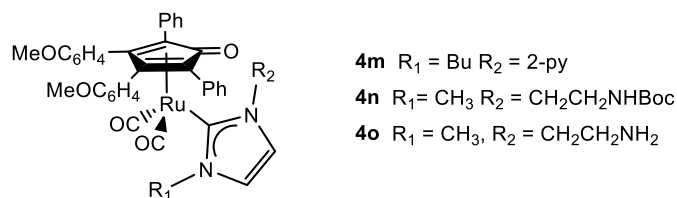
Figure 4.8 Structure of imidazolylidene Ru(0) complexes **4**.

Synthesis of dicarbonyl-η^4-3,4-bis(4-methoxyphenyl)-2,5-diphenylcyclopenta-2,4-dienone) 1-(butyl-3-(2-pyridinyl)-imidazol-2-ylidene)ruthenium (4m): A mixture of 1-butyl-3-(2-pyridinyl)-1H-imidazolium bromide (**1m**) 0.094g (0.33mmol), Ag_2O 0.092g (0.40mmol) and dicarbonyl(η^4-3,4-bis(4-methoxyphenyl)-2,5-diphenylcyclopenta-2,4-dienone) ruthenium dimer (**3**) 0.200g (0.16mmol) in dry CH_2Cl_2 were stirred in the dark

under inert atmosphere at room temperature for 1h. Upon filtration on a celite pad and removal of the solvent the quantitative formation of the dicarbonyl-η^4-3,4-bis(4-methoxyphenyl)-2,5-diphenylcyclopenta-2,4-dienone) 1-(butyl-3-(2-pyridinyl)-imidazol-2-ylidene)ruthenium (**4m**) was verified by ^{1}H-NMR, ^{13}C-NMR, ESI-MS and X-Ray crystal structure. Suitable crystals were obtained by slow diffusion from toluene/hexane double layer ^{1}H-NMR (599.7 MHz, CDCl$_3$) δ (ppm): 8.36 (dd, 1H, CH$_{py}$), 7.60 (m, 4H, CH$_{aryl}$), 7.04-6.97 (m, 10H, CH$_{aryl}$ + 1H, CH$_{py}$ + 2H, CH$_{NHC}$), , 6.60-6.55 (m, 4H, CH$_{aryl}$ + 1H, CH$_{py}$), 3.67 (s, 6H, -OCH$_3$), 3.54 (t, 2H, NCH$_2$), 1.46 (m, 2H, -CH_2CH$_2$-), 1.04 (m, 2H, -CH_2CH$_3$), 0.75 (t, 3H, -CH$_3$); ^{13}C{^{1}H} NMR (150.8 MHz, CDCl$_3$) δ (ppm): 201.77 (CO), 173.20 (C$_{carbene}$), 168.22 (C$_1$=O, Cp), 158.41 (-COCH$_3$), 152.16 (C$_{ipso}$), 148.11 (CH$_{py}$), 138.40 (CH$_{py}$), 135.17 (Cq$_{aryl}$), 133.45 (CH$_{aryl}$), 129.49 (CH$_{aryl}$), 127.43 (CH$_{aryl}$), 125.28 (Cq$_{aryl}$), 124.85 (CH$_{aryl}$), 124.54 (CH$_{NHC}$), 123.89 (CH$_{py}$), 122.43(CH$_{NHC}$), 121.82 (CH$_{py}$), 112.76 (CH$_{aryl}$), 103.10 (C$_{2,5}$, Cp), 79.69 (C$_{3,4}$, Cp), 54.98 (-OCH$_3$), 50.72 (NCH$_2$), 33.08, 19.41 (-CH$_2$CH$_2$), 14.11 (-CH$_3$); IR (CH$_2$Cl$_2$) ν(CO): 2008 cm^{-1}, 1949 cm^{-1}, ν(C=O) 1583 cm^{-1}, ν(C=C) 1609 cm^{-1}, 1518 cm^{-1}. ESI-MS (m/z) (+) = 804 [M+H]$^+$; 826 [M + Na]$^+$. Anal. Calcd (%) for C$_{45}$H$_{39}$N$_3$O$_5$Ru: C, 67.23; H, 4.89; N, 5.23. Found: C, 67.21; H, 4.87; N, 5.24.

Dicarbonyl-(η^4-3,4-bis(4-methoxyphenyl)-2,5-diphenylcyclopenta-2,4-dienone)[1-(2-Boc-NH-ethyl)-3-methyl)-imidazol-2-ylidene]ruthenium (4n): A mixture of 1-1-(2-BocNH-ethyl-)-3-methylimidazolium iodide (**1n**) 0.062g (0.17mmol), Ag$_2$O 0.047g (0.20mmol) and dicarbonyl(η^4-3,4-bis(4-methoxyphenyl)-2,5-diphenylcyclopenta-2,4-dienone) ruthenium dimer (**3**) 0.100g (0.08mmol) in dry CH$_2$Cl$_2$ were stirred in the dark under inert atmosphere at room temperature for 1h. Upon filtration on a celite pad and removal of the solvent the quantitative formation of the Dicarbonyl-(η^4-3,4-bis(4-methoxyphenyl)-2,5-diphenylcyclopenta-2,4-dienone)[1-(2-Boc-NH-ethyl)-3-methylilidene]ruthenium (**4n**) was verified by ^{1}H-NMR and ^{13}C-NMR. ^{1}H-NMR (599.7 MHz, CDCl$_3$) δ (ppm): 7.76 (m, 4H, CH$_{aryl}$), 7.17-7.08 (m, 10H, CH$_{aryl}$), 6.99 (d, 1H, CH$_{NHC}$), 6.79 (d, 1H, CH$_{NHC}$), 6.64 (m, 4H, CH$_{aryl}$), 4.85 (t, 2H, -NCH$_2$), 3.72 (s, 6H, -OCH$_3$), 3.11 (s, 3H, -NCH$_3$), 2.96 (m, 2H, -CH$_2$NHBoc), 1.40 (s, 9H, -CH$_3$). ^{13}C{^{1}H} NMR (150.8 MHz, CDCl$_3$) δ (ppm): 202.13 (CO), 173.16 (C$_{carbene}$), 168.80 (C$_1$=O, Cp), 158.61 (-COCH$_3$), 156.27 (C=O, Boc), 135.00 (Cq$_{aryl}$), 133.60 (CH$_{aryl}$), 129.49 (CH$_{aryl}$), 127.60 (CH$_{aryl}$), 125.64 (Cq$_{aryl}$), 124.54 (CH$_{aryl}$), 124.11 (CH$_{NHC}$), 121.46 (CH$_{NHC}$), 112.95 (CH$_{aryl}$), 103.90 (C$_{2,5}$, Cp), 79.18 (C$_{3,4}$, Cp), 78.90 (Cq, tBu), 55.04 (-OCH$_3$), 49.47 (NCH$_2$), 39.81 (-CH$_2$NHBoc), 38.18 (-NCH$_3$), 28.40 (CH$_3$, tBu). IR (CH$_2$Cl$_2$) ν(CO): 2008 cm^{-1}, 1948 cm^{-1}, ν(C=O, Boc) 1707 cm^{-1}, ν(C=O) 1577 cm^{-1}, ν(C=C) 1602 cm^{-1},1518 cm^{-1}.

Dicarbonyl-(η^4-3,4-bis(4-methoxyphenyl)-2,5-diphenylcyclopenta-2,4-dienone)[1-(aminoethyl)-3-methyl)-imidazol-2-ylidene]ruthenium (4o): A solution of [Dicarbonyl-η^5-3,4-bis(4-methoxyphenyl)-2,5-diphenylhydroxycyclopentadienyl)(1-(2-aminoethyl)-3-dimethylimidazol-2-ylidene)ruthenium]tetrafluoroborato (**12o[BF$_4$]**) in CH$_2$Cl$_2$ was neutralized by a saturated solution of sodium bicarbonate (pH = 7–8). The aqueous layer was extracted with CH$_2$Cl$_2$ and washed with a potassium hydroxide solution (2 M) (3x30 mL), After 1h under mixing the organic phase was extracted with CH$_2$Cl$_2$ then concentrated under vacuum. The slightly brown solid obtained was identified as **4o** by IR, ^{1}H-NMR and ^{13}C-NMR. ^{1}H-NMR (599.7 MHz, CDCl$_3$) δ (ppm): 7.78 (m, 4H, CH$_{aryl}$), 7.15-7.07 (m, 10H, CH$_{aryl}$), 6.97 (s, 1H, CH$_{NHC}$), 6.82 (s, 1H, CH$_{NHC}$), 6.64 (m, 4H, CH$_{aryl}$), NH non si vede, 3.71 (s, 6H, -OCH$_3$), 3.58 (m, 2H, -NCH$_2$), 3.11 (s, 3H, -NCH$_3$), 2.56 (m, 2H, -CH$_2$-). ^{13}C{^{1}H} NMR (150.8 MHz, CDCl$_3$) δ (ppm): 202.33 (CO), 173.14 (C$_{carbene}$), 169.43 (C$_1$=O, Cp), 158.56 (-COCH$_3$), 135.26 (Cq$_{aryl}$), 133.60 (CH$_{aryl}$), 129.40 (CH$_{aryl}$), 127.54 (CH$_{aryl}$), 125.45 (Cq$_{aryl}$), 124.69 (CH$_{aryl}$), 112.92 (CH$_{aryl}$), 124.13 (CH$_{NHC}$), 121.19 (CH$_{NHC}$), 103.92 (C$_{2,5}$, Cp), 78.76 (C$_{3,4}$, Cp), 55.02 (-OCH$_3$), 53.06 (-NCH$_2$), 41.95 (-

CH$_2$*CH*$_2$-), 38.23 (-NCH$_3$). IR (CH$_2$Cl$_2$) v(CO): 2008 cm^{-1}, 1946 cm^{-1}, v(C=O) 1578 cm^{-1}, v(C=C) 1602 cm^{-1},1515 cm^{-1}.

Synthesis of hydroxycyclopentadienyl imidazolylideneRu(II) complexes (12)

12a[X] R$_1$ = R$_2$ = CH$_3$; X = CF$_3$SO$_3$, Cl, BF$_4$.
12c[X] R$_1$ = CH$_3$, R$_2$ = Bu; X = CF$_3$SO$_3$
12d[X] R$_1$ = CH$_3$, R$_2$ = CH$_2$CH$_2$OH; X = CF$_3$SO$_3$
12m[X] R$_1$ = Bu, R$_2$ = 2-py; X = CF$_3$SO$_3$, Cl, BF$_4$
12o[X] R$_1$ = CH$_3$, R$_2$ = CH$_2$CH$_2$NH$_2$; X = CF$_3$SO$_3,$ BF$_4$
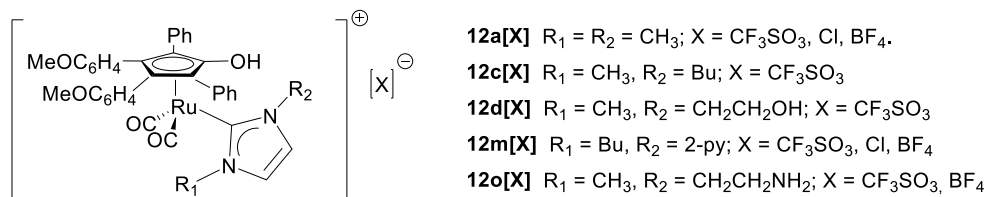
Figure 4.9 Structure of hydroxycyclopentadienyl imidazolylidene ruthenium complexes.

[Dicarbonyl-η^5-3,4-bis(4-methoxyphenyl)-2,5-diphenylhydroxycyclopentadienyl)(1,3-dimethylimidazol-2-ylidene)ruthenium]trifluoromethanesulfonate (12a[CF$_3$SO$_3$]): Dicarbonyl-η^4-3,4-bis(4-methoxyphenyl)-2,5-diphenylcyclopenta-2,4-dienone)(1,3-dimethylimidazol-2-ylidene)ruthenium complex (**4a**) 0.100g (0.143mmol) was dissolved in 10 mL of CH$_2$Cl$_2$ under inert atmosphere. 1.2 equivalent of HCF$_3$SO$_3$ (solution at 0.98% in CH$_2$Cl$_2$) 1.55mL (0.172mmol) were subsequently added. The reaction mixture was stirred for 10 minutes at room temperature, then the solvent was removed under vacuum and the crude washed twice with 10 ml of Et$_2$O. The slightly brown solid obtained was identified as **12a[CF$_3$SO$_3$]** by IR, ^{1}H-NMR, ^{13}C-NMR, ^{19}F-NMR, ESI-MS. The yield was quantitative and suitable crystals for X-Ray diffraction analysis were prepared by toluene/hexane double layer. ^{1}H-NMR (599.7 MHz, CDCl$_3$) δ (ppm): 7.43 (m, 4H, CH$_{aryl}$), 7.27-7.01 (m, 10H, CH$_{aryl}$), 6.97 (s, 2H, CH$_{NHC}$), 6.65 (m, 4H, CH$_{aryl}$), 3.71 (s, 6H, -OCH$_3$), 3.27 (s, 6H, NCH$_{3,NHC}$); ^{13}C{^{1}H} NMR (150.8 MHz, CDCl$_3$) δ (ppm): 199.64 (CO), 161.35 (C$_{carbene}$), 159.88 (-*C*OCH$_3$), 142.77 (C-OH, Cp), 133.86 (CH$_{aryl}$), 130.93 (CH$_{aryl}$), 129.07 (CH$_{aryl}$), 125.27 (Cq$_{aryl}$), 128.38 (Cq$_{aryl}$), 125.97 (CH$_{aryl}$), 121.40 (CH$_{NHC}$), 113.81 (CH$_{aryl}$), 104.85 (C$_{2,5}$, Cp), 87.90 (C$_{3,4}$, Cp), 55.55 (-OCH$_3$), 39.23 (CH$_{3,NHC}$). ^{19}F-NMR (282.4 MHz, CDCl$_3$) δ (ppm): -78.34 (CF$_3$SO$_3$). IR (CH$_2$Cl$_2$) v(CO): 2037 cm^{-1}, 1985 cm^{-1}, v(C=C) 1611 cm^{-1}, 1520 cm^{-1}. ESI-MS (m/z) (+) = 699 [M]$^+$; 149 [M]$^-$. Anal. Calcd (%) for C$_{39}$H$_{33}$F$_3$N$_2$O$_8$RuS: C, 55.18; H, 3.92; N, 3.30. Found: C, 55.14; H, 3.90; N, 3.32.

[Dicarbonyl-η5-3,4-bis(4-methoxyphenyl)-2,5-diphenylhydroxycyclopentadienyl)(1,3-dimethylimidazol-2-ylidene)ruthenium]chloride (12a[Cl]): Dicarbonyl-η^4-3,4-bis(4-methoxyphenyl)-2,5-diphenylcyclopenta-2,4-dienone)(1,3-dimethylimidazol-2-ylidene)ruthenium complex (**4a**) 0.023g (0.0330 mmol) was dissolved in 5 mL of CH$_2$Cl$_2$ under inert atmosphere. Two equivalent of HCl (aqueous solution at 37%, 0.005 mL, 0.0660 mmol) were subsequently added. The reaction mixture was stirred for 2h at room temperature, then the solvent was removed under vacuum and the crude washed twice with 10 ml of Et$_2$O . The slightly brown solid identified as **12a[Cl]** by IR, ^{1}H-NMR, ^{13}C-NMR, ESI-MS obtained in quantitative yield. ^{1}H-NMR (599.7 MHz, CDCl$_3$) δ (ppm): 7.57 (m, 4H, CH$_{aryl}$), 7.23-7.03 (m, 10H, CH$_{aryl}$), 6.93 (s, 2H, CH$_{NHC}$), 6.65 (m, 4H, CH$_{aryl}$), 3.71 (s, 6H, -OCH$_3$), 3.03 (s, 6H, NCH$_{3,NHC}$); ^{13}C{^{1}H} NMR (150.8 MHz, CDCl$_3$) δ (ppm): 199.79 (CO), 162.42 (C$_{carbene}$), 159.24 (-*C*OCH$_3$), 144.52 (C-OH, Cp), 133.47 (CH$_{aryl}$), 130.95 (CH$_{aryl}$), 128.60 (CH$_{aryl}$), 128.18 (Cq$_{aryl}$), 125.35 (CH$_{aryl}$), 121.60 (CH$_{NHC}$), 113.24 (CH$_{aryl}$), 104.55 (C$_{2,5}$, Cp), 86.61 (C$_{3,4}$, Cp), 55.09 (-OCH$_3$), 39.22 (CH$_{3,NHC}$). IR (CH$_2$Cl$_2$) v(CO): 2033 cm^{-1}, 1981 cm^{-1}, v(C=C) 1611 cm^{-1}, 1520 cm^{-1}. ESI-MS (m/z) (+) = 699 [M]$^+$. Anal. Calcd (%) for C$_{38}$H$_{33}$ClN$_2$O$_5$Ru: C, 62.11; H, 4.53; N, 3.81. Found: C, 62.13; H, 4.55; N, 3.79.

[Dicarbonyl-η^5-3,4-bis(4-methoxyphenyl)-2,5-diphenylhydroxycyclopentadienyl)(1,3-dimethylimidazol-2-ylidene)ruthenium]tetrafluoroborato (12a[BF₄]): Dicarbonyl-η^4-3,4-bis(4-methoxyphenyl)-2,5-diphenylcyclopenta-2,4-dienone)(1,3-dimethylimidazol-2-ylidene)ruthenium complex (**4a**) 0.050g (0.072mmol) was dissolved in 10mL of CH_2Cl_2 under inert atmosphere. 1.2 equivalent of tetrafluoroboric acid diethyl ether complex (0.012mL, 0.086mmol) were subsequently added. The reaction mixture was stirred for 1h at room temperature, then the solvent was removed under vacuum and the crude washed twice with 10 ml of Et_2O. The slightly brown solid identified as **12a[BF₄]** by IR, ^{1}H-NMR, ^{13}C-NMR, ^{19}F-NMR was obtained in quantitative yield. ^{1}H-NMR (599.7 MHz, $CDCl_3$) δ (ppm): 7.42 (m, 4H, CH_{aryl}), 7.31-7.03 (m, 10H, CH_{aryl}), 7.05 (s, 2H, CH_{NHC}), 6.68 (m, 4H, CH_{aryl}), 3.74 (s, 6H, $-OCH_3$), 3.29 (s, 6H, $NCH_3,_{NHC}$); ^{13}C{^{1}H} NMR (150.8 MHz, $CDCl_3$) δ (ppm): 199.06 (CO), 160.82 ($C_{carbene}$), 159.57 (-COCH₃), 141.82 (C-OH, Cp), 133.43 (CH_{aryl}), 130.40 (CH_{aryl}), 128.80 (CH_{aryl}), 128.78 (C_{aryl}), 127.89 (C_{aryl}), 125.74 (CH_{aryl}), 120.80 (CH_{NHC}), 113.47 (CH_{aryl}), 104.31 ($C_{2,5}$, Cp), 87.51 ($C_{3,4}$, Cp), 55.15 (-OCH_3), 38.75 ($CH_3,_{NHC}$); ^{19}F-NMR (282.4 MHz, $CDCl_3$) δ (ppm): -152.01 (BF₄). IR (CH_2Cl_2) ν(CO): 2038 cm⁻¹, 1987 cm⁻¹, ν(C=C) 1611 cm⁻¹, 1520 cm⁻¹. Anal. Calcd (%) for $C_{38}H_{33}BF_4N_2O_5Ru$: C, 58.09; H, 4.20; N, 3.57. Found: C, 58.11; H, 4.17; N, 3.58.

[Dicarbonyl-η^5-3,4-bis(4-methoxyphenyl)-2,5-diphenylhydroxycyclopentadienyl)(1-methyl-3-butyl-imidazol-2-ylidene)ruthenium]trifluoromethanesulfonate (12c[CF₃SO₃]): Dicarbonyl-η^4-3,4-bis(4-methoxyphenyl)-2,5-diphenylcyclopenta-2,4-dienone)(1-methyl-3-butyl-imidazol-2-ylidene)ruthenium complex (**4c**) 0.100g (0.135mmol) was dissolved in 10mL of CH_2Cl_2 under inert atmosphere. 1.2 equivalent of HCF_3SO_3 (solution at 0.98% in CH_2Cl_2 1.39 mL, 0.157mmol) were subsequently added. The reaction mixture was stirred for 1h at room temperature, then the solvent was removed under vacuum and the crude washed twice with 10 ml of Et_2O. The slightly brown solid identified as **12c[CF₃SO₃]** by IR, ^{1}H-NMR, ^{13}C-NMR and ^{19}F-NMR was obtained in quantitative yield. ^{1}H-NMR (599.7 MHz, $CDCl_3$) δ (ppm): 7.44 (m, 4H, CH_{aryl}), 7.28-7.02 (m, 10H, CH_{aryl}), 7.05 (2H, CH_{NHC}), 6.66 (m, 4H, CH_{aryl}), 3.72 (s, 6H, $-OCH_3$), 3.70(m, 2H, $-NCH_2$), 3.32 (s, 3H, $NCH_3,_{NHC}$), 1.49 (m, 2H, $-CH_2CH_2-$), 0.97 (m, 2H, $-CH_2CH_3$), 0.77 (m, 3H, $-CH_3$); ^{13}C{^{1}H} NMR (150.8 MHz, $CDCl_3$) δ (ppm): 199.27 (CO), 160.57 ($C_{carbene}$), 159.47 (-COCH₃), 142.83 (C-OH, Cp), 133.43 (CH_{aryl}), 130.55 (CH_{aryl}), 128.60 (CH_{aryl}), 128.09 (C_{aryl}), 126.24 (C_{aryl}), 123.02 (CH_{aryl}), 121.01 (CH_{NHC}), 113.39 (CH_{aryl}), 104.42 ($C_{2,5}$, Cp), 87.45 ($C_{3,4}$, Cp), 55.13(-OCH_3), 50.81 (-NCH_2), 38.91 (-NCH_3), 32.97 (-CH_2CH_2-), 19.48 (-CH_2CH_3), 13.65(-CH_3); ^{19}F-NMR (282.4 MHz, $CDCl_3$) δ (ppm): -78.37. IR (CH_2Cl_2) ν(CO): 2035 cm⁻¹, 1984 cm⁻¹, ν(C=C) 1610 cm⁻¹, 1520 cm⁻¹. ESI-MS (m/z) (+) = 741[M]⁺, 149 [M]⁻. Anal. Calcd (%) for $C_{42}H_{39}F_3N_2O_8RuS$: C, 56.62; H, 4.38; N, 3.15. Found: C, 56.59; H, 4.37; N, 3.16.

[Dicarbonyl-η^5-3,4-bis(4-methoxyphenyl)-2,5-diphenylhydroxycyclopentadienyl)(1-methyl-3-(2-hydroxyethyl-imidazol-2-ylidene)ruthenium]trifluoromethanesulfonate (12d[CF₃SO₃]): Dicarbonyl-η^4-3,4-bis(4-methoxyphenyl)-2,5-diphenylcyclopenta-2,4-dienone)(1-methyl-3-(2-hydroxyethyl-imidazol-2-ylidene)ruthenium complex (**4d**) 0.050g (0.069mmol) was dissolved in 10 mL of CH_2Cl_2 under inert atmosphere. 1.2 equivalent of HCF_3SO_3 (solution at 0.98% in CH_2Cl_2 0.73 mL, 0.082mmol) were subsequently added. The reaction mixture was stirred for 1h at room temperature, then the solvent was removed under vacuum and the crude washed twice with 10 ml of Et_2O. The slightly brown solid identified as **12d[CF₃SO₃]** by IR, ^{1}H-NMR, ^{13}C-NMR, ^{19}F-NMR, ESI-MS was obtained in quantitative yield. Suitable crystals for X-Ray diffraction analysis were prepared by slow diffusion from CH_2Cl_2/Et_2O double layer. ^{1}H-NMR (399.9 MHz, $CDCl_3$) δ (ppm): 7.46 (m, 4H, CH_{aryl}), 7.30-7.03 (m, 10H, CH_{aryl}), 7.40 (s, 1H, CH_{NHC}), 7.01 (s, 1H, CH_{NHC}), 6.68

(m, 4H, CH$_{aryl}$), CH$_2$ not detected, (m, 2H,-NCH$_2$), 3.73 (s, 6H, -OCH$_3$), 3.24 (s, 3H, -NCH$_3$); ^{13}C-NMR (100.6 MHz, CDCl$_3$) δ (ppm): 206.97 (CO), 162.98 (C$_{carbene}$), 159.58 (-COCH$_3$), 142.23 (C-OH, Cp), 133.41 (CH$_{aryl}$), 130.49 (CH$_{aryl}$), 128.84 (CH$_{aryl}$) 128.62 (C$_{aryl}$), 126.08 (C$_{aryl}$), 123.02 (CH$_{aryl}$), 120.75 (CH$_{NHC}$), 113.48 (CH$_{aryl}$), C$_{aryl}$, Cp not detected,, 58.43 (-NCH$_2$) , 55.14 (-OCH$_3$), 51.82 (-CH$_2$OH), 38.45 (-NCH$_3$); ^{19}F-NMR (282.4 MHz, CDCl$_3$) δ (ppm): -78.37. IR (CH$_2$Cl$_2$) ν(CO): 2038 cm^{-1}, 1988 cm^{-1}, ν(C=C) 1610 cm^{-1}, 1520 cm^{-1}. ESI-MS (m/z) (+) = 729 [M]$^+$, 149 [M]$^-$ Anal. Calcd (%) for C$_{40}$H$_{35}$F$_3$N$_2$O$_9$RuS: C, 54.67; H, 3.85; N, 3.19. Found: C, 54.68; H, 3.83; N, 3.22.

[Dicarbonyl-η^5-3,4-bis(4-methoxyphenyl)-2,5-diphenylhydroxycyclopentadienyl)(1-butyl-3-(2-pyridinyl)-imidazol-2-ylidene)ruthenium]trifluoromethanesulfonate (12m[CF$_3$SO$_3$]): Dicarbonyl-η^4-3,4-bis(4-methoxyphenyl)-2,5-diphenylcyclopenta-2,4-dienone)(1-butyl-3-(2-pyridinyl)-imidazol-2-ylidene)ruthenium complex (**4m**) 0.100g (0.124mmol) was dissolved in 10mL of CH$_2$Cl$_2$ under inert atmosphere. 1.2equivalent of HCF$_3$SO$_3$ (solution at 0.98% in CH$_2$Cl$_2$ 1.35mL, 0.149mmol) were subsequently added. The reaction mixture was stirred for 15 minutes at room temperature, then the solvent was removed under vacuum and the crude washed twice with 10 ml of Et$_2$O. The slightly orange solid identified as **12m[CF$_3$SO$_3$]** by IR, ^{1}H-NMR, ^{13}C-NMR, ^{19}F-NMR, ESI-MS was obtained in quantitative yield. ^{1}H-NMR (599.7 MHz, CD$_3$CN) δ (ppm): 7.88 (m, 1H, CH$_{py}$), 7.38 (m, 1H, CH$_{py}$), 7.34 (m, 1H, CH$_{py}$), 7.28 (d, 1H, CH$_{NHC}$), 7.25 (d, 1H, CH$_{NHC}$), 7.23 (m, 1H, CH$_{py}$), 7.17-6.99 (m, 10H, CH$_{aryl}$), 6.78 (m, 4H, CH$_{aryl}$), 6.48 (m, 4H, CH$_{aryl}$), 3.70 (t, 2H, NCH$_2$), 3.68 (s, 6H, -OCH$_3$), 1.72 (m, 2H, -CH_2CH$_2$-), 1.19 (m, 2H, -CH_2CH$_3$), 0.88 (t, 3H, -CH$_3$); ^{13}C{^{1}H} NMR (150.8 MHz, CD$_3$CN) δ (ppm): 199.59 (CO), 166.73 (C$_{carbene}$), 160.80 (-COCH$_3$), 149.27 (C$_{ipso}$), 147.43 (CH$_{py}$), 144.94 (CH$_{py}$), 136.56 (C$_1$-OH, Cp), 134.52-114.29 (C$_{aryl}$), 127.93 (CH$_{NHC}$), 125.71 (CH$_{py}$), 125.13(CH$_{py}$), 121.95 (CH$_{NHC}$), 104.10(C$_{2,5}$, Cp), 94.05 (C$_{3,4}$, Cp), 55.98 (-OCH$_3$), 52.87 (-NCH$_2$), 33.72 (-CH$_2$CH$_2$), 20.42 (-CH$_2$CH$_3$), 13.93 (-CH$_3$); ^{19}F-NMR (282.4 MHz, CD$_3$CN) δ (ppm): -79.33 (CF$_3$SO$_3$). IR (CH$_2$Cl$_2$) ν(CO): 2041 cm^{-1}, 1991 cm^{-1}, ν(C=C) 1610 cm^{-1}, 1520 cm^{-1}. ESI-MS (m/z) (+) = 804 [M]$^+$, 149 [M]$^-$. Anal. Calcd (%) for C$_{46}$H$_{40}$F$_3$N$_3$O$_8$RuS: C, 57.91; H, 4.23; N, 4.41. Found: C, 57.89; H, 4.22; N, 4.38.

[Dicarbonyl-η^5-3,4-bis(4-methoxyphenyl)-2,5-diphenylhydroxycyclopentadienyl)(1-butyl-3-(2-pyridinyl)-imidazol-2-ylidene)ruthenium]chloride (12m[Cl]): Dicarbonyl-η^4-3,4-bis(4-methoxyphenyl)-2,5-diphenylcyclopenta-2,4-dienone)(1-butyl-3-(2-pyridinyl)- imidazol-2-ylidene)ruthenium complex (**4m**) 0.025g (0.031mmol) was dissolved in 5 mL of CH$_2$Cl$_2$ under inert atmosphere. Two equivalent of HCl (aqueous solution at 37%, 0.005mL, 0.061mmol) were subsequently added. The reaction mixture was stirred for 1h at room temperature, then the solvent was removed under vacuum and the crude washed twice with 10 ml of Et$_2$O. The slightly brown solid identified as **12m[Cl]** by IR, ^{1}H-NMR, ^{13}C-NMR obtained in quantitative yield. ^{1}H-NMR (599.7 MHz, CD$_3$CN) δ (ppm): 8.10 (m, 1H, CH$_{py}$), 7.69 (m, 1H, CH$_{py}$), 7.48 (d, 2H, CH$_{NHC}$), 7.45 (d, 2H, CH$_{NHC}$), 7.41-7.19 (m, 10H, CH$_{aryl}$ + 2H, CH$_{py}$), 6.98 (m, 4H, CH$_{aryl}$), 6.65 (m, 4H, CH$_{aryl}$), 3.68 (t, 2H, -NCH$_2$), 3.69 (s, 6H, -OCH$_3$), 1.70 (m, 2H, -CH_2CH$_2$-), 1.14 (m, 2H, -CH_2CH$_3$), 0.84 (t, 3H, -CH$_3$); ^{13}C{^{1}H} NMR (150.8 MHz, CD$_3$CN) δ (ppm): 199.73 (CO), 166.09 (C$_{carbene}$), 160.67 (-COCH$_3$), 150.34 (C$_{ipso}$), 147.87 (CH$_{py}$), 143.52 (CH$_{py}$), 136.47 (C$_1$-OH, Cp), 134.62-114.23 (C$_{aryl}$ + CH$_{py}$), 124.71 (CH$_{NHC}$), 122.13 (CH$_{NHC}$), 102.43 (C$_{2,5}$, Cp), 87.44 (C$_{3,4}$, Cp), 55.95 (-OCH$_3$), 52.65 (-NCH$_2$), 33.24 (-CH$_2$CH$_2$), 20.40 (-CH$_2$CH$_3$), 13.93 (-CH$_3$); IR (CH$_2$Cl$_2$) ν(CO): 2041cm^{-1}, 1992 cm^{-1}, ν(C=C) 1609 cm^{-1}, 1521 cm^{-1}. Anal. Calcd (%) for C$_{45}$H$_{39}$ClN$_3$O$_5$Ru: C, 64.43; H, 4.69; N, 5.01. Found: C, 64.40; H, 4.66; N, 5.02.

[Dicarbonyl-η⁵-3,4-bis(4-methoxyphenyl)-2,5-diphenylhydroxycyclopentadienyl)(1-butyl-3-(2-pyridinyl)-imidazol-2-ylidene)ruthenium]tetrafluoroborate (12m[BF₄]): Dicarbonyl-η⁴-3,4-bis(4-methoxyphenyl)-2,5-diphenylcyclopenta-2,4-dienone)(1-butyl-3-(2-pyridinyl)-imidazol-2-ylidene)ruthenium complex (**4m**) 0.050 g (0.062 mmol) was dissolved in 5 mL of CH_2Cl_2 under inert atmosphere. 1.2 equivalent of tetrafluoroboric acid diethyl ether complex (0.012mL, 0.086mmol) were subsequently added. The reaction mixture was stirred for 1h at room temperature, then the solvent was removed under vacuum and the crude washed twice with 10 ml of Et_2O. The slightly brown solid identified as **12m[BF₄]** by IR, ^{1}H-NMR, ^{19}F-NMR, ^{13}C-NMR, ESI-MS was obtained in quantitative yield. ^{1}H-NMR (599.7 MHz, CD_3CN) δ (ppm): 7.95 (m, 1H, CH_{py}), 7.49-7.16 (m, 10H, CH_{aryl} + 3H, CH_{py} + 2H, CH_{NHC}), 6.98 (m, 4H, CH_{aryl}), 6.69 (m, 4H, CH_{aryl}), 3.69 (s, 6H, $-OCH_3$), 3.67 (t, 2H, NCH_2), 1.75 (m, 2H, $-CH_2CH_2-$), 1.25 (m, 2H, $-CH_2CH_3$), 0.79 (t, 3H, $-CH_3$); ^{13}C{^{1}H} NMR (150.8 MHz, CD_3CN) δ (ppm): 199.65 (CO), 166.30 ($C_{carbene}$), 160.78 ($-COCH_3$), 151.52 (C_{ipso}), 149.07 (CH_{py}), 142.05 (CH_{py}), 134.63 (C_1-OH, Cp), 134.06-114.30 (C_{aryl}), 126.82 (CH_{NHC}), 124.74 (CH_{py}), 124.25 (CH_{py}), 122.20 (CH_{NHC}), 104.16($C_{2,5}$, Cp), 87.35 ($C_{3,4}$, Cp), 56.00 ($-OCH_3$), 52.84 (NCH_2), 33.21 ($-CH_2CH_2-$), 20.55 ($-CH_2CH_3$), 13.91 ($-CH_3$); ^{19}F-NMR (282.4 MHz, CD_3CN) δ (ppm): -151.63 (BF_4). IR (CH_2Cl_2) ν(CO): 2041 cm^{-1}, 1992 cm^{-1}, ν(C=C) 1609 cm^{-1}, 1521 cm^{-1}. Anal. Calcd (%) for $C_{45}H_{39}BF_4N_3O_5Ru$: C, 60.66; H, 4.41; N, 4.71. Found: C, 60.63; H, 4.40; N, 4.69.

[Dicarbonyl-η⁵-3,4-bis(4-methoxyphenyl)-2,5-diphenylhydroxycyclopentadienyl)(1-(2-aminoethyl)-3-dimethylimidazol-2-ylidene)ruthenium]tetrafluoroborato (12o[BF₄]): Dicarbonyl-($η^4$-3,4-bis(4-methoxyphenyl)-2,5-diphenylcyclopenta-2,4-dienone)[1-(2-Boc-NH-ethyl)-3-methyl)-imidazol-2-ylidene]ruthenium (**4n**) 0.084g (0.10mmol) was dissolved in 10 mL of Et_2O under inert atmosphere. 10 equivalents of tetrafluoroboric acid diethyl ether complex (0.14mL, 1.04mmol) were subsequently added. . The reaction mixture was stirred for 1h at room temperature, then the precipitation of a slightly brown solid was observed. The crude was filtered under inert atmosphere and the solid washed twice with 10 ml of Et_2O. The slightly brown solid identified as **12o[BF₄]** by IR, ^{1}H-NMR and ^{13}C-NMR. ^{1}H-NMR (599.7 MHz, CD_3CN) δ (ppm): 7.46-7.36 (m, 10H, CH_{aryl}), 7.23 (d, 1H, CH_{NHC}), 7.21 (d, 1H, CH_{NHC}), 7.12 (m, 4H, CH_{aryl}), 6.71 (m, 4H, CH_{aryl}), 6.40 (br, s, 1H, NH), 3.94 (m, 2H, $-NCH_2$), 3.70 (s, 6H, $-OCH_3$), 3.32 (s, 3H, $-NCH_3$), 3.15 (m, 2H, $-CH_2-$). ^{13}C{^{1}H} NMR (150.8 MHz, CD_3CN) δ (ppm): (CO) not detected, 164.72 ($C_{carbene}$), 160.11 ($-COCH_3$),),142.03 (C_1-OH, Cp), 134.15 – 113.58 (C_{aryl}, CH_{NHC}), 105.52 ($C_{2,5}$, Cp), 84.21 ($C_{3,4}$, Cp), 55.49 ($-OCH_3$), 47.35 ($-NCH_2$), 40.02 ($-NCH_3$), 39.35 ($-CH_2CH_2-$). IR (CH_2Cl_2) ν(CO): 2042 cm^{-1}, 2021 cm^{-1}, 1992 cm^{-1}, 1966 cm^{-1}, ν(C=C) 1610 cm^{-1}, 1520 cm^{-1}.

[Dicarbonyl-η⁵-3,4-bis(4-methoxyphenyl)-2,5-diphenylhydroxycyclopentadienyl)(1-(2-aminoethyl)-3-dimethylimidazol-2-ylidene)ruthenium]tetrafluoroborato (12o[CF₃SO₃]): Dicarbonyl-($η^4$-3,4-bis(4-methoxyphenyl)-2,5-diphenylcyclopenta-2,4-dienone)[1-(aminoethyl)-3-methyl)-imidazol-2-ylidene]ruthenium complex (**4o**) 0.039g (0.005mmol) was dissolved in 5mL of CH_2Cl_2 under inert atmosphere. 1.5equivalents of HCF_3SO_3 (solution at 0.98% in CH_2Cl_2 0.71mL, 0.008mmol) were subsequently added. The reaction mixture was stirred for 15 minutes at room temperature, then the solvent was removed under vacuum and the crude washed twice with 10 ml of Et_2O. The slightly orange solid identified as **12o[CF₃SO₃]** by IR, ^{1}H-NMR, ^{13}C-NMR and ^{19}F-NMR. ^{1}H-NMR (599.7 MHz, $CDCl_3$) δ (ppm): 7.42-7.34 (m, 10H, CH_{aryl}), 7.24 (s, 1H, CH_{NHC}), 7.10 (s, 1H, CH_{NHC}), 7.00 (m, 4H, CH_{aryl}), 6.78 (br, s, 1H, NH), 6.66 (m, 4H, CH_{aryl}), 4.07 (m, 2H, $-NCH_2$), 3.73 (s, 6H, $-OCH_3$), 3.41 (s, 3H, $-NCH_3$), 2.67 (m, 2H, $-CH_2-$). ^{19}F-NMR (282.4 MHz, $CDCl_3$) δ (ppm): -78.52. ^{13}C{^{1}H}

NMR (150.8 MHz, CDCl$_3$) δ (ppm): 198.28 (CO), 162.39 (C$_{carbene}$), 159.66 (-COCH$_3$), 140.38 (C$_1$-OH, Cp), 133.37-113.52 (C$_{aryl}$ + CH$_{NHC}$), 103.92 (C$_{2,5}$, Cp), 88.67 (C$_{3,4}$, Cp), 55.16 (-OCH$_3$), 48.02 (-NCH$_2$), 39.68 (-CH$_2$CH$_2$-), 39.37 (-NCH$_3$). IR (CH$_2$Cl$_2$) ν(CO): 2042 cm^{-1}, 1993 cm^{-1}, ν(C=C) 1612 cm^{-1},1520 cm^{-1}.

Synthesis of cationic methoxycyclopentadienyl imidazolylidene Ru(II) complexes (13)
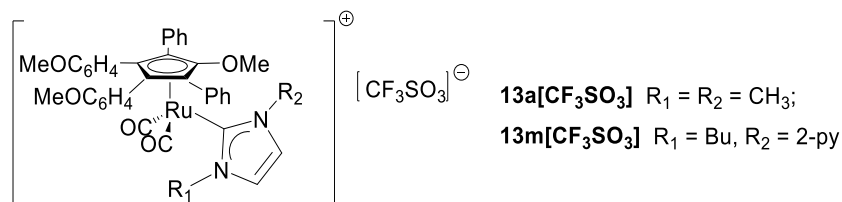

Figure 4.10. Structure of methoxycyclopentadienyl imidazolylidene ruthenium complexes (**13**).

[Dicarbonyl-η^5-3,4-bis(4-methoxyphenyl)-2,5-diphenylmethoxycyclopentadienyl)(1,3-dimethyl-imidazol-2-ylidene)ruthenium]trifluoromethanesulfonate (13a[CF$_3$SO$_3$]): Dicarbonyl-η^4-3,4-bis(4-methoxyphenyl)-2,5-diphenylcyclopenta-2,4-dienone)(1,3-dimethylimidazol-2-ylidene)ruthenium complex (**4a**) 0.100g (0.143mmol) was dissolved in 10 mL of CH$_2$Cl$_2$ under inert atmosphere. Three equivalent of MeCF$_3$SO$_3$ (0.048mL, 0.429 mmol) were subsequently added. The reaction mixture was stirred for 1h at room temperature, then the solvent was removed under vacuum and the crude washed twice with 10 ml of Et$_2$O. The slightly brown solid identified as **13a[CF$_3$SO$_3$]** by IR, ^{1}H-NMR, ^{13}C-NMR, ^{19}F-NMR, ESI-MS was obtained in quantitative yield. ^{1}H-NMR (599.7 MHz, CD$_3$CN) δ (ppm): 7.40-7.31 (m, 10H, CH$_{aryl}$), 7.13 (s, 2H, CH$_{NHC}$), 7.04 (m, 4H, CH$_{aryl}$), 6.66 (m, 4H, CH$_{aryl}$), 3.68 (s, 6H, -OCH$_3$), 3.43 (s, 6H, NCH$_3$), 2.99 (s, 3H, -OCH$_3$); ^{13}C{^{1}H} NMR (150.8 MHz, CD$_3$CN) δ (ppm): 199.52 (CO), 161.90 (C$_{carbene}$), 160.59 (-COCH$_3$), 141.45 (C-OCH$_3$, Cp), 134.53 (CH$_{aryl}$), 132.34 (CH$_{aryl}$), 129.66 (CH$_{aryl}$), 129.28 (C$_{aryl}$), 128.24 (C$_{aryl}$), 126.22 (CH$_{aryl}$), 121.71 (CH$_{NHC}$), 114.04 (CH$_{aryl}$), 104.86 (C$_{2,5}$, Cp), 93.24 (C$_{3,4}$, Cp), 62.47 (-OCH$_3$, Cp), 55.87 (-OCH$_3$), 39.71 (-NCH$_3$); ^{19}F-NMR (282.4 MHz, CD$_3$CN) δ (ppm): -78.23. IR (CH$_2$Cl$_2$) ν(CO): 2045 cm^{-1}, 1995 cm^{-1}; ν(C=C) 1610 cm^{-1}, 1521 cm^{-1}. ESI-MS (m/z) (+) = 713 [M]$^+$; 149 [M]$^-$. Anal. Calcd (%) for C$_{40}$H$_{35}$F$_3$N$_2$O$_8$RuS: C, 55.68; H, 4.09; N 3.25. Found: C, 55.65; H, 4.07; N 3.27.

[Dicarbonyl-η^5-3,4-bis(4-methoxyphenyl)-2,5-diphenylmethoxycyclopentadienyl1-butyl-3-(2-pyridinyl)-imidazol-2-ylidene)ruthenium]trifluoromethanesulfonate (13m[CF$_3$SO$_3$]): Dicarbonyl-η^4-3,4-bis(4-methoxyphenyl)-2,5-diphenylcyclopenta-2,4-dienone)(1-butyl-3-(2-pyridinyl)-imidazol-2-ylidene)ruthenium complex (**4m**) 0.050g (0.072mmol) was dissolved in 10 mL of CH$_2$Cl$_2$ under inert atmosphere. Three equivalent of MeCF$_3$SO$_3$ (0.023mL, 0.216mmol) were subsequently added. The reaction mixture was stirred for 1h at room temperature, then the solvent was removed under vacuum and the crude washed twice with 10 ml of Et$_2$O. The slightly brown solid identified as **13m[CF$_3$SO$_3$]** by IR and ESI-MS was obtained in quantitative yield. . ^{1}H-NMR (599.7 MHz, CD$_3$CN) δ (ppm): 8.47 (m, 1H, CH$_{py}$), 7.87 (m, 1H, CH$_{py}$), 7.71 (m, 1H, CH$_{py}$), 7.65 (d, 1H, CH$_{NHC}$), 7.56 (d, 1H, CH$_{NHC}$), 7.46-6.59 (m, 18H, CH$_{aryl}$ + 1H, CH$_{py}$), 3.69 (s, 6H, -OCH$_3$), 3.63 (t, 2H, NCH$_2$), 3.15 (s, 6H, -OCH$_3$, Cp), 1.52 (m, 2H, -CH_2CH$_2$-), 1.11 (m, 2H, -CH_2CH$_3$), 0.77 (t, 3H, -CH$_3$); ^{13}C{^{1}H} NMR (150.8 MHz, CD$_3$CN) δ (ppm): 199.85 (CO), 167.40 (C$_{carbene}$), 160.61 (-COCH$_3$), 150.52 (C$_{ipso}$), 149.56 (CH$_{py}$), 145.70 (CH$_{py}$), 140.66 (C$_1$-OCH$_3$, Cp), 134.60-114.14 (C$_{aryl}$), 127.56 (CH$_{NHC}$), 124.19 (CH$_{py}$), 121.64 (CH$_{py}$), 120.73 (CH$_{NHC}$), C$_{aryl}$, Cp not detected, 63.36 (-OCH$_3$, Cp), 55.93 (-OCH$_3$), 52.14 (-NCH$_2$), 33.04 (-CH$_2$CH$_2$), 20.15 (-CH$_2$CH$_3$), 14.01 (-CH$_3$); ^{19}F-NMR (282.4 MHz, CD$_3$CN) δ (ppm): -79.32 (CF$_3$SO$_3$). IR

(CH_2Cl_2) v(CO): 2045 cm^{-1}, 1996 cm^{-1}, v(C=C) 1611 cm^{-1}, 1520 cm^{-1}. ESI-MS (m/z) (+) = 818 [M]$^+$; 149 [M]$^-$. Anal. Calcd (%) for $C_{47}H_{42}F_3N_3O_8RuS$: C, 58.32; H, 4.34; N, 4.34. Found: C, 58.30; H, 4.32; N, 4.35.

Synthesis of monocarbonylic Ru carbene complexes

[Carbonyl-η⁵-3,4-bis(4-methoxyphenyl)-2,5-diphenylmethoxycyclopentadienyl)(1-butyl-3-(2-pyridinyl)-imidazol-2-ylidene)ruthenium]trifluoromethanesulfonate (14m[CF₃SO₃])
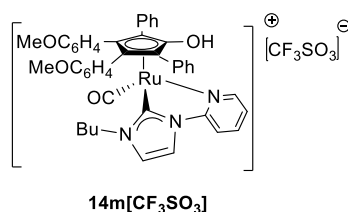

14m[CF₃SO₃]

Figure 4.11. Structure of chelated ruthenium complex (**14m[CF₃SO₃]**).

[Dicarbonyl-η⁵-3,4-bis(4-methoxyphenyl)-2,5-diphenylhydroxycyclopentadienyl)(1-butyl-3-(2-pyridinyl)-imidazol-2-ylidene)ruthenium]trifluoromethanesulfonate(**12m[CF₃SO₃]**) was dissolved in 25 mL of ⁱPrOH. The reaction mixture was irradiated under stirring for 3h, then the solvent was removed under vacuum and the crude washed twice with 20 mL of hexane. The brown solid was identified as 6 and obtained with a yield of 78 %. **14m[CF₃SO₃]** has been completely characterized by IR, ¹H-NMR, ¹³C-NMR, ¹⁹F-NMR, ESI-MS. Suitable crystals for X-Ray diffraction analysis were prepared by slow diffusion from CH_2Cl_2/hexane double layer. ¹H-NMR (599.7 MHz, CDCl₃) δ (ppm): 8.33 (d, 1H, CH$_{py}$), 8.27 (m, 1H, CH$_{py}$), 8.09 (m, 1H, CH$_{py}$), 7.04 (m, 4H, CH$_{aryl}$), 7.30-6.66 (m, 2H, CH$_{NHC}$+ 10H, CHaryl), 3.86 (m, 2H, NCH₂), 3.79 (s, 3H, -OCH₃), 3.74 (s, 3H, -OCH₃), 1.47 (m, 2H, -CH_2CH₂), 0.97 (m, 2H, -CH_2CH₃), 0.72 (t, 3H, -CH₃); ¹³C{¹H} NMR (150.8 MHz, CDCl₃) δ (ppm): 199.57 (CO), 185.63 (C$_{carbene}$), 159.30, 159.08 (-COCH₃), 154.60 (C$_{ipso}$), 153.34 (CH$_{py}$), 141.53 (C₁-OH, Cp), 138.08 (CH$_{py}$), 133.31-112.74 (C$_{aryl}$ + CH$_{NHC}$), 97.38 (C$_{2,5}$, Cp), 84.34 (C$_{3,4}$, Cp), 55.21 (-OCH₃), 50.67 (NCH₂), 32.66, 19.35 (-CH₂CH₂), 13.56 (-CH₃); ¹⁹F-NMR (282.4 MHz, CD₃CN) δ (ppm): -78.19 (CF₃SO₃); IR (CH_2Cl_2) v(CO): 1967 cm^{-1}, v(C=C) 1609 cm^{-1}, 1521 cm^{-1}; ESI-MS (m/z) (+) = 776 [M]$^+$, 149 [M]$^-$. Anal. Calcd (%) for $C_{45}H_{40}F_3N_3O_7RuS$: C, 58.37; H, 4.36; N, 4.54. Found: C, 58.35; H, 4.35; N, 4.51.

[Carbonyl-pyridin-η⁵-3,4-bis(4-methoxyphenyl)-2,5-diphenylhydroxycyclopentadienyl)(1,3-dimethylimidazol-2-ylidene)ruthenium] trifluoromethanesulfonate (15[CF₃SO₃])

15[CF₃SO₃]

Figure 4.12. Structure of monocarbonylic ruthenium carbene complex (**15[CF₃SO₃]**).

[Dicarbonyl-η⁵-3,4-bis(4-methoxyphenyl)-2,5-diphenylhydroxycyclopentadienyl)(1,3-dimethylimidazol-2-ylidene)ruthenium]trifluoromethanesulfonate (**12a[CF₃SO₃]**) 0.060g (0.071mmol) and pyridine 0.023mL (0.283mmol) were dissolved in ⁱPrOH (25 mL). The reaction mixture was irradiated under stirring for 6h and **15[CF₃SO₃]** identified from the reaction mixture by IR and ESI-MS. IR (CH_2Cl_2) v(CO): 1943 cm^{-1}, v(C=C) 1610 cm^{-1},1520 cm^{-1}. ESI-MS (m/z) (+) (CH₃CN) = 671 [M-py]$^+$, 643 [M-py-CO]$^+$

[Carbonyl-pyridin-η⁵-3,4-bis(4-methoxyphenyl)-2,5-diphenylmethoxycyclopentadienyl)(1,3-dimethylimidazol-2-ylidene)ruthenium] trifluoromethanesulfonate (16[CF₃SO₃])

16[CF₃SO₃]

Figure 4.13. Structure of monocarbonylic ruthenium complex (**16[CF₃SO₃]**).

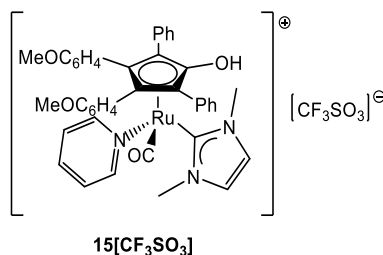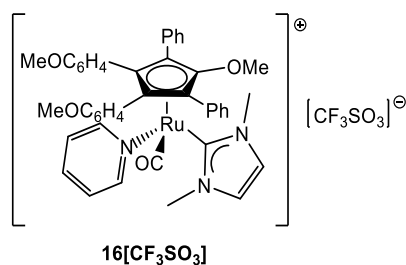[Dicarbonyl-η⁵-3,4-bis(4-methoxyphenyl)-2,5-diphenylmethoxycyclopentadienyl)(1,3-dimethyl-imidazol-2-ylidene)ruthenium]trifluoromethanesulfonato (**13a[CF₃SO₃]**) 0.050g (0.058mmol) and pyridine 0.023mL (0.232mmol) were dissolved in toluene (25 mL). The reaction mixture was irradiated under stirring for 18h and **16[CF₃SO₃]** identified from the reaction mixture by IR and ESI-MS. IR (CH₂Cl₂) ν(CO): 1948 cm⁻¹, ν(C=C) 1610 cm⁻¹,1520 cm⁻¹. ESI-MS (m/z) (+) (MeOH) = 764 [M]⁺; 149 [M]⁻

General procedure for transfer hydrogenation

Complex (15 μmol, 5% mol), additive (1 eq. when needed) and *i*PrOH (3 mL) were stirred at reflux for 15 min. Then 4-fluoroacetophenone (36 μL, 300 μmol) was added and samples were taken at regular intervals. Aliquots (ca. 0.05mL) were diluted with CDCl₃ (0.5 mL) and conversions were determined by ¹⁹F-NMR spectroscopy and GC analysis.

X-ray Crystallography

Crystal data and collection details for **4m·0.5CH₂Cl₂**, **[12a][CF₃SO₃]·0.5toluene**, **[12d][CF₃SO₃]·CHCl₃** and **[14m][CF₃SO₃]** are reported in Table 4.3. The diffraction experiments were carried out on a Bruker APEX II diffractometer equipped with a CCD detector using Mo–Kα radiation. Data were corrected for Lorentz polarization and absorption effects (empirical absorption correction SADABS).[16] Structures were solved by direct methods and refined by full-matrix least-squares based on all data using F^2.[17] All hydrogen atoms were fixed at calculated positions and refined by a riding model, unless otherwise stated. All non-hydrogen atoms were refined with anisotropic displacement parameters.

4m·0.5CH₂Cl₂: The asymmetric unit of the unit cell contains one **4m** complex (on a general position) and half of a CH₂Cl₂ molecule disordered over two symmetry related (by 2) positions. The disordered solvent molecule has been refined isotropically. The crystals are non-merohedrally twinned. The TwinRotMat routine of PLATON[18] was used to determine the twinning matrix and to write the reflection data file (.hkl) containing the two twin components. Refinement was performed using the instruction HKLF 5 in SHELXL and one BASF parameter (0.291(8) after refinement). The Bu-group of the **4m** complex is disordered over two positions and has been refined isotropically using one occupancy factor per disordered group. Similar *U* restraints (SIMU line in SHELXL; s.u. 0.01) have been applied to C, N and O atoms. Restraints to bond distances were applied as follow (s.u. 0.02): 1.53 Å for C–C in the disordered Bu-group of **4m**; 1.75 Å for C–Cl in CH₂Cl₂. The Ph-rings have been constrained to fit regular hexagons (AFIX 66 line in SHELXL).

[12a][CF$_3$SO$_3$]·0.5toluene: The asymmetric unit of the unit cell contains two cations, two anions and one toluene molecule (all located in general positions). The H-atoms bonded to the O-atoms have been located in the Fourier map and refined using the 1.5 fold U_{iso} value of the parent atoms. The O-H distances have been restrained to 0.89 Å (s.u. 0.01). Similar U restraints (SIMU line in SHELXL; s.u. 0.01) have been applied to C and F atoms. The F-atoms have been restrained to isotropic behaviour (ISOR line in SHELXL, s.u. 0.01).

[12d][CF$_3$SO$_3$]·CHCl$_3$: The asymmetric unit of the unit cell contains two cations, two anions and two CHCl$_3$ molecules (all located in general positions). One CHCl$_3$ molecule is disordered over two positions and has been refined using one occupancy parameter per disordered group. The H-atoms bonded to the O-atoms have been initially located in the Fourier map and, then, refined by a riding model. The F-atoms have been restrained to isotropic behaviour (ISOR line in SHELXL, s.u. 0.01).

[14m][CF$_3$SO$_3$]: The asymmetric unit of the unit cell contains one cation and one anion (all located in general positions). The F and O atoms of the CF$_3$SO$_3^-$ anion are disordered and, thus, have been split and refined using one occupancy parameter per disordered group. The chelating NHC ligand in the cation is disordered and, thus, it has been split into two postions and refined using one occupancy parameter per disordered group. The H-atoms bonded to the O-atoms have been initially located in the Fourier map and, then, refined by a riding model. Similar U restraints (SIMU line in SHELXL; s.u. 0.01) have been applied to C, N, F and O atoms. The C, N, O and F atoms of the disordered groups have been restrained to isotropic behaviour (ISOR line in SHELXL, s.u. 0.01). The Ph-rings have been constrained to fit regular hexagons (AFIX 66 line in SHELXL). Restraints to bond distances were applied as follow (s.u. 0.02): 1.53 Å for C–C in the Bu-group; 1.43 Å for C(sp^3)–O; 1.34 Å for C(sp^2)–O.

X-Ray diffraction studies

Table 4.3. Crystal data and experimental details for **4m·0.5CH₂Cl₂, [12a] [CF₃SO₃]·0.5toluene, [12d][CF₃SO₃]·CHCl₃ and [14m][CF₃SO₃]**.

	4m·0.5CH₂Cl₂	[12a][CF₃SO₃]·0.5toluene
Formula	$C_{45.5}H_{40}ClN_3O_5Ru$	$C_{42.5}H_{37}F_3N_2O_8RuS$
Fw	845.33	893.87
T, K	293(2)	294(2)
λ, Å	0.71073	0.71073
Crystal system	Monoclinic	Monoclinic
Space group	*C*2/*c*	*P*2₁/*n*
a, Å	34.655(3)	24.1374(17)
b, Å	10.7672(8)	14.9455(10)
c, Å	23.2262(18)	24.6819(17)
α, °	90	90
β, °	100.455(8)	114.6170(10)
γ, °	90	90
Cell Volume, Å³	8522.6(12)	8094.6(10)
Z	8	8
D_c, g cm⁻³	1.318	1.467
μ, mm⁻¹	0.478	0.508
F(000)	3480	3656
Crystal size, mm	0.18×0.16×0.13	0.19×0.16×0.12
θ limits, °	1.78–25.03	1.54–25.03
Reflections collected	53344	76067
Independent reflections	7457 [R_{int}= 0.1264]	14300 [R_{int}= 0.1315]
Data / restraints /parameters	7457 / 363 / 435	14300/ 513 / 1042
Goodness on fit on F²	1.049	1.004
R_1 (I> 2σ(I))	0.1302	0.0621
wR_2 (all data)	0.3601	0.1331
Largest diff. peak and hole, e Å⁻³	3.643 / –2.129	1.007 / –0.721

	[12d][CF$_3$SO$_3$]·CHCl$_3$	[14m][CF$_3$SO$_3$]
Formula	C$_{41}$H$_{36}$Cl$_3$F$_3$N$_2$O$_9$RuS	C$_{45}$H$_{40}$F$_3$N$_3$O$_7$RuS
Fw	997.20	924.93
T, K	100(2)	100(2)
λ, Å	0.71073	0.71073
Crystal system	Monoclinic	Monoclinic
Space group	*P2$_1$/n*	*P2$_1$/c*
a, Å	12.0563(6)	12.0040(4)
b, Å	20.5906(11)	35.1188(12)
c, Å	35.1658(19)	10.2256(4)
α, °	90	90
β, °	95.724(3)	95.344(2)
γ, °	90	90
Cell Volume, Å^3	8686.3(8)	4292.0(3)
Z	8	4
D$_c$, g cm^{-3}	1.525	1.431
μ, mm^{-1}	0.662	0.480
F(000)	4048	1896
Crystal size, mm	0.19×0.16×0.12	0.19×0.16×0.12
θ limits, °	1.53–26.00	1.16–28.27
Reflections collected	126772	76597
Independent reflections	17081 [*R$_{int}$*= 0.0741]	10513 [*R$_{int}$*= 0.0719]
Data / restraints /parameters	17081 / 144 / 1095	10513/ 967 / 644
Goodness on fit on F^2	1.139	1.129
R$_1$ (*I*> 2σ(*I*))	0.0883	0.1087
wR$_2$ (all data)	0.2451	0.2626
Largest diff. peak and hole, e Å^{-3}	2.741 / −1.475	0.862 / −1.227

Time-conversion profiles

Selected profiles of the conversion in the function of time are summarized in the following:
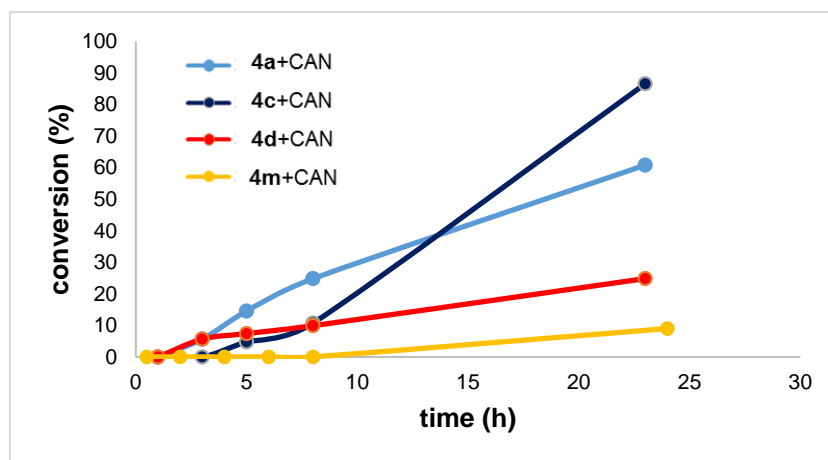
Graphic 4.1. Comparison of conversion for transfer hydrogenation of 4-fluoroacetophenone with 5mol% of the neutral complexes **4a,c,d,m** as pre-catalyst with 1 equivalent (per Ru center) of CAN as additive.
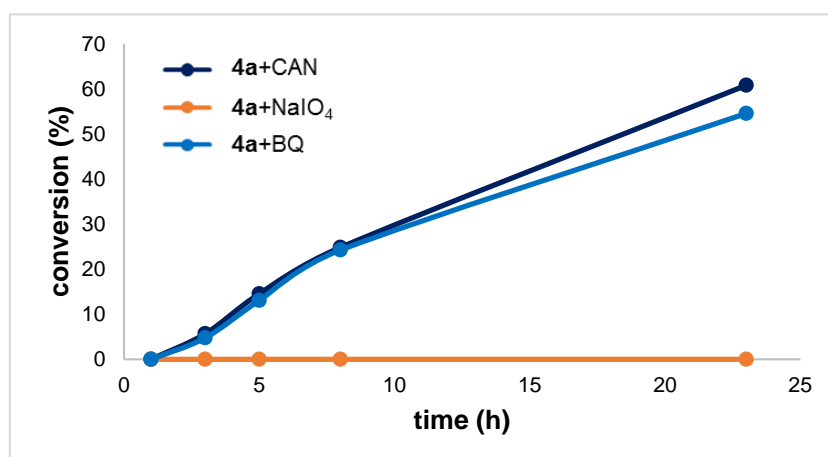
Graphic 4.2. Comparison of conversion for transfer hydrogenation of 4-fluoroacetophenone with 5mol% of the neutral complexes **4a** as pre-catalyst in the presence of 1 equivalent of different oxidant additives.
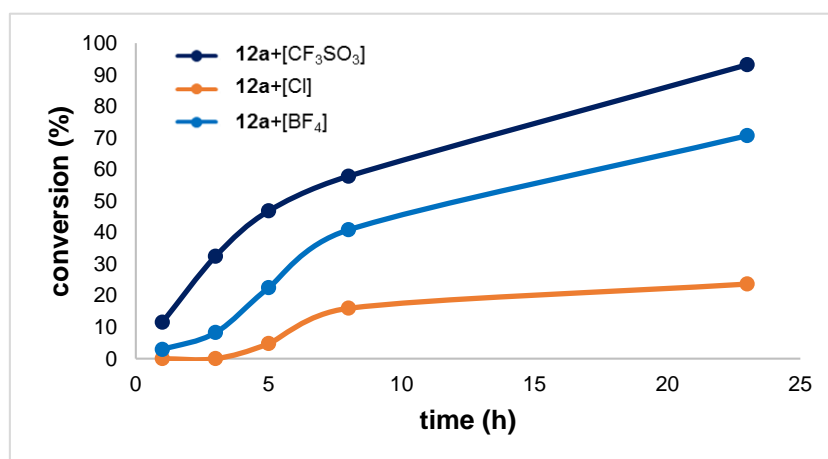
Graphic 4.3. Comparison of conversion for transfer hydrogenation of 4-fluoroacetophenone with 5mol% of the cationic complexes **12a[CF₃SO₃]**, **12a[Cl]** and **12a[BF₄]** as pre-catalysts.
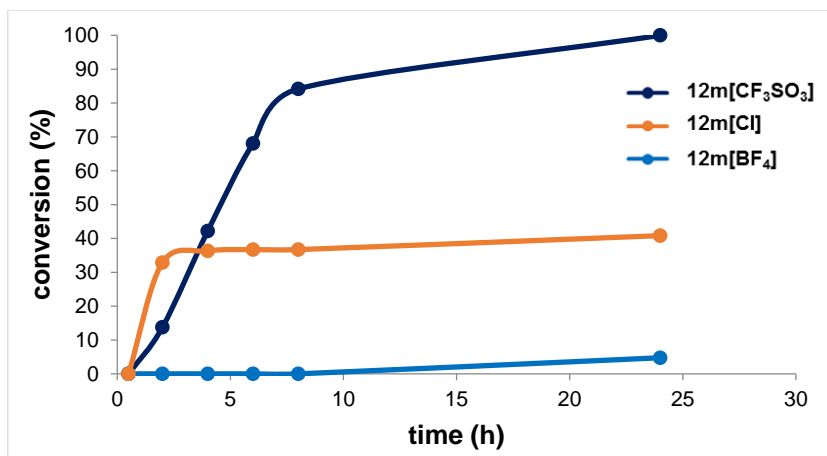
Graphic 4.4. Comparison of conversion for transfer hydrogenation of 4-fluoroacetophenone with 5mol% of the cationic complexes **12m[CF₃SO₃]**, **12m[Cl]** and **12m[BF₄]** as pre-catalysts.
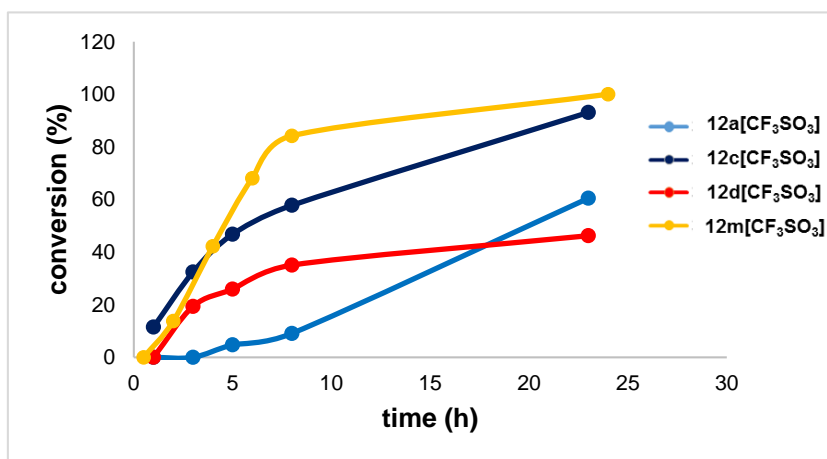
Graphic 4.5. Comparison of conversion for transfer hydrogenation of 4-fluoroacetophenone with 5mol% of the cationic complexes **12a,c,d,m[CF₃SO₃]** as pre-catalysts.
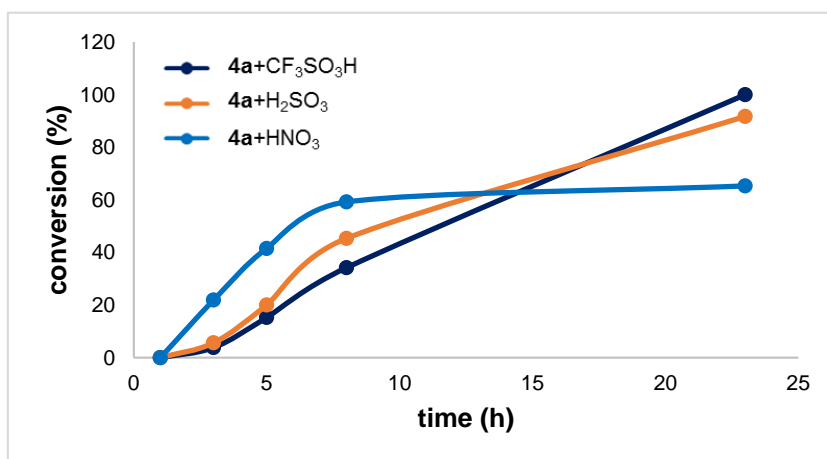
Graphic 4.6. Comparison of conversion for transfer hydrogenation of 4-fluoroacetophenone with 5mol% of the neutral complex **4a** as pre-catalyst with *in situ* addition of various acids.
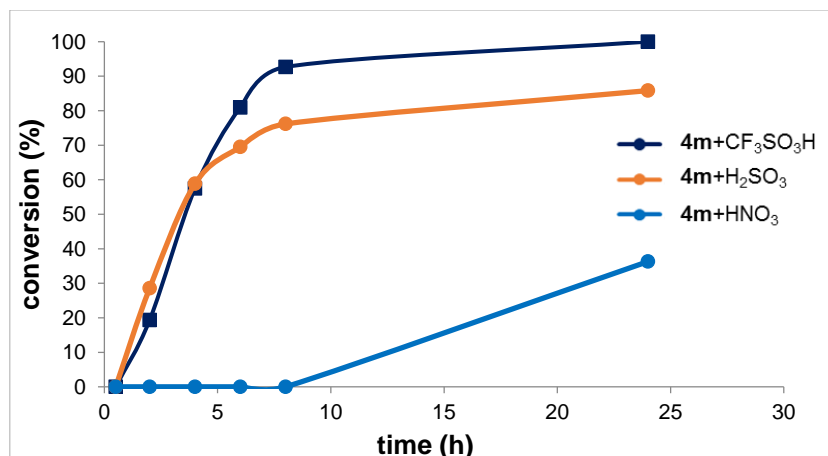
Graphic 4.7. Comparison of conversion for transfer hydrogenation of 4-fluoroacetophenone with 5mol% of the neutral complex **4m** as pre-catalyst with *in situ* addition of various acids.
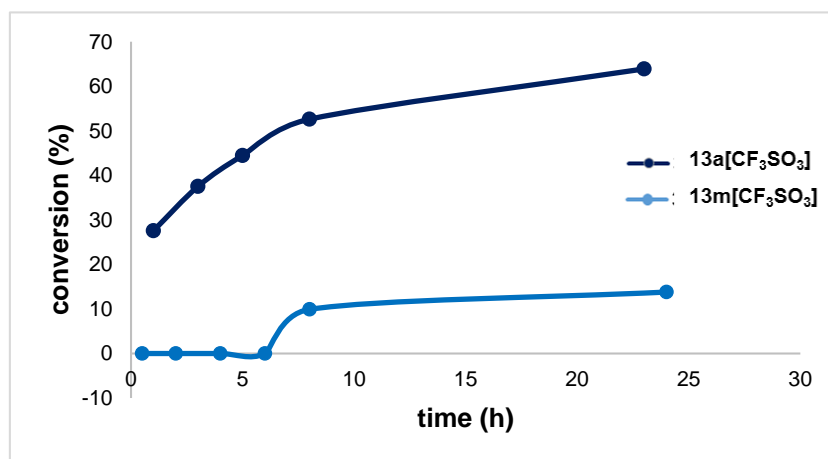
Graphic 4.8. Comparison of conversion for transfer hydrogenation of 4-fluoroacetophenone with 5mol% of the methylated complexes **13a[CF$_3$SO$_3$]** and **13m[CF$_3$SO$_3$]** as pre-catalyst.
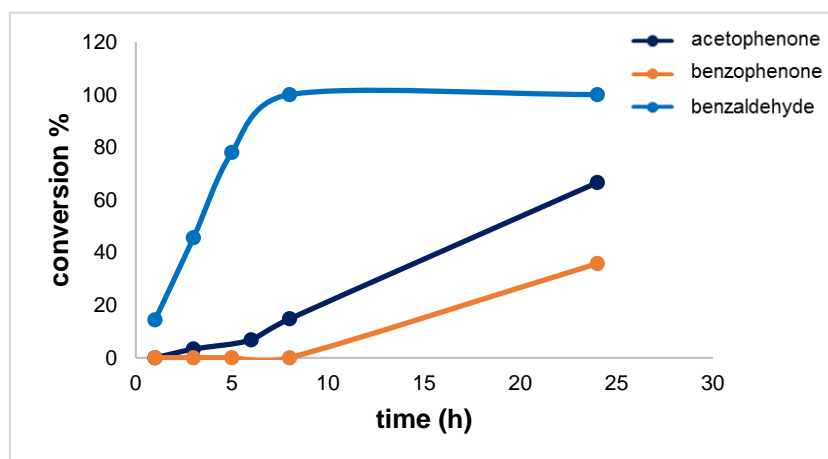
Graphic 4.9. Comparison of conversion for transfer hydrogenation of different substrates such as acetophenone benzophenone and benzaldehyde with 5mol% of the cationic complex **12a[CF$_3$SO$_3$]** as pre-catalyst.

Labeling experiments in isopropanol-d$_8$
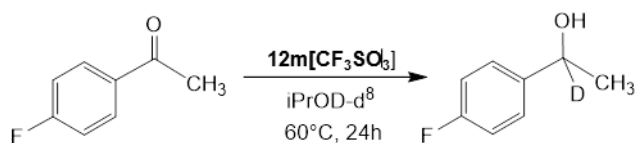
Scheme 4.6. Catalytic Transfer Hydrogention of 4-fluoroacetophenone in iPrOD-d^8 as solvent.

Complex **12m[CF$_3$SO$_3$]** (0.007 g, 7.5 µmol, 5 mol%) was dissolved in 2-propanol d^8 (0.5 mL) in a NMR tube and heated at 60°C for 10 minutes, then the substrate 4-fluoroacetophenone (18 µL, 150 µmol) and the internal standard anisole (10 µL, 150 µmol) were added. The reaction mixture were heated at 60°C for 24h and followed by ^{1}H-NMR spectroscopy at regular intervals (Figures 4.14 and 4.15). The mixture at the end of the catalysis was further characterized by GC-MS analysis (Figures from 4.16 to 4.19).
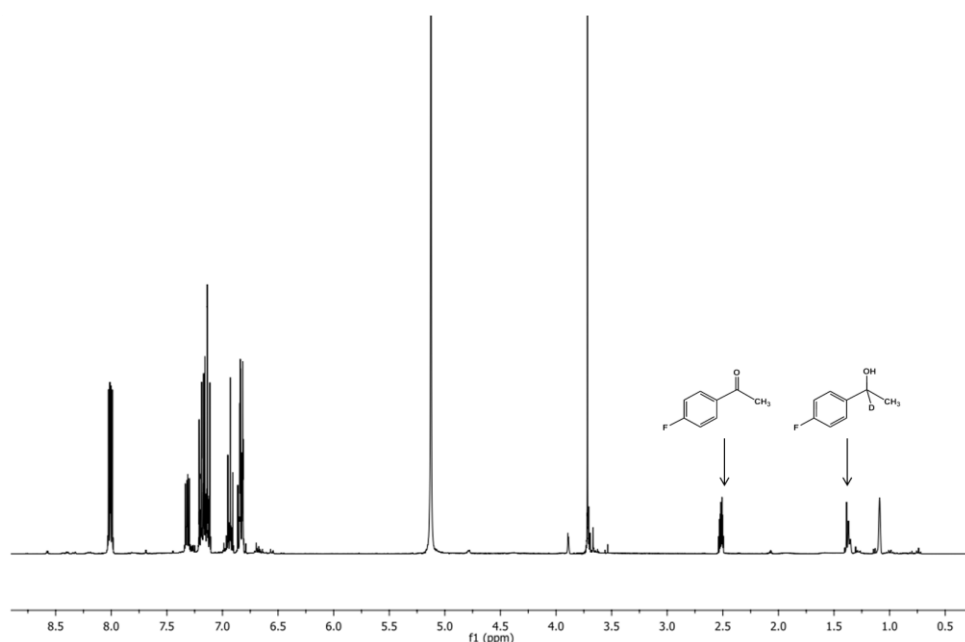
Figure 4.14. ^{1}H-NMR spectrum in 2-propanol-d^8 after 24h of reaction.
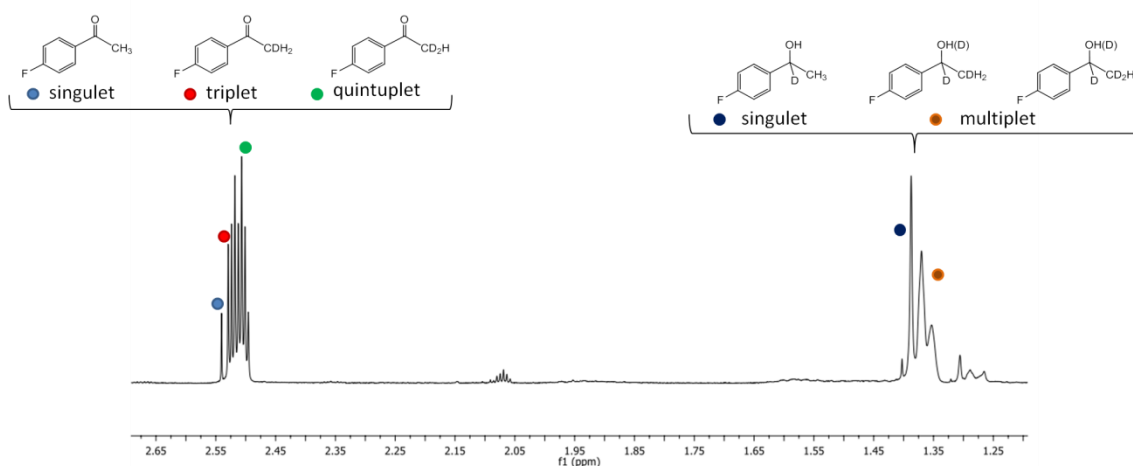
Figure 4.15. Enlargement of the range 1.25-2.65 ppm of the ^{1}H-NMR spectrum in 2-propanol-d^8 after 24h of reaction.

GC-MS analysis were performed on the instrument Focus-DSQ Thermo.
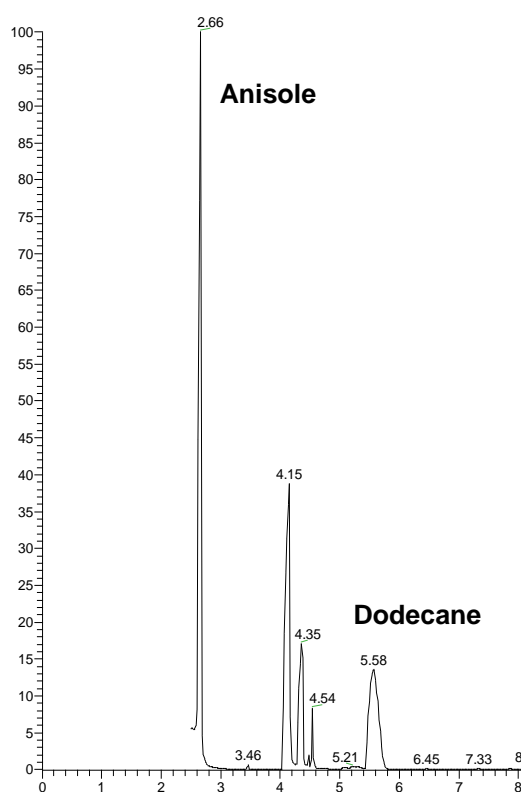
Figure 4.16. GC-MS spectrum in 2-propanol-d^8 after 24h of reaction.
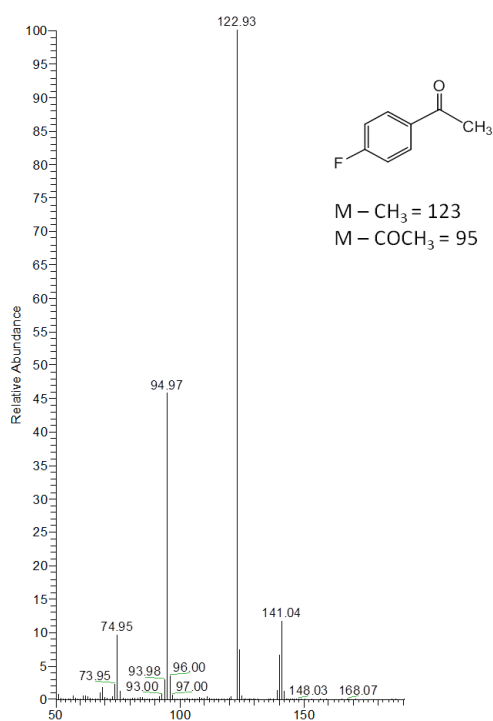
Figure 4.17. GC-MS spectrum in 2-propanol-d^8 after 24h of reaction. Retention time = 4.15 min.
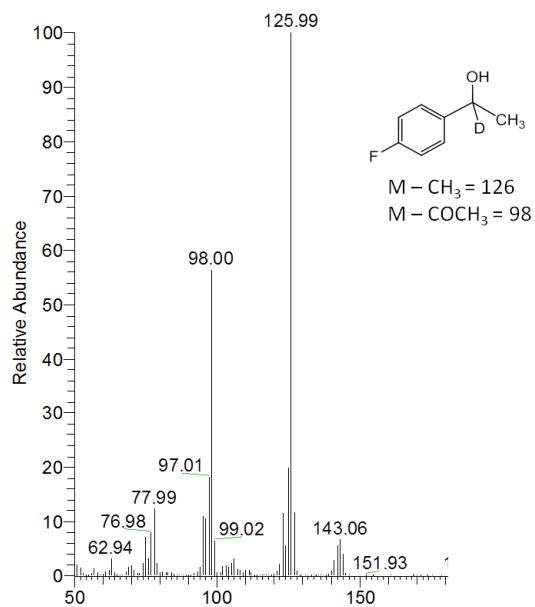
Figure 4.18. GC-MS spectrum in 2-propanol-d^8 after 24h of reaction. Retention time = 4.35 min.
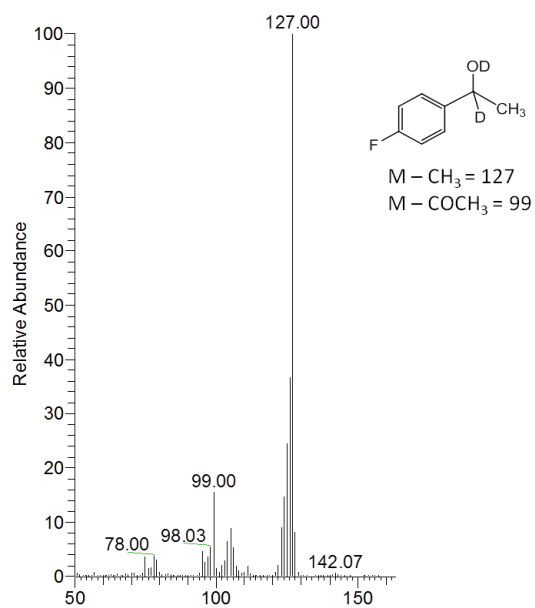
Figure 4.19. GC-MS spectrum in 2-propanol-d^8 after 24h of reaction. Retention time = 4.54 min.

References

[1] For reviews, see: a) F. E. Hahn and M. C. Jahnke, *Angew. Chem. Int. Ed.,* **2008**, *47*, 3122; b) M. Melaimi, M. Soleilhavoup and G. Bertrand, *Angew. Chem. Int. Ed.,* **2010**, *49*, 8810. c) L. Benhamou, E. Chardon, G. Lavigne, S. Bellemin-Laponnaz and V. Cesar, *Chem. Rev.*, **2011**, *111*, 2705. d) L. A. Schaper, S. J. Hock, W. A. Herrmann and F. E. Kühn, *Angew. Chem. Int. Ed.*, **2013**, *52*, 270.

[2] For selected reviews, see: a) D. Bourissou, O. Guerret, F. P. Gabbai and G. Bertrand, *Chem. Rev.,* **2000**, *100*, 39; b) W. A. Herrmann, *Angew. Chem. Int. Ed.,* **2002**, *41*, 1290; c) C. M. Crudden and D. P. Allen, *Coord. Chem. Rev.,* **2004**, *248*, 2247; d) M. Poyatos, J. A. Mata and E. Peris, *Chem. Rev.,* **2009**, *109*, 3677; e) O. Schuster, L. Yang, H. G. Raubenheimer and M. Albrecht, *Chem. Rev.,* **2009**, *109*, 3445; f) L. Mercs and M. Albrecht, *Chem. Soc. Rev.*, **2010**, *39*, 1903; (g) M. N. Hopkinson, C. Richter, M. Schedler and F. Glorius, *Nature*, **2014**, *510*, 485; (h) S. P. Nolan, N-Heterocyclic Carbenes: Effective Tools for Organometallic Synthesis, **2014**, Wiley VCH.

[3] a) M. C. Warner, C. P. Casey and J.-E. Backvall, *Top. Organomet. Chem.,* **2011**, *37*, 85; b) B. L. Conley, M. K. Pennington-Boggio, E. Boz and T. J. Williams, *Chem. Rev.,* **2010**, *110*, 2294; c) T. Pasini, G. Solinas, V. Zanotti, S. Albonetti, F. Cavani, A. Vaccari, A. Mazzanti, S. Ranieri and R. Mazzoni, *Dalton Trans.*, **2014**, *43*, 10224. d) C. Cesari, L. Sambri, S. Zacchini, V. Zanotti and R. Mazzoni *Organometallics* **2014**, *33*, 2814 and reference cited therein.

[4] H. Ohara, W. W. N. O, A. J. Lough and R. H. Morris, *Dalton Trans.*, **2012**, *41*, 8797.

[5] C. Cesari, S. Conti, S. Zacchini, V. Zanotti, M. C. Cassani and R. Mazzoni, *Dalton Trans.*, **2014**, *43*, 17240.

[6] H. Allen, O. Kennard, D. G. Watson, L. Brammer, A. G. Orpen and R. Taylor, *J. Chem. Soc., Perkin Trans.*, **1987**, *2*, S1-S19.

[7] J. A. Cabeza and P. Garcia-Alvarez, *Chem. Soc. Rev.*, **2011**, *40*, 5389.

[8]) Y. Shvo, D. Czarkie, Y. Rahamim and D. F. Chodosh, *J. Am. Chem. Soc.*, **1986**, *108*, 7400; b) C. P. Casey, S. W. Singer, D. R. Powell, R. K. Hayashi and M. Kavana, *J. Am. Chem. Soc.*, **2001**, *123*, 1090; c) L. K. Thalen, D. Zhao, J.–B. Sortais, J. Paetzold, C. Hoben and J.-E. Backwall, *Chem. –Eur. J.*, **2009**, *15*, 3402.

[9] C. Cesari, R. Mazzoni, H. Müller-Bunz and M. Albrecht, *J. Organomet. Chem.*, **2015**, *793*, 256.

[10] M. Benìtez, E. Mas-Marzà, J. A. Mata and E. Peris, *Chem.–Eur. J.*, **2011**, *17*, 10453.

[11] a) A. M. Oertel, V. Ritleng, L. Burr, C. Harwig and M. J. Chetcuti, *Organometallics,* **2011**, *30*, 6685; b) L. B. Benac, E. M. Burgess, L. Burr and A. J. Arduengo, *Organic Syntheses, Coll.*, **1990**, *7,* 195; **1986**, *64*, 92.

[12] L. C. Branco, J. N. Rosa, J. J. Moura Ramos and C. A. M. Afonso, *Chem. Eur. J.*, **2002**, *8*, 3671.

[13] J. A. Loch, M. Albrecht, E. Peris, J. Mata, J. W. Faller and R. H. Crabtree, *Organometallics* **2002**, *21*, 700.

[14] M. Boiani, A. Baschieri, C. Cesari, R. Mazzoni, S. Stagni, S. Zacchini and L. Sambri, *New. J. Chem*. **2012**, *36*, 1469.

[15] Y. Mum, D. Czarkle, Y. Rahamlm and Y. Shvo, *Organometallics*, **1985**, *4*, 1461.

[16] G. M. Sheldrick, *SADABS*, Program for empirical absorption correction, University of Göttingen, Germany, **1996**.

[17] G. M. Sheldrick, *SHELX97*, Program for crystal structure determination, University of Göttingen, Germany, **1997**.

[18] A. L. Spek, PLATON, A Multipurpose Crystallographic Tool, Utrecht University, Utrecht, The Netherlands, **2005**.

CHAPTER V

Synthesis and catalytic performance of poly(propylene imine) (PPIs) dendrimers modified with ruthenium cyclopentadienone N-heterocyclic carbene complexes

Abstract

The organometallic functionalization of the five generations of polypropylene imine dendrimers with up to 64 N-heterocyclic carbene cyclopentadienone ruthenium(0) complexes is obtained by the formation of carbamate linkers between NH_2 peripheral group of the dendrimers and OH functionality in the lateral chain of the NHC employing carbonyldiimidazole as coupling agent. Synthesis, purification and characterization of the five generations and an example of complete and reversible protonation of peripheral ruthenium complexes is described. To the best of our knowledge, this is one of the rare examples in which an NHC is employed as peripheral organometallic ligand in dendritic systems for homogeneous catalysis, in the place of more usual phosphines or nitrogen chelating ligands, based on pyridine or triazoles. Preliminary results on the use of the first generation dendrimers (n=4), in the protonated form, as hydrogen transfer (TH) catalyst in ^{i}PrOH showed higher catalytic activity if compared with the corresponding monomeric species. However, a more detailed study indicated that the higher activity is not ascribable to a true dendritic effect. More likely, the observed activity is due to decomposition of the cationic dendrimer, which led to the release of a peripheral ruthenium monomeric active species recognized as the active form of the famous Shvo catalyst. Preliminary results indicate that cationic and neutral ruthenium NHC functionalized dendrimers do not decompose under oxidizing conditions.

Introduction

Dendritic catalysts are functional macromolecules which exhibit well defined structures and possess a monodisperse nature. Therefore, dendritic catalysts retain some advantages of homogeneous catalysts: fast kinetic behavior, easy tenability and rationalization. Furthermore, they can be easily removed from the reaction mixture by precipitation, membrane or nanofiltration techniques because of their larger size compared to products, which an advantage typical of heterogeneous catalysts. Moreover, it is possible to finely tune the catalytic properties of dendritic catalysts through adjustment of their structure, size, shape, chemical functionality, and solubility. In a few words, dendrimers have been proposed to bridge the gap between homogeneous and heterogeneous catalysis. Grafting catalytic sites on the periphery of dendrimers is the most straightforward approach to construct dendritic catalysts, with potential high loading capacity and high ligand concentrations. Obviously, high catalytic site concentration might result in high reaction rates. At the same time the proximal interactions between catalytic groups and steric crowding at the periphery of dendritic catalysts might lead to cooperative effects and selective reaction profiles, respectively. Many reviews concern the use of dendrimers in homogeneous catalysis,[1] but few are specifically focused on the dendrimer effect in catalysis.[2] Several consequences of dendritic effects have been identified, such as the influence on the rates of reaction, substrate activation, or selectivity. The main reason proposed for such effects in periphery-functionalized dendritic catalysts is cooperativity between proximal catalytic sites in the dendrimer structure. As a general trend, the bulk provided at the periphery upon increasing the dendrimer generation, restricts access of the substrate to the catalytic metal center. This brings about a large number of catalytically active

species in a small nano-object but, on the other hand, restriction of substrate access can sometime lead to a negative dendritic effect resulting from bulk limiting reaction rates.

Dendritic catalysts provided excellent performances in rhodium mediated hydrogenation. Most dendritic catalysts for hydrogenation contain diphosphine or monophosphine since these units demonstrated to be ideal bridge between dendritic support and metals for grafting metal complexes, due to their outstanding capability of coordination, stability, and catalytic performance.[3] Dendritic systems with chiral phosphine ligands applied for Rh and Ir promoted asymmetric hydrogenation, providing positive dendritic effects such as high enantioselectivities (up to 99% ee) and catalytic activities (up to 4850 h−1 TOF).[4]

A lower number of examples concern the field of transfer hydrogenation. A "green" example of dendritic catalysis involves the fluorinated dendritic chiral mono-N-tosylated 1,2-diphenylethylenediamine (FTsDPEN), which was synthesized and applied in the ruthenium(II) complex-catalyzed asymmetric transfer hydrogenation of prochiral ketones in aqueous media.[5]

A tetrabranched phosphoranyl-terminated carbosilane derivative coordinated to four [Ru(*p*-cymene)Cl bipyRu(*p*-cymene)Cl2] units catalyzed hydrogen-transfer of cyclohexanone, with cyclohexadiene or formic acid as stoichiometric hydrogen donor. This *G*1 dendrimer was very active but less than mononuclear species, and the dendritic effect was also negative up to *G*3, which was less active than *G*1.[6]

As reported in the previous chapters, the scope of the thesis is the development of novel ruthenium complexes for bifunctional catalysis[7] containing both cyclopentadienones, which cooperate with the metal center in catalytic redox reactions,[8] and N-heterocyclic carbenes (NHC)[9] (Scheme 5.1), that are valuable ligands due to their easy preparation, the tunability of electronic and steric properties,[10] the rational design of transition metal catalysts[11] and the possibility to decorate the structure with substituents suitable for heterogenization (e.g. – OH functionalization in **4d** and **12d[X]**, Scheme 5.1). In the Chapter IV has been reported the study on the cationic Ru complexes of type **12** which showed good catalytic activity in the transfer hydrogenation of the model substrate 4-fluoroacetophenone. Furthermore, the best catalyst among these complexes contained a pyridine in the lateral chain (**12d[CF₃SO₃]**), which in principle might be involved in the catalytic reaction as a non-innocent ligand. On the other hand, the neutral complexes of type **4** needed to be activated by CAN in order to favor the release of CO and also act as catalys in the same type of reactions.[8b]

4a R₁ = R₂ = CH₃;
4c R₁ = CH₃, R₂ = CH₂CH₂CH₂CH₃;
4d R₁ = CH₃, R₂ = CH₂CH₂OH;
4m R₁ = CH₂CH₂CH₂CH₃, R₂ = 2-pyridine;
4o R₁ = CH₃, R₂ = CH₂CH₂NH₂.

12a[X] X = CF₃SO₃, Cl, BF₄;
12c[X] X = CF₃SO₃;
12d[X] X = CF₃SO₃;
12m[X] X = CF₃SO₃, Cl, BF₄;
12o[X] X = CF₃SO₃, BF₄.
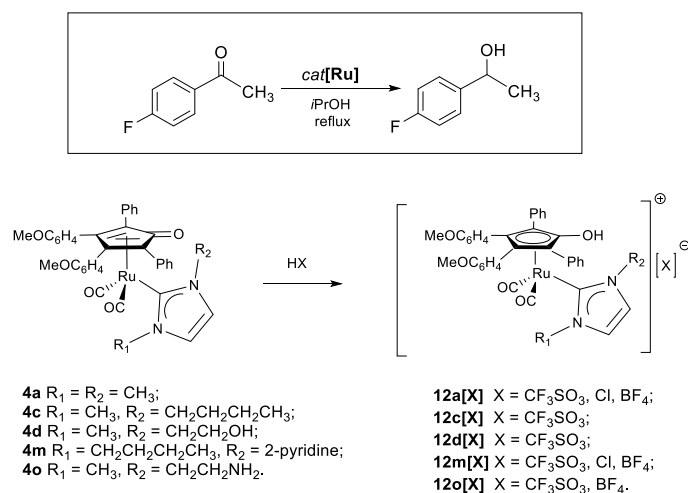
Scheme 5.1. Hydrogen transfer of 4-fluoroacetophenone catalyzed by [Ru] = **4a,c,d,m,o** and **12a,c,d,m,o[X]** complexes at 80°C in iPrOH as solvent and hydrogen source, [Ru] = 5 mol%.

Since NHCs are outstanding ancillary ligands, comparable to phosphine, it is quite surprising the lack of examples in the literature concerning NHC functionalized dendrimers. Indeed, we found only one example of a core functionalized NHC-Rh dendrimer showing a positive dendrimer effect in hydrosililation of ketones communicated in 2005 by Tsuji et al..[12] Hoveida also successfully supported a ruthenium NHC complex for olefin metathesis, but in this case the catalyst was bonded to the dendrimer by the aromatic moiety functionalized with C=Ru double bond without exploiting the ancillary NHC for the immobilization of the catalyst.[13] As stated above, phosphine and diphosphine represented preferential ligands even though nitrogen based chelating ligands containing pyridine or triazole are also frequently employed.[1,2] In order to fill this gap and to evaluate a possible dendrimer effect on the behavior of our catalysts we developed a method, inspired to our previous work on dendrimers,[14] for the straightforward synthesis of the [Ru(NHC)] functionalized five generations of polypropylene imine dendrimers (PPI) with up to 64 organometallic moieties DAB-dendr-[NH(O)CO(NHC)Cp=ORu(CO)$_2$]$_n$ {n=4, 8, 16, 32, 64}. Preliminary results on the use of the first generation (n=4), in both neutral and protonated forms, as hydrogen transfer catalysts in [i]PrOH are herein described.

Results and discussion

5.1 Synthesis and characterization of the ruthenium tetraarylcyclopentadienone NHC-decorate dendrimers

The straightforward preparation of the new CO_2-imidazole functionalized cyclopentadienone NHC ruthenium(0) complex **4p** in 84% yield was achieved by reacting **4d** with a slight excess of CDI (CDI : **4d** = 1.1) in CH_2Cl_2 at room temperature for 2 h as described in Scheme 5.2. The product **4p** is easily purified by extracting the imidazolium co-product in water (see Experimental section).
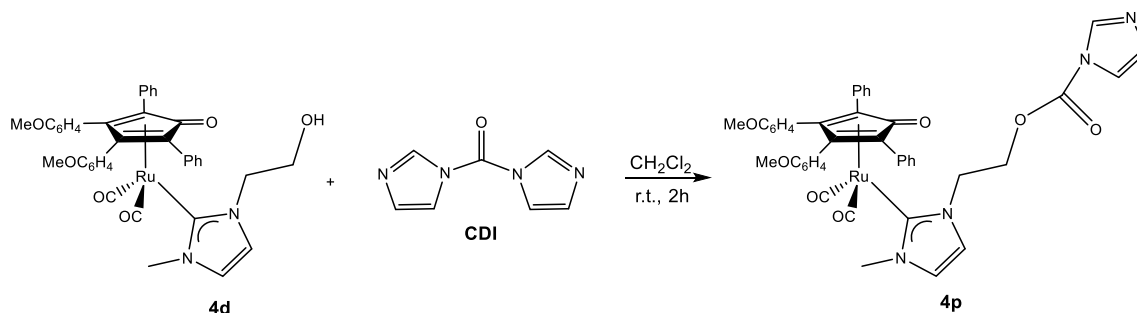
Scheme 5.2 Synthesis of CO_2Im functionalized cyclopentadienone NHC ruthenium complex (**4p**).

The air-stable white-brown solid **4p** has been fully characterized by analytical and spectroscopic measurements. The NMR spectra in $CDCl_3$ show a pattern similar to that of complex **4d**.[8b] In particular, the ^{13}C NMR spectrum shows the downfield shifted resonance of the carbene (δ = 174.80 ppm). Moreover, the imidazole moiety (^{1}H-NMR δ = 8.03, 7.33, 7.08 ^{13}C-NMR δ = 136.95, 130.88, 116.97) displays, as expected, chemical shifts comparable to those of the starting material CDI, whereas at 147.89 ppm resonates the C=O group typical of the carbamate (-OC(O)N-). The IR spectrum shows CO stretching bands (v_{CO} = 2007cm^{-1}, 1948 cm^{-1}) consistent with those of **4d**, and an absorption, v(C=O,-O_2CIm): 1768cm^{-1}, ascribable to the carbamate group. Further evidences were produced by ESI-MS.

The reaction of a 4.8 fold excess of the complex **4p** in CH_2Cl_2 at room temperature with the commercially available poly(propylenimine) dendrimer DAB-*dendr*-(NH$_2$)$_4$ leads, after 2 h, to the quantitative formation of DAB-dendr-[NH(O)CO(NHC)Cp=ORu(CO)$_2$]$_n$ (**17G1**) (Scheme 5.3).
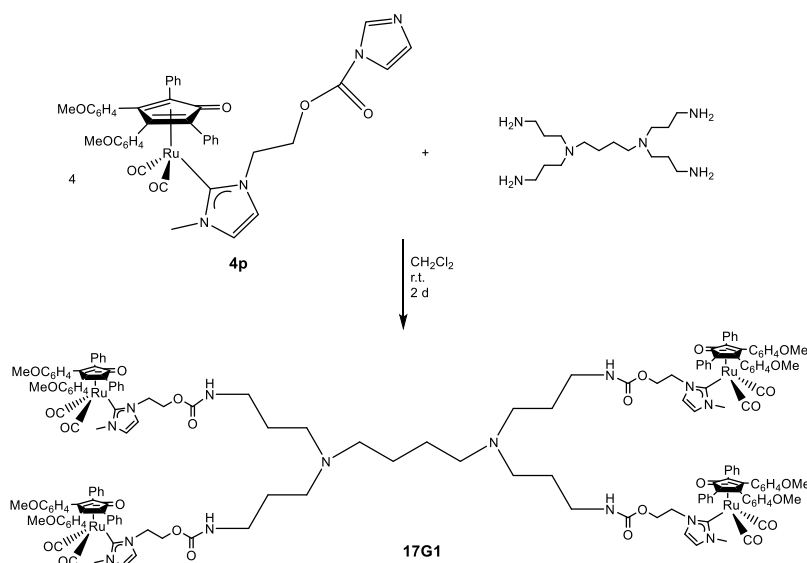
Scheme 5.3. Synthesis of DAB-dendr-[NH(O)CO(NHC)Cp=ORu(CO)$_2$]$_4$ (**17G1**)

Under the same experimental conditions the CO_2-imidazole group of the ruthenium derivative **4p** reacts with the DAB-*dendr-* $(NH_2)n$ {$n = 8, 16, 32, 64$}, up to the fifth generation, to form the completely functionalized new dendritic organometallic macromolecules DAB-dendr-[NH(O)CO(NHC)Cp=ORu(CO)$_2$]$_n$ (**17Gn**) in quantitative yields (Figure 5.1).
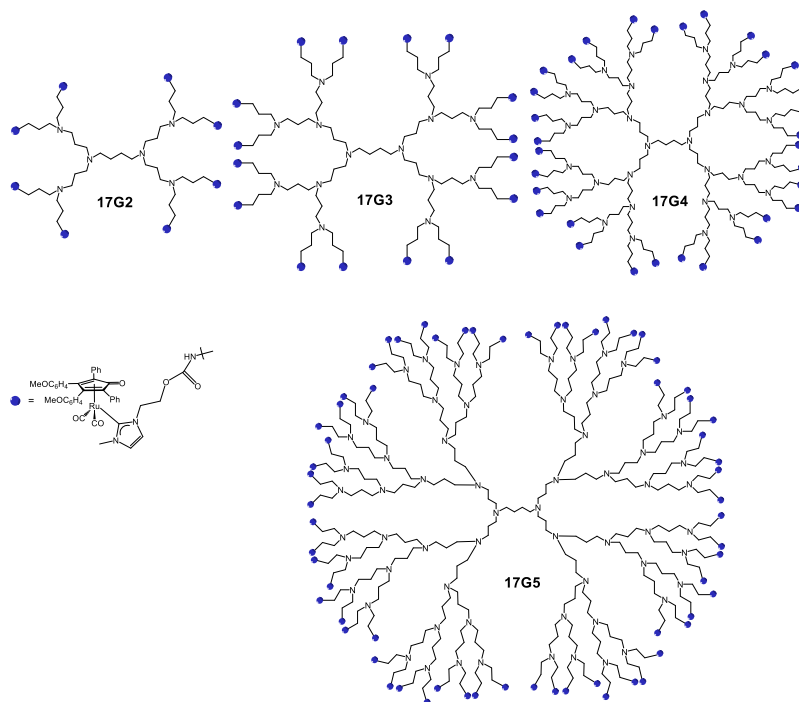
Figure 5.1. Structure of functionalized dendrimers from second to fifth generation: DAB-dendr-[NH(O)CO(NHC)Cp=ORu(CO)$_2$]$_n$ n=8 (**17G2**), n=16 (**17G3**), n=32 (**17G4**) n=64 (**17G5**).

The excess of **4p** and the side products can be removed easily from the crude reaction mixture by water extraction, followed by washing with Et_2O. All five organometallic dendrimers **17Gn** were isolated as brown solids and are air and moisture stable They are soluble in dichloromethane and THF, slightly soluble in Et_2O, insoluble in hexane and toluene and aqueous solvents.

The dendritic compounds were characterized by ^1H, ^{13}C NMR and IR spectroscopy and mass spectrometry when possible. The NMR spectra in $CDCl_3$ combine the signals due to the diaminobutane-based poly(propylenimine) framework (^1H: four broad multiplets in the range of 3.8–1.3 ppm; ^{13}C: four broad resonances in the range of 63–25 ppm) with those derived from the newly introduced peripheral NHC ruthenium moieties (see Figures 5.2 - 5.3 and Experimental section).
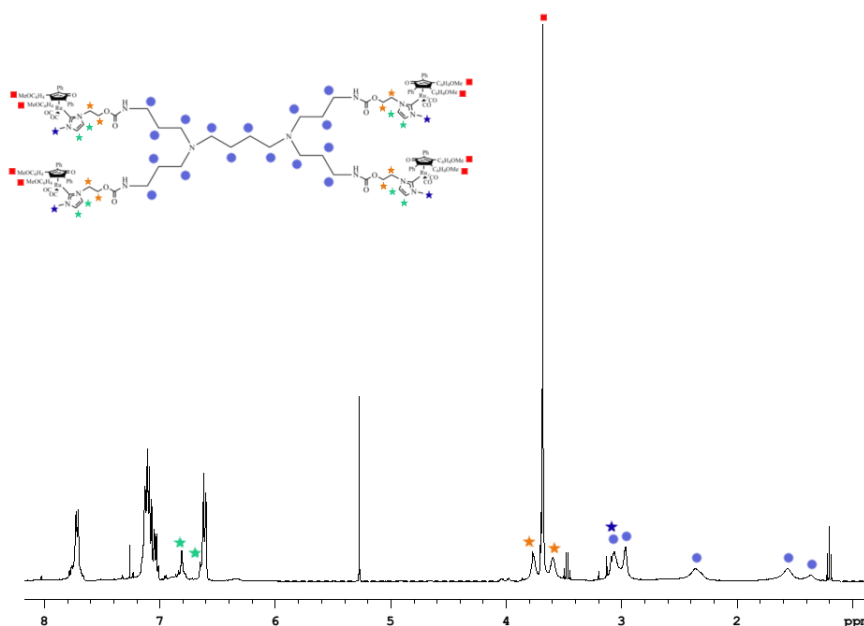
Figura 5.2: ^{1}H-NMR spectrum(CDCl$_3$) of **17G1**.
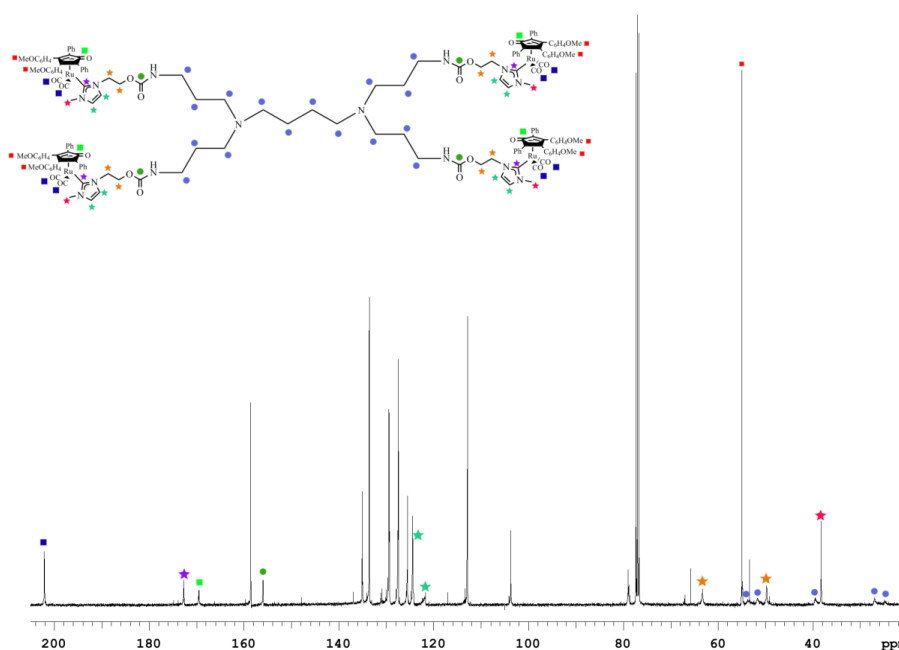
Figura 5.3: ^{13}C-NMR spectrum(CDCl$_3$) of **17G1**.

In addition, evaluation of the signal intensities also provided evidence of the complete polyamines functionalization. Even though all the signals of the proton spectra presented the typical peak broadness of a polymer-like structure, they clearly show that the proton resonances of the two methylene groups in the –NHCCH_2CH_2O$_2$CNH– unit of the organometallic moieties (at 3.77 and 3.59 ppm) are more shielded than those of complex **4p** (4.05 and 3.99 –NHCCH_2CH_2O$_2$CIm).

In the ^{1}H NMR, the signal of the –NH– belonging to the carbamate linkers residing on the surface of the poly(propylenimine) dendrimer is not easily recognizable due to the fact that the resonance is expected in the same region of aromatic signals and that hydrogen bonds –NH…(O)CO– or –NH…cyclopentadienone become more relevant when the interacting groups get in closer contact, namely with increasing generation.

The IR spectra in CH_2Cl_2 of all five dendritic species show a strong absorption at 1718 cm^{-1} (s) due to both (C=O, $-O_2CNH-$) stretching bands.

The structures of the first- (*n* = 4) (**17G1**) generation dendrimers (Scheme 5.3) was confirmed by ESI mass spectroscopy, which showed molecular ions at *m/z* 3355 [M + Na]$^+$. The higher molecular weight of the upper generations **17G2-5** prevented their mass detection.

The straightforward and quantitative reaction between $-CO_2$-imidazole functionalized cyclopentadienone-NHC-ruthenium complexes and DAB-*dendr*-(NH$_2$)*n* {*n* = 4, 8, 16, 32, 64} here described (Figure 5.1) provides a valuable route towards the immobilization of $-OH$ functionalized NHC complexes on organic and inorganic amino functionalized supports.[15]

The reaction of **17G1** with a strong acid such as HCF_3SO_3, leads to the quantitative formation of the hydroxycyclopentadienyl tetra-cationic dendrimer **17G1-H** (Figure 5.4), in which Ru(0) is formally oxidized to Ru(II).
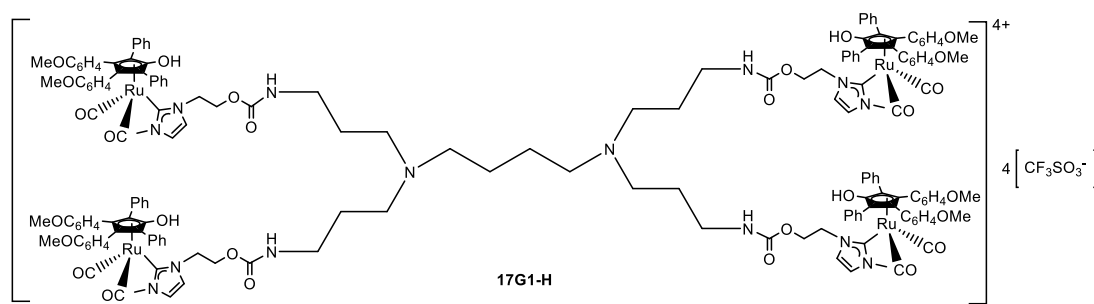
Figure 5.4. Structure of the tetra-cationic DAB-dendr-[NH(O)CO(NHC)Cp-OHRu(CO)$_2$]$_4$ (**17G1-H**).

Infrared spectroscopy provides a convenient technique for monitoring the progress of the protonation in that, in agreement with the reduced back-donation from the metal centre to the carbonyl ligands, ν-C≡O stretch vibrations undergo a significant high-energy shift upon formation of the cationic complex [*e.g.* ν_{CO} = 2006 cm^{-1}, 1947 cm^{-1} (**17G1**), and 2039 cm^{-1}, 1988 cm^{-1} (**17G1-H**)]. It is important to underline that during the protonation stretching bands with intermediate frequency between the neutral and the tetra-cation form (ν_{CO} = 2017 cm^{-1}, 1958 cm^{-1}) appear in the CO region of the IR spectrum. These latter bands are probably associated to the formation of hydrogen bonds between the cationic and the adjacent neutral forms of the ruthenium complex. The change in the coordination from η^4 (cyclopentadienone ligand) to η^5 (hydroxycyclopentadienyl ligand) due to protonation, is further evidenced by ^{13}C-NMR shift of the resonance attributable to the endocyclic carbon involved in the ketone-alcohol transformation [δ 169.56 ppm (C=O, Cp, in **17G1**) vs δ 141.63 ppm (C-OH, Cp, in **17G1-H**)]. Ru-carbene signals are also shifted to higher fields; from δ 172.67 ppm (**17G1**) to δ 160.81 ppm (**17G1-H**) (see Experimental section for more details).

5.2 Synthesis and characterization of the ruthenium 2,5-bis-tetrimethylsilane-3,4 cyclohexane-cyclopentadienone NHC-decorate first generation of PPI dendrimer

Once obtained the five generations of polypropilenimine NHC-Ru functionalized dendrimers (**17G1-5**) we wondered about the possibility to control the solubility by varying the cyclopentadienone ligand, as mentioned in Chapter II (paragraph 2.5). The interest toward this point arose from the synthesis of the new mononuclear complexes **9d** and **18d[Cl]** (Scheme 5.4) which are very similar to **4d** and **14d[X]** except for the substituents of the cyclopentadienone ligands. Indeed, in this case we found a partial solubility of **18d[Cl]** in water (5 mmol/L) that should be potentially transferable to the corresponding functionalized dendrimers.
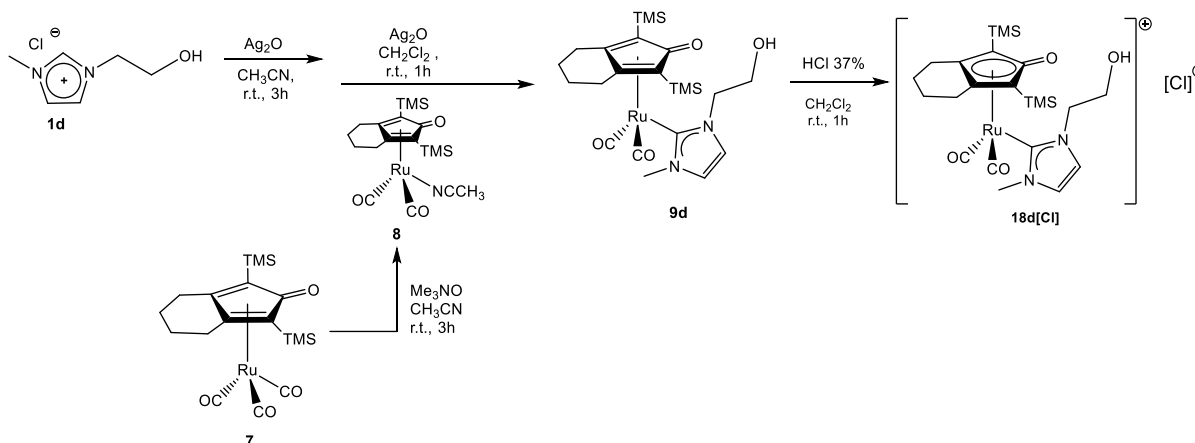
Scheme 5.4 Synthesis of Dicarbonyl-(2,4-bis(trimethylsilyl)bicyclo[3.3.0]nona-1,4-dien-3-one)[1-(2-hydroxyethyl))-3-methylilidene]ruthenium (**9d**) and the corresponding cationic complex Dicarbonyl-(2,4-bis(trimethylsilyl)bicyclo[3.3.0]nona-1,4-dienyl)[1-(2-hydroxyethyl))-3-methylilidene]ruthenium chloride (**18d[Cl]**).

Spectroscopic data of complexes **9d** and **18d[Cl]** are in perfect agreement with those previously reported for similar complexes (synthesis and characterizations of complexes **7**, **8** and **9d** have been reported in the Experimental section of Chapter II).[8, 10, 16] The same is true for the corresponding first generation **19G1** (Figure 5.5) prepared following the same procedure as for the tetraarylcyclopentadienone complex **4d** by a coupling reaction of **9d** and the NH₂ functionality of [DAB-dendr-NH₂]₄ favoured by carbonyldiimidazole. The latter derivative shows similar solubility as **17G1**.
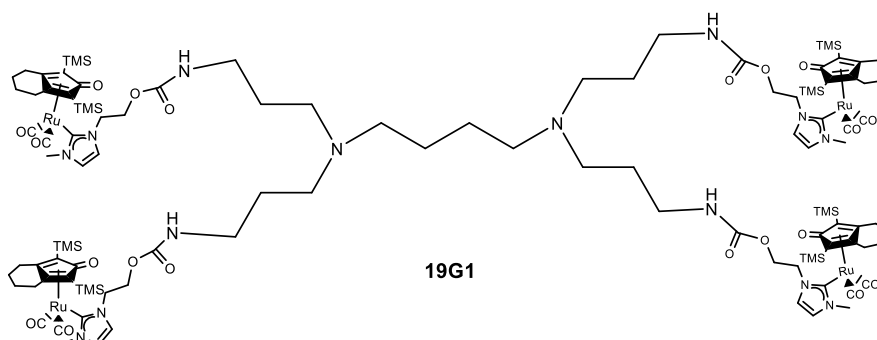
Figure 5.5. Synthesis of DAB-dendr-[NH(O)CO(NHC)Cp(TMS)=ORu(CO)₂]₄ (**19G1**).

Hereafter are described preliminary results obtained in redox catalysis with the neutral and cationic first generations **17G1** and **17G1-H** and their comparison with what found in the case of mononuclear species **4** and **12[X]**.

5.3 Catalytic transfer hydrogenation

The Ru(NHC) peripherally functionalized dendrimers **17G1** and **17G1-H** were evaluated as catalyst precursors under transfer hydrogenation conditions *i.e.* refluxing [i]PrOH as hydrogen source employing 4-fluoroacetophenone as model substrate. Catalytic runs were performed to investigate the stability of complexes on the polypropyleneimine dendrimers and eventual dendrimer effect due to close proximity of complexes in connection with the mononuclear species. The role of CAN in the activation of the **17G1** has been investigated, and the catalytic activity of the ruthenium(0) dendrimer **17G1** compared with the corresponding ruthenium(II) cationic complexes **17G1-H**. Results are reported in Table 5.1: in all cases selectivity is complete and conversion corresponds to yield unless otherwise stated.

The neutral dendrimer **17G1** has no catalytic activity in the absence of additives (entry 1), as already stated in the case of mononuclear complexes[8b] reported in Table 5.1 for the sake of clarity (entry 2-5). In the monomeric neutral form, the addition of one equivalent of an oxidizing agent such as CAN (entry 7-10) promote the CO release giving rise to active intermediates. Under the same conditions a detrimental effect of the dendritic form is observed, in that only 4% conversion is reached after 24h. The degree of oxidation of the metal center remains the key point in order to activate the catalyst, and better conversions are reached employing the cationic monomeric pre-catalysts **12[CF₃SO₃]** as reported in Chapter IV (Table 4.1).[8b] Higher conversions have been found in the case of the tetra-cationic dendrimer **17G1-H** (entry 11 vs. entries 12-15). Forwarding evidence of a possible dendrimer effect. The crude reaction mixture has been analyzed by NMR and IR spectroscopy, after appropriate workup. The study has allowed to identify, in the organic fraction, a ruthenium complex corresponding to the Shvo catalyst.[17] Conversely, in the water soluble fraction the NMR signals (in D_2O) associated to the dendrimer skeleton and imidazolium salt have been found. This result suggests that the catalytic activity of **17G1-H,** as transfer hydrogenation catalyst, is not ascribable to a dendritic effect but is better explained by the decomposition of the cationic dendrimer, leading to the release of a peripheral ruthenium monomeric active species without the NHC moiety. This behavior, not observed in the case of monomeric complexes, should arise from the structure of the dendrimer itself, which contains non innocent nitrogen atoms adjacent to methylenic groups susceptible of both acid-base chemistry and dehydrogenation. On the other hand, a role of the crowding around the mononuclear complexes, which favors their mutual contact should also be taken into consideration. In order to better understand the mechanism related to the detachment of the complex, the reactivity of **17G1-H** is still under investigation.

Table 5.1. Catalytic transfer hydrogenation of 4-fluoroacetophenone.[a]
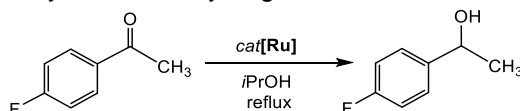
entry	[Ru]	additive	conversion 8h (%)	conversion 24h (%)
1	17G1	---	0	0
2	4a	---	0	0
3	4c	---	0	0
4	4d	---	0	0
5	4m	---	0	0
6	17G1	CAN[b]	0	4
7	4a	CAN[b]	25	61
8	4c	CAN[b]	10	87
9	4d	CAN[b]	10	25
10	4m	CAN[b]	0	9
11	17G1-H	---	>99[c]	>99
12	12a[CF$_3$SO$_3$]	---	58	93
13	12c[CF$_3$SO$_3$]	---	9	60
14	12d[CF$_3$SO$_3$]	---	35	46[g]
15	12m[CF$_3$SO$_3$]	---	84	>99

[a]General conditions: Ruthenium complex (5 mol% Ru), *i*PrOH (3 mL), reflux; conversions determined by ^{19}F NMR spectroscopy; [b]CAN 1 mol equiv. per ruthenium center; [c]conversion is complete already after 6h.

Furthermore, with the aim to understand the role of the solvent, **17G1-H** has been refluxed in ^{i}PrOH for 5h, followed by cooling under inert atmosphere of argon and the solvent removal under vacuum. ^{1}H-NMR performed in a J-young valve NMR tube under inert conditions allow to identify the formation of the hydride derivative [Ru(CO)$_2$HCpOH] (**A**) which, in CDCl$_3$ solution, evolve to the formation of [Ru(CO)$_2$ClCpOH] (**B**) in 24h, also identified by means of IR spectroscopy;[18] Trace of the Shvo complex (in ^{1}H-NMR the bridging hydride is revealed at -18.46 ppm) were also detected, whereas no signals ascribable to the methylene groups of the dendrimer have been observed in the fraction soluble in CDCl$_3$. Moreover, the water soluble fraction evidenced typical NMR signals (in D$_2$O) of both the dendrimer skeleton and imidazolium salt associated to **20G1**. On the light of these results, a proposed decomposition pathway has been formulated (Scheme 5.5).
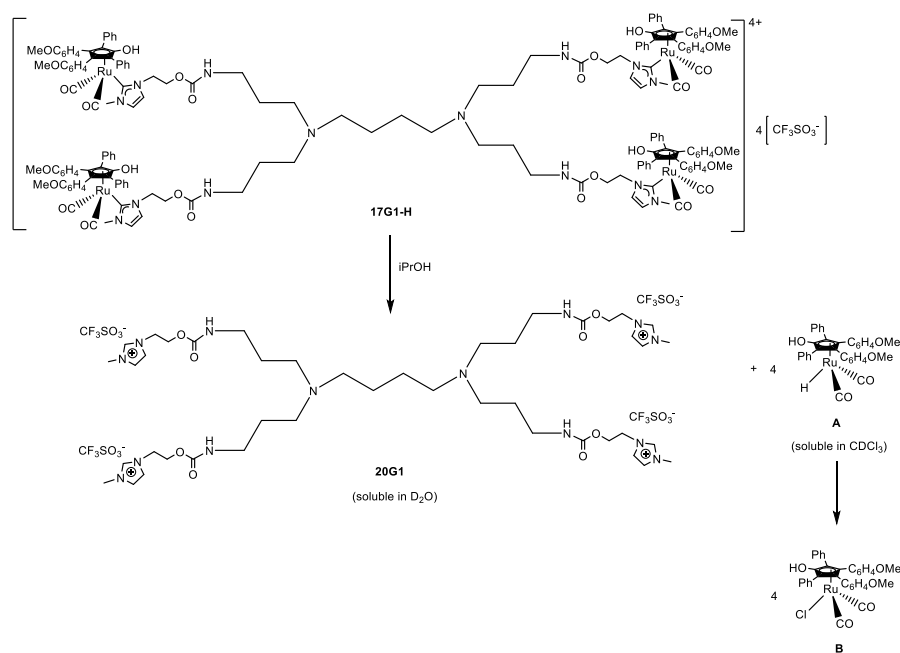
Scheme 5.5 Detachment of ruthenium hydride complex from the first generation **17G1-H**.

Since the solvent iPrOH is supposed to have a crucial role as hydrogen donor in the detachment of the hydroxycyclopentadienyl complex reported in Scheme 5.5, we performed the same decomposition test under reflux in toluene for 16h. In this case the crude reaction product, after solvent removal, was completely insoluble in D_2O but mostly soluble in $CDCl_3$. ^{1}H-NMR of this latter solution showed the pattern ascribable both to dendrimer skeleton and to ruthenium complexes. IR spectrum [v(CO) = 2009, 1951; v(C=O) = 1720 cm^{-1}] revealed the formation of a neutral species in which both the ruthenium terminal carbonyl and carbamate linker are present. The IR frequencies are slightly higher than those found for **17G1**, suggesting formation of a hydrogen bond between C=O of cyclopentadienone and protonated species.[10] A possible explanation is that protons are transferred from the hydroxycyclopentadienyl moiety to the nitrogen atoms available in the dendrimer skeleton. The latter hydrogen maintaining a hydrogen bond with the C=O group of cyclopentadienone. The hypothesis is also in agreement with the small shift of the signals due to -CH_2- (broad signals around 3 ppm and 1.6 ppm) from dendrimer, if compared with **17G1**.

5.4 Catalytic oxidation of alcohols

Since the ruthenium complexes look to remain linked to the dendrimer in refluxing toluene we moved to check the behavior of functionalized dendrimers versus mononuclear complexes under oxidative conditions in the dehydrogenation of benzyl alcohol to benzaldehyde. Preliminary tests were performed on mononuclear ruthenium complexes **4a** and **12a[CF₃SO₃]** in 1,2-dichlorobenzene (DCB) at 150°C (entry 1,2 and 5 in Table 5.2). A fair conversion is obtained with the complex **4a** which reaches a conversion of 71% within 8h (entry 1). Anyway, it seems that after a rapid activation, the catalyst is somehow off (75% after 24h). The presence of an oxidizing additive such as CAN play a detrimental role, giving only a 34% yield (the reaction is completely selective thus conversion correspond to the yield) in 24h. It is important to underline that under hydrogen transfer conditions (see Table 5.1) the same complex is not activated. On the other hand, the cationic complex **12a[CF₃SO₃]** (entry 5) gave good results also in the microscopy reverse transfer hydrogenation. In order to employ a greener solvent and to reduce the energy of the reaction with a lower temperature we checked toluene as solvent. The reaction works also at 110°C (entry 6) with similar results, even though the induction time is shorter in the case of DCB probably due to the higher temperature which can favor the CO release that is the key step of catalyst activation.[8b]

Table 5.2. Catalytic oxidation of benzyl alcohol to benzaldehyde.[a]
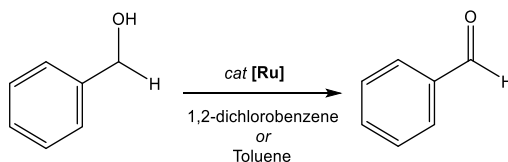
entry	[Ru]	additive	conversion 8h (%)	conversion 24h (%)
1	4a[b]	CAN[c]	21	34
2	4a[b]	---	71	75
3	4a[d]	---	16	67
4	4a[d]	CAN[c]	0	18
5	12a[CF$_3$SO$_3$][b]	---	60	66
6	12a[CF$_3$SO$_3$][d]	---	72	80
7	12a[CF$_3$SO$_3$][d]	Benzoquinone[e]	>99[f]	
8	17G1-H[g]		17	23[h]

[a]General conditions: Ruthenium complex (5 mol% Ru), solvent (3 mL), reflux; conversions determined by GC; [b]solvent: DCB; [c]CAN 1 mol equiv. (dissolved in 1mL of CH$_3$CN) per ruthenium center; [d]solvent: toluene; [e]2 equivalents of benzoquinone per ruthenium center; [e]conversion is complete already after 1 h; [g] Experiment performed in Tol-d$_8$; [h] adding 2 eq. per ruthenium center of benzoquinone to the reaction mixture the conversion arose from 23 to 37% in 2h and 44% in 18h. Further addition of an excess of acetone allow the conversion to reach 68% in two further hours.

In order to prevent the deactivation of the catalyst, a hydrogen acceptor such as benzoquinone has been added to the reaction mixture. This additive, as expected, is able to regenerate the catalyst *in situ* allowing to reach a complete conversion within 1h (entry 7). Performing the reaction with an equimolar quantity of ruthenium center immobilized on dendrimer **17G1-H** a detrimental dendrimer effect is observed (entry 8). In the latter reaction Tol-d$_8$ has been used as solvent in order to better follow the conversion and the destiny of ruthenium complexes. Indeed, by adding oxidizing additive such as benzoquinone or acetone the conversion is increased as expected. (see note *h* in Table 5.2)

With the aim to shed light on the role of solubility in the negative dendrimer effect a sample of **17G1-H** (9.8 mg in 0.6 mL of Tol-d$_8$) has been heated at 110 °C under inert atmosphere (J-young NMR tube under Argon) for 2h. The large majority of the dendrimer remains insoluble, anyway some signals ascribable to the ruthenium fragment are present in solution.

Since the decomposition of the dendrimer under reducing condition looks to be connected to the non-innocent solvent *i*PrOH, we added a slight excess of benzyl alcohol in order to understand if there is an effective role of –CH$_x$OH groups in the complex detachment above described. After 2h at 110°C, without stirring, only 2% conversion is observed. Anyway, the diagnostic signal of Shvo complex is observable at -17.87 ppm. Insoluble fraction has been analyzed in acetone-d$_6$ revealing the presence of the pattern of signals arising from **20G1**.

Anyhow performing the same reaction in acetone-d$_6$, where the dendrimer is completely soluble, neither conversion of benzyl alcohol nor decomposition of **17G1** is observed. Studies with different solvents in order to increase the reaction temperature will be investigated in the near future in order to activate the peripheral complexes avoiding functionalized dendrimer decomposition.

Conclusion

The novel cyclopentadienone-NHC-ruthenium functionalized five generations of polypropylene imine dendrimers (PPI) with up to 64 organometallic moieties DAB-dendr-[NH(O)CO(NHC)Cp=ORu(CO)$_2$]$_n$ {n=4, 8, 16, 32, 64} have been obtained by the formation of carbamate linkers between NH$_2$ peripheral group of the dendrimers and OH functionality in the lateral chain of the NHC employing carbonyldiimidazole as coupling agent. This straightforward and quantitative reaction provides a valuable route towards the immobilization of – OH functionalized NHC complexes on organic and inorganic amino functionalized supports. The dendritic compounds **17G1-5** have been characterized by ^{1}H, ^{13}C NMR and IR spectroscopy and mass spectrometry when possible. The quantitative formation of the hydroxycyclopentadienyl tetra-cationic dendrimer **17G1-H** has been observed by reacting **17G1** with a strong acid such as HCF$_3$SO$_3$.

By varying the cyclopentadienone ligand on the mononuclear ruthenium complexes a partial solubility in water has been found for the trimethylsilyl-functionalized ruthenium cation complex **18d[Cl]** even though the corresponding functionalized first generation dendrimer **19G1** shows similar solubility as **17G1**.

Preliminary results on the use of the first generation dendrimers in the protonated form (**17G1-H**), as hydrogen transfer (TH) catalyst in ^{i}PrOH showed higher catalytic activity if compared with the corresponding monomeric species. However, a more detailed study indicated that this is not ascribable to a true dendritic effect but is better explained by the decomposition of the cationic dendrimer, which led to the release of a peripheral ruthenium monomeric active species recognized as the active form of the famous Shvo catalyst. Preliminary results on dehydrogenation reaction indicate that cationic and neutral ruthenium NHC functionalized dendrimers **17G1** and **17G1-H** do not decompose under oxidizing conditions but in the applied conditions any conversion of the substrate has been achieved. Further investigations will focus on the study of different solvents in order to increase the reaction temperature and to activate the peripheral complexes avoiding functionalized dendrimer decomposition.

Experimental Section

Materials and procedures. Solvents: dichloromethane (CH_2Cl_2), diethyl ether (Et_2O), acetonitrile (CH_3CN), Toluene were dried and distilled prior to use. Acetone has been degassed and stored under inert atmosphere on molecular sieves. Other solvents such as 2-propanol (IPrOH), heptane, hexane, $CDCl_3$, D_2O, Toluene-d_8 (Sigma Aldrich) have been employed without further purification. Reagents: triruthenium-dodecacarbonil ($Ru_3(CO)_{12}$) (Strem), silver oxide, 1-methylimidazole, 1-chloroethanol, 1,3 diphenylacetone, 4,4'dimethoxybenzil (Alfa Aesar), 4-fluoroacetophenone, trifluoromethanesulfonic acid, 1,1'-carbonyldiimidazole (CDI) and DAB-dendr-$(NH_2)_n$ {n = 4, 8, 16, 32, 64}, cerium ammonium nitrate (CAN) (Sigma Aldrich) have been employed as purchased. 1-methyl-3-(2-hydroxyethyl)imidazolium chloride,[27] 3,4-Bis(4-methoxyphenyl)-2,5-diphenylcyclopenta-2,4-dienone,[29] dicarbonyl(η^4-3,4-bis(4-methoxyphenyl)-2,5-diphenylcyclopenta-2,4-dienone) ruthenium dimer,[30] dicarbonyl-η^4-3,4-bis(4-methoxyphenyl)-2,5-diphenylcyclopenta-2,4-dienone)-1-methyl-3-(2-hydroxyethyl-imidazol-2-ylidene)ruthenium,[20] have been prepared as previously reported. The prepared derivatives were characterized by spectroscopic methods. The NMR spectra were recorded using Varian Inova 300 (^{1}H, 300.1; ^{13}C, 75.5 MHz), Varian Mercury Plus VX 400 (^{1}H, 399.9; ^{13}C, 100.6 MHz), Varian Inova 600 (^{1}H, 599.7; ^{13}C, 150.8 MHz) spectrometers at 298 K; chemical shifts were referenced internally to residual solvent peaks. Full ^{1}H- and ^{13}C-NMR assignments were done, when necessary, by gHSQC and gHMBC NMR experiments using standard Varian pulse sequences. Infrared spectra were recorded at 298 K on a Perkin-Elmer Spectrum 2000 FT-IR spectrophotometer. ESI-MS spectra were recorded on Waters Micromass ZQ 4000 with samples dissolved in MeOH or CH_3CN. GC analysis have been performed on an Agilent Technologies 7890A Gas Cromatograph provided with a capillary column Agilent 19091J-433 HP-5 (5%phenyl)-methylpolysiloxane, 30 m x 0.320 mm x 0.25 μm.

Elemental analyses were performed on a Thermo-Quest Flash 1112 Series EA instrument. The conversions were monitored by ^{1}H-NMR ^{19}F-NMR.

Synthesis of Dicarbonyl(η^4-3,4-bis(4-methoxyphenyl)-2,5-diphenylcyclopenta-2,4-dienone)(1-methyl-3-(2-CO$_2$Im-ethyl)imidazol-ylidene)ruthenium (4p).
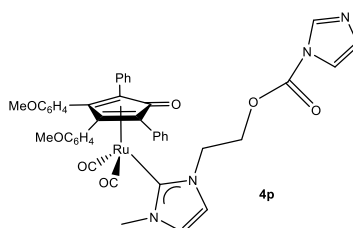
Figure 5.6. Structure of ruthenium carbene complex 4p.

1.44 g (1.98 mmol) of **4d** and 0.97 g (5.99 mmol) of 1,1'-carbonyldiimidazole were reacted under nitrogen atmosphere in 30 mL of anhydrous CH_2Cl_2. The reaction mixture was stirred at room temperature for 2h. The solution was then extracted with water (3x20 mL). Trace of water were removed from organic phase with Na_2SO_4, then the solvent was removed under vacuum and the white/brown product,identified as **4p**, was obtained with an yield of 84%. ^{1}H-NMR (399.9 MHz, $CDCl_3$): δ (ppm): 8.03 (s, 1H, Im); 7.78 (m, 4H, CH_{aryl}), 7.33 (m, 1H, Im), 7.16-7.12 (m, 8H, CH_{aryl}), 7.08 (m, 1H, Im), 7.06 (m, 2H, CH_{aryl}), 6.96 (d, J = 2.00 Hz, 1H, CH_{NHC}), 6.85 (d, J = 2.00 Hz, 1H, CH_{NHC}), 6.65 (m, 4H, CH_{aryl}), 4.05 (m, 2H,-CH_2-), 3.99 (m, 2H,-CH_2-), 3.72 (s, 6H, -OCH_3), 3.14 (s, 3H, -NCH_3). ^{13}C-NMR (100.6MHz, $CDCl_3$, DEPT): δ (ppm): 202.15 (CO), 174.80

($C_{carbene}$), 169.41 (C=O, Cp), 158.64 (-COCH$_3$), 147.89 (-OC(O)N-), 136.95 (CH, Im), 134.91 (Cq$_{aryl}$), 133.55 (CH$_{aryl}$), 130.88 (CH, Im), 129.36 (CH$_{aryl}$), 127.63 (CH$_{aryl}$), 125.63 (Cq$_{aryl}$), 124.70 (CH$_{NHC}$), 124.37 (CH$_{aryl}$), 121.76 (CH$_{NHC}$), 116.97 (CH, Im), 112.96 (CH$_{aryl}$), 104.09 (C$_{2,5}$, Cp), 78.88 (C$_{3,4}$, Cp), 67.02 (-CH$_2$-), 55.00 (-OCH$_3$), 49.20 (-CH$_2$-), 38.41 (CH$_3$, NHC). IR (CH$_2$Cl$_2$): v(CO): 2007cm^{-1}, 1948 cm^{-1}; v(C=O,-O$_2$CIm): 1768cm^{-1}. ESI-MS (m/z) (+): 823 [M+H]$^+$; 845 [M + Na]$^+$.

Synthesis of DAB-dendr-[NH(O)CO(NHC)Cp=ORu(CO)$_2$]$_n$ {n=4, 8, 16, 32, 64; NHC=[-CH$_2$CH$_2$-5-CH$_3$-imidazol-2-ylidene]; Cp=[3,4-(CH$_3$O-C$_6$H$_4$)$_2$-2,5-Ph$_2$(η^4-C$_4$CO)]} (17G)

17G1: DAB-dendr-(NH$_2$)$_4$ (0.02 g, 0.06 mmol) and **4p** (0.26 g, 0.31 mmol) were dissolved in anhydrous CH$_2$Cl$_2$ (10 mL) under inert atmosphere. Reaction mixture was stirred at room temperature for two days. The solution was then extracted with water (3x20 mL). Trace of water were removed from organic phase with MgSO$_4$, then the solvent was removed under vacuum and the crude was washed with Et$_2$O (3x15 mL). The yellow solid was identified as **17G1** (n=4) and obtained with 42% yield. ^{1}H-NMR (399.9 MHz, CDCl$_3$): δ (ppm): 7.72-6.60 (CH$_{aryl}$), 6.81 (m, 4H, CH$_{NHC}$), 6.62 (m, 4H, CH$_{NHC}$), 3.77 (m, 8H, -CH$_2$-), 3.68 (s, 24H, -OCH$_3$), 3.59 (m, 8H, -CH$_2$-), 3.09 (s, 12H, -NCH$_3$), 3.07, 2.97, 2.36, 1.57, 1.36 (br, 32H, CH$_2$, DAB-dendr). ^{13}C-NMR (100.6 MHz, CDCl$_3$): δ (ppm): 202.06 (C=O), 172.67 (C$_{carbene}$), 169.56 (C=O, Cp), 158.53 (-COCH$_3$), 156.00 (-OC(O)N-), 135.04 (Cq$_{aryl}$), 133.55 (CH$_{aryl}$), 129.40 (CH$_{aryl}$), 127.45 (CH$_{aryl}$), 125.50 (Cq$_{aryl}$), 124.44 (CH$_{aryl}$), 124.36 (CH, NHC), 121.80 (CH, NHC), 112.85 (CH$_{aryl}$), 103.73 (C$_{2,5}$, Cp), 78.97 (C$_{3,4}$, Cp), 63.29 (-CH$_2$-), 54.96 (-OCH$_3$), 49.75 (-CH$_2$-), 38.25 (CH$_3$, NHC), 53.73, 51.65, 39.51, 26.99, 24.88 (CH$_2$, DAB-dendr). IR (CH$_2$Cl$_2$): v(C=O): 2006 cm^{-1}, 1947 cm^{-1}; v(C=O, -NHC(O)O-): 1718 cm^{-1}; v(C=C): 1601 cm^{-1}, 1518 cm^{-1}; v(C=O, Cp): 1582 cm^{-1}. ESI-MS (m/z) (+): 3355 [M + Na]$^+$

The upper generations of PPI dendrimers, functionalized with *n* ruthenium complexes, respectively *n* = 8 **17G2**, *n* = 16 **17G3**, n = 32 **17G4** and *n* = 64 **17G5** were prepared with the same procedure, but they required seven days of reaction time.

17G2 (prepared from 0.02 g (0.03 mmol) of DAB-dendr-(NH$_2$)$_8$ and 0.26 g (0.31 mmol) of **4p** with a yield of 25%). ^{1}H-NMR (399.9 MHz, CDCl$_3$): δ (ppm): 7.75-6.61 (CH$_{aryl}$), 6.96 (m, 8H, CH$_{NHC}$), 6.79 (m, 8H, CH$_{NHC}$), 3.77 (m, 16H, -CH$_2$-), 3.70 (s, 48H, -OCH$_3$), 3.59 (m, 16H, -CH$_2$-), 3.10 (s, 24H, -NCH$_3$), 3.20-2.80, 2.60-2.20, 1.96-1.42 (br, 80H, CH$_2$, DAB-dendr). ^{13}C-NMR (100.6 MHz, CDCl$_3$): δ (ppm): 202.18 (C=O), 173.96 (C$_{carbene}$), 169.52 (C=O, Cp), 158.61 (-COCH$_3$), 156.14 (-OC(O)N-), 135.00 (Cq$_{aryl}$), 133.58 (CH$_{aryl}$), 129.49 (CH$_{aryl}$), 127.59 (CH$_{aryl}$), 125.78 (Cq$_{aryl}$), 124.55 (CH$_{aryl}$), 124.30 (CH, NHC), 122.43 (CH, NHC), 112.95 (CH$_{aryl}$), 103.65 (C$_{2,5}$, Cp), 78.68 (C$_{3,4}$, Cp), 63.29 (-CH$_2$-), 55.02 (-OCH$_3$), 50.00 (-CH$_2$-), 38.31 (CH$_3$, NHC), 53.47, 51.54, 39.51, 26.84, 23.63 (CH$_2$, DAB-dendr). IR (CH$_2$Cl$_2$): v(C=O): 2008cm^{-1}, 1948 cm^{-1}; v(C=O, -NHC(O)O-): 1719cm^{-1}; v(C=C): 1603 cm^{-1}, 1518 cm^{-1}; v(C=O, Cp): 1577 cm^{-1}.

17G3: (prepared from 0.02 g (0.01 mmol) of DAB-dendr-(NH$_2$)$_{16}$ and 0.17 g (0.21 mmol) of **4p** with a yield of 32%). ^{1}H-NMR (399.9 MHz, CDCl$_3$): δ (ppm): 7.76-6.61 (CH$_{aryl}$), 6.96 (m, 16H, CH$_{NHC}$), 6.78 (m, 16H, CH$_{NHC}$), 3.77 (m, 32H, -CH$_2$-), 3.71 (s, 96H, -OCH$_3$), 3.67 (m, 32H, -CH$_2$-), 3.10 (s, 48H, -NCH$_3$), 3.20-1.50 (br, 176H, CH$_2$, DAB-dendr). ^{13}C-NMR (100.6 MHz, CDCl$_3$): δ (ppm): 202.17 (C=O), 173.94 (C$_{carbene}$), 169.46 (C=O, Cp), 158.60 (-COCH$_3$), 153.57 (-OC(O)N-), 135.00 (Cq$_{aryl}$), 133.57 (CH$_{aryl}$), 129.29 (CH$_{aryl}$), 127.59 (CH$_{aryl}$), 125.52 (Cq$_{aryl}$), 124.54 (CH$_{aryl}$), 124.29 (CH, NHC), 122.38 (CH, NHC), 112.95 (CH$_{aryl}$), 103.98 (C$_{2,5}$, Cp), 78.67 (C$_{3,4}$, Cp), 63.69 (-CH$_2$-), 55.01 (-OCH$_3$), 50.01 (-CH$_2$-), 38.30 (CH$_3$, NHC), 53.39, 51.39, 38.41, 26.78, 24.02 (CH$_2$,

DAB-dendr). IR (CH$_2$Cl$_2$): ν(C=O): 2008cm^{-1}, 1949 cm^{-1}; ν(C=O, -NHC(O)O-): 1718cm^{-1}; ν(C=C): 1602 cm^{-1}, 1517 cm^{-1}; ν(C=O, Cp): 1577 cm^{-1}.

17G4: (prepared from 0.02 g (6.00 μmol) of DAB-dendr-(NH$_2$)$_{32}$ and 0.20 g (0.25 mmol) of **4p** with a yield of 41%); ^{1}H-NMR (399.9 MHz, CDCl$_3$): δ (ppm): 7.75-6.60 (CH$_{aryl}$), 6.96 (m, 32H, CH$_{NHC}$), 6.79 (m, 32H, CH$_{NHC}$), 3.77 (m, 64H, -CH$_2$-), 3.71 (s, 192H, -OCH$_3$), 3.67 (m, 64H, -CH$_2$-), 3.10 (s, 96H, -NCH$_3$), 3.20-1.50 (br, 368H, CH$_2$, DAB-dendr). ^{13}C-NMR (100.6 MHz, CDCl$_3$): δ (ppm): 202.16 (C=O), 173.88 (C$_{carbene}$), 169.38 (C=O, Cp), 158.60 (-COCH$_3$), 153.58 (-OC(O)N-), 134.97 (Cq$_{aryl}$), 133.57 (CH$_{aryl}$), 129.31 (CH$_{aryl}$), 127.59 (CH$_{aryl}$), 125.54 (Cq$_{aryl}$), 124.53 (CH$_{aryl}$), 124.30 (CH, NHC), 122.38 (CH, NHC), 112.95 (CH$_{aryl}$), 103.96 (C$_{2,5}$, Cp), 78.75 (C$_{3,4}$, Cp), 63.68 (-CH$_2$-), 55.02 (-OCH$_3$), 49.99 (-CH$_2$-), 38.32 (CH$_3$, NHC), 52.47, 51.22, 38.43, 24.10, 19.73 (CH$_2$, DAB-dendr). IR (CH$_2$Cl$_2$): ν(C=O): 2009cm^{-1}, 1947 cm^{-1}; ν(C=O, -NHC(O)O-): 1718cm^{-1}; ν(C=C): 1603 cm^{-1}, 1518 cm^{-1}; ν(C=O, Cp): 1576 cm^{-1}.

17G5: (prepared from 0.02 g (3.00 μmol) of DAB-dendr-(NH$_2$)$_{64}$ and 0.20 g (0.25 mmol) of **4p** with a yield of 43%). ^{1}H-NMR (399.9 MHz, CDCl$_3$): δ (ppm): 7.75-6.58 (CH$_{aryl}$), 6.96 (m, 64H, CH$_{NHC}$), 6.78 (m, 64H, CH$_{NHC}$), 3.77 (m, 128H, -CH$_2$-), 3.71 (s, 384H, -OCH$_3$), 3.66 (m, 128H, -CH$_2$-), 3.10 (s, 192H, -NCH$_3$), 3.20-1.50 (br, 752H, CH$_2$, DAB-dendr). ^{13}C-NMR (100.6 MHz, CDCl$_3$): δ (ppm): 202.16 (C=O), 173.91 (C$_{carbene}$), 169.43 (C=O, Cp), 158.60 (-COCH$_3$), 153.57 (-OC(O)N-), 134.98 (Cq$_{aryl}$), 133.57 (CH$_{aryl}$), 129.30 (CH$_{aryl}$), 127.59 (CH$_{aryl}$), 125.53 (Cq$_{aryl}$), 124.54 (CH$_{aryl}$), 124.30 (CH, NHC), 122.38 (CH, NHC), 112.95 (CH$_{aryl}$), 103.97 (C$_{2,5}$, Cp), 78.70 (C$_{3,4}$, Cp), 63.80 (-CH$_2$-), 55.02 (-OCH$_3$), 49.92 (-CH$_2$-), 38.31 (CH$_3$, NHC), 52.46, 51.35, 38.39, 26.70, 24.09 (CH$_2$, DAB-dendr). IR (CH$_2$Cl$_2$): ν(C=O): 2006cm^{-1}, 1950 cm^{-1}; ν(C=O, -NHC(O)O-): 1717cm^{-1}; ν(C=C): 1602 cm^{-1}, 1518 cm^{-1}; ν(C=O, Cp): 1577 cm^{-1}.

Synthesis of DAB-dendr-[NH(O)CO(NHC)Cp-OHRu(CO)$_2$]$_4$ (17G1-H) 0.150 g (0.045 mmol) of DAB-dendr-[NH(O)CO(NHC)Cp=ORu(CO)$_2$]$_4$ (**17G1**) was dissolved in 10 mL of CH$_2$Cl$_2$ under inert atmosphere. 4.8 equivalent of HCF$_3$SO$_3$ (solution at 1% in CH$_2$Cl$_2$) 1.9mL (0.216 mmol) were subsequently added. The reaction mixture was stirred for 30 minutes at room temperature, then the solvent was removed under vacuum and the crude washed twice with 10 ml of Et$_2$O. The slightly brown solid obtained was identified as **17G1-H** by IR, ^{1}H-NMR, ^{13}C-NMR, ^{19}F-NMR, ESI-MS. The yield was quantitative. ^{1}H-NMR (400 MHz, CDCl$_3$): δ (ppm) 7.36-6.40 (CH$_{aryl}$), 7.02 (m, 4H, CH$_{NHC}$), 6.65 (m, 4H, CH$_{NHC}$), 3.87 (m, 8H, -CH$_2$-), 3.70 (m, 24H, -OCH$_3$), 3.56 (m, 8H, -CH$_2$-), 3.31 (s, 12H, -NCH$_3$), 3.10, 1.84, 1.73, 0.85 (br, 32H, CH$_2$-DAB-dendr). ^{13}C-NMR (400 MHz, CDCl$_3$): δ (ppm) 198.72 (CO), 160.81 (C$_{carbene}$), 159.47 (COCH$_3$), 141.63 (C-OH, Cq), 133.34 (CH$_{aryl}$), 130.48 (CH$_{aryl}$), 128.66 (CH$_{aryl}$), 127.81(Cq$_{aryl}$), 126.21 (Cq$_{aryl}$), 121.66 (CH$_{NHC}$), 120.62 (CH$_{aryl}$), 118.49 (CH$_{NHC}$), 113.38 (CH$_{aryl}$), 104.14 (C$_{2,5}$, Cp), 87.79 (C$_{3,4}$, Cp), 62.71 (CH$_2$), 55.06 (OCH$_3$), 51.87 (CH$_2$), 51.11 (CH$_2$), 49.90 (CH$_2$), 38.93 (NCH$_3$), 37.49 (CH$_2$), 23.67 (CH$_2$), 19.85 (CH$_2$). ^{19}F-NMR (282.4 MHz, CDCl$_3$) δ (ppm): -78.67 (CF$_3$SO$_3$). IR (CH$_2$Cl$_2$): ν(C=O): 2039cm^{-1}, 1988 cm^{-1}; ν(C=O, -NHC(O)O-): 1724, 1701 cm^{-1}; ν(C=C): 1611 cm^{-1}, 1520 cm^{-1}. ESI-MS (m/z) (+): [M/4]$^+$ = 833; (-): [CF$_3$SO$_3$]$^-$ = 149.

Synthesis of DAB-dendr-[NH(O)CO(NHC)Cp=ORu(CO)$_2$]$_4$ {NHC=[-CH$_2$CH$_2$-5-CH$_3$-imidazol-2-ylidene]; Cp=[2,4-bis(trimethylsilyl)bicyclo[3.3.0]nona-1,4-dien-3-one]} (20G)

Dicarbonyl-(2,4-bis(trimethylsilyl)bicyclo[3.3.0]nona-1,4-dienyl)[1-(2-hydroxyethyl))-3-methylilidene]ruthenium chloride (18d[Cl]).
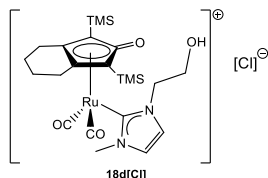
Figure 5.7 Structure of ruthenium cationic complex **18d[Cl]**.

Dicarbonyl-(2,4-bis(trimethylsilyl)bicyclo[3.3.0]nona-1,4-dien-3-one)[1-(2-hydroxyethyl))-3-methylilidene]ruthenium (**9d**) (0.040g, 0.071mmol) was dissolved in 10 mL of CH$_2$Cl$_2$ under inert atmosphere. Two equivalent of HCl (aqueous solution at 37%) were subsequently added. The reaction mixture was stirred for 2 h at room temperature. At the end of the reaction the solvent was removed under vacuum and a slightly brown solid identified as 2cTMS[Cl] by IR, ^{1}H-NMR, ^{13}C-NMR and ESI-MS was obtained in quantitative yield. ^{1}H-NMR (399.9 MHz, CDCl$_3$): δ (ppm) 7.67 (s, 2H, CH$_{NHC}$), 4.36 (t, 2H, -NCH$_2$), 4.04 (t, 2H, CH$_2$OH), 3.91 (s, 3H, -NCH$_3$), 2.50 (m, 4H, CH$_2$), 1.73 (m, 4H, CH$_2$), 0.33 (s, 18H, CH$_3$, TMS). ^{13}C-NMR (150.8 MHz, CDCl$_3$, g-HSQC, g-HMBC): δ (ppm) 199.17 (CO), 164.85 (C$_{carbene}$), 152.58 (C-OH), 125.95 (CH$_{NHC}$), 124.62 (CH$_{NHC}$), 108.26 (C$_{2,5}$, Cp), 81.10 (C$_{3,4}$, Cp), 60.37 (-NCH$_2$), 54.36 (-CH$_2$OH), 41.18 (-NCH$_3$), 24.29 (CH$_2$, 2C), 22.41 (CH$_2$, 2C), 0.98 (CH$_3$, TMS, 6C). IR (CH$_2$Cl$_2$, cm^{-1}): (vCO) 2038cm^{-1}, 1985 cm^{-1}. ESI-MS (m/z) (+):563 [M+H]$^+$; 585 [M + Na]$^+$.

Dicarbonyl-(2,4-bis(trimethylsilyl)bicyclo[3.3.0]nona-1,4-dien-3-one)[1-(2-(imidazolcarbonyloxy)ethyl)-3-methylilidene]ruthenium (9p).

Figure 5.8. Structure of ruthenium cationic complex **9p**.

Dicarbonyl-(2,4-bis(trimethylsilyl)bicyclo[3.3.0]nona-1,4-dien-3-one)[1-(2-hydroxyethyl))-3-methylilidene]ruthenium (**9d**) (0.029 g, 52 μmol) was dissolved in 5 ml of CH$_2$Cl$_2$ under inert atmosphere. Three equivalent of carbonyldiimidazole (CDI) (0.025 g, 156 μmol) were added to the solution and the reaction mixture was stirred for 24h at room temperature. The solution was then extracted with water (3x20ml). Water traces were removed from the organic solution with MgSO$_4$ and the solvent was removed under vacuum. The yellow solid was characterized by IR, ^{1}H-NMR, ^{13}C-NMR and ESI-MS and identified as Dicarbonyl-(2,4-bis(trimethylsilyl)bicyclo[3.3.0]nona-1,4-dien-3-one)[1-(2-(imidazolcarbonyloxy)ethyl)-3-methylilidene]ruthenium (**9p**) obtained with 79% yield. ^{1}H-NMR (599,7 MHz, CDCl$_3$): δ (ppm) 8.12 (s, 1H, CH$_{Imid}$), 7.41 (s, 1H, CH$_{Imid}$), 7.12 (s, 1H, CH$_{NHC}$), 7.09 (s, 1H, CH$_{Imid}$), 7.06 (s, 1H, CH$_{NHC}$), 4.75 (s, 4H, CH$_2$ LINKER), 3.91 (s, 3H, -NCH$_3$), 2.58 (m, 4H, CH$_2$), 1.78 (m, 4H, CH$_2$), 0.19 (s, 18H, TMS). ^{13}C-NMR (150.8 MHz, CDCl$_3$): δ (ppm) 202.74 (CO), 181.03 (C$_{carbene}$), 179.01 (CO, C$_p$), 148.15 (-OC(O)N-), 137.00 (CH, Imid), 131.04

(CH, Imid), 124.19 (CH, NHC), 121.66 (CH, NHC), 117.02 (CH, Imid), 106.07 ($C_{2,5}$, C_p), 68.83 ($C_{3,4}$, C_p), 66.93 (-NCH_2-), 50.74 (-CH_2O-), 40.77 (NCH_3), 24.91 (CH_2), 22.81 (CH_2), 0.60 (CH_3, TMS). ESI-MS (m/z) (+): 657 [M+H]$^+$; 679 [M + Na]$^+$.

20G1: DAB-dendr-(NH_2)$_4$ (2.91 mg, 9.2 µmol) and Dicarbonyl-(2,4-bis(trimethylsilyl)bicyclo[3.3.0]nona-1,4-dien-3-one)[1-(2-(i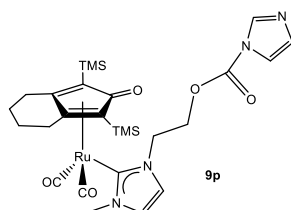midazolcarbonyloxy)ethyl)-3-methylilidene]ruthenium (**9p**) (0,027 g, 41.2 µmol) was dissolved in 5 ml of CH_2Cl_2 under inert atmosphere. The reaction mixture was stirred at room temperature for six days. At the end solvent was removed under vacuum and the brown solid was washed with water (3x20mL). The product, obtained in quantitative yield was identified as **20G1**. ^{1}H-NMR (399.9 MHz, CDCl$_3$): δ (ppm) 7.15 (m, 4H, CH$_{NHC}$), 6.99 (m, 4H, CH$_{NHC}$), 4.52 (s, 8H, CH$_2$ linker), 4.33 (s, 8H, CH$_2$ linker), 3.87 (s, 12H, -NCH_3), 3.19, 2.43, 238, 1.61, 1.41 (br, 32H, CH_2, DAB-dendr), 2.53 (s, 16H, CH_2), 1.76 (s, 16H, CH_2), 0.18 (s, 72H, TMS). ^{13}C-NMR (150.8 MHz, CDCl$_3$, g-HSQC, g-HMBC): δ (ppm) 202.51 (CO), 181.10 (C$_{carbene}$), 177.28 (CO, C$_p$), 155.96 (-OC(O)N-), 123.63 (CH, NHC), 122.22 (CH, NHC), 106.20 (C$_{2,5}$, C$_p$), 68.41 (C$_{3,4}$, C$_p$), 63.57 (-NCH_2-), 51.61 (-CH_2O-), 40.52 (-NCH_3), 24.74 (CH_2), 22.79 (CH_2), 0.63 (CH_3, TMS). IR (CH_2Cl_2): v(CO):1999 cm^{-1}, 1937 cm^{-1}; v(C=O,-O_2CIm):1760 cm^{-1}. ESI-MS (m/z) (+): 2669 [M+H]$^+$; 679 [M + Na]$^+$.

Characterization of dendrimer DAB-dendr-[NH(O)COCH$_2$CH$_2$Im(CH$_3$)]$_4$ (19G1): ^{1}H-NMR (400 MHz, D$_2$O): δ (ppm) 8.81 (m, 4H, NCHN), 7.57 (m, 4H, CH$_{Im}$), 7.46 (m, 4H, CH$_{Im}$), 4.52 (m, 8H, -CH$_2$-), 4.47 (m, 8H, -CH$_2$-), 3.92 (s, 12H, -NCH_3), 3.15, 1.92, 1.78, 0.85 (br, 32H, CH$_2$-DAB-dendr).
^{1}H-NMR (400 MHz, acetone-d$_6$): δ (ppm) 9.06 (m, 4H, NCHN), 7.79 (m, 4H, CH$_{Im}$), 7.70 (m, 4H, CH$_{Im}$), 4.61 (m, 8H, -CH$_2$-), 4.42 (m, 8H, -CH$_2$-), 4.05 (s, 12H, -NCH_3), 3.38-0.85 (br, 32H, CH$_2$-DAB-dendr).

Characterization of Dicarbonyl(η^4-3,4-bis(4-methoxyphenyl)-2,5-diphenylcyclopenta-2,4-hydroxycyclopentadienyl)(H)ruthenium (A): ^{1}H-NMR (399.9 MHz, CDCl$_3$): δ (ppm): 7.46-6.54 (m, 18H, CH$_{aryl}$), 3.71 (s, 6H, -OCH_3), -9.88 (s, 1H, hydride).

Characterization of Dicarbonyl(η^4-3,4-bis(4-methoxyphenyl)-2,5-diphenylcyclopenta-2,4-hydroxycyclopentadienyl)(Cl)ruthenium (B): ^{1}H-NMR (399.9 MHz, CDCl$_3$): δ (ppm): 7.44-6.61 (m, 18H, CH$_{aryl}$), 3.74 (s, 6H, -OCH_3). ^{13}C-NMR (100.6MHz, CDCl$_3$, DEPT): δ (ppm): 197.48 (CO), 159.49 (-COCH$_3$), 140.44 (-C-OH), 132.99-113.35 (CH$_{aryl}$), 99.25 (C$_{2,5}$, Cp), 88.52 (C$_{3,4}$, Cp), 55.14 (-OCH_3). IR (CH_2Cl_2): v(CO): 2038 cm^{-1}, 2018 cm^{-1}.

General method for transfer hydrogenation

Functionalized dendrimer (15 µmol [Ru] (3.75 µmol for 4g1 and 4g1-H , 5 mol% [Ru]), additive (1 eq. when needed) and *i*PrOH (3 mL) were stirred at reflux for 15 min. Then 4-fluoroacetophenone (36 µL, 300 µmol) was added and samples were taken at regular intervals. Aliquots (ca. 0.05mL) were diluted with CDCl$_3$ (0.5 mL) and conversions were determined by ^{19}F-NMR spectroscopy.

General method for dehydrogenation

Ruthenium complex (5%mol, 9.5 µmol) was dissolved in 3mL of the solvent (1,2-dichlorobenzene or toluene). Once reached the reaction temperature (150°C for 1,2-dichlorobenzene and 110 °C for toluene) 19.7 µL of benzyl alcohol (190 µmol) were added. Samples were taken at regular intervals and conversions were determined by GC.

References

[1] (a) D. Wang, D. Astruc, *Coord. Chem. Rev.*, **2013**, *257*, 2317– 2334; (b) D. Astruc, *Nat. Chem.,* **2012**, *4*, 255; D. Mery, D. Astruc, *Coord. Chem. Rev.*, **2006**, *250*, 1965–1979; (c) D. Wang, C. Deraedt, J. Ruiz, D. Astruc, *Acc. Chem. Res.* **2015**, *48*, 1871−1880; (d) D. Astruc, F. Lu, J. Ruiz Aranzaes, *Angew. Chem. Int. Ed.* **2005**, *44*, 7852 – 7872; (e) D. Astruc, E. Boisselier, C. Ornelas *Chem. Rev.* **2010,** *110,* 1857–1959; (f) G.E. Oosterom, J.N.H. Reek, P.C.J. Kamer, P.W.N.M. van Leeuwen, *Angew. Chem. Int.* Ed. **2001**, *40*, 1828; (g) R. van Heerbeek, P.C.J. Kamer, P.W.N.M. van Leeuwen, J.N.H. Reek, *Chem. Rev.* **2002**, *102*, 3717; (h) J.N.H. Reek, S. Arevalo, R. van Heerbeek, P.C.J. Kamer, P.W.N.M. van Leeuwen, *Adv. Catal.*, **2006**, *49*, 71; (i) G. M. Dykes, *J. Chem. Technol. Biotechnol.*, **2001**, *76*, 903; (j) S.-H. Hwang, C. D. Shreiner, C. N. Moorefieldc, G. R. Newkome, *New J. Chem.*, **2007**, *31*, 1192–1217.

[2] (a) A.-M. Caminade, A. Ouali, R. Laurent, C.-O. Turrin, J.-P. Majoral *Chem. Soc. Rev.,* **2015**, *44*, 3890—3899; (b) D. A. Tomalia, *New J. Chem.*, **2012**, *36*, 264–281; (c) B. Helms, J. M. J. Frechet, *Adv. Synth. Catal.*, **2006**, *348*, 1125–1148.

[3] See for example: (a) A. K. Kakkar, *Macromol. Symp.*, **2003**, *196*, 145; (b) B. Yi, H.-P. He, Q.-H. Fan, *J. Mol. Catal. A: Chem.* **2010**, *315*, 82; (c) J. Yu, T. V. RajanBabu, J. R. Parquette, *J. Am. Chem. Soc.,* **2008**, *130*, 7845; (d) R. A. Findeis, L. H. Gade, *Eur. J. Inorg. Chem.* **2003**, 99; (e) B. Natarajan, N. Jayaraman, *J. Organomet. Chem.* **2011**, *696*, 722; (f) L. I. Rodriguez, O. Rossell, M. Seco, G. Muller, *J. Organomet. Chem.* **2009**, *694*, 1938; (g) L.-I. Rodriguez, O. Rossell, M. Seco, G. Muller, *J. Organomet. Chem.* **2007**, *692*, 851.

[4] W.-J. Tang, Y.-Y. Huang, Y.-M. He, Q.-H. Fan, *Tetrahedron Asymm.* **2006**, *17*, 536.
F. Zhang, Y. Li, Z.-W. Li, Y.-M. He, S.-F. Zhu, Q.-H. Fan, Q.-L. Zhou, *Chem. Commun.*, **2008**, 6048; Z.-J. Wang, G.-J. Deng, Y. Li, Y.-M. He, W.-J. Tang, Q.-H. Fan, Org. Lett. **2007**, *9*, 1243.

[5] W. Wang, Q. Wang, *Chem. Commun.* **2010**, *46*, 4616.

[6] Y. Chen, T. Wu, J. Deng, H. Liu, X. Cui, J. Zhu, Y. Jiang, M. C. K. Choi, A. S. C. Chen, *J. Org. Chem.* **2002**, *67*, 5301.

[7] (a) C. Cesari, R. Mazzoni, H. Muller-Bunz and M. Albrecht, *J. Organomet. Chem.*, **2015**, *793*, 256; (b) C. Cesari, A. Cingolani, C. Parise, S. Zacchini, V. Zanotti, M. C. Cassani and R. Mazzoni, *RSC Adv.*, **2015**, *5*, 94707.

[8] (a) M. C. Warner, C. P. Casey and J.-E. Backvall, *Top. Organomet. Chem.*, **2011**, *37*, 85; (b) B. L. Conley, M. K. Pennington-Boggio, E. Boz and T. J. Williams, *Chem. Rev.*, **2010**, *110*, 2294; (c) T. Pasini, G. Solinas, V. Zanotti, S. Albonetti, F. Cavani, A. Vaccari, A. Mazzanti, S. Ranieri and R. Mazzoni, *Dalton Trans.*, **2014**, *43*, 10224; (d) C. Cesari, L. Sambri, S. Zacchini, V. Zanotti and R. Mazzoni, *Organometallics*, **2014**, *33*, 2814 and reference cited therein.

[9] C. Cesari, S. Conti, S. Zacchini, V. Zanotti, M. C. Cassani and R. Mazzoni, *Dalton Trans.*, **2014**, *43*, 17240.

[10] For reviews, see: a) F. E. Hahn and M. C. Jahnke, *Angew. Chem. Int. Ed.,* **2008**, *47*, 3122; b) M. Melaimi, M. Soleilhavoup and G. Bertrand, *Angew. Chem. Int. Ed.,* **2010**, *49*, 8810. c) L. Benhamou, E. Chardon, G. Lavigne, S. Bellemin-Laponnaz and V. Cesar, *Chem. Rev.*, **2011**, *111*, 2705. d) L. A. Schaper, S. J. Hock, W. A. Herrmann and F. E. Kühn, *Angew. Chem. Int. Ed.*, **2013**, *52*, 270.

[11] For selected reviews , see: a) D. Bourissou, O. Guerret, F. P. Gabbai and G. Bertrand, *Chem. Rev.,* 2000, **100**, 39; b) W. A. Herrmann, *Angew. Chem. Int. Ed.,* **2002**, *41*, 1290; c) C. M. Crudden and D. P. Allen, *Coord. Chem. Rev.*, **2004**, *248*, 2247; d) M. Poyatos, J. A. Mata and E. Peris, *Chem. Rev.,* **2009**, *109*, 3677; e) O. Schuster, L. Yang, H. G. Raubenheimer and M. Albrecht, *Chem. Rev.,* **2009**, *109*, 3445; f) L. Mercs and M. Albrecht, *Chem. Soc. Rev.*, 2010, *39*, 1903; (g) M. N. Hopkinson, C. Richter, M. Schedler and F. Glorius, *Nature*, **2014**, *510*, 485; (h) S. P. Nolan, N-Heterocyclic Carbenes: Effective Tools for Organometallic Synthesis, **2014**, Wiley VCH.

[12] T. Fujihara, Y. Obora, M. Tokunaga, H. Sato, Y. Tsuji, *Chem. Commun.*, **2005**, 4526–4528.

[13] S. B. Garber, J. S. Kingsbury, B. L. Gray, A. H. Hoveyda *J. Am. Chem. Soc.* **2000**, *122,* 8168-8179.

[14] L. Busetto, M. C. Cassani, P. W. N. M. van Leeuwen, R. Mazzoni *Dalton Trans.*, **2004**, 2767–2770.

[15] L. Busetto, P. L. Buldini, M. C. Cassani, R. Mazzoni, *J. Organomet. Chem.*, **2006**, *691*, 573–578.

[16] A. Cingolani, C. Cesari, S. Zacchini, V. Zanotti, M. C. Cassani and R. Mazzoni, *Dalton Trans.*, **2015**, *44*, 19063–19067

[17] Y. Shvo, D. Czarkie, Y. Rahamim and D. F. Chodosh, *J. Am. Chem. Soc.*, **1986**, *108*, 7400; b) C. P. Casey, S. W. Singer, D. R. Powell, R. K. Hayashi and M. Kavana, *J. Am. Chem. Soc.*, **2001**, *123*, 1090; c) L. K. Thalen, D. Zhao, J.–B. Sortais, J. Paetzold, C. Hoben and J.-E. Backwall, *Chem. –Eur. J.*, **2009**, *15*, 3402.

[18] H. M. Jung, J. H. Choi, S. O. Lee, Y. H. Kim, J. H. Park, J. Park *Organometallics* **2002,** *21,* 5674-5677

CHAPTER VI

Imidazolium salts of ruthenium anionic cyclopentadienone complexes: ion pair for bifunctional catalysts in ionic liquids

Abstract

A new class of ruthenium anionic complexes that form ion pair with imidazolium salts has been prepared by direct reaction between the dinuclear complex dicarbonyl(η^4-3,4-bis(4-methoxyphenyl)-2,5-diphenylcyclopenta-2,4-dienone and various imidazolium salts. The reaction is clean, general and quantitative and the complexes formed are stable to air and moisture both in the solid state and in solution. The novel complexes show affinity for ionic liquids and represent stable precursors of the catalytic active form of the Shvo catalyst, a well-established homogeneous catalyst for several bifunctional applications in common organic solvents. The novel ion pairs here developed allow the use of green ionic liquids (IL) as solvents and preliminary results demonstrate that they exhibit fair catalytic activity (up to 75% of conversion within 24h) in the transfer hydrogenation of 4-fluoroacetophenone and almost complete conversion in the dehydrogenation of benzyl alcohol. The IL-supported oxidative catalyst can be recycled with a relevant increasing in activity that should be ascribed to a stabilization of the active specie in a more available form by the IL itself. The synthetic method here discussed represents a novelty within the field of IL-supportation and is potentially useful for the heterogenization of the catalysts exploiting SILP technology.

Introduction

Over the past decade, ionic liquids (ILs) have gained recognition in the context of green organic synthesis in that they can be environmentally benign solvents and also behave as a liquid support in various chemical processes.[1] Although ILs were recently introduced as alternative green reaction media in organic synthesis because of their unique chemical and physical properties such as no volatility, non-flammability, thermal and chemical stability, controlled miscibility and ionic conductivity, they have already made a revolutionary impact on a number of fields including: analytical chemistry, electrochemistry, polymer chemistry, nanotechnology and biotechnology, energy[2] and catalysis.[3] Reactions which are successfully performed in ILs include hydrogenation and oxidation.[3] However, redox reactions mediated by bifunctional catalysts such as homogeneous transfer hydrogenation[4] and dehydrogenation, which are reaction of great general interest and particularly within the field of bio-refinery,[5] have been scarcely investigated.

In the previous chapters the new class of ruthenium complexes that combine cyclopentadienone and NHC ligands has been described[6] together with their properties as redox bifunctional catalysts. [7] Their preparation is recalled in Scheme 6.1 in order to make clearer the comparison between the novel ionic pair complexes and the "classic" neutral organometallic compounds of type **4.** The easy functionalization of imidazolium salts, precursors of NHC ligands, allow to tune steric and electronic properties, solubility and the insertion of substituents suitable for heterogenization. Furthermore, by choosing a proper substituent, NHC ligand itself is potentially able to cooperate with the metal and behave as non-innocent species.[7b,8]
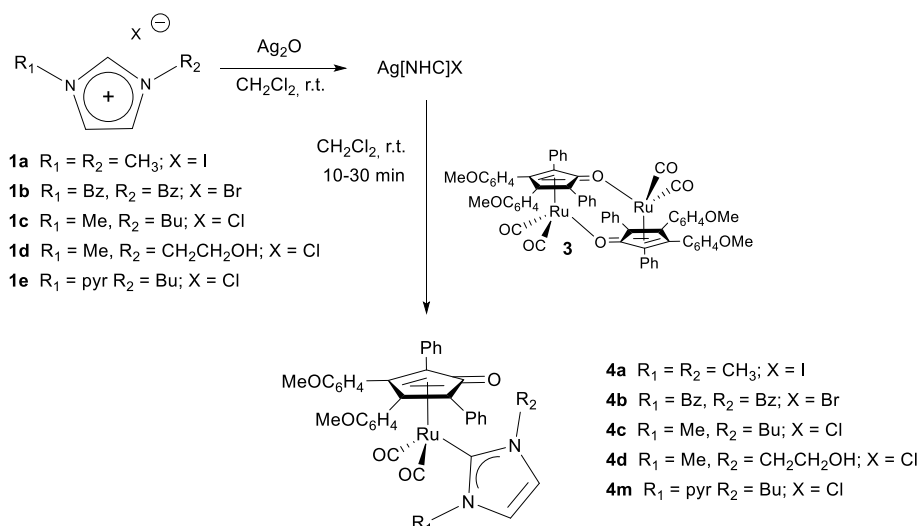
Scheme 6.1 Synthesis of cyclopentadienone imidazolylidene ruthenium(0) complexes **4a–d,m**.

During our study on the reactivity of imidazolium salts with the dinuclear ruthenium carbonyl cyclopentadienone **3**, aimed at obtaining to obtain NHC Ru complexes, we serendipitously observed the formation of a novel class of anionic ruthenium complexes behaving as ILs. Some of these complexes are soluble in ionic liquids such as [BMIM][PF$_6$] and demonstrated to be active in hydrogen transfer employing 2-propanol as the hydrogen donor. Anionic complexes bearing an imidazolium salt as couterion are poorly reported in the literature even though they offer several interesting properties and have been exploited in catalysis,[9] and medicinal chemistry.[10] To the best of our knowledge they have never been employed in transfer hydrogenation. On the other hand, several ionic tagged complexes have been designed in order to obtain catalysts soluble in ionic liquids for ILs-supported catalysis, with the benefit of simplified product isolation and possible catalyst reuse.[11] Here, we report on the synthesis and characterization of a novel class of ruthenium complexes ion paired with imidazolium salts and on their application as hydrogen transfer catalysts.

A comparison between NHC complexes and [Ru][ILs] ion pairs in [BMIM][PF$_6$] is also described for TH and the reverse reaction: dehydrogenation. The easy and quantitative synthetic approach and the stability of the ion-pairs make this procedure available for the immobilization of ruthenium bifunctional catalysts on imidazolium functionalized insoluble supports, such as those employed in the emerging SILP technology.[12]

Results and discussion

6.1 Synthesis and structures of ruthenium complexes

The reactivity of the dinuclear complex **3** with imidazolium salts has been explored using a library of variously functionalized imidazolium salts, prepared according to literature procedures (Figure 6.1).
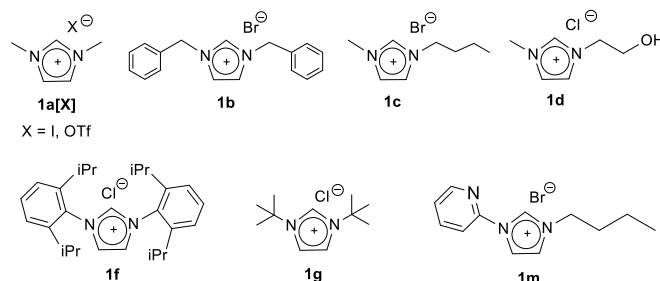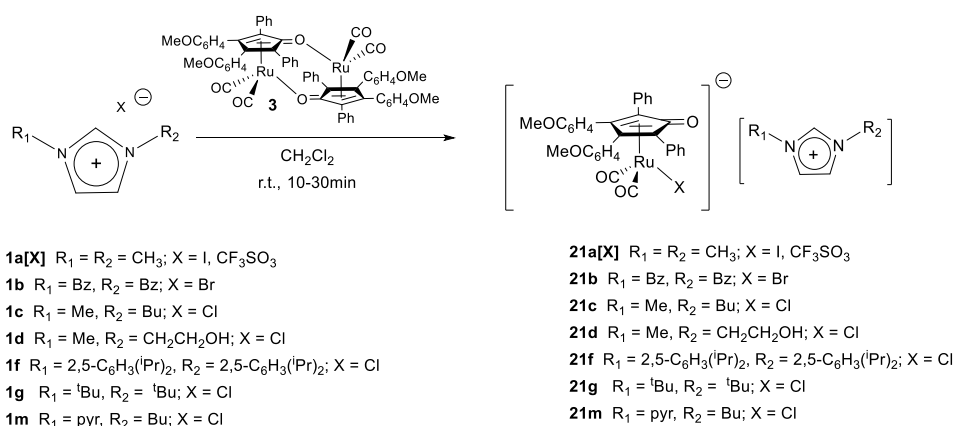

Figure 6.1 Imidazolium salts employed in this work.

Imidazolium salts **1a–m** were reacted directly with the dimeric precursor dicarbonyl(η^4-3,4-bis-(4-methoxyphenyl)-2,5-diphenylcyclopenta-2,4-dienone) (**3**). A quantitative and instant reaction leads to the formation of the ionic pairs **21a–m** consisting of the imidazolium cation and Ru(0) anionic complexes (Scheme 6.2). These latter are obtained upon the coordination of the imidazolium counterion to the 16 electron ruthenium mononuclear form, which is generated as soon as the dimer is dissolved in organic solvents such as dichloromethane.

1a[X] $R_1 = R_2 = CH_3$; X = I, CF_3SO_3
1b $R_1 = Bz, R_2 = Bz$; X = Br
1c $R_1 = Me, R_2 = Bu$; X = Cl
1d $R_1 = Me, R_2 = CH_2CH_2OH$; X = Cl
1f $R_1 = 2,5-C_6H_3(^iPr)_2, R_2 = 2,5-C_6H_3(^iPr)_2$; X = Cl
1g $R_1 = {}^tBu, R_2 = {}^tBu$; X = Cl
1m $R_1 = pyr, R_2 = Bu$; X = Cl

21a[X] $R_1 = R_2 = CH_3$; X = I, CF_3SO_3
21b $R_1 = Bz, R_2 = Bz$; X = Br
21c $R_1 = Me, R_2 = Bu$; X = Cl
21d $R_1 = Me, R_2 = CH_2CH_2OH$; X = Cl
21f $R_1 = 2,5-C_6H_3(^iPr)_2, R_2 = 2,5-C_6H_3(^iPr)_2$; X = Cl
21g $R_1 = {}^tBu, R_2 = {}^tBu$; X = Cl
21m $R_1 = pyr, R_2 = Bu$; X = Cl

Scheme 6.2 Synthesis of cyclopentadienone ruthenium(0) complexes ion paired to imidazolium salts **21a–m**.

The reaction is general, involving both hindered and non-bulky N-heterocyclic carbenes, and tolerant to functional groups: in fact it occurs in the presence of a primary alcohol in the lateral chain (**1d** to **21d**) and in the presence of pyridine (**1m** to **21m**). It proceeds with the halide counterion of the starting imidazolium salt, as well as with trifluoromethanesulfonate. On the other hand, it does not occur with NTf$_2^-$ (bis(trifluoromethylsulfonyl)imide) as counterion, probably due to its peculiar coordination properties.[13] The synthesis of **21a–m** is followed by IR spectroscopy, observing the lowering in vCO stretching frequencies (e.g. **21a**: v(CO) = 2004, 1945 cm^{-1} vs. **3**: 2018, 1967 cm^{-1}). Lower stretching frequencies suggest that the negative charge is more localized on the metal than on the oxygen of the cyclopentadienone ligand (Figure 6.2). This observation is confirmed by the C=O distance in the X-Ray diffraction structure of **21a** (1.225 Å – vide infra - vs 1.245 Å for **4a**[7] and 1.334 Å for the hydroxycyclopentadienyl analogue[8b] **12a[X]** obtained by protonation of **4a**). An η^4 coordination of the cyclopentadienone is thus reasonable and the negative charge on the metal together with the π-donor nature of chloride and congeners allow more back-bonding toward the CO ligands.
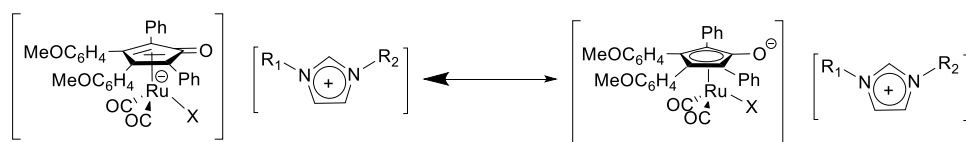
Figure 6.2. Localization of the negative charge in complexes of type **21**. The ruthenium(0) form on the left is the one supported by experimental evidences.

IR spectra of the other ion pairs of type **21** are very similar to that of complex **21a**, except for the hydroxyl-functionalized complex **21d,** that shows increased frequency for terminal CO and lowering of cyclopentadienone v C=O [21d: v(CO) = 2009, 1948 cm^{-1}; v(C=O) = 1566 cm^{-1} vs. **21a**: v(CO) = 2004, 1945 cm^{-1}, 1580 cm^{-1}]. This behavior is in agreement with what observed for NHC ruthenium complexes reported in Chapter II and described in the introduction,[7] and is ascribable to the formation of a hydrogen bond between –OH of the imidazolium salt and the carbonyl group of cyclopentadienone. All the complexes of type **21** show in ^{1}H-NMR and ^{13}C-NMR spectra the typical pattern of the starting reagents moved to different chemical shift; in Figure 6.3 and 6.4 the spectra of **21a[I]** are reported as examples.
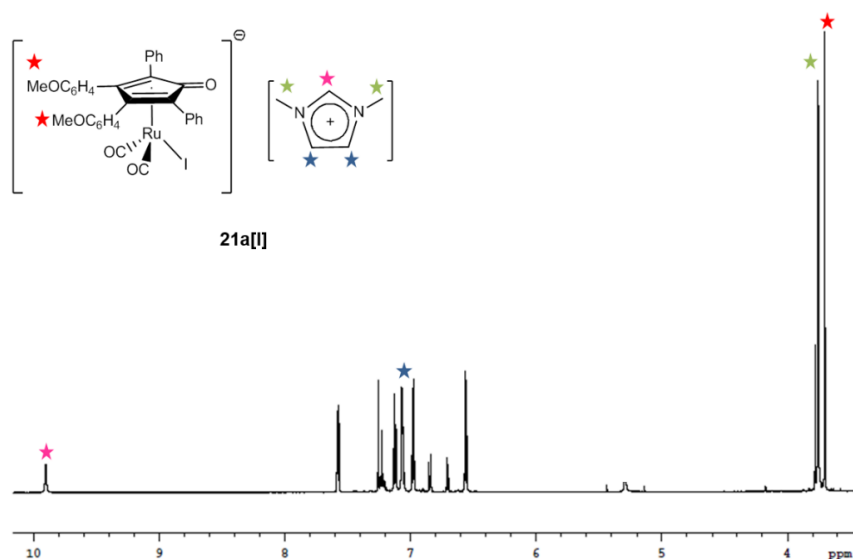
Figure 6.3. ^{1}H-NMR spectrum of **21a[I]** in CDCl$_3$.
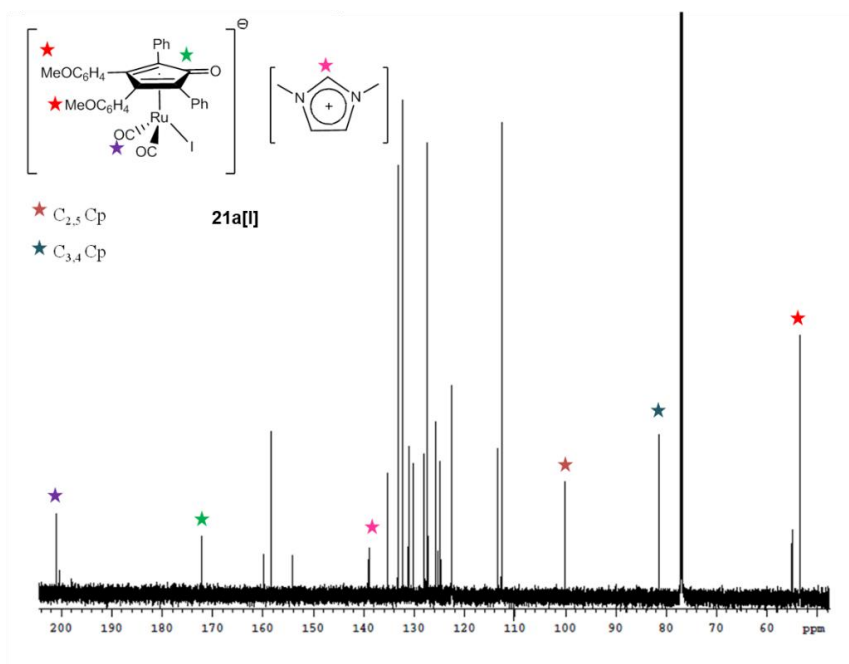
Figure 6.4. ^{13}C-NMR spectrum of **21a[I]** in CDCl$_3$.

More significant indication of the structure reported in Scheme 6.2 is given by ESI-MS analyses which show the molecular anion [Ru(CO)$_2${C$_5$(C$_6$H$_4$OMe)$_2$(Ph)$_2$=O}(X)]$^-$ and the molecular cation [R$_1$ImR$_2$]$^+$. Further confirmation of the structure proposed came from X-Ray diffraction of single crystals obtained for the complexes **21a[I]** and **21f** (Figure 6.5).

The solid state structures of **21a[I]** and **21f** are composed of [{2,5-Ph$_2$-3,4-(p-MeO-C$_6$H$_4$)$_2$(η^4-C$_4$C=O)}Ru(CO)$_2$X]$^-$ (X = I, Cl) complex anions and imidazolium [1,3-R$_2$-C$_3$N$_2$H$_3$]$^+$ (R = Me, ^{t}Bu) cations. The cations display structures similar to those previously reported with other anions.[14] The molecular structures of the [{2,5-Ph$_2$-3.4-(p-MeO-C$_6$H$_4$)$_2$(η^4-C$_4$C=O)}Ru(CO)$_2$X]$^-$ anions are closely related to the neutral {2,5-Ph$_2$-3.4-(p-MeO-C$_6$H$_4$)$_2$(η^4-C$_4$C=O)}Ru(CO)$_2$(L) (L = NHC carbene ligand) complexes, for what concerns the coordination of the cyclopentadienone ligand.[6,7] In particular, the Ru(1)-C(3) distance [2.499(7) and 2.503(7) Å for **21a[I]** and **21f**, respectively] is significantly longer than Ru(1)-C(4-7) [2.201(7)-2.251(6) Å, average 2.225(12) Å for **21a[I]**; 2.149(7)-2.267(7) Å, average 2.213(12) Å for **21f**] as previously found in other complexes where the cyclopentadienone ligand is essentially η^4-coordinated to Ru.[15] For comparison, the same Ru-C contact is shortened to 2.32-2.34 Å in the case of Ru-complexes containing η^5-cyclopentadienone derived ligands.[7,16] In agreement with the above η^4-coordination, the C(3)-O(3) contact [1.242(7) and 1.226(8) Å] is essentially a double bond.

It must be remarked that in both the solid state structures, a C-H···O inter-molecular contact is present involving the C(41)-H(41) group of the imidazolium cation and the O(3) atom of the cyclopentadienone ligand of the anion [C(41)-H(41) 0.93 Å, H(41)···O(3)#1 2.16 Å, C(41)···O(3)#1 2.957(10) Å, <C(41)H(41)O(3)#1 143.1° for **21a[I]**, symmetry #1 x+1,y-1,z; C(41)-H(41) 0.93 Å, H(41)···O(3) 2.49 Å, C(41)···O(3) 3.380(9) Å, <C(41)H(41)O(3) 159.7° for **4a**].
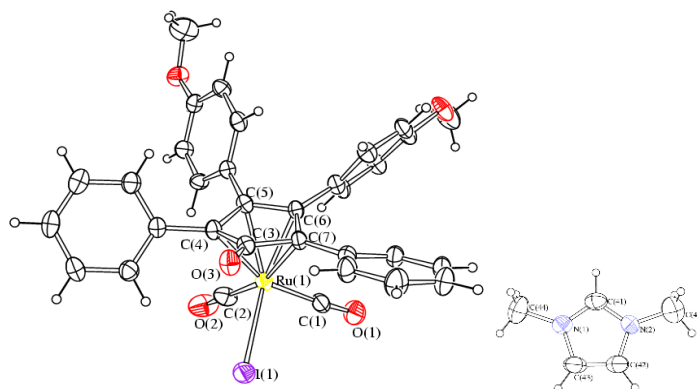
Figure 6.5 ORTEP drawing of **21a[I]**. Displacement ellipsoids are at the 30% probability level.
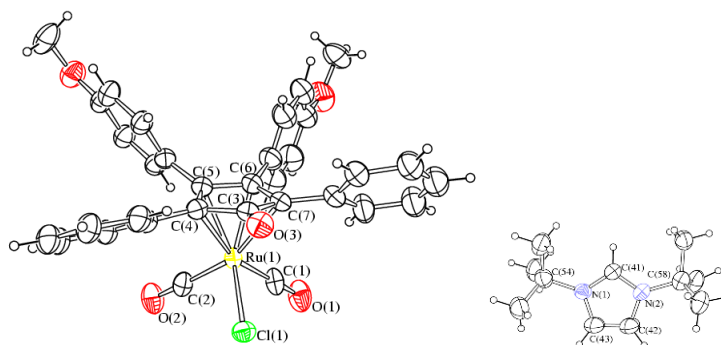
Figure 6.6 ORTEP drawing of **21f**. Displacement ellipsoids are at the 30% probability level.

Table 6.1. Selected bond lengths (Å) and angles (deg) for **21a[I]** and **21f**.

	21a[I]	**21f**
Ru(1)-C(1)	1.900(8)	1.866(8)
Ru(1)-C(2)	1.880(8)	1.872(8)
Ru(1)-X(1)	2.7604(8)	2.4464(18)
Ru(1)-C(3)	2.499(7)	2.503(7)
Ru(1)-C(4)	2.245(7)	2.252(7)
Ru(1)-C(5)	2.201(7)	2.185(7)
Ru(1)-C(6)	2.202(6)	2.149(7)
Ru(1)-C(7)	2.251(6)	2.267(7)
C(1)-O(1)	1.115(7)	1.156(8)
C(2)-O(2)	1.152(8)	1.158(8)
C(3)-O(3)	1.242(7)	1.226(8)
C(3)-C(4)	1.476(8)	1.494(10)
C(4)-C(5)	1.453(8)	1.439(10)
C(5)-C(6)	1.434(8)	1.442(9)
C(6)-C(7)	1.439(8)	1.451(10)
C(7)-C(3)	1.484(8)	1.462(10)
C(41)-N(1)	1.306(9)	1.324(9)
C(41)-N(2)	1.311(9)	1.299(8)
N(1)-C(43)	1.358(9)	1.353(10)
N(2)-C(42)	1.336(9)	1.368(10)
C(42)-C(43)	1.343(11)	1.302(12)
O(3)-C(3)-C(4)	125.3(6)	128.1(7)
O(3)-C(3)-C(7)	129.9(6)	127.2(7)
C(7)-C(3)-C(4)	104.7(6)	104.3(6)
C(3)-C(4)-C(5)	107.9(6)	108.5(6)
C(4)-C(5)-C(6)	107.9(6)	108.0(6)
C(5)-C(6)-C(7)	108.8(6)	107.9(6)
C(6)-C(7)-C(3)	107.8(6)	109.3(6)
N(1)-C(41)-N(2)	110.9(8)	110.1(6)
C(41)-N(2)-C(42)	106.9(8)	107.4(7)
C(41)-N(1)-C(43)	107.0(8)	106.2(7)
N(2)-C(42)-C(43)	108.4(9)	107.2(8)
N(1)-C(43)-C(42)	106.7(8)	109.1(8)

It has to be underline that complex **21a,** treated with Ag_2O in CH_2Cl_2 solution converts to **4a** by transmetallation, and that precipitation of AgI is observed, as expected. Thus, the present method represents another route to easily obtain complexes of type **4**.

6.2 Catalytic transfer hydrogenation

The ruthenium ionic complexes **21a[I]** and **21a[CF₃SO₃]** have been evaluated as catalyst precursors using ionic liquid as reaction solvent under transfer hydrogenation conditions (*i.e.* employing ¹PrOH as hydrogen source and 4-fluoroacetophenone as model substrate). The crude at the end of the reaction has been cooled and then the product extracted with diethyl ether and analyzed by GC. Preliminary catalytic runs were performed in order to investigate the catalytic activity of these kind of ionic complexes in non-conventional media, the results and the comparison between the ruthenium(0) complex **4a** with the corresponding ruthenium(0) anionic complex **21a** in ionic liquid [BMIM][PF₆] are reported in Table 6.2.

Table 6.2. Catalytic transfer hydrogenation of 4-fluoroacetophenone.[a]
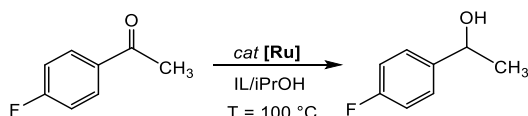
entry	**[Ru]**	solvent (ILs)	conversion 8h (%)	conversion 24h (%)
1	**21a[I]**	[BMIM][PF₆]	69	75
2	**21a[CF₃SO₃]**	[BMIM][PF₆]	63	72
3	**4a**	[BMIM][PF₆]	0	0
4	**21a[I]**	[BMIM][BF₄]	24	24
5	**21a[CF₃SO₃]**	[BMIM][BF₄]	54	57

[a]General conditions: Ruthenium complex (5 mol% Ru), ionic liquid (2 mL), *i*PrOH (2 mL), T = 100°C; conversions determined by ¹⁹F NMR spectroscopy.

The neutral complex **4a** did not present any catalytic activity in the absence of additives even in ionic liquid media (entry 3) as already stated in the case of organic solvent. By contrast, the ionic complexes **21a** show a good catalytic activity without any use of additive. This behavior can be easily explained by the fact that the neutral complexes (**4**) need the release of a CO ligand to be activated (more details in Chapter IV paragraph 4.3); conversely, in the ionic complexes (**21**) the hypothetic de-coordination of iodide or CF₃SO₃⁻ , as imidazolium counterion, would lead to the formation of the 16 electron counting active species ruthenium fragment able to perform the hydrogen transfer from iPrOH to the substrate 4-fluoroacethophenone.
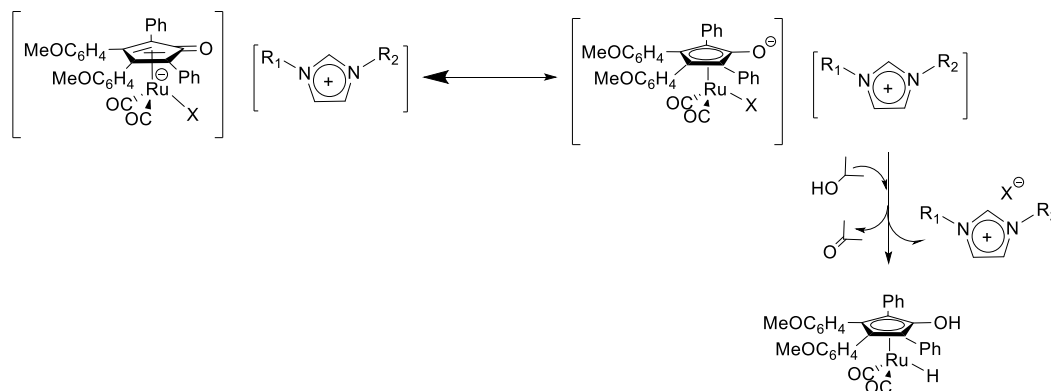
Schema 6.3 Proposed activation of ionic complexes **21**.

Therefore, the catalytic mechanism is similar to that of the Shvo catalyst (see Chapter I paragraph 2.2.2) with the advantage of a possible recover and reuse of the catalyst immobilized in the ionic liquid phase.

The catalytic activity of the ionic complexes **21a[I]** and **21a[CF₃SO₃]**, containing different imidazolium counterions, have been found to be similar, (entries 1, 2), suggesting that there is no influence of the coordination ability of the counterion in the pre-catalyst activation.

The study of the role of different imidazolium salts in the activation of **21**, such as the influence of a pyridine or an -OH substituent on the side chain of the heterocycle, are still under investigation. Further studies will also affect the choice of the hydrogen donor in order to optimized the reaction conditions. In fact, an excess of 2-propanol (2 mL) has been required in these tests due to the fact that the operational temperature is higher than its boiling point. With the aim to understand the role of the ionic liquid, some catalytic runs have been carried out employing [BMIM][BF₄] as reaction solvent, under the same hydrogen transfer conditions. In these cases, a lower conversion is observed compared to the congener [BMIM][PF₆] (24% vs. 69% in 8h; entries 5, 4 respectively). This is probably due to the physical properties of the ILs that depend on the nature of both cation and anion;[3] in this case the different anions can affect some physical properties such as viscosity, density, and solubility that, subsequently, influence the catalytic activity of the complexes. A screening of different ILs as reaction solvent is still under investigation.

6.3 Catalytic dehydrogenation

In addition to transfer hydrogenation, we were also interested to see whether complexes **21** are active in alcohol dehydrogenation in ionic liquid media. The ionic complexes **21** have been employed as catalyst precursors for the oxidation benzyl alcohol (BnOH), as model substrate.

Table 6.3. Catalytic oxidation of benzyl alcohol to benzaldehyde.[a]
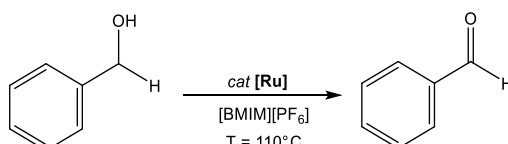
entry	**[Ru]**	solvent	additive	conversion 8h (%)	conversion 24h (%)
1	**21a[I]**	[BMIM][PF₆]	---	36	>99
2	**21a[CF₃SO₃]**	[BMIM][PF₆]	---	35	>99[b]
3	**21d**	[BMIM][PF₆]	---	57	60
4	**21m**	[BMIM][PF₆]	---	>99[c]	---
5	**21a[CF₃SO₃]**	toluene	Benzoquinone[d]	56	>99

[a]General conditions: Ruthenium complex (5 mol% Ru), solvent (2 mL), T = 110°C; conversions determined by GC; [b]recycling test; [c]after 8h the conversion was complete then at 24h of reaction only the presence of a not identified by-product was detected; [d]2 equivalents of benzoquinone per ruthenium center

As for the hydrogen transfer, the complexes **21a[I]** and **21a[CF₃SO₃]** show a similar catalytic activity leading to an almost complete conversion in 24h, while the complex **21d**, having a OH group on the side chain of the imidazole, leads to lower conversion. This result is consistent with what found for the corresponding NHC complex **12d[CF₃SO₃]** probably due to intramolecular dehydrogenation, causing the formation of inactive species. This hypothesis has been described in Chapter IV (paragraph 4.3). The pyridine-functionalized ionic

complex **21m** exhibits the faster activation, in fact, a complete conversion was observed within 8h, however after 24h any traces of the benzaldehyde as detected but only the presence of a not identified by product was observed.

Aimed at comparing the catalytic activity of the complexes **21** in non-conventional solvent (ILs) and in traditional organic solvent, a catalytic test has been performed with **21a[CF₃SO₃]** using toluene as solvent and in the presence of a hydrogen acceptor such as benzoquinone (the same reaction conditions that have been employed for the ruthenium NHC complexes of type **12**, see Chapter V paragraph 5.4). In the case of ion pair, the BQ additive do not accelerate the induction time of the catalytic reaction, leading to the same result as that obtained in ionic liquid without additive. Infact, also in this conditions a complete conversion of the substrate was reached within 24h.

As mentioned in the Introduction, the major advantage of the use of the ionic liquids as reaction solvents is the efficient immobilization of the catalyst in the ionic liquid phase, which means that, after product extraction, the reaction medium and the catalyst can be reused several times. A recycling test has been performed with **21a[CF₃SO₃]**, after the extraction with Et₂O (3x5mL) the mixture (IL with the catalyst inside) was dried under vacuum in order to remove all the volatiles, then, the benzyl alcohol was added to the recycled system and heated at 110°C. After only 2h, complete conversion of the substrate was observed.

Further investigations on the catalytic activity and mechanism of these complexes are being carried out.

Conclusion

The direct and straightforward reaction of the dinuclear ruthenium complex dicarbonyl(η^4-3,4-bis(4-methoxyphenyl)-2,5-diphenylcyclopenta-2,4-dienone (**3**) with a series of variously functionalized imidazolium salts afforded a novel class of anionic ruthenium cyclopentadienone complexes ionic paired with imidazolium salts as counterions. The reaction is clean, general and quantitative and the complexes are stable to air and moisture both in the solid state and in solution. All the complexes obtained have been characterized by means of IR, NMR and ESI-MS techniques and, when possible, with X-ray diffraction studies. The peculiar structure of the novel complexes made them good candidates for redox catalysis in reaction such as hydrogen transfer and dehydrogenation. Indeed, preliminary results demonstrated their activity in such reactions. Moreover, exploiting their affinity for ionic liquids, bifunctional catalysis has been transferred in ILs, such as [BMIM][PF₆], with very promising results. The catalysts are fairly active in hydrogen transfer, although the high temperature and the induction time required, make them still far from being competitive with best ruthenium catalysts available in the literature. Anyway, the use of ionic liquid gives a greener character to the reaction. On the contrary, good preliminary results have been obtained in oxidation reactions, such as the dehydrogenation of benzyl alcohol to aldehyde. Indeed, in this particular reaction the best results is provided by catalyst **21a[CF₃SO₃]** which gives complete conversion of the alcohol in 24h. Furthermore, initial results obtained by recycling this catalyst are very promising and demonstrate that, once activated, the catalyst remains active and protected by the ionic liquid environment until the introduction of a further portion of substrate. Studies on complexes of type **21**, depicted in the present chapter are ongoing and will be further developed in the near future in order to shed more light on both the catalytic activity and recyclability of the ionic pairs in ionic liquid and on the corresponding mechanism. The synthetic methods here discussed represent a novelty within the field of IL-supportation and might be exploited also for the heterogenization of the catalysts using, for example, SILP technology.

Experimental Section

Materials and procedures. Solvents: dichloromethane (CH_2Cl_2), tetrahydrofuran (THF), diethyl ether (Et_2O), petroleum ether referring to a fraction of bp 60-80 °C, acetonitrile (CH_3CN) were dried and distilled prior to use. Acetone has been degassed and stored under inert atmosphere on molecular sieves. Other solvents such as ethylacetate (EtOAc), chloroform, ethanol (EtOH), methanol (MeOH), heptane, toluene, $CDCl_3$, D_2O, CD_3CN (Sigma Aldrich) have been employed without further purification. Reagents: triruthenium-dodecacarbonil ($Ru_3(CO)_{12}$) (Strem), methyl iodide, methyl bromide, bromidric and chloridric acid, silver oxide, 1-methylimidazole, 1,3 diphenylacetone, benzyl bromide, benzyl chloride, paraformaldehyde, *tert*-butylamine, 2,6-dimethylaniline, 2,6-diisopropylaniline, glyoxal, acetic acid, 2,4,6-trimethylaniline, (Sigma Aldrich), 4,4'dimethoxybenzil (Alfa Aesar) have been employed as purchased.

1,3-dimethylimidazolium iodide (**1a[I]**),[17] 1,3-dimethylimidazolium trifluoromethanesulfonate (**1a[OTf]**), 1,3-dimethylimidazolium hexafluorophosphate (**1a[PF6]**), 1,3-dibenzylimidazolium bromide (**1b[Br]**), 1,3-dibenzylimidazolium chloride (**1b[Cl]**),[18] 1-methyl-3-butyl-imidazolium chloride (**1c**), 1-methyl-3-(2-hydroxyethyl)imidazolium chloride (**1d**),[19] N,N'-bis(2,6-diisopropylphenyl)-1,4-diaza-1,3-butadiene, 1,3-bis(2,6-diisopropylphenyl)imidazolium chloride (**1f[Cl]**), 1,3-bis(2,6-diisopropylphenyl)imidazolium bromide (**1f[Br]**),[20] 1,3-di-*tert*-butylimidazolium chloride (**1g**),[21] 1-butyl-3-(2-pyridinyl)-imidazolium bromide (**1m**)[22],3,4-Bis(4-methoxyphenyl)-2,5-diphenylcyclopenta-2,4-dienone,[23] dicarbonyl(η^4-3,4-bis(4-methoxyphenyl)-2,5-diphenylcyclopenta-2,4-dienone) ruthenium dimer (**3**),[24] have been prepared as previously reported.

The prepared derivatives were characterized by spectroscopic methods. The NMR spectra were recorded using Varian Inova 300 (^{1}H, 300.1; ^{13}C, 75.5 MHz), Varian Mercury Plus VX 400 (^{1}H, 399.9; ^{13}C, 100.6 MHz), Varian Inova 600 (^{1}H, 599.7; ^{13}C, 150.8 MHz) spectrometers at 298 K; chemical shifts were referenced internally to residual solvent peaks. Full ^{1}H- and ^{13}C-NMR assignments were done, when necessary, by gHSQC and gHMBC NMR experiments using standard Varian pulse sequences. Infrared spectra were recorded at 298 K on a Perkin-Elmer Spectrum 2000 FT-IR spectrophotometer. ESI-MS spectra were recorded on Waters Micromass ZQ 4000 with samples dissolved in MeOH or CH_3CN. Elemental analyses were performed on a Thermo-Quest Flash 1112 Series EA instrument.

Synthesis of [dicarbonyl-η^4-3,4-bis(4-methoxyphenyl)-2,5-diphenylcyclopenta-2,4-dienone)halogenide][1R$_1$-3R$_2$ imidazolium] ruthenium complexes (21)

21a[X] $R_1 = R_2 = CH_3$; X = I, OTf
21b $R_1 = Bz$, $R_2 = Bz$; X = Br
21c $R_1 = Me$, $R_2 = Bu$; X = Cl
21d $R_1 = Me$, $R_2 = CH_2CH_2OH$; X = Cl
21f $R_1 = 2,5-C_6H_3(^iPr)_2$, $R_2 = 2,5-C_6H_3(^iPr)_2$; X = Cl
21g $R_1 = {}^tBu$, $R_2 = {}^tBu$; X = Cl
21m $R_1 = pyr$, $R_2 = Bu$; X = Cl

Figure 6.7. Structure of the ionic pair **21a-m**.

Imidazolium salts (**1**), were reacted with dicarbonyl(η^4-3,4-bis(4-methoxyphenyl)-2,5-diphenylcyclopenta-2,4-dienone) ruthenium dimer (**3**) (0.5 eq. vs. imidazolium salts). The reaction mixture was stirred until the end of the reaction at room temperature. Upon removal of the solvent the quantitative formation of the [dicarbonyl-η^4-3,4-bis(4-methoxyphenyl)-2,5-diphenylcyclopenta-2,4-dienone)halogenide][1R$_1$-3R$_2$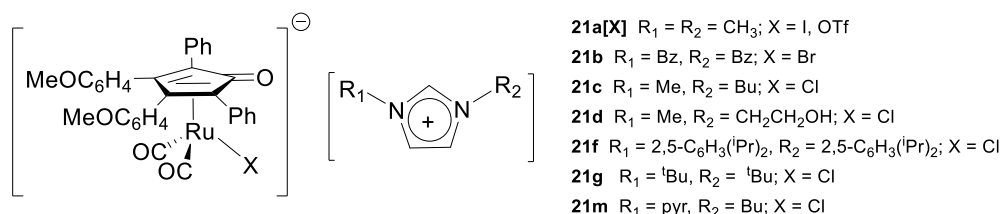 imidazolium] ruthenium complexes (**21**) were verified by ^{1}H-NMR, ^{13}C-NMR, ESI-MS and X-Ray crystal structure when suitable crystals were available.

[dicarbonyl(η^4-3,4-bis(4-methoxyphenyl)-2,5-diphenylcyclopenta-2,4-dienone)(iodine)ruthenium][1,3-dimethylimidazolium] (21a[I]): 1,3-dimethylimidazolium iodide (**1a**) 0.011 g (0.0499 mmol), **3** 0.030 g (0.0249 mmol), CH$_2$Cl$_2$, room temperature, 1h. The beige solid obtained was identified as **21a[I]**. Complex **21a[I]** is stable to air, moisture, in solution of organic solvents and in the presence of water. Suitable crystals for X-Ray diffraction has been obtained by toluene/hexane double layer. **21a[I]** has been analyzed by IR, ^{1}H-NMR, ^{13}C-NMR, ESI-MS and X-Ray diffraction. ^{1}H-NMR (599.7 MHz, CDCl$_3$): δ 9.91 (s, NCHN), 7.58-6.55 (m, 18H, CH$_{aryl}$), 7.07 (s, 2H, CH$_{im}$), 3.75 (s, 6H, NCH$_3$), 3.70 (s, 6H, -OCH$_3$). ^{13}C-NMR (150.8 MHz, CDCl$_3$, g-HSQC, g-HMBC, DEPT): δ 201.00 (CO), 172.12 (C=O, Cp), 158.40 (-COCH$_3$), 138.96 (NCHN), 135.21-112.66 (C$_{aryl}$), 122.55 (CH$_{im}$), 100.09 (C$_{2,5}$, Cp), 81.40 (C$_{3,4}$, Cp), 55.01 (-OCH$_3$), 36.55 (NCH$_3$). IR (CH$_2$Cl$_2$, cm^{-1}): 2004, 1944 (v_{CO}); 1580 ($v_{C=O}$), 1604, 1518 ($v_{C=C}$). ESI-MS (m/z) (+): 97 [M]$^+$; (-): 729 [M]$^-$. Anal. Calcd (%) for C$_{38}$H$_{33}$IN$_2$O$_5$Ru: C, 55.28; H, 4.03; N, 3.39. Found: C, 55.26; H, 4.00; N, 3.41.

[dicarbonyl(η^4-3,4-bis(4-methoxyphenyl)-2,5-diphenylcyclopenta-2,4-dienone)(trifluoromethanesulfonate)ruthenium][1,3-dimethylimidazolium] (21a[OTf]): 1,3-dimethylimidazolium trifluoromethanesulfonate (**1a[OTf]**) 0.012 g (0.0499 mmol), **2** 0.030 g (0.0249 mmol), CH$_2$Cl$_2$, room temperature, 2h. The beige solid obtained was identified as **21a[OTf]**. Complex **21a[OTf]** is stable to air, moisture, in solution of organic solvents and in the presence of water. **21a[OTf]** has been analyzed by IR, ^{1}H-NMR, ^{13}C-NMR, ^{19}F-NMR, ESI-MS. ^{1}H-NMR (599.7 MHz, CDCl$_3$): δ 9.71 (s, NCHN), 7.85-6.55 (m, 18H, CH$_{aryl}$), 7.19 (s, 2H, CH$_{im}$), 3.80 (s, 6H, NCH$_3$), 3.70 (s, 6H, -OCH$_3$). ^{13}C-NMR (150.8 MHz, CDCl$_3$): δ 201.09 (CO), 172.13 (C=O, Cp), 158.38 (-COCH$_3$), 138.24 (NCHN), 135.20-112.64 (C$_{aryl}$), 122.85 (CH$_{im}$), 100.24 (C$_{2,5}$, Cp), 81.34 (C$_{3,4}$, Cp), 54.99 (-OCH$_3$), 36.62 (NCH$_3$). ^{19}F-NMR (282.4 MHz, CDCl$_3$): δ -78.61 (s, 3F). IR (CH$_2$Cl$_2$, cm^{-1}): 2004, 1944 (v_{CO}); 1579 ($v_{C=O}$), 1604, 1518 ($v_{C=C}$). ESI-MS (m/z) (+): 97 [M]$^+$; (-): 751 [M]$^-$. Anal. Calcd (%) for C$_{39}$H$_{33}$F$_3$N$_2$O$_8$RuS: C, 55.25; H, 3.92; N, 3.30. Found: C, 55.21; H, 3.89; N, 3.31.

[dicarbonyl(η^4-3,4-bis(4-methoxyphenyl)-2,5-diphenylcyclopenta-2,4-dienone)(bromine)ruthenium][1,3-dibenzylimidazolium] (21b): 1,3-dibenzylimidazolium bromide (**1b**) 0.011 g (0.0332 mmol), **3** 0.020 g (0.0166 mmol), CH$_2$Cl$_2$, room temperature, 30 min. The beige solid obtained was identified as **21b**. Complex **21b** is stable to air, moisture, in solution of organic solvents and in the presence of water. **21b** has been analyzed by IR, ^{1}H-NMR, ^{13}C-NMR, ESI-MS. ^{1}H-NMR (599.7 MHz, CDCl$_3$): δ 10.66 (s, NC*H*N), 7.66-6.54 (m, 20H, CH$_{aryl}$, CH$_{im}$), 5.08 (s, 4H, CH$_2$Ph), 3.70 (s, 6H, -OCH$_3$). ^{13}C-NMR (150.8 MHz, CDCl$_3$): δ 200.85 (CO), 171.34 (C=O, Cp), 158.42 (-COCH$_3$), 138.96 (NCHN), 136.13-112.67 (C$_{aryl}$, CH$_{im}$), 99.47 (C$_{2,5}$, Cp), 81.98 (C$_{3,4}$, Cp), 55.01 (-OCH$_3$), 53.26 (CH$_2$Ph). IR (CH$_2$Cl$_2$, cm^{-1}): 2006, 1945 (v_{CO}); 1580 ($v_{C=O}$), 1605, 1517 ($v_{C=C}$). ESI-MS (m/z) (+): 249 [M]$^+$; (-): 683 [M]$^-$. Anal. Calcd (%) for C$_{50}$H$_{41}$BrN$_2$O$_5$Ru: C, 64.52; H, 4.44; N, 3.00. Found: C, 64.55; H, 4.42; N, 2.99.

[dicarbonyl(η^4-3,4-bis(4-methoxyphenyl)-2,5-diphenylcyclopenta-2,4-dienone)(bromine)ruthenium][1-methyl-3-butyl-imidazolium] (21c): 1-methyl-3-butylimidazolium bromide (**1c**) 0.005 g (0.0332 mmol), **3** 0.020 g (0.0166 mmol), CH$_2$Cl$_2$, room temperature, 30 min. The beige solid obtained was identified as **21c**. Complex **21c** is stable to air, moisture, in solution of organic solvents and in the presence of water. **21c** has been analyzed by IR, ^{1}H-NMR, ^{13}C-NMR, ESI-MS. ^{1}H-NMR (599.7 MHz, CDCl$_3$): δ 8.46 (s, NC*H*N), 7.55-6.59 (CH$_{aryl}$, CH$_{im}$), 4.10 (t, 2H, NCH$_2$), 3.78 (s, 3H, -NCH$_3$), 3.67 (s, 6H, -OCH$_3$), 1.77, 1.32 (m, 2H, -CH$_2$CH$_2$-), 0.93 (t, 3H, -CH$_3$). ^{13}C-NMR (150.8 MHz, CDCl$_3$): δ 200.97 (CO), 171.55 (C=O, Cp), 158.38 (-COCH$_3$), 135.21 (NCHN), 133.19-112.64 (C$_{aryl}$, CH$_{im}$), 99.64 (C$_{2,5}$, Cp), 81.66 (C$_{3,4}$, Cp), 55.00 (-OCH$_3$), 48.88 (-NCH$_2$), 36.02

(-NCH$_3$), 31.90, 19.42 (-CH$_2$CH$_2$-), 13.45 (-CH$_3$). IR (CH$_2$Cl$_2$, cm^{-1}): 2005, 1944 (ν_{CO}); 1581 ($\nu_{C=O}$), 1605, 1517 ($\nu_{C=C}$). ESI-MS (m/z) (+): 139 [M]$^+$; (-): 683 [M]$^-$. Anal. Calcd (%) for C$_{41}$H$_{39}$BrN$_2$O$_5$Ru: C, 59.91; H, 4.77; N, 3.40. Found: C, 59.94; H, 4.80; N, 3.40.

[dicarbonyl(η^4-3,4-bis(4-methoxyphenyl)-2,5-diphenylcyclopenta-2,4-dienone)(chloro)ruthenium][3-(2-hydroxyethyl)-1-methyl-imidazolium] (21d): 3-(2-hydroxyethyl)-1-methyl-imidazolium (**1d**) 0,03 g (0,17 mmol), **3** 0,10 g (0,08 mmol), CH$_2$Cl$_2$, room temperature, 1h. The beige solid obtained was identified as **21d**. Complex **21d** is stable to air, moisture, in solution of organic solvents and in the presence of water. **21d** has been analyzed by IR, ^{1}H-NMR, ^{13}C-NMR, ESI-MS. ^{1}H-NMR (599.7 MHz, CDCl$_3$): δ 9.40 (s, NCHN), 7.57-6.54 (C$_{aryl}$), 6.97 (s, 2H, CH$_{Im}$), 6.82 (s, 2H, CH$_{Im}$), 4.06 (br, H, OH), 3.99 (m, 2H,-NCH$_2$-), 3.69 (s, 6H, -OCH$_3$), 3.47 (m, 2H, -CH$_2$OH), 3.44 (s, 3H, -NCH$_3$). ^{13}C-NMR (150.8 MHz, CDCl$_3$): δ 200.97 (CO), 169.79 (C=O, Cp), 158.44 (-COCH$_3$), 138.48 (-NCHN-), 134.52-112.65 (C$_{aryl}$), 125.97 (CH$_{Im}$), 121.96 (CH$_{Im}$), 99.64 (C$_{2,5}$, Cp), 82.47 (C$_{3,4}$, Cp), 59.69 (-CH$_2$-), 54.93 (-OCH$_3$), 51.50 (-CH$_2$-), 35.70 (NCH$_3$). IR (CH$_2$Cl$_2$, cm^{-1}): 2009, 1948 (ν_{CO}), 1566 cm^{-1} ($\nu_{C=O}$), 1605, 1518 ($\nu_{C=C}$). ESI-MS (m/z) (+): 127 [M]$^+$; (-): 638 [M]$^-$. Anal. Calcd (%) for Anal. Calcd (%) for C$_{39}$H$_{35}$ClN$_2$O$_6$Ru: C, 61.23; H, 4.60; N, 3.66. Found: C, 61.24; H, 4.58; N, 3.67.

[dicarbonyl(η^4-3,4-bis(4-methoxyphenyl)-2,5-diphenylcyclopenta-2,4-dienone)(chloro)ruthenium][1,3-bis(2,6-diisopropylphenyl)imidazolium] (21f): 1,3-bis(2,6-diisopropylphenyl)imidazolium chloride (**1f**) 0.013 g (0.0332 mmol), **3** 0.020 g (0.0166 mmol), CH$_2$Cl$_2$, room temperature, 1h. The beige solid obtained was identified as **21f**. Complex **21f** is stable to air, moisture, in solution of organic solvents and in the presence of water. **21f** has been analyzed by IR, ^{1}H-NMR, ^{13}C-NMR, ESI-MS. ^{1}H-NMR (599.7 MHz, CDCl$_3$): δ 8.54 (s, NCHN), 7.98 (s, 2H, CH$_{Im}$), 7.57-6.51 (CH$_{aryl}$), 3.67 (s, 6H, -OCH$_3$), 2.41 (sept., J = 6.8 Hz, 4H, CH$_{iPr}$), 1.28 (d, J = 6.8 Hz, 12H, CH$_{3iPr}$), 1.14 (d, J = 6.8 Hz, 12H, CH$_{3iPr}$). ^{13}C-NMR (150.8 MHz, CDCl$_3$): δ 201.76 (CO), 170.80 (C=O, Cp), 158.15 (-COCH$_3$), 135.13 (NCHN), 145.15-112.49 (C$_{aryl}$), 128.30 (CH$_{im}$), 100.01 (C$_{2,5}$, Cp), 88.56 (C$_{3,4}$, Cp), 54.94 (-OCH$_3$), 28.84 (CH$_{iPr}$), 24.72 (CH$_{3iPr}$), 23.77 (CH$_{3iPr}$). IR (CH$_2$Cl$_2$, cm^{-1}): 2000, 1937 (ν_{CO}); 1591 ($\nu_{C=O}$), 1607, 1517 ($\nu_{C=C}$). ESI-MS (m/z) (+): 389 [ImIPr]$^+$; 602 {[Ru(CO)$_2$CpO] + Na$^+$}. Anal. Calcd (%) for C$_{60}$H$_{61}$ClN$_2$O$_5$Ru: C, 70.19; H, 5.99; N, 2.75. Found: C, 70.21; H, 6.01; N, 2.77.

[dicarbonyl(η^4-3,4-bis(4-methoxyphenyl)-2,5-diphenylcyclopenta-2,4-dienone)(chloro)ruthenium][1,3-bis(2,6-diisopropylphenyl)imidazolium] (21g): 1,3-di-*tert*-butylimidazolium chloride (**1g**) 0.010 g (0.0499 mmol), **3** 0.030 g (0.0249 mmol), CH$_2$Cl$_2$, room temperature, 1h. The beige solid obtained was identified as **21g**. Complex **21g** is stable to air, moisture, in solution of organic solvents and in the presence of water. Suitable crystals for X-Ray diffraction has been obtained by CDCl$_3$/petroleum ether double layer. **21g** has been analyzed by IR, ^{1}H-NMR, ^{13}C-NMR, ESI-MS and X-Ray diffraction. ^{1}H-NMR (599.7 MHz, CDCl$_3$): δ 9.81 (s, NCHN), 7.62-6.52 (C$_{aryl}$), 7.36 (s, 2H, CH$_{Im}$), 3.68 (s, 6H, -OCH$_3$), 1.59 (s, 18H, CH$_{3tBu}$). ^{13}C-NMR (150.8 MHz, CDCl$_3$): δ 201.76 (CO), 171.10 (C=O, Cp), 158.16 (-COCH$_3$), 134.16 (NCHN), 135.32-112.45 (C$_{aryl}$), 119.50 (CH$_{im}$), 100.20 (C$_{2,5}$, Cp), 82.47 (C$_{3,4}$, Cp), 60.50 (Cq$_{tBu}$), 54.91 (-OCH$_3$), 30.01 (CH$_{3tBu}$). IR (CH$_2$Cl$_2$, cm^{-1}): 2001, 1938 (ν_{CO}); 1578 ($\nu_{C=O}$), 1607, 1518 ($\nu_{C=C}$). ESI-MS (m/z) (+): 180 [M]$^+$; (-): 638 [M]$^-$. Anal. Calcd (%) for C$_{44}$H$_{45}$ClN$_2$O$_5$Ru: C, 70.19; H, 5.99; N, 3.42. Found: C, 70.21; H, 6.01; N, 3.44.

[dicarbonyl(η^4-3,4-bis(4-methoxyphenyl)-2,5-diphenylcyclopenta-2,4-dienone)(chloro)ruthenium][1-(butyl-3-(2-pyridinyl)-imidazolium] (21m): 1-(butyl-3-(2-pyridinyl)-imidazolium (**1m**) 0,034 g (0,17 mmol), **3** 0,10 g (0,08 mmol), CH$_2$Cl$_2$, room temperature, 1h. The beige solid obtained was identified as **21m**. Complex **21m** is stable to air, moisture, in solution of organic solvents and in the presence of water. **21m** has been

analyzed by IR, ^{1}H-NMR, ^{13}C-NMR, ESI-MS. ^{1}H-NMR (599.7 MHz, CDCl$_3$): δ 10.85 (s, NC*H*N), 8.36 (dd, 1H, CH$_{py}$), 8.19 (1H, CH$_{py}$), 8.01 (1H, CH$_{py}$), 7.60-6.55 (CH$_{aryl}$, CH$_{im}$), 3.77 (t, 2H, NCH$_2$), 3.70 (s, 6H, -OCH$_3$), 1.60, 1.14 (m, 2H, -CH$_2$CH$_2$-), 0.86 (t, 3H, -CH$_3$). ^{13}C-NMR (150.8 MHz, CDCl$_3$): δ 200.93 (CO), 171.01 (C=O, Cp), 158.39 (-*C*OCH$_3$), 147.95-112.63 (C$_{aryl,py}$), 137.76 (-NCHN-), 124.54 (CH$_{im}$), 120.07 (CH$_{im}$), 99.92 (C$_{2,5}$, Cp), 82.36 (C$_{3,4}$, Cp), 55.00 (–OCH$_3$), 49.54 (NCH$_2$), 31.48, 19.36 (–CH$_2$CH$_2$), 13.56 (–CH$_3$). IR (CH$_2$Cl$_2$, cm^{-1}): 2006, 1945 (ν$_{CO}$), 1577 cm^{-1} (ν$_{C=O}$), 1602, 1518 (ν$_{C=C}$). ESI-MS (m/z) (+): 202 [M]$^+$; (-):683 [M]$^-$. Anal. Calcd (%) for Anal. Calcd (%) for C$_{45}$H$_{40}$BrN$_3$O$_5$Ru: C, 50.85; H, 4.52; N, 4.75. Found: C, 50.92; H, 4.56; N, 4.73.

General method for hydrogenation

Ruthenium ionic complex (15 µmol, 5% mol) was dissolved in a mixture of ionic liquid (Bmim[PF$_6$] or Bmim[BF$_4$], 2 mL) and *i*PrOH (2 mL) in a10mL two neck-flask and stirred at 100°C for 10 min. Then 4-fluoroacetophenone (36 µL, 300 µmol) was added and samples were taken at regular intervals. Aliquots (ca. 0.05mL) were diluted with CDCl$_3$ (0.5 mL) and conversions were determined by ^{19}F-NMR spectroscopy and GC analysis.

General method for dehydrogenation

Ruthenium ionic complex (5%mol, 9.5 µmol) was dissolved in 2mL of the ionic liquid Bmim[PF$_6$]. Once reached the reaction temperature (110°C) 19.7 µL of benzyl alcohol (190 µmol) were added. Samples were taken at regular intervals and conversions were determined by GC.

X-Ray diffraction studies

Crystal data and collection details for **21a[I]** and **21f·0.5CH$_2$Cl$_2$** are reported in Table 6.4. The diffraction experiments were carried out on a Bruker APEX II diffractometer equipped with a CCD detector using Mo–Kα radiation. Data were corrected for Lorentz polarization and absorption effects (empirical absorption correction SADABS).[25] Structures were solved by direct methods and refined by full-matrix least-squares based on all data using F^2.[26] All hydrogen atoms were fixed at calculated positions and refined by a riding model. All non-hydrogen atoms were refined with anisotropic displacement parameters.

21a[I]: The asymmetric unit of the unit cell contains one anion and one cation (located on general positions). Similar *U* restraints (SIMU command in SHELXL; s.u. 0.01) have been applied to the C atoms.

21f·0.5CH$_2$Cl$_2$: The asymmetric unit of the unit cell contains one anion and one cation (located on general positions), as well as half of a CH$_2$Cl$_2$ molecule disordered over four positions two by two related by a 2-fold axis. The CH$_2$Cl$_2$ molecule has been refined isotropically. One Ph and one p-MeO-C$_6$H$_4$ group in the anion and one ^{t}Bu substituent in the cation are disordered. Disordered groups have been split into two positions and refined using one occupancy factor per disordered group. Similar *U* restraints (SIMU command in SHELXL; s.u. 0.005) have been applied to C and O atoms. Some of the C and O atoms of the disordered groups have been restrained to isotropic behaviour (ISOR command in SHELXL, s.u. 0.005). The disordered aromatic rings have been constrained to fit regular hexagons (AFIX 66 command in SHELXL). Restraints to bond distances were applied as follow (s.u. 0.01): 1.75 Å for C–Cl in CH$_2$Cl$_2$.

Table 6.4 Crystal data and experimental details for **21a[I]** and **21f·0.5CH₂Cl₂**.

	21a[I]	**21f·0.5CH₂Cl₂**
Formula	$C_{38}H_{33}IN_2O_5Ru$	$C_{44.5}H_{46}Cl_2N_2O_5Ru$
Fw	825.63	860.80
T, K	298(2)	293(2)
λ, Å	0.71073	0.71073
Crystal system	Triclinic	Monoclinic
Space group	$P\bar{1}$	*C2/c*
a, Å	10.0781(13)	40.674(11)
b, Å	10.2434(13)	10.346(3)
c, Å	17.587(2)	24.634(7)
α, °	79.250(2)	90
β, °	86.754(2)	122.090(3)
γ, °	74.504(2)	90
Cell Volume, Å³	1718.8(4)	8782(4)
Z	2	8
D_c, g cm⁻³	1.595	1.302
μ, mm⁻¹	1.400	0.523
F(000)	824	3560
Crystal size, mm	0.16×0.13×0.11	0.18×0.16×0.14
θ limits, °	2.10–25.02	1.66–26.00
Reflections collected	16644	43695
Independent reflections	6053 [R_{int}= 0.0954]	8633 [R_{int}= 0.1049]
Data / restraints /parameters	6053 / 210 / 424	8633/ 707 / 633
Goodness on fit on F^2	0.939	1.017
R_1 (*I*> 2σ(*I*))	0.0519	0.0763
wR_2 (all data)	0.0943	0.2420
Largest diff. peak and hole, e Å⁻³	0.463 / –0.419	1.266 / –0.641

References

[1] P. Wasserscheid, W. Keim, *Angew. Chem. Int. Ed.* **2000**, *39*, 3772–3789.

[2] N. Gunasekaran *Adv. Synth. Catal.* **2015**, *357*, 1990 – 2010.

[3] For recent reviews in catalysis in ionic liquids: a) V. I. Parvulescu, C. Hardacre, *Chem. Rev.* **2007**, *107*, 2615–2665; b) D. Betz, P. Altmann, M. Cokoja, W. A. Herrmann, F. E. Kuhn *Coord. Chem. Rev.*, **2011**, *255*, 1518–1540; c) C. D. Hubbard, P. Illner and R. van Eldik *Chem. Soc. Rev.*, **2011**, *40*, 272–290; d) H. Olivier-Bourbigou, L. Magna, D. Morvan *Applied Catal. A: General*, **2010**, *373*, 1–56; f) Q. Zhang, S. Zhang and Y. Deng *Green Chem.*, **2011**, *13*, 2619–2637.

[4] See for example: (a) T. J. Geldbach and P. J. Dyson, *J. Am. Chem. Soc.*, **2004**, *126*, 8114–8115; (b) I. Kawasaki, K. Tsunoda, T. Tsuji, T. Yamaguchi, H. Shibuta, N. Uchida, M. Yamashita and S. Ohta, *Chem. Commun.*, **2005**, 2134–2136; (c) J. Wang, J. Feng, R. Qin, H. Fu, M. Yuan, H. Chen and X. Li, *Tetrahedron: Asymmetry*, **2007**, *18*, 1643–1647; (d) H. L. Ngo, A. Hu and W. Lin, *Chem. Commun.*, **2003**, 1912–1913.

[5] a) T. Pasini, G. Solinas, V. Zanotti, S. Albonetti, F. Cavani, A. Vaccari, A. Mazzanti, S. Ranieri, R. Mazzoni, *Dalton Trans.* **2014**, *43, 10224-10234; b)* R. J. van Putten, J. C. van der Waal, E. de Jong, C. B. Rasrendra, H. J. Heeres and J. G. de Vries, *Chem. Rev.*, **2013**, *113*, 1499; c) K. L. Luska, P. Migowski and W. Leitner *Green Chem.*, **2015**, *17*, 3195–3206; d) R. A. Sheldon *Green Chem.*, **2014**, *16*, 950–963.

[6] C. Cesari, S. Conti, S. Zacchini, V. Zanotti, M. C. Cassani and R. Mazzoni, *Dalton Trans.*, **2014**, *43*, 17240.

[7] (a) C. Cesari, R. Mazzoni, H. Muller-Bunz and M. Albrecht, *J. Organomet. Chem.*, **2015**, *793*, 256; (b) C. Cesari, A. Cingolani, C. Parise, S. Zacchini, V. Zanotti, M. C. Cassani and R. Mazzoni, *RSC Adv.*, **2015**, *5*, 94707.

[8] H. Ohara, W. W. N. O, A. J. Lough and R. H. Morris, *Dalton Trans.*, **2012**, *41*, 8797.

[9] H.-h. Gao, C.-h. Yan, X.-P. Tao, Y. Xia, H.-M. Sun, Q. Shen and Y. Zhang *Organometallics* **2010**, *29*, 4189–4192; M. V. Jiménez, J. J. Pérez-Torrente, M. I. Bartolomé, V. Gierz, F. J. Lahoz, and L. A. Oro *Organometallics* **2008,** *27,* 224–234; P. Zhang, Y. Gong, Y. Lv, Y. Guo, Y. Wang, C. Wang and H. Li *Chem. Commun.*, **2012**, *48*, 2334–2336

[10] G. Suss-Fink *Dalton Trans.*, **2010**, *39*, 1673–1688; G. Sava, A. Bergamo, S. Zorzet, B. Gava, C. Casrsa, M. Cocchietto, A. Furlani, V. Scarcia, B. Serli, E. Iengo, E. Alessio and G. Mestroni, *Eur. J. Cancer*, **2002**, *38*, 427; H.Keller and B.Keppler, *US Patent*, **1989**, 4843069; G. Mestroni, E. Alessio and G. Sava, *Int. Patent*, **1998**, PCT C 07F 15/00, A61K 31/28, WO 98/00431.

[11] R. Sebesta, I. Kmentova and S. Toma *Green Chem.*, **2008**, *10*, 484–496; M. R. dos Santos, J. R. Diniz, A. M. Arouca, A. F. Gomes, F. C. Gozzo, S. M. Tamborim, A. L. Parize, P. A. Z. Suarez, and B. A. D. Neto *ChemSusChem* **2012**, *5*, 716 – 726; T. N. Gieshoff, A. Welther, M. T. Kessler, M. H. G. Prechtl and A. J. von Wangelin *Chem. Commun.,* **2014**, *50*, 2261

[12] K. L. Luska, P. Migowskia and W. Leitner Green Chem., **2015**, *17*, 3195–3206.

[13] D. B. Williams, M. E. Stoll, B. L. Scott, D. A. Costa and W. J. Oldham, Jr. *Chem. Commun.*, **2005**, 1438–1440

[14] see for instance: K. Fujii, T. Mukai, K. Nishikawa, *Chem. Lett.* **2014**, *43*, 405; D. B. Cordes, M. Smiglak, C. C. Hines, N. J. Bridges, M. Dilip, G. Srinivasan, A. Metlen, R. D. Rogers, *Chem. –Eur. J.* **2009**, *15*, 13441; D. V. Konarev, S. S. Khasanov, A. Otsuka, H. Yamochi, G. Saito, R. N. Lyubovskaya, *Inorg. Chem.* **2012**, *51*, 3420; A. J. Arduengo III, H. V. R. Dias, R. L. Harlow, M. Kline, *J. Am. Chem. Soc.* **1992**, *114*, 5530; T. Pugh, R. A. Layfield, *Dalton Trans.* **2014**, *43*, 4251; Y. Zhang, M. Schmitt, L. Falivene, L. Caporaso, L. Cavallo, E. Y. –X. Chen, *J. Am. Chem. Soc.* **2013**, *135*, 17925; E. Rijnberg, B. Richter, K. –H. Thiele, J. Boersma, N. Veldman, A. L. Spek, G. van Koten, *Inorg. Chem.* **1998**, *37*, 56

[15] B. Schneider, I. Goldberg, D. Reshef, Z. Stein, Y. Shvo, *J. Organomet. Chem.* **1999**, *588*, 92

[16] H. M. Jung, J. H. Choi, S. O. Lee, Y. H. Kim, J. H. Park, J. Park, *Organometallics* **2002**, *21*, 5674

[17] a) A. M. Oertel, V. Ritleng, L. Burr, C. Harwig and M. J. Chetcuti, *Organometallics,* **2011**, *30*, 6685; b) L. B. Benac, E. M. Burgess, L. Burr and A. J. Arduengo, *Organic Syntheses, Coll.*, **1990**, *7*, 195; **1986**, *64*, 92.

[18] S. Patil, J. Claffey, A. Deally, M. Hogan, B. Gleeson, L. M. Menéndez Méndez, H. Müller-Bunz, F. Paradisi and M. Tacke, *Eur. J. Inorg. Chem.,* **2010***, 7*, 1020.

[19] L. C. Branco, J. N. Rosa, J. J. Moura Ramos and C. A. M. Afonso, *Chem. Eur. J.*, **2002**, *8*, 3671.

[20] a) L. Jafarpour, E. D. Stevens and S. P. Nolan, *J. Organomet. Chem.*, **2000**, *606*, 49; b) A. J. Arduengo, R. Krafczyk, H. A. Schmutzler, J. Craig, R. Goerlich, W. J. Marshall and M. Unverzagt, *Tetrahedron*, **1999**, *55*, 14523.

[21] a) W. A. Herrmann, V. P. W. Böhm, C. W. K. Gstöttmayr, M. Grosche, C. P. Reisinger and T. Weskamp, *J. Organomet. Chem.*, **2001**, *616–617*, 616; b) E. C. Hurst, K. Wilson, I. J. S. Fairlamb and V. Chechick, *New J. Chem.*, **2009**, *33*, 1837.

[22] J. A. Loch, M. Albrecht, E. Peris, J. Mata, J. W. Faller and R. H. Crabtree, *Organometallics* **2002**, *21*, 700.

[23] K. R. J. Thomas, M. Velusamy, J. T. Lin, C. H. Chuen and Y. T. Tao, *J. Mater. Chem.*, **2005**, *15*, 4453.

[24] Y. Mum, D. Czarkle, Y. Rahamlm and Y. Shvo, *Organometallics*, **1985**, *4*, 1461.

[25] Sheldrick, G. M. *SADABS*, Program for empirical absorption correction, University of Göttingen, Germany, **1996**.

[26] Sheldrick, G. M. *SHELX97*, Program for crystal structure determination, University of Göttingen, Germany, **1997**.

CHAPTER VII

Straightforward synthesis of iron cyclopentadienone *N*-heterocyclic carbene complexes

Abstract

Novel iron complexes bearing both cyclopentadienone and *N*-heterocyclic carbene ancillary ligands have been obtained by a straightforward synthesis from $Fe_2(CO)_9$. The preparation represents a rare example of silver transmetallation involving iron. The reaction is general and occurs in the presence of variously functionalized NHC and cyclopentadienones.

Introduction

Iron is the most abundant transition metal in Earth's crust; it is cost effective and environmentally benign. Furthermore, its low toxicity is vouched for its involvement in several biological processes that make iron as one of the most important elements in nature.[1] For a long time noble metals such as Pd, Rh, Ir, Ru have dominated the field of homogeneous catalysis and only in the last decade the use of iron complexes in catalysis has witnessed a strong acceleration.[2] In particular iron cyclopentadienone complexes have recently received a special attention due to their easy preparation from simple and cheap materials, air–water stability and, most important, their unique catalytic features arising from the presence of a non-innocent ligand able to trigger powerful redox properties.[3] Furthermore, in addition to the economic benefits, developing iron-based complexes produces an opportunity to access complementary chemoselectivities and discover new reactivity patterns.

One important aspect in coordination chemistry is the control and fine-tuning of electronic and steric properties of the ligand sphere. Good candidates for this goal are *N*-heterocyclic carbenes (NHC), widespread used ligands for coordination and catalysis (for more details see Chapter I, paragraph 1.1).[4] NHC ligands are easily prepared and, due to the robust bond formed with most metal centers, are highly resistant toward decomposition. A series of reports in the last few years have shown that iron-NHC complexes have considerable potential for unique and wide-ranging applications including: novel coordination chemistry, homogeneous catalysis, and bio-mimetic chemistry.[5] Developments in homogeneous catalysis involving iron-NHC complexes are represented by cross-coupling Kochi reactions, C-C bond formation reactions, hydrosilylation,[6] allylic alkylation, C−X bond formation (X = B, N, Mg, S), reduction reactions, transfer hydrogenation[7] and cyclization reactions.[1]

In the previous chapters it has been evidenced that ruthenium carbonyls containing both NHC and cyclopentadienone ligands take advantage of the properties of both ligands affording novel metal-cyclopentadienone bifunctional catalysts in which steric and electronic properties, solubility and the introduction of substituents suitable for heterogenization can be finely tuned through the NHC ancillary ligand. Furthermore, by choosing a proper substituent such as a pyridine (*e.g.* complex **12m[CF₃SO₃]**), the NHC ligand itself could cooperate with the metal as non-innocent species.

The access to the new class of Ru(0) carbene complexes of type **4** (see Chapter II) has been provided by the cleavage of the dimeric Ru(0) cyclopentadienone dicarbonyl precursor (**3**) in the presence of the silver carbene intermediate **2** as shown in Scheme 7.1.[8]
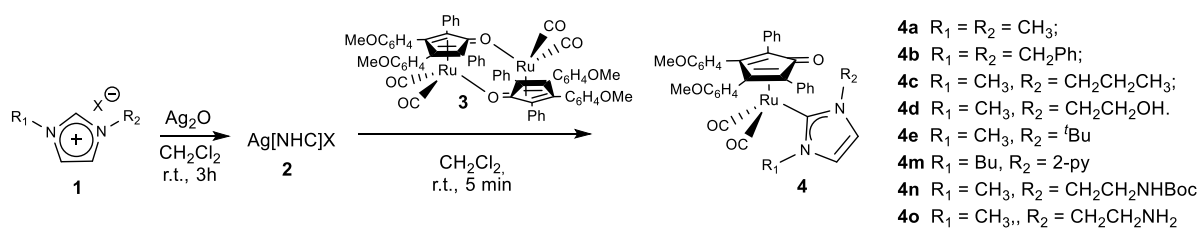
Scheme 7.1. Synthesis of dicarbonyl-cyclopentadienone-*N*-heterocyclic carbene ruthenium complexes (**4**).

The reaction, clean and quantitative, can be also performed in one pot by generating the silver-NHC complex *in situ*. The same procedure has been successively extended to triazolylidene ligands (see Chapter III); the both imidazolylidene (**4**) and triazolylidene (**11**) complexes showed to be active in transfer hydrogenation and alcohol oxidation in the presence of additives such as cerium ammonium nitrate (see Chapter IV).[9]

In order to expand the scope of this reaction to iron, a cyclopentadienone triscarbonyl iron complex has been chosen as precursor. This chapter concerns a novel synthesis of cyclopentadienone NHC iron complexes suitable for catalytic reactions such as those investigated for the ruthenium analogues. To the best of our knowledge this is the first report in which iron complexes containing both a cyclopentadienone and a NHC ligand are reported.

Results and Discussion

7.1 Synthesis of Iron carbene complexes

Inspired by our previous work on ruthenium (paragraph 2.5), we tried to take advantage of microwave irradiation[10] for the synthesis of the triscarbonyl cyclopentadienone precursor (**22**) with significant reduction of the reaction time. Indeed, after screening different temperatures and times, best reaction conditions have been found at 140°C, with a reaction time of 70 minutes. Under these conditions a yield of 50% has been reached which is identical to that obtained with the classical protocol (heating under reflux for 18 h).[11]
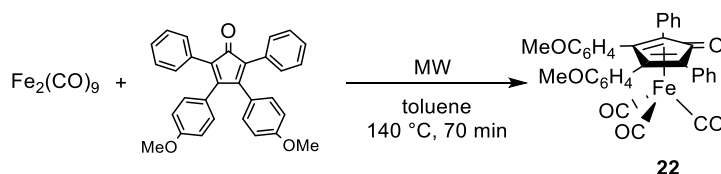
Scheme 7.2. Microwave assisted synthesis of triscarbonyl-(η^4-3,4-bis(4-methoxyphenyl)-2,5-diphenylcyclopenta-2,4-dienone)iron (**22**).

Crystals of **22**, suitable for X-ray diffraction, have been obtained with the double layer technique (dichloromethane/hexane). The structure of **22** is described in the Experimental Section.

After having optimized the preparation of **22**, one of the terminal carbonyls has been replaced upon reaction with Me$_3$NO in acetonitrile, with the more labile acetonitrile ligand, leading to the formation of biscarbonyl-acetonitrile(η^4-3,4- bis(4-methoxyphenyl)-2,5-diphenylcyclopenta-2,4-dienone)iron (**23**). Complex **23** has been treated with silver-NHC complexes (**2**), obtained *in situ* by reaction of imidazolium salts **1** and Ag$_2$O.[8] The latter reaction, performed in refluxing toluene, leads to the formation of the desired NHC complexes **24a-d,n,q** generally in good or excellent yields (50-80%, Scheme 3). The low yield (18%) observed for **24d** can be probably ascribed to the presence of an –OH group in the NHC side chain which might interact with the C=O group of cyclopentadienone and/or with the metal center, with detrimental influence on transmetallation.

Indeed, indication of an intramolecular hydrogen bond between the cyclopentadienone and –OH group in complex **24d** can be inferred from IR and ^{13}C NMR spectra. In the IR spectra the low-energy shift of the carbonyl band of **24d** [v(CO) = 1576 cm^{-1}] compared with those of **24a-c,n,q** [v(CO) = 1584-1587 cm^{-1}] suggests a η^4 to an η^5 coordination change of cyclopentadienone. Furthermore the ^{13}C-NMR shift of the C=O signal (**24a-c,n,q**: 166-167 ppm vs. **24d**: 163 ppm) and the broadness of CH$_2$ signals in ^{1}H-NMR are in agreement with H-bond formation.

The same behaviour was observed for a similar ruthenium complex (**4d**, Chapter II) for which the H-bond formation was also confirmed by X-Ray diffraction.[8] To further confirm the influence of –OH group on transmetallation to iron complexes, the corresponding silver complex of the –OMe functionalized imidazolium salt **1q** has been reacted with **23** affording **24q** in 55% yield.

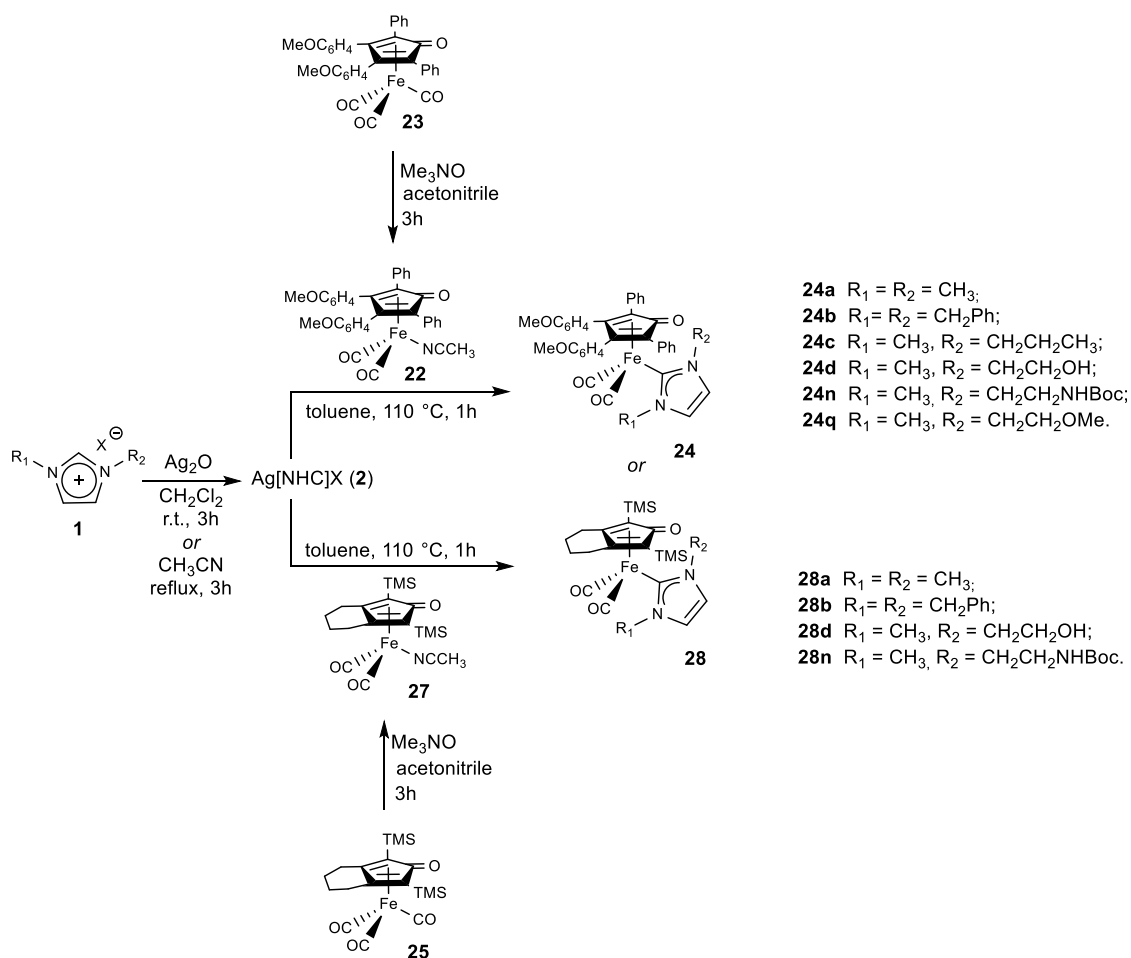**Scheme 7.3.** Synthesis of dicarbonyl-cyclopentadienone-*N*-heterocyclic carbene iron complexes (**24a-d,n,q**) and

28a,b,d,n).

The reaction is general with non-bulky NHCs and tolerant of functional groups: in fact it occurs in the presence of a primary alcohol and amide in the lateral chain (**1d,n** to **24d,n**). The synthesis of **24a-d,n,q** has been followed by IR spectroscopy observing in all cases a lowering in the CO stretching frequencies (*e.g.* **24a**: v(CO) = 1988, 1930 cm^{-1} *vs.* **22**: 2008, 1954 cm^{-1}) due to the strong NHC σ donor properties. ^{13}C-NMRs show a diagnostic signal for the Fe-C$_{carbene}$ within the range 182-185 ppm (*e.g.* ^{13}C-NMR spectrum of **24c** in Figure 7.1) and molecular ions of complexes **24a-d,n,q** are detectable by ESI-MS. Complexes **24a-d,n,q** are air- and moisture-stable both in solid state and in solution and are soluble in the most common organic solvents.
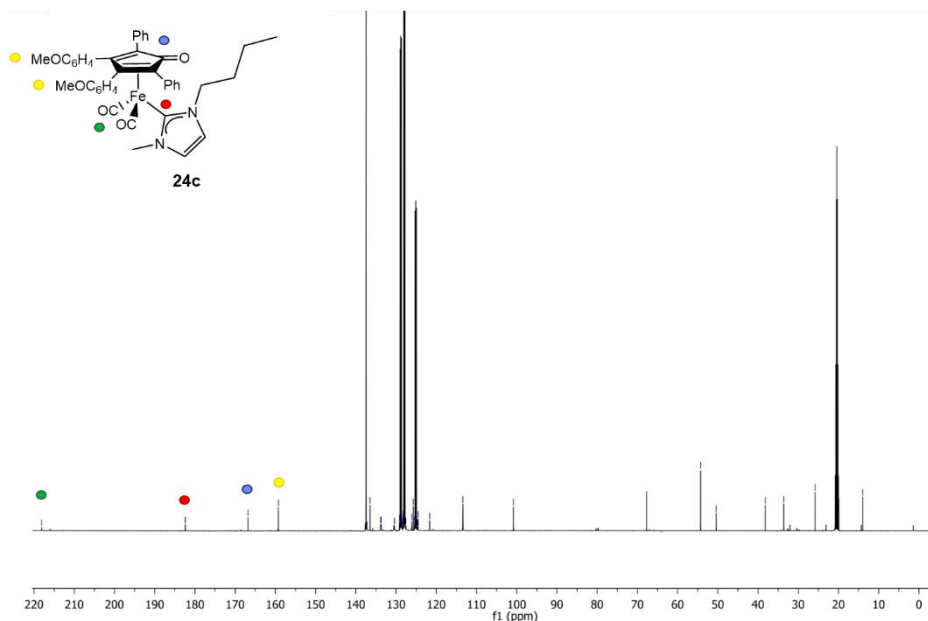
Figure 7.1 ^{13}C-NMR spectrum of **24c** in C_7D_8.

The neutral iron complex **24a** treated with a strong acid such as HCF_3SO_3 (Scheme 7.4) displayed the same behaviour of the analogue ruthenium complex (**4a**) leading to the quantitative formation of the hydroxycyclopentadienyl cationic complexes **25a[CF₃SO₃]**.

IR spectroscopy revealed a significant high-energy shift of the CO stretching frequencies upon protonation [*e.g.* $v(CO) = 1988$ cm^{-1}, 1930 cm^{-1} (**24a**), and 2023 cm^{-1}, 1977 cm^{-1} (**25a[CF₃SO₃]**)], as observed for the related ruthenium cationic complex **12a[CF₃SO₃]** (see Chapter IV).

The change in the coordination from η^4 (cyclopentadienone ligand) to η^5 (hydroxycyclopentadienyl ligand) is further evidenced by ^{13}C-NMR shift of the resonance due to the endocyclic carbon involved in the ketone-alcohol transformation [δ 166.57 ppm (C=O, Cp, in **24a**) vs δ 136.12 ppm (C-OH, Cp, in **25a[CF₃SO₃]**)]. Fe-carbene signals are also shifted to higher fields; from δ 182.41 ppm (2**4a**) to δ 169.62 ppm (**25a[CF₃SO₃]**).
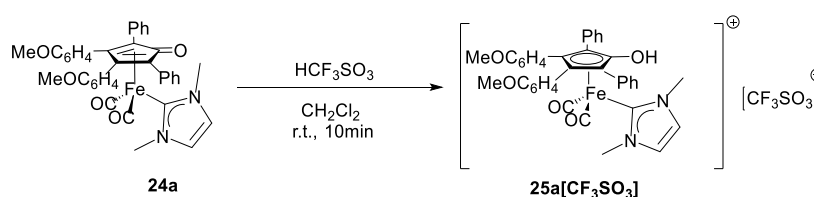
Scheme 7.4 Synthesis of hydroxycyclopentadienyl imidazolylidene iron complex **25a[CF₃SO₃]**.

In order to further extent the ligand scope, the Knölker's cyclopentadienone triscarbonyl complex,[12] has been obtained, exploiting microwave irradiation (see Experimental section, Scheme 7.5). As previously observed for **22**, the synthesis is by far faster than that reported in the literature affording **26** in good yield (83%) (Scheme 7.3). By treating **26** with Me_3NO in CH_3CN, the intermediate **27** has been obtained and employed as precursor for the synthesis of NHC complexes by transmetallation with silver-NHC complexes prepared *in situ* (Scheme 7.3). Complexes **28a,b,d,** have been characterized by spectroscopy and mass spectra (see Experimental section). The protonation reaction of **28a** with triflic acid leads to the quantitative formation of the hydroxycyclopentadienyl cationic complex **29a[CF₃SO₃]**.

Noteworthy –OH functionalized complex **28d** (y = 13 %) resembles the behavior of the congener **24d** further confirming an influence of the hydroxyl group on the reactivity of these complexes.

Complexes **24a**, **24b**, **24c** and **28a** have been also characterized by X-Ray diffraction studies. The molecular structure of **24a** is reported in Figure 7.2, whereas those of **24b** and **24c** are given in the Experimental section (Figures 7.11 and 7.12). Their structures are similar to those previously reported for analogous Ru-complexes (see Chapter II).[8] In particular, the Fe(1)-C(3) distance [2.348(3) Å in **24a**] is significantly longer than Fe(1)-C(4-7) [2.053(3)- 2.162(3) Å, average 2.118(6) Å in **24a**] and C(3)-O(3) [1.246(4) Å in **24a**] is essentially a double bond,[13] in agreement with C=O bond, absorptions around 1585 cm^{-1} were found in the IR spectra of complexes **24**. The Fe(1)-C(34) contact [1.980(3) Å in **24a**] is in the typical range for the interaction between Fe(0) and a *N*-heterocyclic carbene.[7a]
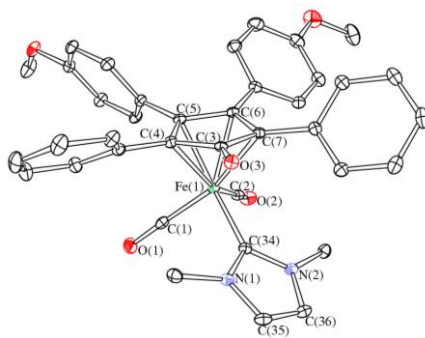

Figure 7.2. ORTEP drawing of **24a**. Displacement ellipsoids are at the 30% probability level. H-atoms have been omitted for clarity. Selected bond lengths (Å): Fe(1)-C(1) 1.754(3), Fe(1)-C(2) 1.765(3), Fe(1)-C(3) 2.348(3), Fe(1)-C(4) 2.162(3), Fe(1)-C(5) 2.053(3), Fe(1)-C(6) 2.099(3), Fe(1)-C(7) 2.156(3), Fe(1)-C(34) 1.980(3), C(3)-O(3) 1.246(4).

The structure of **28a** is similar to **24a** apart from the different substituents on the cyclopentadienone ring (Figure 7.3).
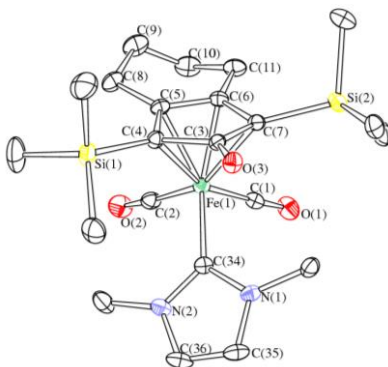
Figure 7.3. ORTEP drawing of **28a**. Displacement ellipsoids are at the 30% probability level. H-atoms have been omitted for clarity. Selected bond lengths (Å): Fe(1)-C(1) 1.747(3), Fe(1)-C(2) 1.754(3), Fe(1)-C(3) 2.359(2), Fe(1)-C(4) 2.153(3), Fe(1)-C(5) 2.091(3), Fe(1)-C(6) 2.067(2), Fe(1)-C(7) 2.177(2), Fe(1)-C(34) 1.996(3), C(3)-O(3) 1.250(3).

The reaction reported in Scheme 7.3 is one of the rare examples of transmetallation from silver complexes to first row transition metals, such as iron[1,14] and the first example in which transmetallation is employed in the synthesis of piano stool complexes. Such complexes were initially obtained upon reaction of diamines with mononuclear [FeCp(SnPh$_3$)(CO)(CS)] or dinuclear [Fe$_2$Cp$_2$(CO)$_2$(μ-CO)(μ-C(SMe$_2$)(CN))]$^+$ thiocarbonyl complexes.[15] Later on, the procedure consisting in the deprotonation of the imidazolium salts followed by reaction of the resulting carbene with an iron halide precursor (*e.g.* [FeCp(CO)$_2$I]) was introduced.[16] Finally, an

elegant synthetic approach, was described by Royo *et al.*[17] based on the formation of bidentate cyclopentadienyl functionalized iron(II)-NHC by direct reaction of the imidazolium proligands with $Fe_3(CO)_{12}$. The disadvantage of the deprotonation method is that the generation of a free, often unstable, carbene intermediate requires special bases, rigorous air and moisture-free conditions and yields are generally scarcely reproducible. On the other hand, transmetallation with silver complexes does not require any particular reaction conditions and can be applied to a broad range of imidazolium salts bearing various *N*-substituents.

In our case transmetallation might be favored by the presence of the non-innocent cyclopentadienone ligand,[18] which can interact with silver[8] and labilize the silver-carbene bond. The oxidation state of iron might also have an influence on the reactivity, as suggested by the related complex $[FeCp(CO)_2(CH_3CN)]BF_4$, obtained reacting $[FeCp(CO)_2]_2$ with $AgBF_4$, that does not undergo transmetallation with silver-NHC complexes. Furthermore, a possible role of the NHCs donor properties, in addition to steric effects, should not be excluded (complex **23** is unreactive towards hindered silver-NHC such as 1,3-bis(2,6-diisopropylphenyl)imidazol-2-ylidene silver chloride). Indeed, NHCs with bulky substituents generally display better donor properties, as evaluated by TEP values (Tolman Electronic Parameters). A combination of these steric and electronic effects might increase both stability and inertness of the silver complexes intermediates and consequently disfavor carbene transmetallation.[19]

7.2 Catalytic transfer hydrogenation

The Iron carbene complexes **24a** and **25a[CF₃SO₃]** were evaluated as catalyst precursors under transfer hydrogenation conditions *i.e.* refluxing 'PrOH as hydrogen source employing 4-fluoroacetophenone as model substrate. Catalytic runs were performed in order to compare the catalytic activity of the iron carbene complexes **24a** and **25a[CF₃SO₃]** with the precursor biscarbonyl-acetonitrile(η^4-3,4-bis(4-methoxyphenyl)-2,5-diphenylcyclopenta-2,4-dienone)iron (**23**), containing more labile acetonitrile ligand, and with the analogues ruthenium complexes **4a** and **12[CF₃SO₃]** previously tested in the same catalytic reaction (more details in Chapter IV, paragraph 4.2). The role of additives such as CAN (cerium ammonium nitrate) and Me₃NO in the activation of **24a** has been also investigated.

Table 7.1. Catalytic transfer hydrogenation of 4-fluoroacetophenone.[a]
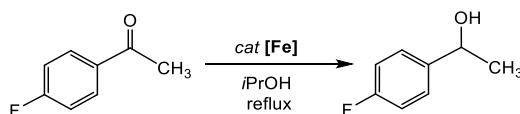
entry	**[Fe]**	additive	conversion 24h (%)
1	**24a**	---	0
2	**24a**	CAN[b]	0
3	**24a**	Me₃NO[c]	0
4	**25a[CF₃SO₃]**	---	0
5	**23**	---	96
6	**23**[d]	---	58
7	**4a-[Ru]**	CAN	61
8	**12a[CF₃SO₃]-[Ru]**	---	93

[a]General conditions: Iron complex (5 mol% Fe), 'PrOH (3 mL), reflux; conversions determined by ¹⁹F NMR spectroscopy; [b]CAN 1 mol equiv. per iron center; [c]Me₃NO 1.5 mol equiv. per iron center, [d]catalyst loading reduced to 2 mol% Fe.

The catalytic results shown in Table 7.1 reveal that the iron carbene complexes **24** and **25a[CF₃SO₃]** are not active in the transfer hydrogenation of 4-fluoroacetophenone. In fact, no conversion of the substrate has been observed for the both, neutral (**24a**) and cationic complexes (**25a[CF₃SO₃])** (entries 3,4), even by adding promoters such as CAN or Me₃NO (entries 2,3). In particular, the use of CAN as additive lead to a complete oxidation and subsequently decomposition of the catalyst, while with Me₃NO or in absence of additive the initial complex **24a** or **25a[CF₃SO₃]** has been recovered unaltered at the end of the reaction. The catalytic tests performed with biscarbonyl-acetonitrile(η⁴-3,4- bis(4-methoxyphenyl)-2,5-diphenylcyclopenta-2,4-dienone)iron (**23**) as pre-catalyst lead to an almost complete conversion of the substrate in 24h. This is reasonably due to the presence of the labile ligand acetonitrile as the equivalent of a vacant coordination site. Conversely, in the carbonylic-NHC transition metal-carbene complexes, coordinative insaturation is obtained by CO removal (Chapter IV paragraph 4.3). Whereas CO release in ruthenium complexes can be reached through the oxidation of the metal center (upon protonation or treatment with CAN), this doesn't occur for the congener iron complexes. The iron complexes of type **24** and **25[X]** need a different way to be activated; therefore, a screening of several reaction conditions and parameters (temperature, solvent, additives), as well as higher catalytic loadings, are still under investigation.

7.3 Catalytic alcohol oxidation

Iron carbene complexes have been also tested as catalyst precursor under oxidative conditions in the dehydrogenation of benzyl alcohol to benzaldehyde. In particular, it has been investigated the catalytic activity of the bis-trimethylsilyl-cyclopentadienone substituted iron carbene complexes **28a** and **29a[CF₃SO₃]**,which are more stable in solution compared to the analogues complexes with tetraaryl-cyclopentadienone substituent (type **24** and **25**).

A screening of different solvents and additives have been performed; the results are reported in Table 7.2.

Table 7.2. Catalytic oxidation of benzyl alcohol. [a]
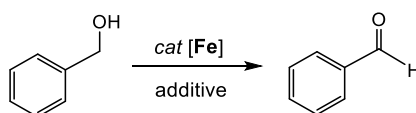
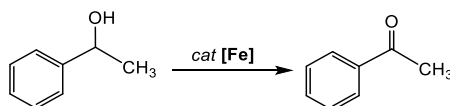| entry	**[Fe]**	solvent	additive	conversion 24h (%)
1	**28a**	toluene	---	0
2	**28a**	toluene	BQ[b]	0
3	**28a**	1,4-dioxane	Me₃NO[c]	4
4	**28a**	1,4-dioxane	Me₃NO[d]	10
5	**28a**	1,4-dioxane	Me₃NO[e]	15
6	**29a[CF₃SO₃]**	toluene	---	11
7	**29a[CF₃SO₃]**	toluene	BQ[b]	11
8	**29a[CF₃SO₃]**	1,4-dioxane	Me₃NO[c]	11
9	**29a[CF₃SO₃]**	acetone	---	0
10	**26**	toluene	BQ[b]	3

[a]General conditions: Iron complex (5 mol% Fe), solvent (3 mL), reflux; conversions determined by GC; [b]BQ 10 mol equiv. per iron center; [c]Me₃NO 7 mol equiv. per iron center, [d]Me₃NO 25 mol equiv. per iron center; [e]catalyst loading increased to 10 mol% Fe.

The neutral iron complex **24a** did not present any catalytic activity in refluxing toluene, even in the presence of benzoquinone. This additive, with the analogues ruthenium complexes, is able to regenerate the catalyst *in situ,* (see Chapter V, paragraph 5.4), whereas, in the case of iron complexes, leads to their decomposition.. Moreover, catalytic tests performed with the well-known catalyst triscarbonyl-(2,4-bis(trimethylsilyl)bicyclo[3.3.0]nona-1,4-dien-3-one)iron (**26**) (entry 10) in the presence of BQ, show that the complex is not able to convert the substrate but, as reported in the literature,[3] it needs an additive such as Me$_3$NO in order to exhibit catalytic activity.

On these basis, catalytic tests have been also performed in 1,4-dioxane as solvent with Me$_3$NO as additive, in these conditions some conversion has been observed: 4% with 7 mol% of Me$_3$NO, up to 10% with Me$_3$NO loading raised to 25 mol% (entries 3, 4). Increasing the catalyst loading to 10mol% with 25mol% of Me$_3$NO resulted in only 15% of conversion (entry 5). More catalytic runs have been carried out with the cationic complex **29a[CF$_3$SO$_3$]** testing different solvents and additives: under all the applied reaction conditions a low conversion (11%) has been observed (entries 6, 7 ,8) and the presence of the carbene-free iron(0) precursor **26** has been detected at the end of the reaction. Using acetone as solvent (entry 9) no conversion has been reached but the complex **29a[CF$_3$SO$_3$]** has been recovered unaltered in the reaction crude, indicating that the complex is stable but not activated under these conditions.

With the aim to test the complexes on more active substrates, the reactivity of **28a** and **29a[CF$_3$SO$_3$]** has been extended to 1-phenylethanol. Indeed, secondary alcohols are more prone to oxidation.[20] Furthermore, in these experiments, the concentration of the substrate in the reaction mixture has been increased to 0.25 M. The catalytic results are reported in Table 7.3

Table 7.3. Catalytic oxidation of 1-phenylethanol.[a]

entry	[Fe]	solvent	conversion 24h (%)
1	**29a[CF$_3$SO$_3$]**	toluene	35
2	**29a[CF$_3$SO$_3$]**	acetone[b]	27
3	**28a**	acetone[b]	41[c]

[a]General conditions: Iron complex (5 mol% Fe), substrate concentration = 0.25 M, reflux; conversions determined by GC; [b] test performed in a sealed glass ampoules equipped with a Young valve heating at 90°C; [c]yield ~ 21% the byproduct is identidied as bis(alpha-methylbenzyl) ether.

The cationic complex **29a[CF$_3$SO$_3$]** under these conditions exhibits some catalytic activity in the oxidation of 1-phenylethanol both in toluene and acetone, leading to a conversion of 35% and 27% respectively (entry 1, 2). Furthermore, 41% of conversion has been observed employing the neutral complex **28a** as catalyst precursor, even though the effective yield is lower (~ 21%) because of the formation of the bis(alpha-methylbenzyl) ether as by-product.

The observed catalytic activity of both neutral and cationic complexes **28a** and **29a[CF$_3$SO$_3$]** in these catalytic tests is encouraging and a screening of different substrates and NHCs (with different substituents) will be matter of further studies in this field in order find active iron NHC complexes.

7.4 Electrochemical measurement

Electrochemical analysis of the carbene iron(0) complex **24a** by cyclic voltammetry measurements reveal a reversible oxidation of **24a** in CH_2Cl_2 solution with $E_{1/2}$ = +0.581(±4) *vs* SCE (Figure 7.4). The redox process likely involves a Fe^0/Fe^{II} oxidation which is reversible according to the peak-current ratio (i_{pc}/i_{pa} = 0.95 at 100 mV s^{-1}) that is maintained quite constant at different scan rates.
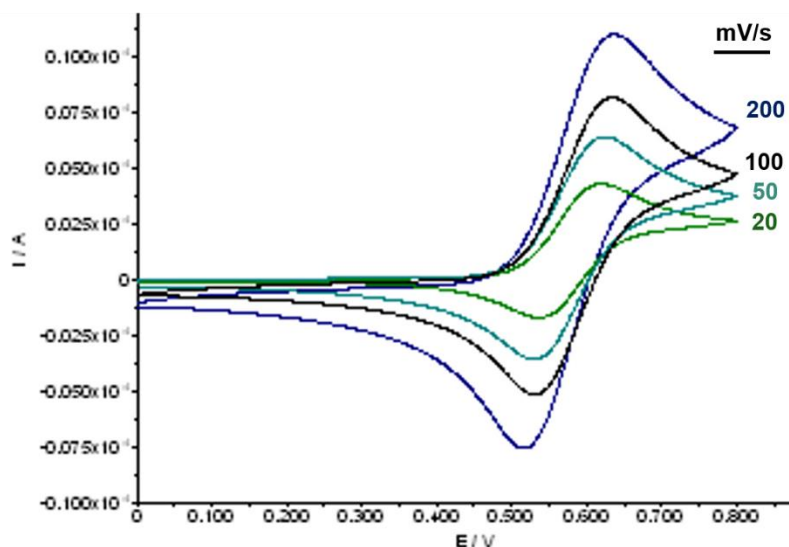
Figure 7.4. Cyclic voltammograms for **24a** in CH_2Cl_2 at at different scan rates (potential *vs* SCE, Fc as internal standard).

The electrochemical data of the imidazolylidene iron(0) complex **24a** evidences a similar behaviour of the triazolylidene ruthenium(0) complex **11a** (see Chapter III, paragraph 3.4), but with a lower potential (**11a**: $E_{1/2}$ = +0.952(±3)) and a more reversible oxidation mechanism. This feature suggests that under electrochemical conditions the iron complexes undergo oxidation of the metal center that can be the key point of the activation in the catalytic reactions. Investigations on the catalytic activity of this complex in these conditions are being carried out.

From an electrochemical point of view this complex show good electrochemical reversibility, regeneration at low potential, and generation of stable redox form. These features indicate that iron cyclopentadienone NHC complexes **(24)** are promising electrocatalysts and redox mediators,[21] potentially useful for the development of novel sensors for amperometric detection of interesting molecules, such as dopamine (DA).[22]

Conclusions

A very efficient and rapid synthetic route for obtaining a new class of Fe(0) complexes, which contain both *N*-heterocyclic carbenes and cyclopentadienone ligands has been developed. The synthetic approach takes advantage of transmetallation from silver-NHC complexes, which is a method rarely exploited in the case of iron-NHC complexes. Transmetallation could be favored either by non-innocent cyclopentadienone ligand or by iron valence. Donor and steric properties of NHCs can also play a role. The novel synthetic method for the preparation of complexes of type **24** and **28** is general and pave the way for future developments in iron mediated redox homogeneous catalysis. The iron complexes didn't show good catalytic activity as transfer hydrogenation catalysts, but under oxidative conditions some promising results have been obtained, even though the conversions observed are so far low. Moreover, the interesting electrochemical properties displayed by the iron complex **24a** indicate possible development and applications in the field of electrocatalytic processes and amperometric sensor devices.

Experimental Section

Materials and procedures. Solvents: dichloromethane (CH_2Cl_2), tetrahydrofuran (THF), diethyl ether (Et_2O), petroleum ether referring to a fraction of bp 60-80 °C, acetonitrile (CH_3CN) were dried and distilled prior to use. Acetone has been degassed and stored under inert atmosphere on molecular sieves. Other solvents such as ethylacetate (EtOAc), chloroform, ethanol (EtOH), methanol (MeOH), heptane, toluene, $CDCl_3$, D_2O, CD_3CN (Sigma Aldrich) have been employed without further purification. Reagents: $Fe_2(CO)_9$ (Strem), methyl iodide, chloridric acid, silver oxide, 1-methylimidazole, 1,3 diphenylacetone, benzyl bromide, 4,4'dimethoxybenzil (Alfa Aesar) have been employed as purchased.

1,3-dimethylimidazolium iodide (**1a**),[23] 1,3-dibenzylimidazolium bromide (**1b**),[24] 1-methyl-3-butyl-imidazolium chloride, 1-methyl-3-(2-hydroxyethyl)imidazolium chloride (**1d**),[25] 1-(2-BocNH-ethyl)-3-methylimidazolium iodide (**1e**)[26] 1-methyl-3-(2-methoxyethyl)imidazolium chloride (**1f**), 1,3-bis(2,6-diisopropylphenyl)imidazolium bromide,[27] 1,3-dimethylimidazol-2-ylidene silver iodide (**2a**),[28] 1,3-dibenzylimidazol-2-ylidene silver bromide (**2b**),[29] 1-methyl-3-(2-hydroxyethyl)imidazol-2-ylidene silver chloride (**2d**),[30] 1,3-bis(2,6-diisopropylphenyl)imidazol-2-ylidene silver bromide,[31] 3,4-Bis(4-methoxyphenyl)-2,5-diphenylcyclopenta-2,4-dienone,[32] have been prepared following procedures reported in the literature.

The prepared derivatives were characterized by spectroscopic methods. The NMR spectra were recorded using Varian Inova 300 (^1H, 300.1; ^{13}C, 75.5 MHz), Varian Mercury Plus VX 400 (^1H, 399.9; ^{13}C, 100.6 MHz), Varian Inova 600 (^1H, 599.7; ^{13}C, 150.8 MHz) spectrometers at 298 K; chemical shifts were referenced internally to residual solvent peaks. Full ^1H- and ^{13}C-NMR assignments were done, when necessary, by gHSQC and gHMBC NMR experiments using standard Varian pulse sequences. Infrared spectra were recorded at 298 K on a Perkin-Elmer Spectrum 2000 FT-IR spectrophotometer. ESI-MS spectra were recorded on Waters Micromass ZQ 4000 with samples dissolved in MeOH or CH_3CN. Elemental analyses were performed on a Thermo-Quest Flash 1112 Series EA instrument.

Synthesis of Iron complexes

Triscarbonyl-(η^4-3,4-bis(4-methoxyphenyl)-2,5-diphenylciclopenta-2,4-dienone)iron (22)
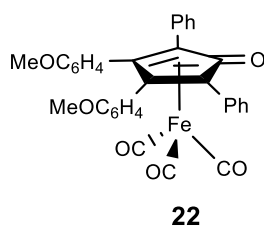
Figure 7.5. Structure of triscarbonyl cyclopentadienone precursor (**22**).

In a 75 mL Teflon tube equipped with magnetic stirrer, 3,4-Bis(4-methoxyphenyl)-2,5-diphenylcyclopenta-2,4-dienone 0.53 g (1.2 mmol) and $Fe_2(CO)_9$ 0.728 g (2 mmol) were dissolved in 40 mL of toluene. The container is closed with a cap, equipped with a temperature sensor, and placed into microwave. The reaction is heated to 140 °C for 70 min. Upon removal of the solvent, the crude was purified to afford the yellow triscarbonyl-η^4-3,4-bis(4-methoxyphenyl)-2,5-diphenylcyclopenta-2,4-dienone)iron complex (**22**) by neutral alumina column chromatography using dichloromethane/ethyl acetate (100/0 to 0/100). Yield = 50%

Suitable crystals of **5** for X-Ray diffraction were obtained by slow diffusion (CH₂Cl₂/Hexane). **22** has been analyzed by IR, ^{1}H-NMR, ^{13}C-NMR, ESI-MS and X-Ray diffraction. ^{1}H-NMR (399.9 MHz, CDCl₃): δ (ppm) 7.55-6.69 (m, 18H, C_{aryl}), 3.76 (s, 6H, -OCH₃). ^{13}C-NMR (150.8 MHz, CDCl₃, g-HSQC, g-HMBC): δ (ppm) 208.58 (CO), 169.75 (C=O, Cp), 159.58 (-COCH₃), 133.05-121.56 (C_{aryl}), 113.40 (CH$_{aryl}$), 103.44 ($C_{2,5}$, Cp), 82.75 ($C_{3,4}$, Cp), 55.12 (-OCH₃). IR (CH₂Cl₂, cm^{-1}): (v_{CO}) 2067, 2013, 1997; ($v_{C=O}$) 1636; ($v_{C=C}$) 1609, 1518. ESI-MS (m/z) (+): 585 [M+H]⁺; 607 [M + Na]⁺; 623 [M+K]⁺. Anal. Calcd (%) for C₃₄H₂₄O₆Fe: C, 69.88; H, 4.14. Found: C, 68.97; H, 3.93.

Dicarbonyl-(η⁴-3,4-bis(4-methoxyphenyl)-2,5-diphenylcyclopenta-2,4-dienone)(acetronitrile)iron (23)
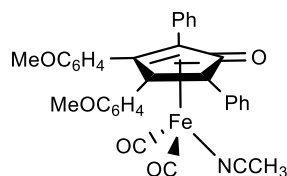
23

Figure 7.6 Structure of Dicarbonyl-(η⁴-3,4-bis(4-methoxyphenyl)-2,5-diphenylcyclopenta-2,4-dienone)(acetronitrile)iron precursor (**23**)

In a dried 15 mL Schlenk flask, triscarbonyl-(η⁴-3,4-bis(4methoxyphenyl)-2,5-diphenylcyclopenta-2,4-dienone)iron (**22**) 0.145 g (0.249 mmol) and trimethylamine-N-oxide 0.028 g (0.374 mmol) were dissolved in 3 mL of anhydrous acetonitrile. Reaction mixture was stirred at room temperature and protected from light for 3 hours. A yellow precipitate appeared. The solid was filtered and washed with diethyl ether and hexane. Yield: 54%

23 has been analyzed by IR, ^{1}H-NMR, ^{13}C-NMR, ESI-MS. ^{1}H-NMR (399.9 MHz, C₇D₈): δ (ppm) 8.24-6.433 (m, 18H, CH$_{aryl}$); 3.10 (s, 6H, -OCH₃); 0.72 (s, 3H, -NCCH₃). ^{13}C-NMR (150.8 MHz, C₇D₈, g-HSQC, g-HMBC): δ (ppm) 214.21 (CO), 169.74 (C=O, Cp), 159.56 (-COCH₃), 134.99-124.45 (C_{aryl}), 113.44 (CH$_{aryl}$), 101.41 ($C_{2,5}$, Cp), 81.31 ($C_{3,4}$, Cp), 54.32 (-OCH₃), 2.48 (CH₃, CH₃CN). IR (CH₂Cl₂, cm^{-1}): (v_{CO}) 2008, 1954; ($v_{C=O}$) 1636; ($v_{C=C}$) 1608, 1515. ESI-MS (m/z) (+): 557 [M-CH₃CN]⁺, 583 [M-CH₃]⁺, 598 [M+H]⁺. Anal. Calcd (%) for C₃₅H₂₇NO₅Fe: C, 70.36; H, 4.56. Found: C, 70.75; H, 4.35.

Synthesis of dicarbonyl-η⁴-3,4-bis(4-methoxyphenyl)-2,5-diphenylcyclopenta-2,4-dienone)(NHC)iron complexes (24)
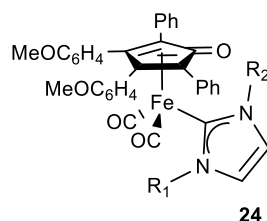
24a R₁ = R₂ = CH₃;
24b R₁ = R₂ = CH₂Ph;
24c R₁ = CH₃, R₂ = CH₂CH₂CH₃;
24d R₁ = CH₃, R₂ = CH₂CH₂OH;
24n R₁ = CH₃, R₂ = CH₂CH₂NHBoc;
24q R₁ = CH₃, R₂ = CH₂CH₂OMe.

24

Figure 7.7 Structure of imidazolylidene Fe(0) complexes **24**.

Imidazolium salts (**1**), silver oxide (1.2 eq.), triscarbonyl-η⁴-3,4-bis(4-methoxyphenyl)-2,5-diphenylcyclopenta-2,4-dienone) iron precursor (**22**) and trimethylammine-N-oxide (1.5 eq.) were reacted in CH₃CN under inert atmosphere and with protection from light. After stirring the reaction for the time and at the temperature required in order to reach complete conversion to silver complexes (**2**), the solvent was removed under vacuum, then the solid dissolved in toluene. The reaction mixture was stirred for 1 hour at 110 °C. Upon

removal of the solvent, the crude was purified to afford the dicarbonyl-η^4-3,4-bis(4-methoxyphenyl)-2,5-diphenylcyclopenta-2,4-dienone)(NHC)iron complexes (**24**) by neutral alumina column chromatography using dichloromethane/ethyl acetate (100/0 to 0/100). Formation of the iron complexes (**24**) was verified by IR, ^{1}H-NMR, ^{13}C-NMR, ESI-MS and X-Ray crystal structure, when suitable crystals were available.

Dicarbonyl-(η^4-3,4-bis(4-methoxyphenyl)-2,5-diphenylcyclopenta-2,4-dienone)(1,3-dimethyl-ilidene)iron (24a): Triscarbonyl-(η^4-3,4-bis(4-methoxyphenyl)-2,5-diphenylcyclopenta-2,4-dienone)iron (**22**) 0.150 g, (0.256 mmol), trimethylammine-N-oxide 0.029 g (0.384 mmol), 1,3-dimethylimidazolium iodide (**1a**) 0.057 g (0.256 mmol) and silver oxide 0.071 g (0.307 mmol), room temperature, 3h. Yield: 60%.

Suitable crystals of **24a** for X-Ray diffraction were obtained by slow diffusion (THF/Hexane). **24a** has been analyzed by IR, ^{1}H-NMR, ^{13}C-NMR, ESI-MS and X-Ray diffraction. ^{1}H-NMR (399.9 MHz, C_7D_8): δ (ppm) 8.33-6.50 (m, 18H, CH_{aryl}), 5.88 (s, 2H, CH_{NHC}) 3.10 (s, 6H, -OCH_3), 2.93 (s. 6H, -NCH_{3NHC}). ^{13}C-NMR (150.8 MHz, C_7D_8, g-HSQC, g-HMBC): δ (ppm) 218.11 (CO), 182.41 ($C_{carbene}$), 166.57 (C=O, Cp), 159.30 (-$COCH_3$), 123.96 (CH_{NHC}), 136.44-125.66 (CH_{aryl}), 113.39 (CH_{aryl}), 100.73 ($C_{2,5}$, Cp), 79.76 ($C_{3,4}$, Cp), 54.28 (-OCH_3) 38.18 (-NCH_3). IR (CH_2Cl_2, cm^{-1}): (v_{CO}) 1988, 1930; ($v_{C=O}$) 1585; ($v_{C=C}$) 1603, 1518. ESI-MS (m/z) (+): 653 [M+H]$^+$; 675 [M + Na]$^+$; 691 [M+K]$^+$. Anal. Calcd (%) for $C_{38}H_{32}N_2O_5Fe$: C, 69.95; H, 4.94. Found: C, 69.33; H, 4.63.

Dicarbonyl-(η^4-3,4-bis(4-methoxyphenyl)-2,5-diphenylcyclopenta-2,4-dienone)(1,3-dibenzylimidazole)iron (24b): Triscarbonyl-(η^4-3,4-bis(4-methoxyphenyl)-2,5-diphenylcyclopenta-2,4-dienone)iron (**22**) 0.030 g (0.005 mmol), trimethylammine-N-oxide 0.006 g (0.080 mmol), 1,3-dibenzylimidazolium bromide (**1b**) 0.016 g (0.005 mmol), and silver oxide 0.014 g (0.016 mmol), 80 °C, 3h. Yield : 70 %.

Suitable crystals of **24b** for X-Ray diffraction were obtained by slow diffusion (Toluene/Hexane). **24b** has been analyzed by IR, ^{1}H-NMR, ^{13}C-NMR, ESI-MS and X-Ray diffraction. ^{1}H-NMR (399.9 MHz, C_7D_8) δ (ppm): 8.43-6.46 (m, 28H, CH_{aryl}), 6.06 (s, 2H, -CH_{NHC}), 5.15 (m, -CH_2), 4.50 (m, -CH_2) 3.06 (s, 6H, -OCH_3). ^{13}C-NMR (150.8 MHz, C_7D_8, g-HSQC, g-HMBC) δ (ppm): 217.43 (CO), 184.99 ($C_{carbene}$), 167.37 (C=O, Cp), 159.27 (-$COCH_3$), 137.34-123.15 (C_{aryl}), 127.78 (CH_{NHC}), 113.36 (CH_{aryl}), 101.31 ($C_{2,5}$, Cp), 80.08 ($C_{3,4}$, Cp), 54.57 (-CH_2), 54.22 (-OCH_3). IR (CH_2Cl_2, cm^{-1}): (v_{CO}) 1989, 1933; ($v_{C=O}$) 1586; ($v_{C=C}$) 1603, 1518. ESI-MS (m/z) (+): 805 [M+H]$^+$; 827 [M + Na]$^+$; 843 [M+K]$^+$. Anal. Calcd (%) for $C_{50}H_{40}N_2O_5Fe$: C, 74.63; H, 5.01. Found: C, 74.19; H, 4.65.

Dicarbonyl-(η^4-3,4-bis(4-methoxyphenyl)-2,5-diphenylcyclopenta-2,4-dienone)(1-methyl-3-butyl-imidazol-ylidene)iron (24c): Triscarbonyl-(η^4-3,4-bis(4-methoxyphenyl)-2,5-diphenylcyclopenta-2,4-dienone)iron (**5**) 0.030 g (0.005 mmol), trimethylammine-N-oxide 0.006 g (0.075 mmol), 1-methyl-3-butyl-imidazolium bromide (**1c**) 0.011 g (0.005mmol) and silver oxide 0.014 g (0.006 mmol), 80 °C, 3 hours. Yield: 50 %.

Suitable crystals of **24c** for X-Ray diffraction were obtained by slow diffusion (Toluene/Hexane). **24c** has been analyzed by IR, ^{1}H-NMR, ^{13}C-NMR, ESI-MS and X-Ray diffraction. ^{1}H-NMR (399.9 C_7D_8) δ (ppm): 8.97-7.13 (m, 18H, CH_{aryl}), 6.85 (d, H, -CH_{NHC}), 6.69 (d, H, -CH_{NHC}), 4.19 (m, 2H, $CH_{2\ NHC}$), 3.73 (s, 6H, -OCH_3), 3.60 (s. 6H, -$CH_{3\ NHC}$), 2.73 (m, 2H, $CH_{2\ NHC}$), 1.53 (t, 2H, $CH_{2\ NHC}$), 1.36 (t, 3H, $CH_{3\ NHC}$). ^{13}C-NMR (150.8 MHz, C_7D_8, g-HSQC, g-HMBC) δ (ppm): 216.04 (CO), 182.41 ($C_{carbene}$), 166.83 (C=O, Cp), 159.29 (-$COCH_3$), 129.18-121.65 (C_{aryl}), 124.54 (CH_{NHC}), 113.40 (CH_{aryl}), 100.87 ($C_{2,5}$, Cp), 80.26 ($C_{3,4}$, Cp), 54.27 (-OCH_3), 50.39 (-NCH_2-), 38.22 (-NCH_3), 33.63 (-CH_2-), 25.83 (-CH_2-), 13.99(-CH_3). IR (CH_2Cl_2, cm^{-1}): (v_{CO}) 1987, 1931; ($v_{C=O}$)

1587; ($v_{C=C}$) 1607, 1518. ESI-MS (m/z) (+): 695 [M+H]$^+$; 717 [M + Na]$^+$; 733 [M+K]$^+$. Anal. Calcd (%) for C$_{41}$H$_{38}$N$_2$O$_5$Fe: C, 70.90; H, 5.51. Found: C, 69.19; H, 5.13.

Dicarbonyl-(η⁴-3,4-bis(4-methoxyphenyl)-2,5-diphenylcyclopenta-2,4-dienone)[1-(2-hydroxyethyl)-3-methylilidene]iron (24d): Triscarbonyl-(η⁴-3,4-bis(4-methoxyphenyl)-2,5-diphenylcyclopenta-2,4-dienone)iron 0.060 g (0.103 mmol), trimethylammine-N-oxide 0.012 g (0.155 mmol), 13-(2-hydroxyethyl)-1-methylimidazole chloride (**24d**) 0.016 g (0.103 mmol) and silver oxide 0.029 g (0.124 mmol), room temperature, 3 h. Chromatography eluent: dichloromethane/ethyl acetate/MeOH (100/0/0 to 0/0/100). Yield: 18 %.

24d has been analyzed by IR, ^{1}H-NMR, ^{13}C-NMR, ESI-MS. ^{1}H-NMR (399.9 MHz, C$_7$D$_8$) δ (ppm): 8.10 (m, 18H, CH$_{aryl}$), 6.63 (s, 1H, CH$_{NHC}$), 6.07 (s, 1H, CH$_{NHC}$), (CH$_2$ not visible), 3.10 (s, 6H, -OCH$_3$), 2.90 (s, 3H, -NCH$_3$). ^{13}C-NMR (150.8 MHz, C$_7$D$_8$, g-HSQC, g-HMBC) δ (ppm): 218.60 (CO), 181.69 (C$_{carbene}$), 163.0 (C=O, Cp), 159.46 (-COCH$_3$) 134.80-125.37 (CH$_{aryl}$), 124.48 (CH$_{NHC}$), 121.99 (CH$_{NHC}$), 113.47 (CH$_{aryl}$), (not visible C$_{3,4}$, Cp), (not visible C$_{2,5}$, Cp), 59.24 (-CH$_2$), 53.30 (-OCH$_3$), 52.40 (-CH$_2$), 37.92 (-NCH$_3$). IR (CH$_2$Cl$_2$, cm^{-1}) (v_{CO}) 1991, 1935; ($v_{C=O}$) 1576 (broad); ($v_{C=C}$) 1604, 1517. ESI-MS (m/z) (+): 683 [M+H]$^+$, 705 [M+Na]$^+$. Anal. Calcd (%) for C$_{39}$H$_{34}$N$_2$O$_6$Fe: C, 68.63; H, 5.02. Found: C, 68.35; H, 4.69.

Dicarbonyl-(η⁴-3,4-bis(4-methoxyphenyl)-2,5-diphenylcyclopenta-2,4-dienone)[1-(2-Boc-NH-ethyl)-3-methylilidene]iron (24n): Triscarbonyl-(η⁴-3,4-bis(4-methoxyphenyl)-2,5-diphenylcyclopenta-2,4-dienone)iron (**5**) 0.150 g (0.257 mmol), trimethylammine-N-oxide 0.029 g (0.386 mmol), 1-(2-BocNH-ethyl-)-3-methylimidazolium iodide (**1n**) 0.091 g (0.257 mmol) and silver oxide 0.071 g (0.308 mmol), room temperature,1 h. Yield : 53 %.

7e has been analyzed by IR, ^{1}H-NMR, ^{13}C-NMR, ESI-MS. ^{1}H-NMR (399.9 MHz, C$_7$D$_8$) δ (ppm): 8.10-6.48 (m, 18H, CH$_{aryl}$), 6.68 (s, H, CH$_{NHC}$), 5.98 (s, H, CH$_{NHC}$), 3.12 (s, 2H, -CH$_2$), 3.11 (s, 6H, OCH$_3$), 2.96 (s, 2H, CH$_2$), 2.79 (s, 3H, NCH$_3$), 1.45 (s, 9H, -CH$_{3 BOC}$). ^{13}C-NMR (150.8 MHz, C$_7$D$_8$, g-HSQC, g-HMBC) δ (ppm): 217.63 (CO), 182.44 (C$_{carbene}$), 164.51 (C=O, Cp), 159.43(-COCH$_3$), 156.86 (C=O, BOC), 137.68-121.84 (C$_{aryl}$), 125.41 (CH$_{NHC}$), 121.84 (CH$_{NHC}$), 113.46 (CH$_{Aryl}$), 98.92 (C$_{2,5}$, Cp), 88.59 (C$_{3,4}$, Cp), 77.94 (C, BOC), 58.32 (CH$_2$), 54.38 (-OCH$_3$), 49.33 (NCH$_2$), 37.82(NCH$_3$), 28.66 (-CH$_3$, BOC). IR (CH$_2$Cl$_2$, cm^{-1}): (v_{CO}) 1991, 1935; ($v_{C=O}$) 1576 (broad); ($v_{C=C}$) 1604, 1517. ESI-MS (m/z) (+) = 782[M+H]$^+$, 804 [M+Na]$^+$. Anal. Calcd (%) for C$_{44}$H$_{43}$N$_3$O$_7$Fe: C, 67.61; H, 5.54. Found: C, 66.95; H, 5.06.

Dicarbonyl-(η⁴-3,4-bis(4-methoxyphenyl)-2,5-diphenylcyclopenta-2,4-dienone)[1-(2-methoxyethyl)-3-methylilidene]iron (24q): Triscarbonyl-(η⁴-3,4-bis(4-methoxyphenyl)-2,5-diphenylcyclopenta-2,4-dienone)iron (**5**) 0.060 g (0.100 mmol), trimethylammine-N-oxide 0.012 g (0.150 mmol), 3-(2-methoxyethyl)-1-methylimidazole chloride (**1q**) 0.016 g (0.103 mmol) and silver oxide 0.028 g (0.120 mmol, room temperature,1 h. Yield : 55 %.

7f has been analyzed by IR, ^{1}H-NMR, ^{13}C-NMR, ESI-MS. ^{1}H-NMR (399.9 MHz, C$_7$D$_8$) δ (ppm): 8.29-6.49 (m, 18H, CH$_{aryl}$), 6.95 (s, 1H, CH$_{NHC}$), 6.00 (s, 1H, CH$_{NHC}$), 3.86 (br, 2H, CH$_2$), 3.09 (s, 6H, -OCH$_3$), 2.92 (s, 3H, -NCH$_3$) 2.88 (s, 3H, -OCH$_3$), 2.08 (br, 2H, CH$_2$). ^{13}C-NMR (150.8 MHz, C$_7$D$_8$, g-HSQC, g-HMBC) δ (ppm): 218.05 (CO), 182.42 (C$_{carbene}$), 166.72 (C=O, Cp), 159.34 (-COCH$_3$), 136.23-125.61 (CH$_{aryl}$), 124.24 (CH$_{NHC}$), 123.53 (CH$_{NHC}$), 113.41 (CH$_{aryl}$), 100.83 (C$_{3,4}$, Cp), 79.97 (C$_{2,5}$, Cp), 72.72 (-CH$_2$), 58.17 (-OCH$_3$), 54.30 (-OCH$_3$), 50.73 (CH$_2$), 38.14 (-NCH$_3$). IR (CH$_2$Cl$_2$, cm^{-1}): (v_{CO}) 1987, 1931; ($v_{C=O}$) 1586 (broad); ($v_{C=C}$) 1518. ESI-MS (m/z) (+) = 697 [M+H]$^+$, 719 [M+Na]$^+$. Anal. Calcd (%) for C$_{40}$H$_{36}$N$_2$O$_6$Fe: C, 68.97; H, 5.21. Found: C, 68.80; H, 4.99.

Dicarbonyliodo-(η⁴-3,4-bis(4-methoxyphenyl)-   2,5-diphenylhydroxycyclopentadienyl)(1,3-dimethyl-ilidene)iron triflate (25a[CF₃SO₃]): Dicarbonyl-(η⁴-3,4-bis(4-methoxyphenyl)-2,5-diphenylcyclopenta-2,4-dienone)(1,3-dimethyl-ilidene)iron complex (**24a**) 0.020g (0.031mmol) was dissolved in 5 mL of CH₂Cl₂ under inert atmosphere. 1.2 equivalent of HCF₃SO₃ (solution at 0.98% in CH₂Cl₂) were subsequently added. The reaction mixture was stirred for 10 minutes at room temperature, then the solvent was removed under vacuum and the crude washed twice with 10 ml of hexane. The orange solid obtained was identified as **25a[CF₃SO₃]** by IR, ¹H-NMR, ¹³C-NMR, ¹⁹F-NMR, ESI-MS. ¹H-NMR (399.9 MHz, CD₃CN)

δ (ppm): 7.45-6.71 (m, 18H, CH$_{aryl}$), 7.14 (s, 2H, CH$_{NHC}$), 3.71 (s, 6H, -OCH₃), 3.39 (s. 6H, -NCH₃). ¹³C-NMR (150.8 MHz, CD₃CN) δ (ppm): 215.00 (CO), 169.62 (C$_{carbene}$), 160.83 (-*C*OCH₃), 136.12 (C-OH), 131.97-127.56 (C$_{aryl}$), 121.62 (CH$_{NHC}$), 114.21 (CH$_{aryl}$), 98.92 (C$_{2,5}$, Cp), 88.59 (C$_{3,4}$, Cp), 55.98 (-OCH₃), 39.55 (-NCH₃). ¹⁹F-NMR (282.4 MHz, CD₃CN) δ (ppm): -79.10 (CF₃SO₃). IR (CH₂Cl₂) ν$_{(CO)}$ 2023 cm⁻¹, 1977 cm⁻¹; ν$_{(C=C)}$ 1610 cm⁻¹, 1521 cm⁻¹. ESI-MS (m/z) (+) = 653 [M]⁺; 149 [M]⁻.

Triscarbonyl-(2,4-bis(trimethylsilyl)bicyclo[3.3.0]nona-1,4-dien-3-one)iron (26)
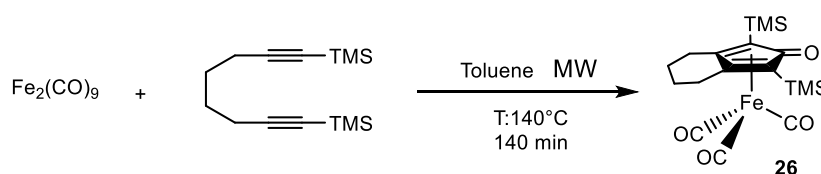
Scheme 7.5 Microwave assisted synthesis of triscarbonyl-(η⁴-2,4-bis(trimethylsilil)biciclo[3.3.0]nona 1,4-dien-3-one)4-methoxyphenyl)iron (**26**).

In a 75 mL Teflon tube equipped with magnetic stirrer, 1,7-octadiyne 0.027 g (0.11 mmol) and Fe₂(CO)₉ 0.039 g (0.11 mmol) were dissolved in 40 mL of toluene. The container is closed with a cap, equipped with a temperature sensor, and placed into microwave reactor. The reaction is heated to 140 °C for 140 min. Upon removal of the solvent, the crude was purified to afford the yellow triscarbonyl-(2,4-bis(trimethylsilyl)bicyclo[3.3.0]nona-1,4-dien-3-one)iron (**26**) by neutral alumina column chromatography using dichloromethane/ethyl acetate (100/0 to 0/100). Yield = 83%

26 has been analyzed by IR, ¹H-NMR. ¹H-NMR (399.9 MHz, CDCl₃): δ (ppm) 2.56 (m, 4H, CH₂), 1.82 (m, 4H, CH₂), 0.27 (s, 18H, CH₃, TMS). IR (CH₂Cl₂, cm⁻¹): (ν$_{CO}$) 2063, 2004, 1987.

Dicarbonyl-(2,4-bis(trimethylsilyl)bicyclo[3.3.0]nona-1,4-dien-3-one)[acetonitrile]iron (27)
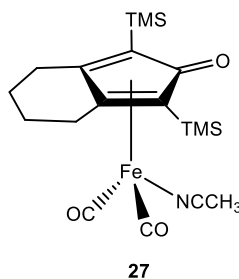
Figure 7.8. Structure of iron triscarbonyl bis(TMS)-substituted cyclopentadienone complex (2**7**).

In a dried 15 mL Schlenk flask, triscarbonyl-(2,4-bis(trimethylsilyl)bicyclo[3.3.0]nona-1,4-dien-3-one)iron (**26**) 0.039 g (0.094 mmol) and trimethylamine-N-oxide 0.011 g (0.14 mmol) were dissolved in 3 mL of anhydrous acetonitrile. Reaction mixture was stirred at room temperature and protected from light for 3 hours. A yellow precipitate appeared. The solid was filtered and washed with diethyl ether and hexane. Yield : 78%.

27 has been analyzed by IR, ^{1}H-NMR. ^{1}H-NMR (399.9 MHz, CDCl$_3$): δ (ppm) 2.28 (m, 4H, CH$_2$), 2.23 (s, 3H, CH$_3$), 1.56 (m, 4H, CH$_2$), 0.24 (s, 18H, CH$_3$, TMS). IR (CH$_2$Cl$_2$, cm^{-1}): (v$_{CO}$) 1999, 1938.

Synthesis of dicarbonyl-(2,4-bis(trimethylsilyl)bicyclo[3.3.0]nona-1,4-dien-3-one)(NHC)iron complexes (28)
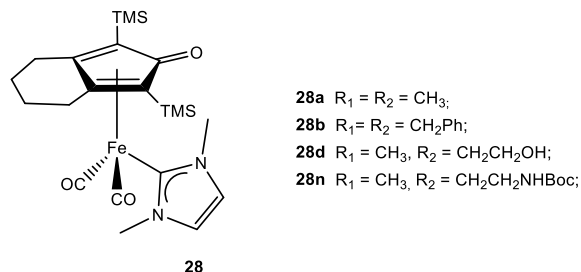
28a R$_1$ = R$_2$ = CH$_3$;
28b R$_1$= R$_2$ = CH$_2$Ph;
28d R$_1$ = CH$_3$, R$_2$ = CH$_2$CH$_2$OH;
28n R$_1$ = CH$_3$, R$_2$ = CH$_2$CH$_2$NHBoc;

Figure 7.9 Structure of bis(TMS)-substituted cyclopentadienone Fe carbene complex (**28**)

Same general procedure for complex **24**. Precursor is triscarbonyl-(2,4-bis(trimethylsilyl)bicyclo[3.3.0]nona-1,4-dien-3-one)iron (**26**).

Dicarbonyl-(2,4-bis(trimethylsilyl)bicyclo[3.3.0]nona-1,4-dien-3-one)[1,3-dimethyl-ilidene]iron (28a): Triscarbonyl-(2,4-bis(trimethylsilyl)bicyclo[3.3.0]nona-1,4-dien-3-one)iron (**26**) 0.035 g (0.084 mmol), trimethylammine-N-oxide 0.009 g (0.12 mmol), 1,3-dimethylimidazolium iodide 0.019 g (0.084 mmol) and silver oxide 0.035 g (0.084 mmol), room temperature, 3 h. Yield : 86 %

Suitable crystals of **28a** for X-Ray diffraction were obtained by slow diffusion (Toluene/Hexane). **28a** has been analyzed by IR, ^{1}H-NMR, ^{13}C-NMR, ESI-MS and X-Ray diffraction. ^{1}H-NMR (399.9 CDCl$_3$) δ (ppm): 6.98 (s, 2H, CH$_{NHC}$), 3.91 (s, 6H, CH$_3$), 2.45 (t, 4H, CH$_2$), 1.85-1.87 (m, 4H, CH$_2$), 0.174 (s, 18H, CH$_3$, TMS). ^{13}C-NMR (150.8 MHz, C$_7$D$_8$, g-HSQC, g-HMBC) δ (ppm): 217.00 (CO), 182.00 (C$_{carbene}$), (C=O, Cp) (not visible), 123.79 (CH$_{NHC}$), 103.72 (C$_{3,4q}$), 65.00 (C$_{2,5q}$), 39.94 (CH$_3$), 24.52 (CH$_2$), 22.55 (CH$_2$), 0.23 (CH$_3$, TMS). IR (CH$_2$Cl$_2$, cm^{-1}): (v$_{CO}$) 1983, 1922. ESI-MS (m/z): 487 [M+H]$^+$, 509 [M+Na]$^+$, 525 [M+K]$^+$. Anal. Calcd (%) for C$_{22}$H$_{34}$N$_2$O$_3$Si$_2$Fe: C, 54.31; H, 7.04. Found: C, 54.82; H, 6.72.

Dicarbonyl-(2,4-bis(trimethylsilyl)bicyclo[3.3.0]nona-1,4-dien-3-one)[1,3-dibenzylimidazol-lilidene]iron (28b): Triscarbonyl-(2,4-bis(trimethylsilyl)bicyclo[3.3.0]nona-1,4-dien-3-one)iron (**26**) 0.077 g (0.018 mmol), trimethylammine-N-oxide 0.021 g (0.28 mmol), 1,3-dibenzylimidazolium bromide 0.060 g (0.018 mmol) and silver oxide 0.051 g (0.022 mmol), 80 °C 3 h. Yield : 61%.

28b has been analyzed by IR, ^{1}H-NMR, ^{13}C-NMR, ESI-MS. ^{1}H-NMR (399.9 CDCl$_3$) δ (ppm): 7.42-7.18 (10H, CH$_{aryl}$), 6.82 (s, 2H, CH$_{NHC}$), 5.6 (br, 4H, NCH$_2$), 2.49 (m, 4H, CH$_2$), 1.78-1.72 (m, 4H, CH$_2$), 0.19 (s, 18H, CH$_3$, TMS). ^{13}C-NMR (150.8 MHz, C$_7$D$_8$, g-HSQC, g-HMBC) δ (ppm): 216.14 (CO), 186.32 (C$_{carbene}$), 177.02 (C=O, Cp), 136.30 (C$_{aryl}$), 128.75 (CH$_{aryl}$), 127.88 (CH$_{aryl}$), 126.81(CH$_{aryl}$), 123.30 (CH$_{aryl}$), 103.91 (C$_{3,4q}$), 70.12 (C$_{2,5q}$), 55.15 (-NCH$_2$-), 23.94 (CH$_2$), 22.04 (CH$_2$), 0.98 (CH$_3$, TMS). IR (CH$_2$Cl$_2$, cm^{-1}): (v$_{CO}$) 1986, 1924. ESI-MS (m/z): 639 [M+H]$^+$, 661 [M+Na]$^+$, 677 [M+K]$^+$. Anal. Calcd (%) for C$_{34}$H$_{42}$N$_2$O$_3$Si$_2$Fe: C, 63.93; H, 6.63. Found: C, 64.22; H, 6.21.

Dicarbonyl-(2,4-bis(trimethylsilyl)bicyclo[3.3.0]nona-1,4-dien-3-one)[1-(2-hydroxyethyl))-3-methylilidene]iron (28d): Triscarbonyl-(2,4-bis(trimethylsilyl)bicyclo[3.3.0]nona-1,4-dien-3-one)iron (**26**) 0.048 g (0.103 mmol), trimethylammine-N-oxide 0.012 g (0.155 mmol), 3-(2-hydroxyethyl)-1-methylimidazole

chloride 0.020 g (0.103 mmol) and silver oxide 0.037 g (0.160 mmol), room temperature, 3 h. Chromatography eluent: dichloromethane/ethyl acetate/MeOH (100/0/0 to 0/0/100). Yield = 13 %

28c has been analyzed by IR, ^{1}H-NMR, ^{13}C-NMR, ESI-MS. ^{1}H-NMR (399.9 CDCl$_3$) δ (ppm): 7.27 (d, 1H, -CH$_{NHC}$), 7.04 (d, 1H, -CH$_{NHC}$), 4.33 (t, CH$_2$, NHC), 4.00 (t. 2H, -CH$_2$, NHC), 3.83 (s, 3H, -NCH$_3$), 2.52-2.45 (m, 4H, CH$_2$), 1.85-1.75 (m, 4H, CH$_2$), 0.18 (s, 18H, CH$_3$, TMS). ^{13}C-NMR (150.8 MHz, C$_7$D$_8$, g-HSQC, g-HMBC) δ (ppm): 217.68 (CO), 183.60 (C$_{carbene}$), 171.22 (C=O, Cp), 126.63 (C$_{3,4}$, Cp), 124.28 (CH$_{NHC}$), 120.91 (CH$_{NHC}$), 75.27 (C$_{2,5}$, Cp), 59.06 (-CH$_2$-), 52.66 (-CH$_2$-), 40.24 (-NCH$_3$), 25.01 (-CH$_2$-, Cp), 22.43 (-CH$_2$-, Cp), 0.21 (CH$_3$, TMS). IR (CH$_2$Cl$_2$, cm^{-1}): (v$_{CO}$) 1986, 1926. ESI-MS (m/z): 517 [M+H]$^+$, 539 [M+Na]$^+$. Anal. Calcd (%) for C$_{23}$H$_{36}$N$_2$O$_4$Si$_2$Fe: C, 53.48; H, 7.02. Found: C, 53.54; H, 6.67.

Dicarbonyl-(2,4-bis(trimethylsilyl)bicyclo[3.3.0]nona-1,4-dien-3-one)[1-(2-BocNH-ethyl)-3-methylilidene]iron (28n): Triscarbonyl-(η^4-3,4-bis(4-methoxyphenyl)-2,5-diphenylcyclopenta-2,4-dienone)iron (**26**) 0.082 g (0.197 mmol), trimethylammine-N-oxide 0.022 g (0.296 mmol), 1-(2-BocNH-ethyl-)-3-methylimidazolium iodide 0.070 g (0.197 mmol) and silver oxide 0.055 g (0.236 mmol), room temperature, 1 h. Yield = 52 %.

28n has been analyzed by IR, ^{1}H-NMR, ^{13}C-NMR, ESI-MS. ^{1}H-NMR (399.9 CDCl$_3$) δ (ppm): 7.19 (s, 1H, -CH$_{NHC}$), 6.98 (s, 1H, -CH$_{NHC}$), 6.41 (br, 1H, NH), 4.33 (t, CH$_2$, NHC), 3.85 (s, 6H, -NCH$_3$), 3.65 (t. 2H, -CH$_2$, NHC), 2.47 (t, 4H, CH$_2$), 1.83-1.77 (m, 4H, CH$_2$), 1.35 (s, 9H, CH$_3$, BOC), 0.17 (s, 18H, CH$_3$, TMS). ^{13}C-NMR (150.8 MHz, C$_7$D$_8$, g-HSQC, g-HMBC) δ (ppm): 217.61 (CO), 184.56 (C$_{carbene}$), 174.08 (C=O, Cp), 156.66 (C=O, BOC), 123.91 (CH$_{NHC}$), 121.17 (CH$_{NHC}$), 103.26 (C$_{3,4}$, Cp), 78.80 (Cq, BOC), 73.31 (C$_{2,5}$, Cp), 49.55 (-NCH$_2$-), 40.16 (-NCH$_3$), 38.73 (-NCH$_2$-), 28.32 (CH$_3$, BOC), 24.87 (-CH$_2$), 22.47 (-CH$_2$), 0.29 (CH$_3$, TMS) IR (CH$_2$Cl$_2$, cm^{-1}): (v$_{CO}$) 1982, 1922. ESI-MS (m/z): 638 [M+Na]$^+$, 654 [M+K]$^+$. Anal. Calcd (%) for C$_{28}$H$_{46}$N$_3$O$_5$Si$_2$Fe: C, 54.53; H, 7.52. Found: C, 54.53; H, 7.10.

Dicarbonyliodo-(2,4-bis(trimethylsilyl)bicyclo[3.3.0]nona-1,4-dienyl)(1,3-dimethyl-ilidene)iron triflate (29a[CF$_3$SO$_3$]): Dicarbonyl-(η^4-3,4-bis(4-methoxyphenyl)-2,5-diphenylcyclopenta-2,4-dienone)(1,3-dimethyl-ilidene)iron complex (**28a**) 0.020g (0.035mmol) was dissolved in 5 mL of diethyl ether under inert atmosphere. 3.3 µL of HCF$_3$SO$_3$ (solution at 98% in CH$_2$Cl$_2$) were subsequently added. The reaction mixture was stirred for 10 minutes at room temperature, then the precipitate obtained was filtered, washed with 10 ml of hexane and died under vacuum. The orange solid obtained was identified as **29a[CF$_3$SO$_3$]** by IR, ^{1}H-NMR, ^{13}C-NMR, ^{19}F-NMR, ESI-MS. ^{1}H-NMR (399.9 MHz, CDCl$_3$) δ (ppm): 7.28(s, 2H, CH$_{NHC}$), 3.39 (s, 6H, -NCH$_3$). 2.41 (m, 4H, CH$_2$), 1.79 (m, 4H, CH$_2$), 0.29 (s, 18H, CH$_3$, TMS). ^{13}C-NMR (150.8 MHz, CDCl$_3$, g-HSQC, g-HMBC): δ (ppm) 214.16 (CO), 170.93 (C$_{carbene}$), C-OH not visible, 126.26 (CH$_{NHC}$), 104.00 (C$_{2,5}$, Cp), 82.43 (C$_{3,4}$, Cp), 39.87 (-NCH$_3$), 23.79 (CH$_2$, 2C), 21.97 (CH$_2$, 2C), 0.99 (CH$_3$, TMS, 6C). ^{19}F-NMR (282.4 MHz, CDCl$_3$) δ (ppm): -78.18 (CF$_3$SO$_3$).IR (CH$_2$Cl$_2$, cm^{-1}): (vCO) 2018cm^{-1}, 1969 cm^{-1}.

X-Ray diffraction studies

Crystal Structure of 22

The crystal structure of **22** closely resembles those previously reported for other $Fe(CO)_3$-cyclopentadienone complexes.[33] The X-ray crystal structure clearly illustrates the η^4 character of the bonding of the cyclopentadienone ligand. The average bonding distance from the iron to the tetracyclone ring carbons C(4)-C(7) is 2.11 Å and is markedly shorter than the distance to the ketonic carbon Fe(1)-C(3) [2.4074(19) Å].

Figure 7.10. ORTEP drawing of **22**. Displacement ellipsoids are at the 30% probability level. H-atoms have been omitted for clarity. Selected bond lengths (Å): Fe(1)-C(1) 1.807(2), Fe(1)-C(2) 1.800(2), Fe(1)-C(34) 1.809(2), Fe(1)-C(3) 2.4074(19), Fe(1)-C(4) 2.1257(19), Fe(1)-C(5) 2.1065(19), Fe(1)-C(6) 2.1016(19), Fe(1)-C(7) 2.1027(19), C(3)-O(3) 1.230(2).

Crystal Structure of 24b and 24c

Figure 7.11. ORTEP drawing of **24b**. Displacement ellipsoids are at the 30% probability level. H-atoms have been omitted for clarity. Selected bond lengths (Å): Fe(1)-C(1) 1.7678(18), Fe(1)-C(2) 1.7671(17), Fe(1)-C(3) 2.3784(16), Fe(1)-C(4) 2.1442(15), Fe(1)-C(5) 2.0912(15), Fe(1)-C(6) 2.0766(15), Fe(1)-C(7) 2.1758(16), Fe(1)-C(34) 2.0138(17), C(3)-O(3) 1.2444(19).
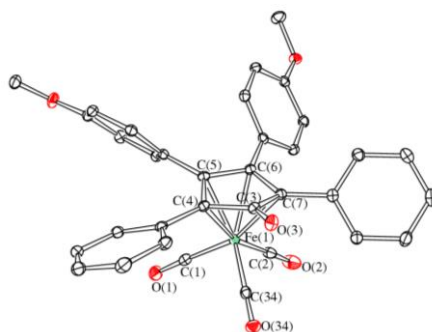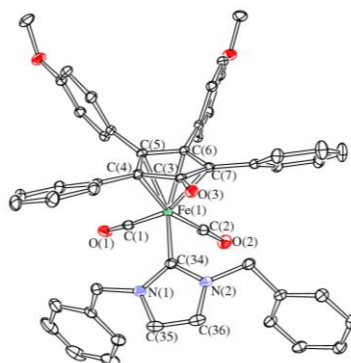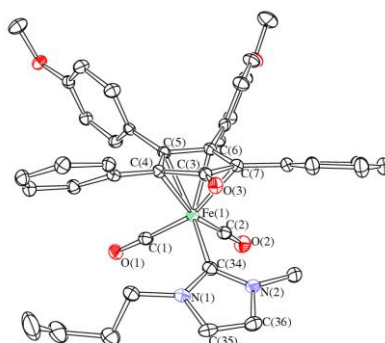

Figure 7.12 ORTEP drawing of **24c**. Displacement ellipsoids are at the 30% probability level. H-atoms have been omitted for clarity. Selected bond lengths (Å): Fe(1)-C(1) 1.764(3), Fe(1)-C(2) 1.766(4), Fe(1)-C(3) 2.392(3), Fe(1)-C(4) 2.161(3), Fe(1)-C(5) 2.079(3), Fe(1)-C(6) 2.082(3), Fe(1)-C(7) 2.168(3), Fe(1)-C(34) 2.000(3), C(3)-O(3) 1.240(4).

X-ray Crystallography

Crystal data and collection details for **22·0.5C₆H₁₄**, **24a·thf·C₆H₁₄**, **24b**, **24c** and **28a** are reported in Table 7.4. The diffraction experiments were carried out on a Bruker APEX II diffractometer equipped with a CCD detector using Mo–Kα radiation. Data were corrected for Lorentz polarization and absorption effects (empirical absorption correction SADABS).[34] Structures were solved by direct methods and refined by full-matrix least-squares based on all data using F^2.[35] All hydrogen atoms were fixed at calculated positions and refined by a riding model. All non-hydrogen atoms were refined with anisotropic displacement parameters.

The C_6H_{14} molecule of **22·0.5C₆H₁₄** is located on an inversion center.

The C_6H_{14} and THF molecules of **24a·thf·C₆H₁₄** are disordered and, therefore, they have been split into two positions each and refined isotropically using one occupancy parameter per disordered group. The disordered molecules have been restrained to have similar geometries (SAME line in SHELXTL; s.u. 0.02) and similar *U* parameters (SIMU line in SHELXTL; s.u. 0.01). Restraints to bond distances were applied as follow (s.u. 0.02): 1.53 Å for C–C and 1.43 Å for C–O in THF and C_6H_{14}.

Table 7.4

*Crystal data and experimental details for **22·0.5C₆H₁₄**, **24a·thf·C₆H₁₄**, **24b**, **24c** and **28a**.*

	22·0.5C₆H₁₄	**24a·thf·C₆H₁₄**
Formula	$C_{37}H_{31}FeO_6$	$C_{48}H_{54}FeN_2O_6$
Fw	627.47	810.78
T, K	100(2)	100(2)
λ, Å	0.71073	0.71073
Crystal system	Monoclinic	Monoclinic
Space group	$P2_1/n$	$P2_1/n$
a, Å	14.3553(2)	9.4831(7)
b, Å	11.8026(2)	23.5286(19)
c, Å	17.6616(3)	19.2990(16)
α, °	90	90
β, °	90.0710(10)	103.518(4)
γ, °	90	90
Cell Volume, Å³	2992.40(8)	4186.8(6)
Z	4	4
D_c, g cm⁻³	1.393	1.286
μ, mm⁻¹	0.552	0.412
F(000)	1308	1720
Crystal size, mm	0.22×0.18×0.14	0.25×0.21×0.16
θ limits, °	1.83–25.03	1.73–26.00
Reflections collected	42504	64046
Independent reflections	5268 [R_{int}= 0.0285]	8231 [R_{int}= 0.0740]
Data / restraints /parameters	5268 / 0 / 397	8231/ 121 / 505

Goodness on fit on F^2	1.024	1.023
R_1 ($I > 2\sigma(I)$)	0.0335	0.0641
wR_2 (all data)	0.0881	0.1870
Largest diff. peak and hole, e Å^{-3}	1.714 / −0.278	1.401 / −0.827

	24b	**24c**	**28a**
Formula	$C_{50}H_{40}FeN_2O_5$	$C_{41}H_{38}FeN_2O_5$	$C_{22}H_{34}FeN_2O_3Si_2$
Fw	804.69	694.58	486.54
T, K	100(2)	100(2)	100(2)
λ, Å	0.71073	0.71073	0.71073
Crystal system	Monoclinic	Monoclinic	Triclinic
Space group	$P2_1/n$	$P2_1/n$	$P\bar{1}$
a, Å	14.8500(8)	12.7360(4)	8.3374(2)
b, Å	15.3813(8)	17.9148(5)	10.1477(3)
c, Å	17.4682(10)	15.2500(4)	15.9325(4)
α, °	90	90	75.869(2)
β, °	101.570(3)	95.190(2)	77.444(2)
γ, °	90	90	76.216(2)
Cell Volume, Å^3	3908.9(4)	3465.22(17)	1251.27(6)
Z	4	4	2
D_c, g cm^{-3}	1.367	1.331	1.291
μ, mm^{-1}	0.439	0.483	0.723
F(000)	1680	1896	516
Crystal size, mm	0.19×0.15×0.12	0.16×0.13×0.10	0.18×0.16×0.11
θ limits, °	1.65–27.00	1.76–26.00	1.34–27.00
Reflections collected	64623	39892	21430
Independent reflections	8525 [R_{int}= 0.0444]	6797 [R_{int}= 0.0844]	5441 [R_{int}= 0.0497]
Data / restraints /parameters	8525 / 0 / 523	6797 / 18 / 442	5441 / 0 / 279
Goodness on fit on F^2	1.015	1.040	1.016
R_1 ($I > 2\sigma(I)$)	0.0336	0.0472	0.0399
wR_2 (all data)	0.0866	0.1309	0.0987
Largest diff. peak and hole, e Å^{-3}	0.370 / −0.428	0.584 / −0.488	0.281 / −0.232

References

1 K. Riener, S. Haslinger, A. Raba, M. P. Hogerl, M. Cokoja, W. A. Herrmann and F. E. Kuhn, *Chem. Rev.*, **2014**, *114*, 5215.

2 (a) C. Bolm, J. Legros, J. Le Paih, and L. Zani, *Chem. Rev.* **2004**, *104*, 6217; (b) B. D. Sherry and A. Fürstner, *Acc. Chem. Res.*, **2008**, *41*, 1500; (c) A. Correa, O. Garcia Mancheño and C. Bolm, *Chem. Soc. Rev.*, **2008**, *37*, 1108; (d) S. Gaillard and J.-L. Renaud, *ChemSusChem*, **2008**, *1*, 505; (e) S. Enthaler, K. Junge and M. Beller, *Angew. Chem., Int. Ed.*, **2008**, *47*, 3317; (f) W. M. Czaplik, M. Mayer, J. Cvengroš and A. J. von Wangelin, *ChemSusChem*, **2009**, *2*, 396; (g) R. H. Morris, *Chem. Soc. Rev.*, **2009**, *38*, 2282; (h) A. Fürstner, *Angew. Chem., Int. Ed.*, **2009**, *48*, 1364; (i) B. A. F. Le Bailly and S. P. Thomas, *RSC Adv.*, **2011**, *1*, 1435; (l) K. Junge, K. Schröder and M. Beller, *Chem. Commun.*, **2011**, *47*, 4849; (m) K. Gopalaiah, *Chem. Rev.*, **2013**, *113*, 3248.

3 (a) A. Quintard and J. Rodriguez, *Angew. Chem. Int. Ed.*, **2014**, *53*, 4044; (b) C. P. Casey and H. Guan, *J. Am. Chem. Soc.* **2007**, *129*, 5816; (c) S. Fleischer, S. S. Zhou, K. Junge and M. Beller, *Angew. Chem. Int. Ed.,* **2013**, *52*, 5120; (d) C. P. Casey and H. Guan, *Organometallics*, **2012**, *31*, 2631; (e) C. P. Casey and H. Guan, *J. Am. Chem. Soc.,* **2009**, *131*, 2499.

4 For selected reviews on NHC: (a) W. A. Herrmann, *Angew. Chem., Int. Ed.,* **2002**, *41*, 1290; (b) R. H. Crabtree, *J. Organomet. Chem.*, **2005**, *690*, 5451; (c) S. Díez-González and S. P. Nolan, *Coord. Chem. Rev.*, **2007**, *251*, 874; (d) O. Kühl, *Chem. Soc. Rev.*, **2007**, *36*, 592; (e) S. T. Liddle, I. S. Edworthy and P. L. Arnold, *Chem. Soc. Rev.*, **2007**, *36*, 1732; (f) F. E. Hahn and M. C. Jahnke, *Angew. Chem., Int. Ed.,* **2008**, *47*, 3122; (g) S. Díez-González, N. Marion and S. P. Nolan, *Chem. Rev.*, **2009***, 109*, 3612; (h) H. Jacobsen, A. Correa, A. Poater, C. Costabile and L. Cavallo, *Coord. Chem. Rev.*, **2009**, *253*, 687; (i) O. Kühl, *Coord. Chem. Rev.*, **2009**, *253*, 2481; (l) L. A. Schaper, S. J. Hock, W. A. Herrmann and F. E. Kühn, *Angew. Chem., Int. Ed.*, **2013**, *52*, 270; (m) D. J. Nelson and S. P. Nolan, *Chem. Soc. Rev.,* **2013**, *42*, 6723; (n) M. N. Hopkinson, C. Richter, M. Schedler and F. Glorius, *Nature*, **2014**, *510*, 485; (o) S. P. Nolan, *N-Heterocyclic Carbenes: Effective Tools for Organometallic Synthesis*, Wiley VCH, **2014**.

5 M. J. Ingleson and R. A. Layfield, *Chem. Commun.*, **2012**, *48*, 3579.

6 (a) D. Bezier, J.-B. Sortais and C. Darcel, *Adv. Synth. Catal.*, **2013**, *355*, 19; (b) S. Warratz, L. Postigo, and B. Royo, *Organometallics*, **2013**, *32*, 893; (c) J. M. S. Cardoso, A. Fernandes, B. de P. Cardoso, M. D. Carvalho, L. P. Ferreira, M. J. Calhorda and B. Royo, *Organometallics*, **2014**, *33*, 5670; (d) R. Lopes, J. M. S. Cardoso, L. Postigo and B. Royo, *Catal Lett*, **2013***, 143*, 1061; (e) J. M.S. Cardoso, R. Lopes and B. Royo *J. Organomet. Chem.*, **2015**, *775*, 173.

7 a) V. V. K. M. Kandepi, J. M. S. Cardoso, E. Peris, and B. Royo, *Organometallics*, **2010**, *29*, 2777; b) T. Hashimoto, S. Urban, R. Hoshino, Y. Ohki, K. Tatsumi and F. Glorius, *Organometallics*, **2012**, *31*, 4474.

8 C. Cesari, S. Conti, S. Zacchini, V. Zanotti, M. C. Cassani and R. Mazzoni, *Dalton Trans.***, 2014**, *43*, 17240.

9 C. Cesari, R. Mazzoni, H. Müller-Bunz and M. Albrecht, *J. Organomet. Chem.*, **2015**, *793*, 256.

10 C. Cesari, L. Sambri, S. Zacchini, V. Zanotti and R. Mazzoni, *Organometallics*, **2014**, *33*, 2814;

11 S. Moulin, H. Dentel, A. Pagnoux-Ozherelyeva, S. Gaillard, A. Poater, L. Cavallo, J.-F. Lohier, and J.-L. Renaud, *Chem. Eur. J.*, **2013**, *19*, 17881

12 (a) H.-J. Knölker, J. Heber and C. H. Mahler, *Synlett*, **1992**, 1002; (b) H.-J. Knölker and J. Heber, *Synlett,* **1993**, 924; (c) H.-J. Knölker, E. Baum and R. Klauss, *Tetrahedron Lett.*, **1995**, *36*, 7647; (d) H.-J. Knölker, H. Goesmann and R. Klauss, *Angew. Chem. Int. Ed.,* **1999**, *38*, 702.

13 H. Allen, O. Kennard, D. G. Watson, L. Brammer A. G. Orpen and R. Taylor, *J. Chem. Soc., Perkin Trans.*, **1987**, *2*, S1-S19.

14 (a) Require electrochemical conditions: B. Liu, Y. Zhang, D. Xu and W. Chen, *Chem. Commun.*, **2011**, *47*, 2883; (b) Polydentate ligands: B. Liu, Q. Xia and W. Chen, *Angew. Chem. Int. Ed.***, 2009**, *48*, 5513. Such findings were later questioned in ref. 17; (c) Polydentate ligands: Z. Lu, S. A. Cramer and D. M. Jenkins, *Chem. Sci.*, **2012**, *3*, 3081; (d) A. Raba, M. Cokoja, S. Ewald, K. Riener, E. Herdtweck, A. Pothig, W. A. Herrmann and F. E. Kuhn, *Organometallics*, **201**2, *31*, 2793.

15 Dinuclear piano stool iron complexes: V. Zanotti, S. Bordoni, L. Busetto, L. Carlucci, A. Palazzi, R. Serra, V. G. Albano, M. Monari and F. Prestopino, *Organometallics*, **1995**, *14*, 5232; first mononuclear piano stool complex: M. H. Quick and R. J. Angelici, *J. Organomet. Chem.*, **1978**, *160*, 231.

16 (a) P. Buchgraber, L. Toupet, and V. Guerchais, *Organometallics,* **2003**, *22*, 5144; (b) L. Mercs, G. Labat, A. Neels, A. Ehlers, and M. Albrecht, *Organometallics*, **2006**, *25*, 5648; (c) L. Mercs, A. Neels, H. Stoeckli-Evans and M. Albrecht, *Dalton Trans.*, **2009**, 7168.

17 J. M. S. Cardoso and B. Royo, *Chem. Commun.*, **2012**, *48*, 4944.

18 B. L. Conley, M. K. Pennington-Boggio, E. Boz, and T. J. Williams, *Chem. Rev.*, **2010**, *110*, 2294.

19 (a) D. G. Gusev, *Organometallics*, **2009**, *28*, 6458; (b) R. Tonner and G. Frenking, *Organometallics*, **2009**, *28*, 3901; (c) A. Furstner, M. Alcarazo, H. Krause and C. W. Lehmann, *J. Am. Chem. Soc.*, **2007**, *129*, 12676.

20 S. A. Moyer, T. W. Funk, *Tetrahedron Letters*, **2010**, *51*, 5430–5433.

21 M. A. Rampi, O. J. A. Schueller and G. M. Whitesides, Appl. Phys. Lett., **1998**, 72, 1781; (b) D. J. Wold, R. Haag, M. A. Rampi and C. D. Frisbie, *J. Phys. Chem. B*, **2002**, *106*, 2813; (c) A. Callegari, M. Marcaccio, D. Paolucci, F. Paolucci, N. Tagmatarchis, D. Tasis, E. Vazquez and M. Prato, *Chem. Commun.*, **2003**, 2576 – 2577.

22 E. Scavetta, R. Mazzoni, F. Mariani, R. G. Margutta, A. Bonfiglio, M. Demelas, S. Fiorilli, M. Marzocchi, B. Fraboni, *J. Mater. Chem. B*, **2014**, 2, 2861–2867.

[23] (a) A. M. Oertel, V. Ritleng, L. Burr, C. Harwig and M. J. Chetcuti, *Organometallics,* **2011**, *30*, 6685; (b) L. B. Benac, E. M. Burgess, L. Burr and A. J. Arduengo, *Organic Syntheses, Coll.*, **1990**, *7*, 195; **1986**, *64*, 92.

[24] S. Patil, J. Claffey, A. Deally, M. Hogan, B. Gleeson, L. M. Menéndez Méndez, H. Müller-Bunz, F. Paradisi and M. Tacke, *Eur. J. Inorg. Chem.,* **201**0*, 7*, 1020.

[25] L. C. Branco, J. N. Rosa, J. J. Moura Ramos and C. A. M. Afonso, *Chem. Eur. J.*, **2002**, *8*, 3671.

[26] L. Busetto, M. C. Cassani, C. Femoni, A. Macchioni, R. Mazzoni and D. Zuccaccia, *J. Organomet. Chem.*, **2008**, *693*, 2579.

[27] (a) L. Jafarpour, E. D. Stevens and S. P. Nolan, *J. Organomet. Chem.*, **2000**, *606*, 49; (b) A. J. Arduengo, R. Krafczyk, H. A. Schmutzler, J. Craig, R. Goerlich, W. J. Marshall and M. Unverzagt, *Tetrahedron*, **199**9, *55*, 14523.

[28] W. Chen and F. Liu, *J. Organomet. Chem.*,**2003**, *673*, 5.

[29] S. Patil, A. Deally, F. Hackenberg, L. Kaps, H. Muller-Bunz, R. Schobert and M. Tacke *Helv. Chim. Acta*, **2011**, *94*, 1551.

[30] S. Hameury, P. de Frémont, P. -A. R. Breuil, H. Olivier-Bourbigou and P. Braunstein, *Dalton Trans.*, **2014**, *43*, 4700.

[31] D. V. Partyka and N. L. Deligonul, *Inorg. Chem.*, **2009**, *48*, 9463.

[32] K. R. J. Thomas, M. Velusamy, J. T. Lin, C. H. Chuen and Y. T. Tao, *J. Mater. Chem.*, **2005**, *15*, 4453.

[33] (a) H. K. Gupta, N. Rampersad, M. Stradiotto and M. J. McGlinchey, *Organometallics*, 2000, *19*, 184; (b) T. Rukachalsirkul, S. Arabl, F. Harstock, N. J. Taylor and A. J. Carty, *Organometallics*, **1984**, *3*, 1587; (c) G. G. Cash and R. C. Pettersen, *Inorg. Chem.*, **1978**, *17*, 650; (d) I. Emme, T. Labahn and A. de Meijere, *Eur. J. Org. Chem.*, **2006**, 399.

[34] Sheldrick, G. M. *SADABS*, Program for empirical absorption correction, University of Göttingen, Germany, **1996.**

[35] Sheldrick, G. M. *SHELX97*, Program for crystal structure determination, University of Göttingen, Germany, **1997.**

CHAPTER VIII

Microwave-assisted synthesis of functionalized Shvo's type complexes

Abstract

A simple and expeditious microwave-assisted procedure for the synthesis of a variety of Shvo's type ruthenium complexes has been developed by reacting $Ru_3(CO)_{12}$ with variously functionalized tetraarylcyclopentadienones under microwave irradiation in MeOH. Ligand precursors have been also prepared under microwave heating by a bis-aldol condensation of 1,3 diphenylacetone with variously functionalized aromatic diketones. All the reactions resulted to be very fast and clean, leading to good yields and selectivities.

Introduction

Hydroxycyclopentadienylruthenium hydride dimer complexes, well known as Shvo's type complexes,[1] have been inspired the work reported in this thesis, since the Shvo catalyst is the one of most relevant example of the bifunctional catalysis and cooperativity of a metal centre (ruthenium) with a non-innocent ligand (cyclopentadienone), based on the cyclopentadienone/hydroxycyclopentadienyl reversible transformation.

As mentioned in Chapter I (paragraph 2.2), Shvo's type complexes are precursors of useful and versatile catalysts, successfully applied in a broad variety of hydrogen-transfer processes, such as hydrogenation of carbonyls and imines, oxidation of alcohols and amines.[2] More recently, applications have been extended to a broader number of reactions including: synthesis of primary amines by using ammonia,[3] biomimetic aerobic oxidation,[4] chemoenzymatic dynamic kinetic resolution of amines,[5] *N*-acylation of heterocycles with aldehydes,[6] ammonia−borane dehydrogenation,[7] and α,β-deuteration of bioactive amines.[8] Furthermore, the catalyst, supported on silica, has been used in the hydroformylation and hydrogenation of propene to butanol[9] and, combined with Rh complexes, it has been exploited in tandem reactions, resulting in the isomerization/hydroformylation/hydrogenation of internal alkenes to yield n-alcohols.[10] Promising perspectives are also in the field of green chemistry, in the transformation of renewable feedstocks,[11] including upgrading of bio-oil by hydrogenation[11a] and selective conversion of levulinic and formic acids into γ-valerolactone.[12]

Stimulated by the possibility to decorate the cyclopentadienyl of Shvo's complexes with various functionalities, we investigated the synthesis of new hydroxypropargyl arylcyclopentadienone ligands. These functionalized tetraarylcyclopentadienones, besides providing a tool for controlling the properties of the catalyst, are themselves fascinating compounds, with interesting properties as organogels,[13] and useful applications in material science.[14]

The considerable potential of the Shvo catalyst, which might be further improved by use of functionalized tetraarylcyclopentadienones, is unfortunately affected by the lack of a simple and efficient synthetic method. Indeed, different synthetic approaches have been developed since its first synthesis,[2a-c,15] but all the reported procedures still require high temperatures and long reaction times.

In this chapter a new rapid, clean and general method for the synthesis of variously functionalized Shvo's type complexes, which takes advantage of microwave heating, is described.

Furthermore, microwave irradiation also provides easier access to the corresponding tetraarylcyclopentadienone ligands.

Results and Discussion

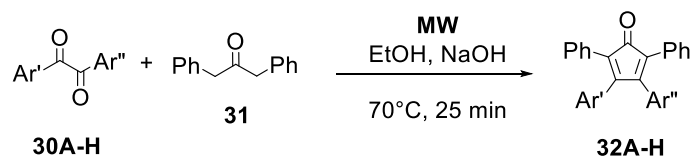## 8.1 Microwave assisted tetraarylcyclopentadienone ligands synthesis

Most common synthetic routes to tetraarylcyclopentadienones involve reaction of diaryl- α-diketones **30** with the diphenylacetone **31**, in the presence of KOH or NaOH, in refluxing EtOH for variable reaction times (2-16h) (Scheme 1).[13,16]

R= H (**30A**, **32A**), OMe (**30B**, **32B**), Br (**30C**, **32C**),

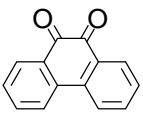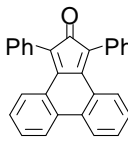(**30D**, **32D**)   (**30E**, **32E**)
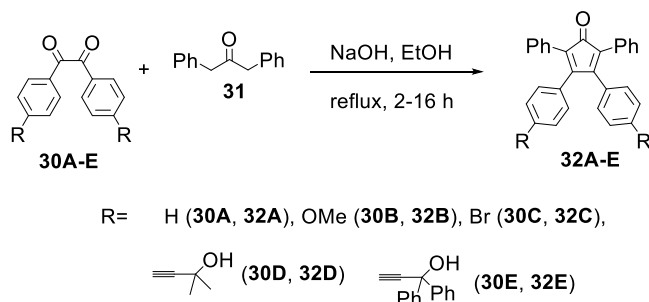
Scheme 8.1: Examples of conventional synthesis of tetraarylcyclopentadienones **32**.

In consideration of the fact that microwave irradiation has proved to be efficient in the acceleration of many organic reactions, becoming a standard tool in organic synthesis,[17] we have applied this technique for the base catalyzed bis-aldol condensation of 1,3 diphenylacetone with α-diketones. As initial approach, we investigated benzil (**30A**, Scheme 8.1) as model substrate to study its condensation with 1,3-diphenylacetone and NaOH, employing EtOH as solvent. The mixture was stirred and heated in a microwave teflon closed reaction vessel. Optimization studies led to identify the best reaction conditions in heating at 70°C for 25 min to obtain tetraphenylcyclopentadienone (**32A**) in 78% yields. No significant variation has been observed leaving the mixture under microwave irradiation for a longer time (*e.g.* 50 min). On the other hand, a shorter reaction time (15 min) did not give complete conversion of the starting material, leading to lower yields (55%). Similar results were observed by lowering the temperature: T = 30 °C, Yield = 27%; T = 50 °C, Yield = 40%. Finally, yields decrease performing the reaction at 120°C (Yield = 32%) due to partial decomposition of the product.

Once established the optimized reaction conditions (T = 70°C and t = 25 min) for the un-functionalized benzil, we investigated the substrate scope with diketones **30B-H** as reported in Table 8.1. We found that the procedure can be extended to several variously substituted diketones in that microwave irradiation affords yields comparable to the classic reflux methods, but with much shorter reaction times. Comparisons with reaction yields reported in the literature are shown in Table 8.1. The only exception is the synthesis of **32H** (Table 8.1, entry 8), which better occurs at room temperature, in that typically suffers from thermal oxidative degradation.[18]

Table 8.1: Scope of the microwave assisted condensation.[a]

Entry	Starting material	Ar'	Ar''	Product	Yield (%)
1	**30A**	Ph	Ph	**32A**	78 (91)[b,19]
2	**30B**	4-MeO-C$_6$H$_4$	4-MeO-C$_6$H$_4$	**32B**	75 (86)[b,16f]
3	**30C**	4-Br-C$_6$H$_4$	4-Br-C$_6$H$_4$	**32C**	70 (85)[b,16e]
4	**30D**	4-(HOMe$_2$C-C≡C)-C$_6$H$_4$	4-(HOMe$_2$C-C≡C)-C$_6$H$_4$	**32D**	58 (60)[b,13]
5	**30E**	4-(HOPh$_2$C-C≡C)-C$_6$H$_4$	4-(HOPh$_2$C-C≡C)-C$_6$H$_4$	**32E**	33 (32)[b,13]
6	**30F**	4-(C$_6$H$_{11}$-C≡C)-C$_6$H$_4$	4-(C$_6$H$_{11}$-C≡C)-C$_6$H$_4$	**32F**	23
7	**30G**	2-Cl-C$_6$H$_4$	3,4-(MeO)$_2$-C$_6$H$_4$	**32G**	25
8	**30H**			**32H**	20 (48, r.t.)[c,18]

a) Reaction conditions: **30** (1.19 mmol), **31** (1 equiv.), NaOH (1 equiv.), 0.1 M in EtOH, T=70 °C, t=25 min; b) In parenthesis, literature yields (when available) for the classical thermal procedure (80°C); c) reaction performed at room temperature.

Results evidence that microwave irradiation promotes a significant acceleration of the reaction. In fact, reaction times, which typically range from 2 to 16 h in the classic thermal methods for the preparation of **32B-E**, are shortened to 25 min in the corresponding microwave assisted procedures.
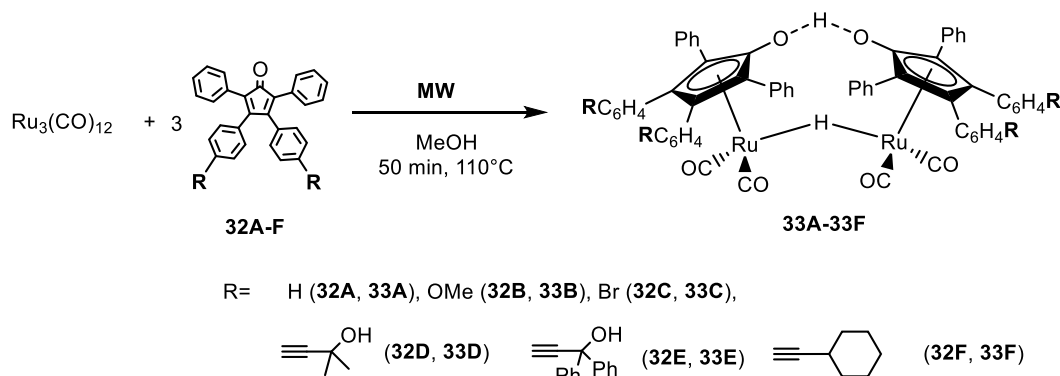
Likewise conventional methods,[16] yields are influenced by the aryl functionalization (Table 1), and the work up procedure is particularly convenient when the products are insoluble in EtOH (**32A-C**, **32F**, **32H**), in that it simply consists of a filtration. Conversely, in the case of soluble products, (**32D-E** and **32G**) purification requires column chromatography on silica gel. All the compounds have been characterized by IR, ¹H- and ¹³C-NMR spectroscopy and by comparison with literature data, when available. For the new compounds **30F**, **32F** and **32G** complete characterization is reported in the experimental section.

8.2 Microwave-assisted synthesis of hydroxycyclopentadienylruthenium hydride dimer (Shvo's type) complexes

The dinuclear complexes **{**[3,4-(R-C$_6$H$_4$)$_2$-2,5-Ph$_2$(η^5-C$_4$CO)]$_2$H**}**Ru$_2$(CO)$_4$(μ-H) [*e.g.* R = H, OMe, Cl] are typically prepared by heating Ru$_3$(CO)$_{12}$ and tetraarylcyclopentadienones in MeOH for 40h. An alternative two-step approach involves the synthesis of the precursor 3,4-(R-C$_6$H$_4$)$_2$-2,5-Ph$_2$(η^4-C$_4$CO)Ru(CO)$_3$, which is subsequently transformed in the corresponding dinuclear Shvo's type complex by a 48 h long reaction in acetone/water in the presence of Na$_2$CO$_3$. The latter method leads to lower yields and more difficult purification of the product.

A drawback of the reported methods [2,15] is the long reaction time that prompted us to explore the potential of microwave heating in the organometallic synthesis of Shvo's type complexes **33**. Indeed, microwave irradiation has been widely used for transition metal catalyzed reactions, but there are few reports about its application in the syntheses of organometallic[20] and coordination[21] compounds. We have found that this technique

impressively reduces the reaction time (from 40 h to 50 min) required for reacting $Ru_3(CO)_{12}$ with tetraarylcyclopentadienones in methanol (12 mL) (Scheme 8.2). It is noteworthy that the syntheses of complexes **33** can be performed with not-anhydrous solvents in air.

R= H (**32A**, **33A**), OMe (**32B**, **33B**), Br (**32C**, **33C**),

≡⟨OH (**32D**, **33D**)   ≡⟨OH Ph Ph (**32E**, **33E**)   ≡⟨⟩ (**32F**, **33F**)

Scheme 8.2. Microwave assisted synthesis of Shvo's type complexes **33A-F.**

First we optimized the synthetic procedure for **33A** by heating a mixture of 3 eq. of tetraphenylcyclopentadienone **32A** with $Ru_3(CO)_{12}$ in MeOH (12 mL) in a teflon closed reaction vessel at variable temperatures and times. Best reaction conditions have been found at 110 °C for 50 min, leading to the complete conversion of $Ru_3(CO)_{12}$ and subsequent isolation of microcrystalline Shvo's complex **33A** by precipitation, filtration and washing with MeOH. Complex **33A** was obtained in about 75% yield.

The substrate scope has been then extended to several tetraarylcyclopentadienones with different R substituents leading to yields comparable or higher with respect to classical methods (Table 8.2). Yields above 70% have been obtained for complexes **33A**, **33B**, **33C** and **33F** (entry 1-3, 6 in Table 8.2), which can be easily separated by precipitation in methanol, whereas complexes containing propargyl substituents (**33D**, **33E**) require separation by column chromatography, leading to lower yields (22-25%: entry 4 and 5 in Table 8.2).

Table 8.2 Scope of the microwave assisted Shvo's complexes synthesis.[a]

Entry	Cyclopentadienone	R	Product	Yield (%)[b,c]
1	**32A**	H-	**33A**	75 (67)
2	**32B**	MeO-	**33B**	73 (70)
3	**32C**	Br-	**33C**	72 (62)
4	**32D**	$(HOMe_2C\text{-}C{\equiv}C)\text{-}$	**33D**	24 (22)
5	**32E**	$(HOPh_2C\text{-}C{\equiv}C)\text{-}$	**33E**	23 (25)
6	**32F**	$(C_6H_{11}\text{-}C{\equiv}C)\text{-}$	**33F**	74 (72)

a) Reaction conditions: $Ru_3(CO)_{12}$ (0.16mmol), **32** (0.48 mmol), MeOH (12 mL), T=110 °C, t=50 min; b) In parenthesis yields for the classical thermal procedure in our hands – in agreement with literature procedures when available (methanol reflux, 40 h); c) **33H** has been also obtained by **32H** in 15% yield, the poor yield is ascribable to the instability of **32H** at high temperatures.[18]

FT-IR spectra of compounds **33** show the typical pattern in the region of CO stretching (*e.g.* for **33C**: v(CO): 2041, 2010, 1982 cm⁻¹). ¹H NMR spectra exhibit the diagnostic signal of the bridging hydride, at about -18 ppm

in CDCl₃ (*e.g.* for **33C**: -18.40), and ^{13}C-NMR spectra are consistent with typical resonances that involve terminal CO (at about 200.20-201.12 ppm), and quaternary carbons of hydroxycyclopentadienyl ligands (*e.g.* C₁-OH = 154.49-155.63; C₂,₅ = 101.88-102.75; C₃,₄ = 87.78-87.88). Signals of alkyne-containing substituents in **33D-33F** present a negligible shift if compared with the corresponding resonances of not coordinated cyclopentadienones (*e.g.* for **32D** vs **33D** the quaternary carbons of the group -C≡CC(CH₃)₂OH resonate at 95.21, 81.79, 65.63[13] and 94,93, 81,59, 65,52 respectively) indicating that formation of the complexes has a little influence on the substituents placed on the five-member ring. ESI-MS allowed to identify the molecular ion of **33C-33H** (see Experimental section).

Suitable crystals for X-Ray analysis have been obtained for **33B** as its **33B·CH₂Cl₂** solvate, and for the new complex **33C** (Figures 8.1 and 8.2). Since structural data for complex **33B** have not been reported previously, its crystallographic structure is herein reported. The structures of **33B** and **33C** are very similar to those previously reported for analogous complexes, for what concern their geometries and bonding parameters and, therefore, they will not be discussed any further.[1a, 15b,d]
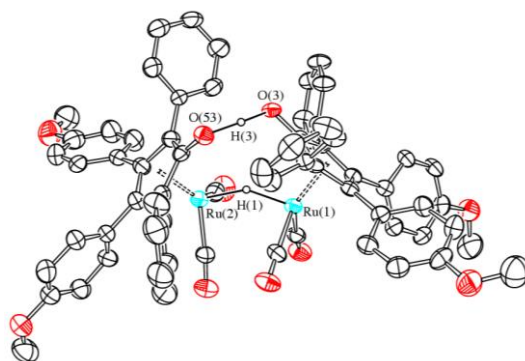
Figure 8.1. ORTEP drawing of **33B** with key atoms labelled. Thermal ellipsoids are at the 30% probability level. H-atoms, apart from H(1) and H(3), have been omitted for clarity. Selected bond lengths (Å) and angles (°): Ru(1)-H(1) 1.68(2); Ru(2)-H(1) 1.68(2); Ru(1)-Cp(av) 2.256(18); Ru(2)-Cp(av) 2.69(2); Ru(1)-CO(av) 1.886(15); Ru(2)-CO(av) 1.880(16); O(3)-H(3) 1.276(18); O(53)-H(3) 1.248(18); Ru(1)-H(1)-Ru(2) 149.8(8); O(3)-H(3)-O(53) 158(7).
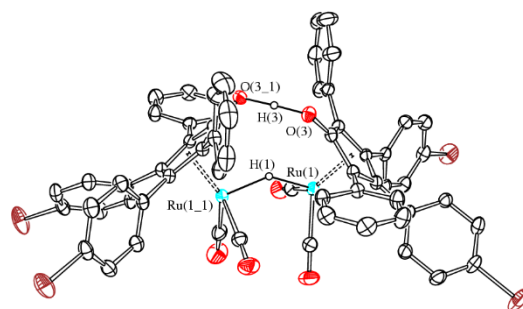
Figure 8.2 ORTEP drawing of **33C** with key atoms labelled. Thermal ellipsoids are at the 30% probability level. H-atoms, apart from H(1) and H(3), have been omitted for clarity. Selected bond lengths (Å) and angles (°): Ru(1)-H(1) 1.724(13); Ru(1)-Cp(av) 2.264(4); Ru(1)-CO(av) 1.895(4); O(3)-H(3) 1.2676(19); Ru(1)-H(1)-Ru(1_1) 140.0(2); O(3)- H(3)-O(3_3) 178(4). Symmetry transformations used to generate equivalent atoms Ru(1_1) and O(53_1): -x,y,-z+1/2.

Conclusions

In this chapter a very efficient procedure for the synthesis of variously functionalized tetraarylcyclopentadienones and the corresponding dinuclear ruthenium hydride Shvo's type complexes based on microwave irradiation has been described. This class of complexes are of great interest in modern homogeneous catalytic processes, with promising applications in biomass conversion into chemicals and bio-fuel. The new synthetic procedure, designed to obtain Shvo complexes provided with different substituents and functional groups, has demonstrated to tolerate various functionalities, avoiding protection and deprotection steps, with consequent advantages in terms of atom economy. The reaction needs a relatively low amount of solvent, and, with few exceptions, does not require long and solvent consuming purification steps. The most relevant advantage is reduction of the reaction time, which in the case of complexes **33**, goes from days (40 h) to minutes (50 min) without affecting the reaction yields. Also the ligand synthesis takes advantage of a significant reduction of solvent used and reaction time, which goes from 2-16 h, under the classic refluxing method, to 25 min under microwave heating. Functionalization toward novel complexes of type **33** containing alkyne and -OH groups should be exploited for Shvo's catalysts immobilization on solid support by means of "click" or "coupling" reactions. In principle, catalyst heterogenization should make easier recover and recycling of the catalyst for industrial applications.

Experimental section

Materials and procedures. Solvents: THF was dried and distilled under nitrogen prior to use, ethanol (EtOH), methanol (MeOH), dichloromethane (CH_2Cl_2), ethyl acetate, diethyl ether, petroleum ether referring to a fraction of bp 60-80 °C, $CDCl_3$ (Sigma Aldrich) and reagents: 1,3-diphenylacetone, benzil, NaOH, 4,4'-dimethoxybenzil, 2-chloro-3',4'-dimethoxybenzil, 9,10-phenanthrenequinone, 2-methyl-3-butin-2-ol, 1,1-diphenyl-2-propyn-2-ol, triethylamine (Et_3N), 2,3-butanedione, 2,3-pentanedione, 1-phenyl-1,2-propanedione, (Sigma Aldrich) 4,4'-dibromobenzil, (Alfa Aesar) dichlorobis-(triphenylphosphine)palladium(II), copper iodide (CuI), triruthenium- dodecacarbonil ($Ru_3(CO)_{12}$) (Strem) have been used as purchased, 4,4'-bis(2-methyl-3-butin-2-ol)-benzil and 4,4'-bis(2-phenyl-3-butin-2-ol)-benzil, have been prepared as previously reported.[13] The prepared derivatives were characterized by spectroscopic methods. ^1H and ^{13}C NMR were measured at rt with 399.9 MHz and 100.6 MHz NMR spectrometer; chemical shifts were referenced internally to residual solvent peaks for ^1H ($CDCl_3$: 7.26 ppm) and ^{13}C NMR ($CDCl_3$: 77.00 ppm); infrared spectra were recorded at 298 K with a FT-IR spectrophotometer. ESI-MS spectra were recorded with samples dissolved in MeOH or CH_3CN.

General procedure for microwave experiments

Microwave reactions were carried out in a "high throughput rotor" microwave oven using Teflon vessels equipped with temperature sensor and pressure control. The instrument power has been set at maximum 600 W. The instrument has been programmed in order to reach the reaction temperature within 5 min and to keep it for the required reaction time. Thereafter the irradiation was stopped and the sample cooled down to room temperature.

All the experiments have been followed by temperature and pressure control while the power of pulsed microwave irradiation is automatically modulated by the instrument in order to follow the desired temperature program. All the experiments herein discussed registered a microwave power plot in the range between 0 and 100 W.

General procedure for the microwave assisted synthesis of cyclopentadienones (32).

Into a 75 mL Teflon vessel with a magnetic stirrer were placed α-diketone **30** (1.19 mmol), 1,3-diphenylacetone **31** (0.250 g, 1.19 mmol), 12 mL of EtOH and NaOH (0.0479 g, 1.19 mmol). The vessel was sealed with a lid equipped with a temperature sensor and placed in the microwave oven. The reaction mixture was heated for 25 min at 70 °C. The dark-purple product was purified by filtration when solid, or by column chromatography. Spectral data for new compounds are reported.

Tetraphenylcyclopentadienone (**32A**) Reactants: benzil (**30A**) (0.250 g, 1.19 mmol), 1,3-diphenylacetone **31** (0.250 g, 1.19 mmol), 12 mL of EtOH and NaOH (0.0479 g, 1.19 mmol). The dark-purple crystalline solid was purified by filtration and washed three times with 5 mL of EtOH (0.357 g, 78% yield).

3,4-Bis(4-methoxyphenyl)-2,5-diphenylcyclopenta-2,4-dienone (**32B**) Reactants: 4,4'-dimethoxybenzil (**30B**) (0.490 g, 1.81 mmol), 1,3-diphenylacetone **31** (0.380 g, 1.81 mmol), NaOH (0.0724 g, 1.81 mmol). Dark-purple crystalline solid purified by filtration (0.607 g, 75% yield).

3,4-Bis(4-Bromophenyl)-2,5-diphenylcyclopenta-2,4-dienone (**32C**) Reactants: 4,4'-dibromobenzil (**30C**) (0.452 g, 1.23 mmol), 1,3-diphenylacetone **31** (0.261 g, 1.23 mmol), NaOH (0.0492 g, 1.23 mmol). Dark-purple crystalline solid purified by filtration (0.471g, 70% yield).

3,4-Bis(4-(3-hydroxy-3-methylbut-1-ynyl)phenyl)-2,5-diphenylcyclopenta-2,4-dienone (**32D**) Reactants: 4,4'-bis(2-methyl-3-butin-2-ol)-benzil (**30D**) (0.307 g, 0.820 mmol), 1,3-diphenylacetone **31** (0.172 g, 0.820 mmol), NaOH (0.0328 g, 0.820 mmol). Dark-purple solid: purified by chromatography on silica gel (CH$_2$Cl$_2$/ethylacetate: 95/5) (0.261 g, 58% yield).

3,4-Bis(4-(3-hydroxy-3,3-diphenyl-prop-1-ynyl)phenyl)-2,5-diphenylcyclopenta-2,4-dienone (**32E**) Reactants: 4,4'-bis(2-phenyl-3-butin-2-ol)-benzil (**30E**) (0.761 g, 1.22 mmol), 1,3-diphenylacetone **2** (0.262 g, 1.22 mmol), NaOH (0.0490 g, 1.22 mmol). Dark-purple solid: purified by chromatography on silica gel (CH$_2$Cl$_2$) (0.320 g, 33% yield).

4,4'-bis(cyclohexylethynyl)benzil (**30F**) 4,4'-dibromobenzil (**30B**) (0.500 g, 1.22 mmol) and cyclohexylacetylene (0.385 mL, 2.99 mmol) were dissolved in 50 mL of THF in a two neck round bottom flask under nitrogen atmosphere. Dichlorobis-(triphenylphosphine)palladium(II) (0.168 g, 0.240 mmol), CuI (0.0473 g, 0.251 mmol) and Et$_3$N (5 mL) were added and the mixture was stirred for 1 h at room temperature. Then the solvent was removed under vacuum and the crude was purified by chromatography on silica gel (petroleum ether/Et$_2$O=95/5) giving the desired product 4,4'-bis(cyclohexylethynyl)benzil (**30F**) (0.478 g, 82% yields) as a pale yellow solid. ^{1}H-NMR (399.9 MHz, CDCl$_3$) δ 7.79 (d, $J_{H,H}$=8.7, 4H, CH$_{aryl}$), 7.49 (d, $J_{H,H}$=8.7, 4H, CH$_{aryl}$), 2.60-2.45 (m, 2H), 1.85-1.55 (m, 8H), 1.55-1.15 (m, 12H); ^{13}C-{^{1}H}NMR (100.6 MHz, CDCl$_3$) δ 193.8 (C=O), 132.0 (CH), 131.4 (C), 131.2 (C), 129.7 (CH), 100.0 (C), 80.1 (C), 32.4 (CH$_2$), 29.8 (CH), 25.8 (CH$_2$), 24.8 (CH$_2$). IR (CH$_2$Cl$_2$): υ(C=O): 1673 cm^{-1}. GC-MS: 423 (M+1). Anal. Calcd (%) for C$_{30}$H$_{30}$O$_2$: C, 85.27; H, 7.16. Found: C, 85.23; H 7.18.

3,4-bis-[4-(cyclohexylethynyl)phenyl]-2,5-diphenylcyclopenta-2,4-dienone (**32F**) Reactants: 4,4'-bis(cyclohexylethynyl)benzil (**30F**) (0.100 g, 0.240 mmol), 1,3-diphenylacetone **2** (0.0494 g, 0.240 mmol), NaOH (0.0096 mg, 0.240 mmol). Dark purple solid purified by filtration (0.0330 g, 23% yield). ^{1}H-NMR (399.9 MHz, CDCl$_3$) δ 7.20–7.10 (m, 14H, CH$_{aryl}$), 6.76 (d, $J_{H,H}$=8.7, 4H, CH$_{aryl}$), 2.55-2.45 (m, 2H), 1.85-1.60 (m, 8H), 1.55-1.20 (m, 12H); ^{13}C-{^{1}H}NMR (100.6 MHz, CDCl$_3$) δ 199.9 (C=O), 153.6 (C), 132.0 (C), 131.3 (CH), 130.5 (C), 130.1 (CH), 129.3 (CH), 128.1 (CH), 127.6 (CH), 125.5 (C), 124.3 (C), 96.1 (C), 80.3 (C), 32.6 (CH$_2$), 29.7 (CH), 25.9 (CH$_2$), 24.9 (CH$_2$). IR (CH$_2$Cl$_2$): υ(C=O): 1712 cm^{-1}. GC-MS: 598 (M+1). Anal. Calcd for C$_{45}$H$_{40}$O: C, 90.56; H, 6.76. Found: C, 90.50; H, 6.75.

3-(2-chlorophenyl)-4-(3,4-dimethoxyphenyl)-2,5-diphenylcyclopenta-2,4-dienone (**32G**) Reactants: 2-chloro-3',4'-dimethoxybenzil (**30G**) (0.366 g, 1.19 mmol), 1,3-diphenylacetone **31** (0.250 g, 1.19 mmol), NaOH (0.0479 g, 1.19 mmol). Dark purple solid purified by chromatography on silica gel (CH$_2$Cl$_2$/petroleum ether=9/1) (0.142 g, 25% yield). ^{1}H-NMR (399.9 MHz, CDCl$_3$) δ 7.30–7.00 (m, 17H, CH$_{aryl}$), 3.71 (s, 3H, OMe), 3.30 (s, 3H, OMe); ^{13}C-{^{1}H}NMR (100.6 MHz, CDCl$_3$) δ 200.0 (C=O), 154.4 (C), 152.3 (C), 149.3 (C), 148.0 (C), 134.1 (C), 133.7 (C), 131.1 (C), 130.6 (C), 130.3 (CH), 130.2 (CH), 129.8 (CH), 129.7 (CH), 129.3 (CH), 128.13 (CH), 128.09 (CH), 127.9 (C), 127.8 (CH), 127.4 (CH), 126.9 (CH), 125.4 (C), 123.6 (C), 122.4 (CH), 112.0 (CH), 110.5 (CH), 55.7 (CH$_3$), 55.4 (CH$_3$). IR (CH$_2$Cl$_2$): υ(C=O): 1713 cm^{-1}. GC-MS: 480 (M+1). Anal. Calcd for C$_{31}$H$_{23}$ClO$_3$: C, 77.74; H, 4.84. Found: C, 77.82; H, 4.85.

1,3-Diphenyl-2*H***-cyclopenta[l]phenanthrene-2-one** (**32H**) Reactants: 9,10-Phenanthrenequinone (**30H**) (0.248 g, 1.19 mmol), 1,3-diphenylacetone **31** (0.250 g, 1.19 mmol), NaOH (0.0479 g, 1.19 mmol). The dark-green crystalline solid (0.0909 g, 20% yield) was purified by filtration.

General procedure for the microwave assisted synthesis of Shvo's type complexes {[3,4-(R-C$_6$H$_4$)$_2$-2,5-Ph$_2$(η^5-C$_4$CO)]$_2$H}Ru$_2$(CO)$_4$(μ-H) (4).

Into a 75 mL Teflon vessel with a magnetic stirrer were placed tetraarylcyclopentadienone **32** (3 eq.), Ru$_3$(CO)$_{12}$ (1 eq.), methanol (12 mL). The vessel was sealed with a lid equipped with a temperature sensor and placed in the microwave oven. The reaction mixture was heated for 50 min at 110 °C.

{[2,3,4,5-Ph$_4$(η^5-C$_4$CO)]$_2$H}Ru$_2$(CO)$_4$(μ-H) (33A) Reactants: tetraphenylcyclopentadienone **32A** (0.180 g, 0.48 mmol), Ru$_3$(CO)$_{12}$ (0.100g, 0.16mmol), methanol (12 mL). The complex **33A** was purified by filtration (0.260 g, 75% yield). The purity of the product was verified by comparison of ^{1}H, ^{13}C-NMR and IR spectra with literature data.[15] The same reaction was performed under classic heating method (methanol, 80°C, 40 h) leading to a yield of 67%.

{[3,4-(OMe-C$_6$H$_4$)$_2$-2,5-Ph$_2$(η^5-C$_4$CO)]$_2$H}Ru$_2$(CO)$_4$(μ-H) (33B) Reactants: 3,4-Bis(4-methoxyphenyl)-2,5-diphenylcyclopenta-2,4-dienone **32B** (0.213g, 0.48 mmol), Ru$_3$(CO)$_{12}$ (0.100g, 0.16mmol), methanol (12 mL). The complex **33B** was purified by filtration (0.211 g, 73% yield). The purity of the product was verified by comparison of ^{1}H, ^{13}C-NMR and IR spectra with literature data.[15] Suitable crystals of **33B** were obtained by precipitation from MeOH. The same reaction was performed under classic heating method (methanol, 80°C, 40 h) leading to a yield of 70%.

{[3,4-(Br-C$_6$H$_4$)$_2$-2,5-Ph$_2$(η^5-C$_4$CO)]$_2$H}Ru$_2$(CO)$_4$(μ-H) (33C) Reactants: 3,4-Bis(4-Bromophenyl)-2,5-diphenylcyclopenta-2,4-dienone **32C** (0.260g, 0.48 mmol), Ru$_3$(CO)$_{12}$ (0.100g, 0.16mmol), methanol (12 mL). The complex **33C** was purified by filtration (0.242 g, 72% yield). Suitable crystal of **33C** were obtained by precipitation from MeOH. ^{1}H-NMR (399.9 MHz, CDCl$_3$) δ 7.45-6.85 (m, 36H, CH$_{aryl}$), 3.43 (s, 1H, OH), -18.40 (s, 1H, RuHRu); ^{13}C-{^{1}H}NMR (100.6 MHz, CDCl$_3$) δ 200.20 (CO), 154.49 (C$_1$-OH, Cp), 130.96-127.13 (Cq$_{aryl}$ and CH$_{aryl}$), 101.88 (C$_{2,5}$; Cp), 87.84 (C$_{3,4}$; Cp); IR (CH$_2$Cl$_2$) ν(CO): 2041, 2010, 1982 cm^{-1}; ESI-MS (CH$_3$OH, m/z) =1399 [M+H]$^+$, 1421 [M+Na]$^+$. Anal. Calcd (%) for C$_{62}$H$_{38}$Br$_4$O$_6$Ru$_2$: C, 53,22; H, 2.78. Found: C, 53,34; H, 2,76. The same reaction was performed under classic heating method (methanol, 80°C, 40 h) leading to a yield in **33C** of 62%.

{[3,4-(4-C≡CC(CH$_3$)$_2$OH-C$_6$H$_4$)$_2$-2,5-Ph$_2$(η^5-C$_4$CO)]$_2$H}Ru$_2$(CO)$_4$(μ-H) (33D) Reactants: 3,4-bis(4-(3-hydroxy-3-methylbut-1-ynyl)phenyl)-2,5-diphenylcyclopenta-2,4-dienone **32D** (0.263 g, 0.48 mmol), Ru$_3$(CO)$_{12}$ (0.100g, 0.16mmol), methanol (12 mL). The complex {[3,4-(4-C≡CC(CH$_3$)$_2$OH-C$_6$H$_4$)$_2$-2,5-Ph$_2$(η^5-C$_4$CO)]$_2$H}Ru$_2$(CO)$_4$(μ-H) (**33D**), soluble in MeOH, was purified by column chromatography on silica gel (eluent: CH$_2$Cl$_2$/EtOAc 95:5), (0,081 g, 24% yield). ^{1}H-NMR (399.9 MHz, CDCl$_3$) δ 7,62-6,89 (m, 36H, CH$_{aryl}$); 1,55 (s, 24H, CH$_3$); -18,38 (s, 1H, RuHRu); OH variable. ^{13}C-{^{1}H}NMR (100.6 MHz, CDCl$_3$) δ 201,12 (CO); 155,52 (C$_1$-OH, Cp); 131,81-126,75 (CH$_{aryl}$ and Cq$_{aryl}$); 102,48 (C$_{2,5}$; Cp); 94,93 (-*C*≡CC(CH$_3$)$_2$OH); 87,78 (C$_{3,4}$; Cp); 81,59 (-C≡*C*C(CH$_3$)$_2$OH); 65,52 (-C≡C*C*(CH$_3$)$_2$OH); 31,37 (CH$_3$). IR (CH$_2$Cl$_2$) ν(CO): 2040; 2011; 1981 cm^{-1}. ESI-MS (m/z) (-) = 1413 [M - H]$^-$. Anal. Calcd (%) for C$_{82}$H$_{66}$O$_{10}$Ru$_2$: C, 69.59; H, 4.67. Found: C, 69.69; H, 4,65.

The same reaction was performed under classic heating conditions (methanol, 80°C, 40 h) leading to a yield in **33D** of 22%.

{[3,4-(4-C≡CC(Ph)₂OH-C₆H₄)₂-2,5-Ph₂(η⁵-C₄CO)]₂H}Ru₂(CO)₄(μ-H) (**33E**) Reactants: 3,4-bis(4-(3-hydroxy-3,3-diphenyl-prop-1-ynyl)phenyl)-2,5-diphenylcyclopenta-2,4-dienone **32E** (0.382 g, 0.48 mmol), Ru₃(CO)₁₂ (0.100g, 0.16mmol), methanol (12 mL). The complex {[3,4-(4-C≡CC(Ph)₂OH-C₆H₄)₂-2,5-Ph₂(η⁵-C₄CO)]₂H}Ru₂(CO)₄(μ-H) (**33E**), soluble in MeOH, was purified by column chromatography on silica gel (eluent: CH₂Cl₂/EtOAc 95:5), (0,105 g, 23% yield). ^{1}H-NMR (399.9 MHz, CDCl₃) δ (ppm): 8.08-6.72 (m, 76H, CH$_{aryl}$); -18.42 (s, 1H, RuHRu); OH variable. ^{13}C-{^{1}H}NMR (100.6 MHz, CDCl₃) δ 201,32 (CO); 155,63 (C₁-OH, Cp); 144,82 (C$_{ipso}$, -(Ph)₂OH) 133,30-126,02 (CH$_{aryl}$ and Cq$_{aryl}$); 102,75 (C$_{2,5}$; Cp); 94,22 (-*C*≡CC(CH₃)₂OH); 87,88 (C$_{3,4}$; Cp); 86,92 (-C≡*C*C(Ph)₂OH); 74,85 (-C≡C*C*(Ph)₂OH). IR (CH₂Cl₂) ν(CO): 2039; 2010; 1981 cm^{-1}. ESI-MS (m/z) (-) = 1909 [M - H]⁻. Anal. Calcd (%) for C₁₂₂H₈₂O₁₀Ru₂: C, 76.65; H, 4.29. Found: C, 76.58; H, 4,32. The same reaction was performed under classic heating method (methanol, 80°C, 40 h) leading to a yield in **33E** of 25%.

{[3,4-(4-(C₆H₁₁-C≡C)-C₆H₄)₂-2,5-Ph₂(η⁵-C₄CO)]₂H}Ru₂(CO)₄(μ-H) (**33F**) Reactants: 3,4-bis-[4-(cyclohexylethynyl)phenyl]-2,5-diphenylcyclopenta-2,4-dienone **33F** (0.287 g, 0.48 mmol), Ru₃(CO)₁₂ (0.100g, 0.16mmol), methanol (12 mL). The complex {[3,4-(4-(C₆H₁₁-C≡C)-C₆H₄)₂-2,5-Ph₂(η⁵-C₄CO)]₂H}Ru₂(CO)₄(μ-H) (**33F**) was purified by filtration (0.268 g, 74% yield). ^{1}H-NMR (399.9 MHz, CDCl₃) δ (ppm): 7.41-6.82 (m, 36H, CH$_{aryl}$); 2.52-1.05 (m, 44H, cyclohexane), -18.46 (s, 1H, RuHRu); OH variable. ^{13}C-{^{1}H}NMR (100.6 MHz, CDCl₃) δ 201,04 (CO); 155,11 (C₁-OH, Cp); 132.0 -124.3 (CH$_{aryl}$ and Cq$_{aryl}$), 102,63 (C$_{2,5}$; Cp); 95.7, 81.0 (-C≡C-), 88,01 (C$_{3,4}$; Cp); 33.0 (CH₂), 29.7 (CH), 26.0 (CH₂), 24.9 (CH₂). IR (CH₂Cl₂) ν(CO): 2037; 2019; 1976 cm^{-1}. ESI-MS (m/z) (+) = 1511 [M + H]⁺. Anal. Calcd (%) for C₉₄H₈₂O₆Ru₂: C, 74.70; H, 5.43. Found: C, 74.77; H, 5.38. The same reaction was performed under classic heating method (methanol, 80°C, 40 h) leading to a yield in **33F** of 72%.

{[3,4-phenanthren-2,5-Ph₂(η⁵-C₄CO)]₂H}Ru₂(CO)₄(μ-H) (**33H**) Reactants: 1,3-Diphenyl-2*H*-cyclopenta[l]phenanthren-2-one **32H** (0.183 g, 0.48 mmol), Ru₃(CO)₁₂ (0.100g, 0.16mmol), methanol (12 mL). The complex **33H** was purified by filtration (0.039 g, 15% yield). ^{1}H-NMR (399.9 MHz, CDCl₃)δ 8.83-7.17 (m, 36H, CH$_{aryl}$), -19.68 (s, 1H, RuHRu), OH variable; IR (CH₂Cl₂) ν(CO): 2037, 2008, 1981cm^{-1}; ESI-MS (CH₃OH, m/z) =1083 [M+H]⁺. Anal. Calcd (%) for C₆₂H₃₈O₆Ru₂: C, 68.76; H, 3.51. Found: C, 68.88; H, 3.49.

X-ray Crystallography

Crystal data and collection details for **33B·CH₂Cl₂** and **33C** are reported in Table 8.3. The diffraction experiments were carried out on a diffractometer equipped with a CCD detector using Mo–Kα radiation. Data were corrected for Lorentz polarization and absorption effects (empirical absorption correction SADABS).[22] Structures were solved by direct methods and refined by full-matrix least-squares based on all data using F^2.[23] All hydrogen atoms were fixed at calculated positions and refined by a riding model, except H(1) and H(3) in both structures which were located in the Fourier map and refined isotropically using the 1.2 fold U_{iso} value of the parent atoms. All non-hydrogen atoms were refined with anisotropic displacement parameters.

33B·CH₂Cl₂: The asymmetric unit of the unit cell contains one **33B** complex and one CH₂Cl₂ molecule (all located on general positions). The CH₂Cl₂ molecule is disordered over three independent positions and, therefore, it has been split and refined isotropically using one occupancy parameter per disordered group; the sum of the site occupation factors of the three images has been restrained to unit (SUMP 1.0 0.001 1.0 2 1.0

3 1.0 4 line in SHELXL). Some C and O atoms of **33B** have been restrained to isotropic behaviour (ISOR line in SHELXL, s.u. 0.01). The Ru(1)-H(1) and Ru(2)-H(1) distances have been restrained to be similar (SADI line in SHELXL, s.u. 0.01); the same restraint has been applied also to the O(3)-H(3) and O(53)-H(3) distances. The three images of CH_2Cl_2 have been restrained to have similar geometries (SAME line in SHELXL, s.u. 0.02) and similar *U* parameters (SIMU line in SHELXL, s.u. 0.02). Restraints to bond distances were applied as follow (s.u. 0.02): 1.75 Å for C–Clin CH_2Cl_2.

33C: The asymmetric unit of the unit cell contains half of a complex molecule located on a 2-fold axis passing through H(1) and H(3).

Table8.3. Crystal data and experimental details for **33B·CH₂Cl₂** and **33C**.

	33B·CH₂Cl₂	**33C**
Formula	$C_{67}H_{52}Cl_2O_{10}Ru_2$	$C_{62}H_{38}Br_4O_6Ru_2$
Fw	1290.13	1400.70
T, K	293(2)	294(2)
λ, Å	0.71073	0.71073
Crystal system	Triclinic	Monoclinic
Space group	$P\bar{1}$	$C2/c$
a, Å	11.5361(19)	27.2316(18)
b, Å	17.408(3)	9.6582(6)
c, Å	17.936(5)	20.5820(13)
α, °	118.895(3)	90
β, °	97.620(3)	100.8750(10)
γ, °	101.411(2)	90
Cell Volume, Å³	2979.9(10)	5316.0(6)
Z	2	4
D_c, g cm⁻³	1.438	1.750
μ, mm⁻¹	0.655	3.628
F(000)	1312	2744
Crystal size, mm	0.19×0.16×0.12	0.21×0.16×0.14
θ limits, °	1.34–25.03	1.52–25.99
Reflections collected	28343	26736
Independent reflections	10500 [R_{int}= 0.0942]	5212 [R_{int}= 0.0222]
Data / restraints /parameters	10500 / 148 / 748	5212 / 0 / 336
Goodness on fit on F²	0.978	1.025
R_1 (*I*> 2σ(*I*))	0.0726	0.0266
wR_2 (all data)	0.2177	0.0722
Largest diff. peak and hole, e Å⁻³	1.295 / –0.516	0.728 / –0.679

References

[1] a) Shvo, Y.; Czarkie, D.; Rahamim, Y. *J. Am. Chem. Soc.* **1986**, *108*, 7400; b) Blum, Y.; Czarkie, D.; Rahamin, Y.; Shvo Y. *Organometallics* **1985**, *4*, 1459.

[2] a) Warner, M. C.; Casey, C. P.; Backvall, J.-E. *Top. Organomet. Chem.* **2011**, *37*, 85; b) Conley, B. L.; Pennington-Boggio, M. K.; Boz, E.; Williams, T. J. *Chem. Rev.* **2010**, *110*, 2294; c) Karvembu, R.; Prabhakaran, R.; Natarajan, N. *Coord. Chem. Rev.* **2005**, *249*, 911; d) Casey, C. P.; Johnson, J. B.; Singer, S. W.; Cui, Q. *J. Am. Chem. Soc.* **2005**, *127,* 3100; e) Casey, C. P.; Bikzhanova, G. A.; Cui, Q.; Guzei, I. A. *J. Am. Chem. Soc.* **2005**, *127*, 14062; f) Samec, J. S. M.; Ell, A. H.; Aberg, J. B.; Privalov, T.; Eriksson, L.; Backvall, J. E. *J. Am. Chem. Soc.* **2006**, *128*, 14293; d) Casey, C. P.; Clark, T. B.; Guzei, I. A. *J. Am. Chem. Soc.* **2007**, *129*, 11821; g) Casey, C. P.; Beetner, S. E.; Johnson, J. B. *J. Am. Chem. Soc.* **2008**, *130*, 2285; h) Casey, C. P.; Guan, H. *Organometallics* **2012**, *31*, 2631; i) Johnson, J. B.; Backvall, J. E. *J. Org. Chem.* **2003**, *68*, 7681; l) Casey, C. P.; Bikzhanova, G. A.; Backvall, J. E.; Johansson, L.; Park, J.; Kim, Y. H.; *Organometallics* **2002**, *21*, 1955; m) Comas-Vives, A.; Ujaque, G.; Lledos, A. *Organometallics* **2007**, *26,* 4135; n) Comas-Vives, A.; Ujaque, G.; Lledos, A. *Organometallics* **2008**, *27,* 4854; o) Zhang, X.; Guo, X.; Chen, Y.; Tang, Y.; Lei, M.; Fang, W. *Phys. Chem. Chem. Phys.* **2012**, *14*, 6003; p) Hollmann, D.; Jiao, H.; Spannenberg, A.; Bahn, S.; Tillack, A.; Parton, R.; Altink, R.; Beller, M. *Organometallics* **2009**, *28,* 473.

[3] Bahn, S.; Imm, S.; Neubert, L.; Zhang, M.; Neumann, H.; Beller, M. *Chem. Eur. J.* **2011**, *17*, 4705.

[4] Babu, B. P.; Endo, Y.; Backvall, J.-E. *Chem. Eur. J.* **2012**, *18*, 11524.

[5] Vaz, B. G.; Milagre, C. D. F.; Eberlin, M. N.; Milagre, H. M. S. *Org. Biomol. Chem.* **2013**, *11*, 6695.

[6] Zhang, J.; Hong, S. H. *Org. Lett.* **2012**, *14*, 4646.

[7] Lu, Z.; Conley, B. L.; Williams, T. J. *Organometallics* **2012**, *31*, 6705.

[8] Neubert, L.; Michalik, D.; Bahn, S.; Imm, S.; Neumann, H.; Atzrodt, J.; Derdau, V.; Holla, W.; Beller, M. *J. Am. Chem. Soc.* **2012**, *134*, 12239.

[9] Hanna, D. G.; Shylesh, S.; Parada, P. A.; Bell, A. T. *J. Catal.* **2014**, *311*, 52.

[10] Yuki, Y.; Takahashi, K.; Tanaka, Y.; Nozaki, K. *J. Am. Chem. Soc.* **2013**, *135*, 17393.

[11] a) Busetto, L.; Fabbri, D.; Mazzoni, R.; Salmi, M.; Torri, C.; Zanotti, V. *Fuel* **2011**, *90*, 1197; b) Pasini, T.; Solinas, G.; Zanotti, V.; Albonetti, S.; Cavani, F.; Vaccari, A.; Mazzanti, A.; Ranieri, S. Mazzoni, R. *Dalton Trans.*, **2014**, *Accepted Manuscript* , DOI: 10.1039/C4DT00304G

[12] Fabos, V.; Mika, L. T.; Horvath, I. T. *Organometallics* **2014**, *33*, 181.

[13] Boiani, M.; Baschieri, A.; Cesari, C.; Mazzoni, R.; Stagni, S.; Zacchini, S.; Sambri, L. *New J. Chem.* **2012**, *36*, 1469.

[14] a) Qin, T.; Zhou, G.; Scheiber, H.; Bauer, R. E.; Baumgarten, M.; Anson, C. E.; List, E. J. W.; Müllen, K. *Angew. Chem., Int. Ed.* **2008**, *47*, 8292; b) Liang, Y.; Schwab, M. G.; Zhi, L.; Mugnaioli, E.; Kolb, U.; Feng, X.; Müllen, K. *J. Am. Chem. Soc.* **2010**, *132*, 15030. c) Qin, T.; Ding, J.; Wang, L.; Baumgarten, M.; Zhou, G.; Müllen, K. *J. Am. Chem. Soc.* **2009**, *131*, 14329. d) Zhi, L.; Wu, J.; Müllen, K. *Org. Lett.* **2005**, *7*, 5761; e) Bauer, R.; Liu, D.; Heyen, A. V.; Schryver, F. D.; Feyter, S. D.; Müllen, K. *Macromolecules* **2007**, *40,* 4753.

[15] see for example: a) Matute, M.; Backvall, J. E. *J. Org. Chem* **2004**, *69*, 9191; b) Casey, C. P.; Singer, S.; Powell, D. R.; Hayashi, R. K.; Kavana, M. *J. Am. Chem. Soc.* **2001**, *123*, 1090; c) Menashe, N.; Salant, E.; Shvo, Y. *J. Organomet. Chem.* **1996**, *514*, 97; d) Thalen, L. K.; Zhao, D.; Sortais, J. B.; Paetzold, J.; Hoben, C.; Backwall, J. E. *Chem. Eur. J.* **2009**, *15*, 3402.

[16] a) Gourdon, A. *Eur. J. Org. Chem.* **1998**, 2797; b) Bernhardt, S.; Baumgarten, M.; Wagner, M.; Müllen, K. *J. Am. Chem. Soc.* **2005**, *127*, 12392; c) Shifrina, Z. B.; Rajadurai, M. S.; Firsova, N. V.; Bronstein, L. M.; Huang, X.; Rusanov, A. L.; Müllen, K. *Macromolecules* **2005**, *38,* 9920; d) Sadhukhan, S. K.; Viala, C.; Gourdon, A. *Synthesis* **2003**, 1521; e) Maly, K. E.; Gagnon, E.; Maris, T.; Wuest, J. D. *J. Am. Chem. Soc.* **2007**, *129*, 4306. f) Thomas, K. R. J.; Velusamy, M.; Lin, J. T.; Chuen, C. H.; Tao, Y. T. *J. Mater. Chem.* **2005**, *15*, 4453.

[17] See for example: a) Loupy, A. In *Microwaves in Organic Synthesis*; Wiley-VCH: Weinheim, Germany, 2002; b) Kappe, C. O. *Angew. Chem., Int. Ed.* **2004**, *43*, 6250; c) Roberts, B. A.; Strauss, C. R. *Acc. Chem. Res.* **2005**, *38*, 653; e) Polshettiwar, V.; Varma, R. S. *Acc. Chem. Res.* **2008**, *41*, 629; f) Kappe, C. O.; Stadler, A. In *Microwaves in Organic and Medical Chemistry*, Wiley-VCH: Weinheim, Germany, 2005; g) Kappe, C. O.; Pieber, B.; Dallinger, D. *Angew. Chem. Int. Ed.* **2013**, *52*, 1088.

[18] Marchand, A. P.; Srinivas, G.; Watson, W. H. *Arkivoc* **2003**, (*iii*), 8.

[19] Johnson, J. R.; Grummitt, O. *Organic Syntheses Coll.* **1955**, *3*, 806.

[20] see for examples: a) Tonneman, J.; Risse, J.; Grote, Z.; Scopelliti, R.; Severin, K. *Eur. J. Inorg. Chem.* **2013**, 4558; b) Albrecht, C.; Gauthier, S.; Wolf, J. ; Scopelliti, R. K. Severin, *Eur. J. Inorg. Chem.* **2009**, 1003; c) Garringer, S. M.; Hesse, A. J.; Magers, J. R.; Pugh, K. R.; O'Reilley, S. A.; Wilson, A. M. *Organometallics* **2009**, *28*, 6841; d) Beckford, F. A.; Scott, A.; Gonzales-Sarrias, A.; Seeram, N. P. *Appl. Organomet. Chem.* **2013**, *27*, 425; e) Leadbeater, N. E.; Shoemaker, K. M. *Organometallics* **2008**, *27*, 1254; f) VanAtta, S. L.; Duclos, B. A.; Green, D. B. *Organometallics* **2000**, *19*, 2397; g) Barnard, T. M.; Leadbeater, N. E. *Chem. Commun.* **2006**, 3615.

[21] See for example: a) Beckford, F. A.; Shaloski Jr., M.; Leblanc, G.; Thessing, J.; Lewis-Alleyne, L. C.; Holder, A. A.; Li, L.; Seeram, L. *Dalton Trans.* **2009**, 10757; b) Zagermann, J.; Molon, M.; Metzler-Nolte, N. *Dalton Trans.* **2011**, *40*, 1011; c) Herrero, S.; Jimenez-Aparicio, R.; Perles, R.; Priego, J. L.; Urbanos, F. *Green Chem.* **2010**, *12*, 965; d) Delgado, P.; Gonzales-Prieto, R.; Jimenez-Aparicio, R.; Perles, J.; Priego, J. L.; Torres, R. M. *Dalton Trans.* **2012**, *41*, 11866; e) Herrero, S.; Jimenez-Aparicio, R.; Perles, J.; Priego, J. L.; Urbanos, F. *Green Chem.*, **2011**, *13*, 1885.

[22] Sheldrick, G. M. *SADABS*, Program for empirical absorption correction, University of Göttingen, Germany, 1996**.**

[23] Sheldrick, G. M. *SHELX97*, Program for crystal structure determination, University of Göttingen, Germany, 1997.

CHAPTER IV

Oxidant free one-pot transformation of bio-based 2,5-bis-hydroxymethylfuran into α-6-hydroxy-6-methyl-4-enyl-2H-pyran-3-one in water

Abstract

A new synthetic route for obtaining α-6-hydroxy-6-methyl-4-enyl-2H-pyran-3-one, a useful synthon for the preparation of biologically active compounds, has been developed from the bio-based platform derivative (2,5-bis-hydroxymethylfuran) BHMF. The reaction occurs with good selectivity in water, under mild conditions and employing a heterogeneous recyclable acid (Amberlyst 15®) as catalyst, avoiding the use of oxidizing agents. The reaction provides access to poly-oxygenated compounds characterized by a molecular motif commonly found in many natural products.

Introduction

As already stated in the conclusion of the previous chapter, Shvo's type complexes are promising catalysts for application of in the valorization of bio-oil and biomass derivatives. Indeed the research group in which I performed my PhD, has developed a new process for the quantitative reduction of 5-hydroxymethylfurfural (HMF) to BHMF exploiting the selective behavior of Shvo catalyst in the hydrogenation of aldehyde to alcohol.[1] Biomass and biomass-derived chemicals hold promise in transitioning to a more sustainable bio-based economy displaying a new portfolio of products, not equivalent to those presently manufactured by classical synthetic routes from hydrocarbons.[2] In particular, furans (e.g. 5-hydroxymethylfurfural HMF) are important biomass-derived molecules which can be used as starting materials for the synthesis of a variety of potentially useful compounds.[3] The structural moieties present in HMF allow synthetic transformations to other target molecules by means of selective reactions such as: oxidation of the formyl group,[4] reduction of the formyl group and/or the furan ring,[5] deoxygenation of the hydroxyl groups to 2,5-dimethylfuran,[6] etherification and carbonylation,[7] and hydrogenolysis transformations.[8] In particular, selective reduction of 5-hydroxymethylfurfural (HMF) provides access to the diol 2,5-bishydroxymethylfuran (BHMF), a valuable building block for the production of polymers and polyurethane foams.[3c,9] HMF reduction to BHMF can be performed under stoichiometric conditions in the presence of NaBH4[10] or by using aqueous solutions of HCHO and NaOH,[11] in the presence of catalysts such as: copper chromite,[12] Ni Raney,[13] Pt-, Pd- or Ru-supported catalysts.[5,14] Main drawbacks are the toxicity of some of the catalysts employed, and the high temperature (140-200 °C) and pressure (70-75 bar) required.[1e] Therefore, the development of novel processes for biomass derived building blocks transformation employing lower temperature, ,low hydrogen pressure and exploiting less toxic catalysts, such as the one above cited,[1] is indeed of great interest.

Aimed at developing a heterogeneous bi-functional redox/acidic catalyst for the transformation of HMF in a linear bis-alcohol with terminal –OH groups, we first tested the heterogeneous acid catalyst Amberlyst 15® on BHMF in order to favor concomitant hydrolysis and the opening of the furan ring. In our plan The subsequent planned step would be to modify the acidic support by adding the Shvo catalyst. In particular, by using the complexes **33** described in the previous chapter, we planned to insert the redox catalyst for the reduction steps. Nonetheless, we found out that the acid catalyst allows a series of unexpected rearrangements that led to the formation of a secondary alcohol function, making almost useless the incorporation of the Shvo catalyst.

Anyway, the compound obtained is interesting by itself and this is the reason why we decided to study in more detail the effect of acid catalysis on BHMF. In this final chapter then, the transformation of BHMF into α-6-hydroxy-6-methyl-4-enyl-2H-pyran-3-one upon treatment with a heterogeneous acid catalyst (Amberlyst 15[®]) in water and in the absence of oxidizing agent is described. The same treatment in alcohol leads to etherification of the OH functionalities and no rearrangements are observed.[15] Amberlyst 15[®] is non-hazardous in nature and easily separable from reaction mixture. Thus, on the basis of its physical properties such as high H- exchange capacity (4.7 meq/g) and surface area (42 m^2/g) it combines very useful acidic properties, with benign environmental character, reusability and commercial availability.[16] The present reaction is consistent with most requirements typical of green methodologies, in that it is atom economic,[17] one-pot reaction[18] and performed in water as solvent,[19] with the possibility to recycle the catalyst. Furthermore, the product obtained represents an attractive synthon for the preparation of sugar analogues and compounds showing biological activity.[20]

Result and discussion

9.1 Catalyst screening

The substrate BHMF has been treated in the presence of different heterogeneous acid catalysts such as Amberlite IRC50® and Amberlyst 15®. Amberlite IRC50® did not produce any conversion of BHMF at 100 °C, even upon different catalyst loading (up to $1g_{CAT}/mmol_{BHMF}$). Concerning the reaction with Amberlyst 15®, no conversion occurred with $0.1g/mmol_{BHMF}$, while with a loading of $0.8g_{CAT}/mmol_{BHMF}$ decomposition of BHMF was detected by the formation of an insoluble black product. Lowering the catalyst/substrate ratio to $0.5g_{CAT}/mmol_{BHMF}$, a complete conversion of BHMF was observed within 30 minutes at 70 °C, leading to the formation of a mixture of products. The high catalyst loading (actually one H^+ sites each BHMF) suggests that a high acid content for the catalyst is required in order to promote the reaction as confirmed by the inactivity of Amberlite IRC 50® (0.43 meq H^+/g vs Amberlyst 15® 4.7 meq H^+/g). ^{1}H-NMR and ^{13}C-NMR (g-HSQC e g-HMBC) allowed the identification of α-6-hydroxy-6-methyl-4-enyl-2H-pyran-3-one (**34**) (Scheme 9.1) as major product.
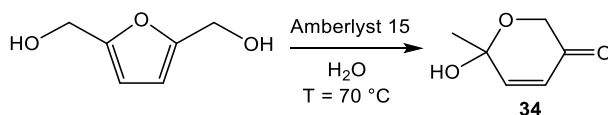
Scheme 9.1. Reaction of BHMF in water with Amberlyst 15® (t = 30 min; T = 70 °C, H_2O = 20 mL).

The ^{1}H-NMR signals, assigned to the pyranone **34** (Figure 9.3), are consistent with those reported for the same product obtained by a different synthetic approach,[21] better known as the Achmatowicz rearrangement[68] which is the oxidative rearrangement of 2-(α-hydroxyalkyl) furan, to form 6-hydroxy-3(2H)-pyranones (Scheme 9.2). The Achmatowicz rearrangement occurs under a variety of conditions, including treatment with: Br_2/MeOH,[22] peracids (e.g. m-CPBA,[23] magnesium monoperoxypthalate[24]), NBS,[25] dioxiranes (DMDO[26]), metal-based oxidations (PCC,[27] VO(acac)$_2$/t-BuOOH[28] and titanium(IV) silicalite (TS-1)/H_2O_2[29]).
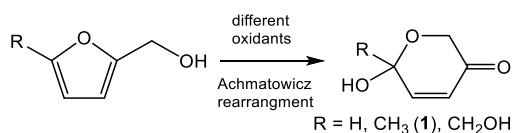
**Scheme 9.2.** Some example of Achmatowicz rearrangement.

Analogies between the reaction of BHMF (Scheme 9.1) and the Achmatowicz rearrangement are obviously based on the similar nature of the pyranone products. However, there are relevant and peculiar differences, in that our reaction provides access to **34** without oxidants. On the other hand, the Achmatowicz rearrangements shown in Scheme 9.2 do not take place when the reactions occur under the conditions shown in Scheme 1. For example, treatment of furfuryl alcohol with Amberlyst 15® ($0.5g_{CAT}/mmol_{Furfuryl\ alcohol}$, H_2O 20 mL, T = 70°C, t = 30 min) does not lead to the formation of pyranone products. A further observation is that BHMF, under Achmatowicz conditions is transformed into a more oxidized product (see Scheme 9.2, R= CH_2OH), compared to **34,** which is instead obtained from 2-methyl-5-hydroxymethylfuran.

It has to be underlined that the number of methods developed to undertake the oxidative Achmatowicz rearrangement accounts for both the usefulness 6-hydroxy-3(2H)-pyranones, and the lack of a single, very effective and reliable synthetic route. Methods proposed so far exhibit limits mostly arising from the harshness of the reaction conditions and the lack of selectivity associated. Drawbacks include tedious work-up, use of

expensive reagents or high energy-demand, non-scalability, formation of salt waste or low catalyst recyclability. For example, although the NBS and peroxyacid mediated reactions usually offer simple procedures, it was found that these methods are unreliable and unsuitable for all but very small-scale work. On the other hand, the bromomethoxylation procedure is highly sensitive to temperature and produces stoichiometric amounts of NaBr. In contrast to the above-mentioned methods, using TS-1 as a heterogeneous catalyst and aqueous H_2O_2 as an inexpensive oxygen source, small-sized furfuryl alcohols are readily converted into 6-hydroxy-2H-pyran-3(6H)-ones with high yield and high oxidant efficiency. Moreover, the use of other Ti-substituted molecular sieves possessing larger pores, such as zeolite Ti-Beta or mesoporous Ti-MCM-41, provide access to the oxidation of more bulky furfuryl alcohols.[30] More recently, it has been reported a greener method based on non-toxic singlet oxygen ($^1O_2$), run in MeOH in the presence of a reducing agent,[31] and in water exploiting light and spirulina as the photosensitizer.[32] In our reaction, the presence of two hydroxyl groups on the furan ring makes the oxidant source unnecessary, and results in a greener approach to pyranones.

9.2 Screening of the reaction conditions

The reaction has been performed also under nitrogen atmosphere. Both GC-MS and NMR spectra (^{1}H and ^{13}C-NMR) confirm the formation of α-6-hydroxy-6-methyl-4-enyl-2H-pyran-3-one (**34**) as well as of the by-products 1,3-dihydroxyhexan-2,5-dione (**35**) and 1,4-dihydroxyhexan-2,5-dione (**36**). (Scheme 9.3 and Figure 9.6).
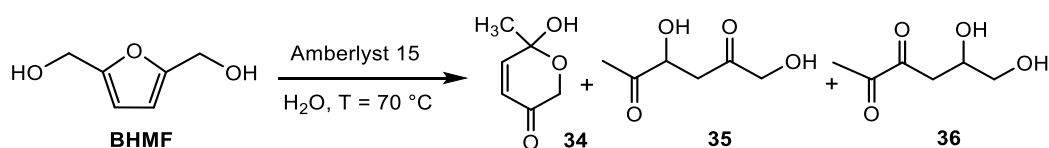
Scheme 9.3. Reaction conditions: 0.5g$_{CAT}$/mmol$_{BHMF}$, N_2, degassed water, 70°C, t = 30 min.

Conversion, yield and selectivity were established on the crude from ^{1}H-NMR spectra, once identified all the products in the mixture which are solely **34**, **35** and **36**. As reported in Table 9.1 the reaction under nitrogen atmosphere (entry 2) shows a better selectivity in the formation of **34** than in the presence of air (entry 1). It is worth noting that lower temperatures (e.g. 50 °C, entry 3) have a detrimental effect on both yield and selectivity. Product **34** has been purified by column chromatography on deactivated silica (treated with a Et$_2$O solution of NEt$_3$). The product was eluted with Et$_2$O and isolated with a 25% yield.

Table 9.1. Acid catalyzed BHMF conversion to **34**. Reaction conditions: 0.5g$_{CAT}$/mmol$_{BHMF}$, t=30 min.

Entry	Atmosphere	T (°C)	Conversion (%)	Yield (%)	Selectivity (%)
1	Air	70	91	45	49
2	N_2	70	76	50	70
3	N_2	50	12	5	46

Finally, the reaction behavior in function of the reaction time is reported in Figure 9.1. The reaction reaches complete conversion within 60 minutes and the selectivity results lower than 100% already at the beginning of the reaction suggesting that a parallel reaction is involved, with formation of the side products **35** and **36**.
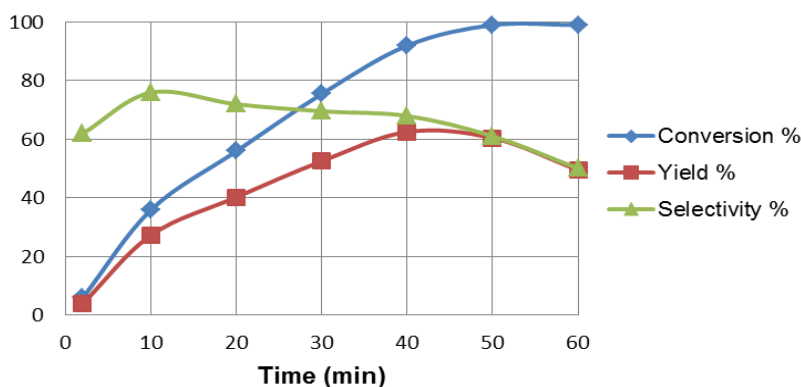
Figure 9.1. BHMF conversion, yield and selectivity of **34** in function of time. Reaction conditions: $0.5g_{CAT}/mmol_{BHMF}$, T = 70°C, under N_2.

9.3 Catalyst recycling

The resin employed under the reaction conditions of Table 9.1 - entry 2 (T = 70 °C, t = 30 min) was washed with water and dried for 14 h, then was further employed for recycling tests maintaining the same activity for four cycles (Figure 9.2). FT-IR (KBr) analysis of the resin before and after use and comparison with the spectra of BHMF and **34** indicates that neither reagents nor products remain absorbed over the resin.
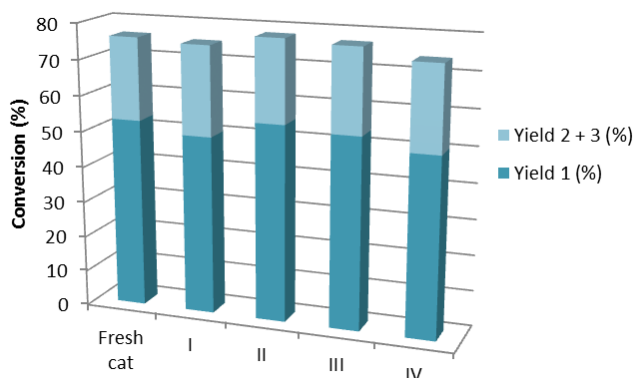

Figure 9.2. Recycling of Amberlyst 15®. Reaction conditions: $0.5g_{CAT}/mmol_{BHMF}$ T = 70 °C, t = 30 min, under N_2.
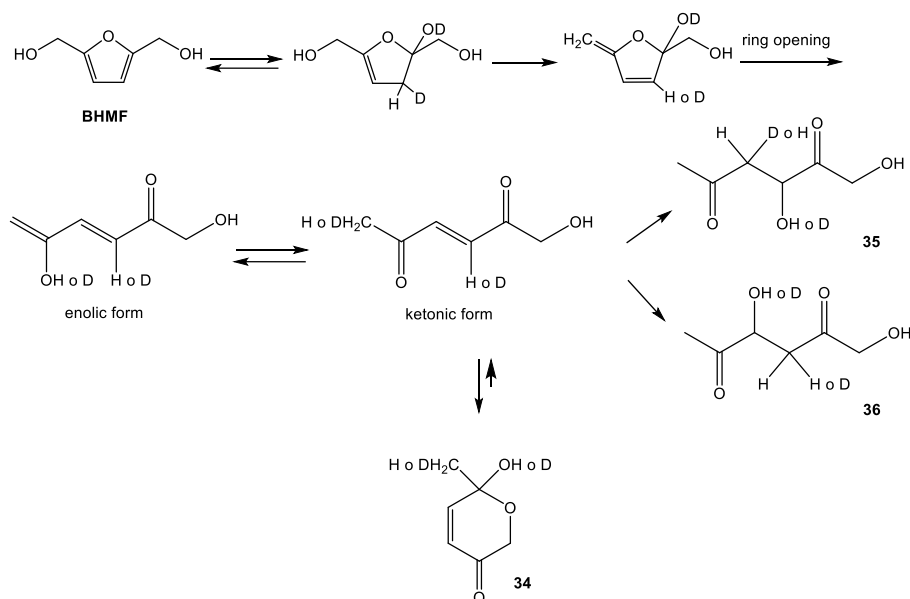
9.4 Reaction mechanism

Based on the nature of the reaction products, a tentative reaction mechanism has been depicted (Scheme 9.4). It consists of a hydration of one C=C double bond of BHMF followed by a dehydration that involve the hydroxymethyl group on the other side of the ring. Then the ring of 2-hydroxymethyl-5-methylen-2,5-dihydrofuran-2-ol undergoes ring opening giving rise to a keto-enol equilibrium. When the linear molecule is in its ketonic form a nucleophilic attack of the hydroxyl group on the terminal carbon lead to the ring closure and to the formation of compound **34** which is the major compound. The side products **35** and **36** are likely derived from parallel hydration of the ketonic intermediate before ring closure. However, following the reaction up to 5 h the complete conversion of the product **34** into **35** and **36** is observed (GC-MS e ^{1}H-NMR) that means that a consecutive hydration/ring opening of compound **34** also contributes to the formation of **35** and **36**.
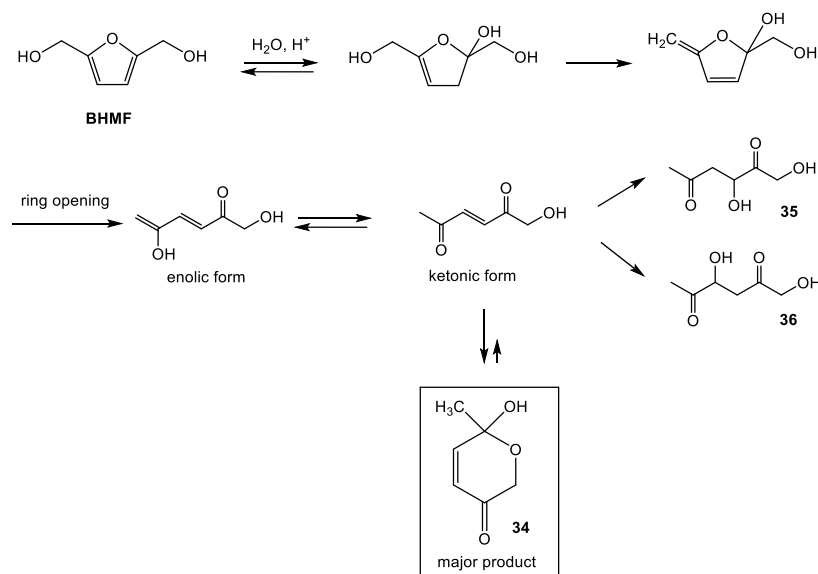
Scheme 9.4. Proposed mechanism for the reaction of BHMF in water with Amberlyst 15®.

In order to validate the proposed mechanism, the reaction has been also performed in D_2O with the same reaction conditions (0.5g_{CAT}/mmol$_{BHMF}$; T = 70 °C, t = 30 min). ^{1}H-NMR spectrum of the mixture shows the appearance of signals due to H/D coupling in the range in which signals attributable to CH_3 (δ 1.4-1.5 ppm) and to CH_2 (δ 2.0-2.2 ppm) are found, which is consistent with the hydration and dehydration steps in the proposed mechanism (see Scheme 9.5 and Figure 9.3).

Scheme 9.5: Mechanism proposed for the reaction of BHMF with Amberlyst 15 in D_2O. Sites involved in the hydration and subsequently in the deuterium insertion are highlighted.

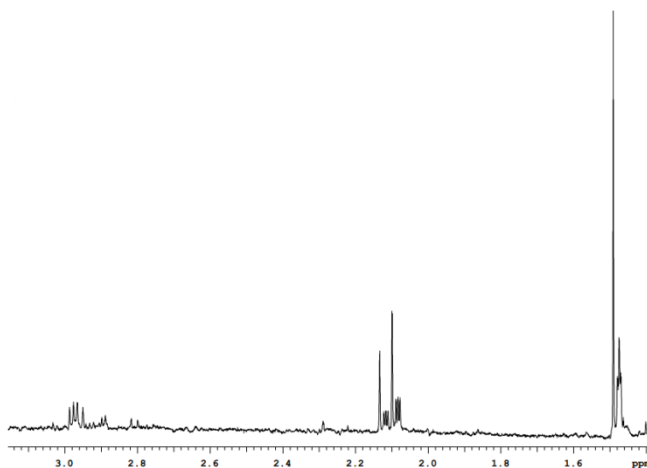Below a portion of the NMR spectrum in which H-D coupling have been detected:

Figure 9.3 Portion of the ^{1}H-NMR spectrum in D_2O. Reaction conditions: Amberlyst 15/BHMF (5:1) in D_2O at 70°C, t = 30 min.

9.5 Homogeneous vs. heterogeneous acid catalysis

The reactivity of BHMF with a homogeneous acid catalyst (HCl) has been investigated in water at 70 °C for 30 minutes by varying the solution pH (Table 9.2). The formation of a mixtures of compounds **34**, **35** and **36** with a general behavior similar to that found for the Amberlyst 15® resin (entry 1) is observed, however lower yields and selectivity in **34** are obtained in the case of the homogeneous system (HCl, entries 2-5). Data in Table 9.3 also evidence that a low pH favors the conversion.

Table 9.2. Reaction of BHMF with HCl at different pH.

Entry	Cat [H$^+$]	Conversion (%)	Yield of **34** (%)	Selectivity of **34** (%)
1	Amberlyst 15 (0.5g$_{CAT}$/mmol$_{BHMF}$)	76	53	70
2	HCl (pH 1)	99	16	16
3	HCl (pH 2)	76	14	18
4	HCl (pH 3)	49	13	27
5	HCl (pH 4)	19	6	29

Employing H_2SO_4 instead of HCl as acid led to complete decomposition probably due to the oxidizing properties of the acid. The latter experiments confirm the role of acid in the formation of **34** from BHMF, as well as the need of a strong acidity in order to obtain complete conversion in due time (pH=1 for a complete conversion in 30 min). Moreover, the heterogeneous catalyst results, by far, more effective in terms of selectivity, which is not obvious to explain. The heterogeneous catalyst might provide both a very high acid concentration, necessary to promote hydration-dehydration steps, and some selectivity effects due to the lower availability of the acid sites, which should favor the formation of **34**. Indeed, due to steric reasons, the ketonic form in equilibrium with **34** (Scheme 9.4) should have easier access to the acidic sites, compared to **34**, making ring opening reaction less favorable compared to the reverse reaction and resulting in the observed selectivity.

Conclusions

In this novel and efficient acid-mediated BHMF rearrangement to α-6-hydroxy-6-methyl-4-enyl-2H-pyran-3-on in water neither ungreen oxidizing agents nor harsh conditions are required. The heterogeneous recyclable acid catalyst Amberlyst 15® allows good selectivity and mild conditions. The new method starts from a bio-based platform derivative such as BHMF and the protocol employs green, nontoxic reagents and conditions. Furthermore, it is highly step-economic and highly efficient from the perspective of atom economy. The product obtained represents an attractive synthon for the preparation of biologically active compounds, making the protocol a step forward in the direction of the green approach to pharmaceuticals from biomasses. Mechanistic investigation opens the street for the development of a general method for the transformation of variously functionalized dihydroxy-furans.

Experimental section

Materials. Solvents: water has been freshly distilled; diethylether, methanol (MeOH), toluene, CDCl₃, toluene-d₈, CD₃CN, (Sigma Aldrich), reagents: H₂SO₄, HCl, furfuryl alcohol (Sigma Aldrich), 5-hydroxymethylfurfural (HMF) (SAFC), and resins Amberlite IRC50®, Amberlyst 15® wet, have been employed as purchased, 2,5-bishydroxymethylfuran (BHMF) has been prepared as described in the literature.[1]

Analytical methods. The NMR spectra were recorded using Varian Inova 300 (^{1}H, 300.1; ^{13}C, 75.5 MHz), Varian Mercury 400 (^{1}H, 399.9; ^{13}C, 100.6 MHz), Varian Inova 600 (^{1}H, 599.7, ^{13}C, 150.8 MHz) spectrometers. Infrared spectra were recorded at 298 K on a Perkin-Elmer Spectrum 2000 FT-IR spectrophotometer. GC analyses have been performed on an Agilent Technologies 6890N instrument (column: Agilent 19091J-433 HP-5). HPLC analyses where performed on an Agilent Technologies 1260 Infinity instrument, equipped with a C-18 core shell column 50x4.6mm employing a solution of 80% of 0.01 M H₃PO₄ and 20% acetonitrile as mobile phase.

BHMF rearrangement

Amberlyst 15®. BHMF (54.8 mg, 0.43 mmol) is dissolved in a suspension of Amberlyst 15® (256 mg) in water (20 mL). For reactions performed under nitrogen atmosphere the aqueous suspension of Amberlyst 15® is degassed and purged with nitrogen. The mixture is warmed to the desired temperature and the suspension maintained under stirring for the time requested and then cooled in a water bath. The catalyst is filtered off and the solvent removed under vacuum (at a temperature lower than 40 °C). The reaction crude is analysed by GC-MS, ^{1}H- and ^{13}C-NMR and HPLC. From those analyses the following products are identified in variable mixtures. BHMF, α-6-hydroxy-6-methyl-4-enyl-2H-pyran-3-one (**34**), 1,3-dihydroxyhexan-2,5-dione (**35**), 1,4-dihydroxyhexan-2,5-dione (**36**).

HCl or H₂SO₄. BHMF (54.8 mg, 0.43 mmol) is dissolved in a water (20 mL) solution of the desired quantity of HCl or H₂SO₄. The reaction mixture is stirred at 70 °C for 30 min. Then it is cooled to room temperature and neutralized with NaOH. Water is removed under vacuum and the crude dissolved in CH₂Cl₂. After anhydrification on Na₂SO₄ the solution is filtered and the solvent removed under vacuum. The crude has been analyzed by ^{1}H-NMR.

Characterization of 2,5-hydroxymethylfuran (BHMF)

BHMF
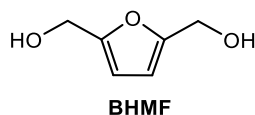
^{1}H NMR (399.9 MHz, CD₃CN): δ 3.19 (s, 2H, -O**H**); 4.44 (s, 4H, -C**H₂**OH); 6.20 (s, 2H, -C**H**). ^{13}C NMR (100.6 MHz, CD₃CN): δ 57.87 (s, 2C, -**C**H₂OH); 109.50 (s, 2C, -**C**H); 156.37 (s, 2C, -**C**q)

^{1}H NMR (399.9 MHz, D₂O): δ 4.56 (s, 4H, -C**H₂**OH); 4.79 (s, 2H, -O**H**); 6.36 (s, 2H, -C**H**).^{13}C NMR (100.6 MHz, D₂O): δ 58.37 (s, 2C, -**C**H₂OH); 111.59 (s, 2C, -**C**H); 156.17 (s, 2C, -**C**q)

^{1}H NMR (399.9 MHz, CDCl₃): δ 4.60 (s, 4H, -C**H₂**OH); 6.25 (s, 2H, -C**H**); –O**H** variable. ^{13}C NMR (100.6 MHz, CDCl₃): δ 58.00 (-**C**H₂OH); 108.45 (**C**H); 155.08 (**C**q).

^{1}H NMR (399.9 MHz, Toluene-d$_8$): δ 4.18 (C**H$_2$**-OH); 5.89 (-C**H**); 4.32 (-O**H**).^{13}C NMR (100.6 MHz, Toluene-d$_8$): δ 58.13 (-**C**H$_2$OH); 108.65 (**C**H); 155.31 (**C**q).

GC-MS t.r.: 10.77 min - 128 [M$^+$]; 109 [M$^+$-OH]; 97 [M$^+$-CHO]. HPLC r.t.: 1,7 minutes
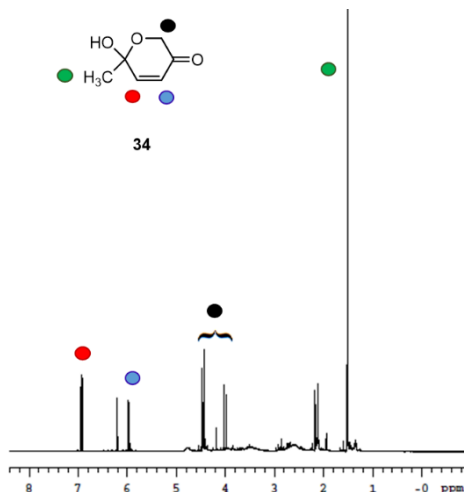
NMR spectra of selected reaction mixtures

Figure 9.4. ^{1}H-NMR spectrum in CD$_3$CN. Reaction conditions: Amberlyst 15/BHMF (5:1), T = 70 °C, t = 30 min, air, water.
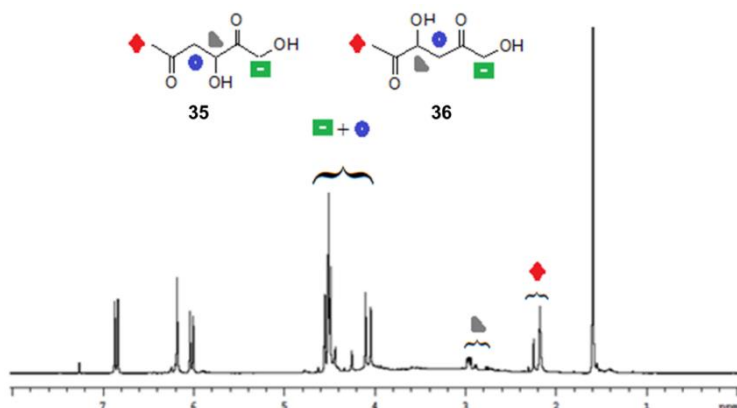

Figure 9.5. ^{1}H-NMR in CDCl$_3$. Reaction conditions: Amberlyst 15/BHMF (5:1), N$_2$, degassed water, 70°C, t = 30 min.
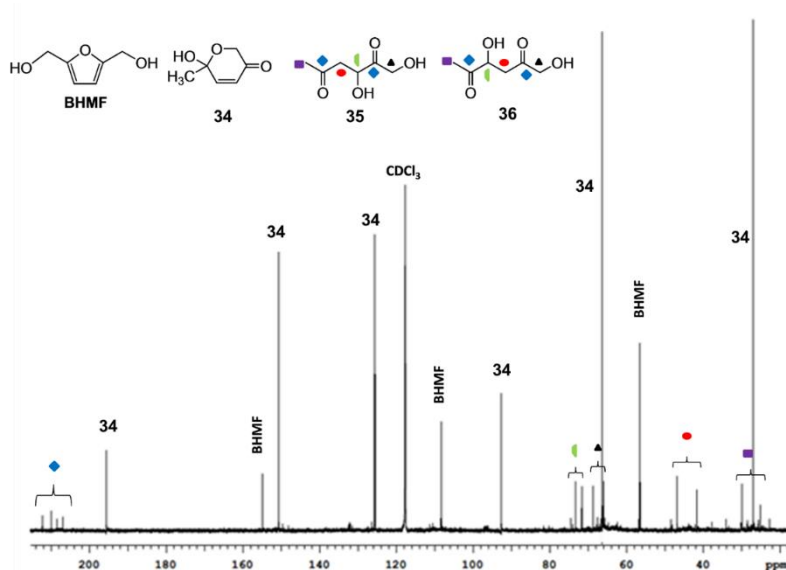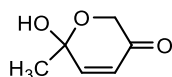

Figura 9.6. ^{13}C-NMR in CDCl$_3$. Reaction conditions: Amberlyst 15/BHMF (5:1), N$_2$, degassed water, 70°C, t = 30 min.

Characterization of α-6-hydroxy-6-methyl-4-enyl-2H-pyran-3-one (34)

34

^{1}H NMR (399.9 MHz, CD$_3$CN): δ 1.51 (s, 3H, CH$_3$); 4.01, 4.45 (d, ^{2}J (H,H) = 17.2 Hz, 2H -CH$_2$); 5.96 (d, ^{2}J (H,H) = 10.4 Hz, 2H -CHCO); 6.93 (d, ^{2}J (H,H) = 10.4 Hz -CHC(OH)CH$_3$); OH variable;^{13}C NMR (100.6 MHz, CD$_3$CN): δ 27.70 (CH$_3$); 67, (-CH$_2$-); 93.40 (-C(OH)CH$_3$); 126.37 (-CHCO); 151.36-CHC(OH)CH$_3$; 196.31 (CO).

^{1}H NMR (399.9 MHz, CDCl$_3$): δ 1.65 (s, 3H, CH$_3$); 4.12, 4.57 (d, ^{2}J (H,H) = 17.1 Hz, 2H -CH$_2$); 6.08 (d, ^{2}J (H,H) = 10.2 Hz, 2H -CHCO); 6.87 (d, ^{2}J (H,H) = 10.2 Hz -CHC(OH)CH$_3$); OH variable;

^{1}H NMR (399.9 MHz, D$_2$O): δ 1.67 (s, 3H, CH$_3$); 4.34, 4.63 (d, ^{2}J (H,H) = 23.2 Hz, 2H -CH$_2$); 6.22, 7.18 (d, ^{2}J (H,H) = 10.4 Hz, 2H -CHCO); 6.87 (d, ^{2}J (H,H) = 10.2 Hz -CHC(OH)CH$_3$); OH variable;

IR (CH$_2$Cl$_2$): ν(C=O) = 1706 cm^{-1}. IR (KBr): ν(C=O) = 1704 cm^{-1}.

GC-MS t.r.: 8.38 min - 128 [M$^+$]; 113 [M$^+$-CH$_3$]; 111 [M$^+$-OH]; 98 [M$^+$-CH$_2$O].

HPLC r.t.: 4,7 minutes

Characterization of 1,3-dihydroxyhexan-2,5-dione (3) e 1,4-dihydroxyhexan-2,5-dione (4)
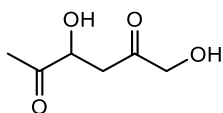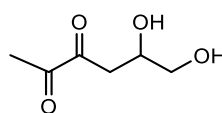
35   **36**

^{1}H NMR (399.9 MHz, CD$_3$CN): 2.14, 2.19 (s, 3H + 3H, CH$_3$ (**35** and **36**)); 3.00-2.50 (m, 2H + 2H –CH$_2$CO- (**35** and **36**)); 4.18, 4.44 (s, 2H, CH$_2$OH (**35** and **36**)); 4.41, 4.46 (m, 1H, CH (**35** and **36**)); OH variable. ^{13}C NMR (100.6 MHz, CD$_3$CN): 25.84, 30.58 (CH$_3$ (**35** and **36**); 42.38, 47.56 (CH$_2$CO (**35** and **36**); 66.68, 69.43 (CH$_2$OH (**35** and **36**); 72.36, 73.98 (CH (**35** and **36**); 207.62, 209.18, 210.63, 212.96 (CO (**35** and **36**).

^{1}H NMR (399.9 MHz, CDCl$_3$): 2.17, 2.24 (s, 3H + 3H, CH$_3$ (**3** and **4**)); 3.00-2.60 (m, 2H + 2H –CH$_2$CO- (**35** and **36**)); 4.22, 4.50 (s, 2H, CH$_2$OH (**35** and **36**)); 4.43, 4.44 (m, 1H, CH (**35** and **36**)); OH variable.

HPLC (**35** and **36**): r.t.: 1,0 e 1,2 minutes

References

[1] T. Pasini, G. Solinas, V. Zanotti, S. Albonetti, F. Cavani, A. Vaccari, A. Mazzanti, S. Ranieri and R. Mazzoni, *Dalton Trans*., **2014**, *43*, 10224.

[2] (a) R.-J. van Putten, J. C. van der Waal, E. de Jong, C. B. Rasrendra, H. J. Heeres and J. G. de Vries, *Chem. Rev*., **2013**, *113*, 1499. (b) R. W. Gosselink, S. A. W. Hollak, S.-W. Chang, J. van Haveren, K. P. de Jong, J. H. Bitter and D. S. van Es, *ChemSusChem*, **2013**, *6*, 1576. (c) P. N. R. Vennestrøm, C.M. Osmundsen, C. H. Christensen and E. Taarning, Angew. *Chem., Int. Ed.* **2011**, *50*, 10502. (d) E. L. Kunkes, D. A. Simonetti, R. M. West, J. C. Serrano-Ruiz, C. A.Gartner and J. A. Dumesic, *Science*, **2008**, *322*, 417.(e) D. R. Dodds and R. A. Gross, *Science*, **2007**, *318*, 1250. (f) L. Petrus and M. A. Noordermeer, *Green Chem*., **2006**, 861. (g) R. A. Sheldon, *Chem. Soc. Rev*., **2012**, *41*, 1437. (h) P. Gallezot *Chem. Soc. Rev*., **2012**, *41*, 1538. (i) C. Chatterjee, F. Pong and A. Sen, *Green Chem*., **2015**, *17*, 40. (l) M. J. Climent, A. Corma and S. Iborra, *Green Chem*., **2011**, *13*, 520. (m) C. H. Christensen, J. Rass-Hansen, C. C. Marsden, E. Taarning and K. Egeblad, *ChemSusChem*, **2008**, *1*, 283. (n) P. Gallezot, Green Chem., **2007**, *9,* 295. (o) A. Corma, S. Iborra and A. Velty *Chem. Rev.* **2007**, *107*, 2411. (p) J. N. Chheda, G. W. Huber and J. A. Dumesic, Angew. *Chem. Int. Ed.* **2007**, *46*, 7164.

[3] For recent reviews on HMF as a building block platform: a) see ref. 1 and A. A. Rosatella, S. P. Simeonov, R. F. M. Frade and C. A. Afonso, *Green Chem.* **2011**,*13*, 754.

[4] (a) T. Pasini, M. Piccinini, M. Blosi, R. Bonelli, S. Albonetti, N. Dimitratos, J. A. Lopez-Sanchez, M. Sankar, Q. He, C. J. Kiely, G. J. Hutchings and F. Cavani, *Green Chem.* **2011**, *13*, 2091. (b) S. Albonetti, T. Pasini, A. Lolli, M. Blosi, M. Piccinini, N. Dimitratos, J. A. Lopez-Sanchez, D. J. Morgan, A. F. Carley, G. J. Hutchings and F. Cavani, *Catal. Today* **2012**, *195*, 120. (c) S. A. Davis, L. R. Houk, E. C. Tamargo, A. K. Datye and R. J. Davis, *Catal. Today*, **2011***, 160*, 55. (d) M. A. Lilga, R. T. Hallen and M. Gray, *Top. Catal*., **2010**, *53*, 1264. e) Y. Y. Gorbanev, S. K. Klitgaard, J. M. Woodley, C. Christensen and A. Riisager, *ChemSusChem* **2009**, *2*, 672. (f) O. Casanova, S. Iborra and A. Corma, *ChemSusChem* **2009**, *2*, 1138. (g) E. Taarning, I. S. Nielsen, K. Egeblad, R. Madsen and C. H. Christensen, *ChemSusChem* **2008**, *1*,75. (h) A. Gandini, D. Coelho, M. Gomes, B. Reis and A. Silvestre, *J. Mat. Chem*., **2009**, *19*, 8656.

[5] (a) Y. Nakagawa and K. Tomishige, *Catal. Commun***., 2010**, *12*, 154. (b) R. Alamillo, M. Tucker, M. Chia, Y. Pagan-Torres and J. Dumesic, *Green Chem.* **2012**, *14*, 1413.

[6] (a) T. S. Hansen, K. Barta, P. T. Anastas, P. C. Ford and A. Riisager, *Green Chem.* **2012**, *14*, 2457. (b) M. Chidambaram and A. T. Bell, *Green Chem.* **2010**, *12*, 1253. (c) T. Thananatthanachon and T. B. Rauchfuss, Angew. *Chem. Int. Ed.* **2010**, *49*, 6616. (d) Y. Roman-Leshkov, C.J. Barrett, Z. Y. Liu and J. A. Dumesic, *Nature* **200**7, *447*, 982.

[7] (a) M. Balakrishnan, E. R. Sacia and A. T. Bell, *Green Chem.* **2012**, *14*, 1626. (b) P. Che, F. Lu, J. Zhang, Y. Huang, X. Nie, J. Gao and J. Xu, *Biores. Technol.* **2012**, *119*, 433. (c) P. Lanzafame, D. M. Temi, S. Perathoner, G. Centi, A. Macario, A. Aloise and G. Giordano, *Catal. Today* **2011**, *175*, 435. (d) O. Casanova, S. Iborra and A. Corma, *J. Cata*l. **2010**, *275*, 236. (e) O. Casanova, S. Iborra and A. Corma, *J. Catal.* **2009**, *265*, 109. (f) G. Papadogianakis, L. Maat and R. A. Sheldon, *J. Mol. Catal. A: Chem*. **1997**, *116*, 179.

[8] (a) T. Buntara, S. Noel, P. H. Phua, I. Melian-Cabrera, J. G. de Vries and H. J. Heeres, *Angew Chem. Int. Ed.* **2011**, *50*, 7083. (b) M. Chia, Y. J. Pagan-Torres, D. Hibbitts, Q. Tan, H. N. Pham, A. K. Datye, M. Neurock, R. J. Davis and J. A. Dumesic, *J. Am. Chem. Soc.* **2011**, *133*, 12675.

[9] (a) A. Gandini, *Green Chem*., **2011**, *13,* 1061. (b) C. Moreau, M. N. Belgacem and A. Gandini, *Top. Catal***., 2004**, *27*, 11.

[10] (a) J. M. Timko and D. J. Cram, *J. Am. Chem. Soc.* **1974**, *96*, 7159. (b) S. Goswami, S. Dey and S. Jana, *Tetrahedron*, **2008** *64*, 6358. (c) F. W. Lichtenthaler, A. Brust and E. Cuny, *Green Chem.* **2001**, *3*, 201.

[11] J. H. Turner, P. A. Rebers, P. L. Barrick and R. H. Cotton, *Anal. Chem*. **1954**, *26*, 898.

[12] T. Utne, J. D. Garber and R. E. J. Jones *US Patent 3,083,236* (**1963**) assigned to Merck &Co.

[13] T. J. Connolly, J. L. Considine, Z. Ding, B. Forsatz, M. N. Jennings, M. F. MacEwan, K. M. McCoy, D. W. Place, A. Sharma and K. Sutherland *Org. Proc. Res. Dev.* **2010**, *14*, 459.

[14] (a) J. Lewkowski, Arkivoc **2001**, *2*, 17. (b) V. Schiavo, G. Descotes and J. Mentech, *Bull. Soc. Chim. Fr.* **1991**, 704. (c) A. C. Cope and W. N. Baxter, *J. Am. Chem. Soc.* **1955**, *77*, 393.

[15] (a) E. R. Sacia, M. Balakrishnan, A. T. Bell, *J. Catal.* **2014**, *313*, 70. (b) M. Balakrishman, E. R. Sacia, A. T. Bell, *Green Chem*., **2012**, *13*4, 1626.

[16] (a) R. Pal, T. Sarkar, S. Khasnobis, *Arkivoc*, **2012**, 570. (b) S. R. Lanke, B. M. Bhanage, *Catal. Commun.* **2013**, *41*, 29. (c) V. V. Patil, G. S. Shankarling, *Catal. Commun***. 2014**, *57*, 138.

[17] B. M. Trost, *Science,* **1991**, *254*, 1471.

[18] P. A. Wender and B. L. Miller, *Nature**,* **2009**, *460*, 197.

[19] I. S. Young and P. S. Baran, *Nat. Chem*., **2009**, *1*, 193.

[20] (a) P. D. Weeks, T. M. Brennan, D. P. Brannegan, D. E. Kuhla, M. L. Elliott, H. A. Watson, B. Wlodecki, R. Breitenbach, *J. Org. Chem.* **1980**, *45*, 1109. (b) S. F. Martin, D. E. Guinn, *J. Org. Chem.* **1987**, *52*, 5588. (c) P. DeShong, R. E. Waltermire, H. L. Ammon, *J. Am. Chem. Soc.* **1988**, *110*, 1901. (d) F. M. Hauser, S. R. Ellenberger,W. P. Ellenberger, *Tetrahedron Lett.* **1988**, *29*, 4939. (e) S. F. Martin, P. W. Zinke, *J. Am. Chem. Soc.* **1989**, *111*, 2311. (f) S. F. Martin, H.-J. Chen, C.-P. Yang, *J. Org. Chem.* **1993**, *58*, 2867. (g) P. A.

Wender, K. D. Rice, M. E. Schnute, *J. Am. Chem. Soc.* **1997**, *119*, 7897. (h) M. Takeuchi, T. Taniguchi, K. Ogasawara, *Synthesis* **1999**, 341. (i) J. M. Harris, M. D. Keranen, G. A. O-Doherty, *J. Org. Chem.* **1999***, 64*, 2982.

[21] D. Noutsias, I. Alexopoulou, T. Montagnon, G. Vassilikogiannakis, *Green Chem.*, **2012**, *14*, 601.

[22] Achmatowicz Jr., P. Bukowski, B. Szechner, Z. Zwierzchowska, A. Zamojski*, Tetrahedron*, **1971**, 1973.

[23] Y. Lefebvre, Tetrahedron Lett., 1972, 13, 133; R. Laliberte, G. Medawar and Y. Lefebvre, *J.* Med. Chem., **1973**, *16*, 1084.

[24] C. Dominguez, A. G. Csaky and J. Plumet, *Tetrahedron Lett.*, **1990**, *31*, 7669.

[25] E. A. Couladouros and M. P. Georgiadis, *J. Org. Chem.,* **1986**, *51,* 2725.

[26] B. M. Adger, C. Barrett, J. Brennan, M. A. McKervey and R. W. Murray, *J. Chem. Soc., Chem*. Commun., **1991**, 1553.

[27] G. Piancatelli, A. Scettri and M. D'Auria, *Tetrahedron Lett.*, **1977**, *18*, 2199.

[28] T.-L. Ho and S. G. Sapp, *Synth. Commun.*, **1983,** *13*, 207.

[29] J. Wahlen, B. Moens, D. E. De Vos, P. L. Alsters, P. A. Jacobs, *Adv. Synth. Catal.*, **2004**, *346*, 333.

[30] (a) M. A. Camblor, A. Corma, A. Martinez, J. Perez-Pariente*, J. Chem. Soc. Chem*. Commun., **1992**, 589. (b) [77] A. Corma, M. T. Navarro, J. Perez-Pariente, J. *Chem. Soc. Chem. Commun.,* **1994**, 147.

[31] D. Noutsias, A. Kouridaki and G. Vassilikogiannakis, *Org. Lett.,* **2011**, *13*, 1166.

[32] T. Montagnon, D. Kalaitzakis, M. Triantafyllakis, M. Stratakis and G. Vassilikogiannakis *Chem. Commun.,* **2014**, *50,* 15480.

List of publications

The most of the results presented in this thesis have been documented in 8 publications:

- "A new tetraarylcyclopentadienone based low molecular weight gelator: synthesis, self-assembly properties and anion recognition" M. Boiani, A. Baschieri, C. Cesari, R. Mazzoni, S. Stagni, S. Zacchini and L. Sambri, *New J. Chem.*, **2012**, *36*, 1469–1478.

- "Microwave-Assisted Synthesis of Functionalized Shvo Type Complexes" C. Cesari, L. Sambri, S. Zacchini, V. Zanotti, R. Mazzoni, *Organometallics*, **2014**, *33*, 2814-2819.

- "Sterically driven synthesis of ruthenium and ruthenium-silver N-heterocyclic carbene complexes." C. Cesari, S. Conti, S. Zacchini, V. Zanotti, M.C. Cassani, R. Mazzoni, *Dalton Trans.*, **2014**, *43*, 17240-3.

- "Ruthenium(0) complexes with triazolylidene spectator ligands: Oxidative activation for (de)hydrogenation catalysis." C. Cesari, R. Mazzoni, H. Muller-Bunz, M. Albrecht, *J. Organomet. Chem*, **2015**, *793,* 256-262.

- "Diiron complexes bearing bridging hydrocarbyl ligands as electrocatalysts for proton reduction." R. Mazzoni, A. Gabiccini, C. Cesari, V. Zanotti, I. Gualandi, D. Tonelli, *Organometallics*, **2015**, *34*, 3228-3235.

- "Oxidant free one-pot transformation of bio-based 2,5-bis-hydroxymethylfuran into α-6-hydroxy-6-methyl-4-enyl-2H-pyran-3-one in water" A. Gelmini, S. Albonetti, F. Cavani, C. Cesari, A. Lolli, V. Zanotti, R. Mazzoni, *Applied Catalysis B: Environmental*, **2016**, 180, 38-43.

- "Straightforward synthesis of iron cyclopentadienone N-heterocyclic carbene complexes" A. Cingolani, C. Cesari, S. Zacchini, V. Zanotti, M.C. Cassani, R. Mazzoni, *Dalton Trans.*, **2015**, *44*, 19063-19067.

- "Ruthenium hydroxycyclopentadienyl N-heterocyclic carbene complexes as transfer hydrogenation catalysts" C. Cesari, A. Cingolani, C. Parise, S. Zacchini, V. Zanotti, M.C. Cassani, R. Mazzoni, *RSC Adv.*, **2015**, *5*, 94707-94718.